DISCOVERY AND CHARACTERIZATION OF THE INTERPHASE FUNCTION OF MITOTIC MOTORS IN PROTEIN SYNTHESIS

by

Kristen Marie Bartoli

B.S., Temple University, 2004

Submitted to the Graduate Faculty of

University of Pittsburgh School of Medicine in partial fulfillment

of the requirements for the degree of

Doctor of Philosophy

University of Pittsburgh

2010

UNIVERSITY OF PITTSBURGH

SCHOOL OF MEDICINE

This dissertation was presented

by

Kristen Marie Bartoli

It was defended on

September 1, 2010

and approved by

Stefan Duensing, M.D., Associate Professor, Microbiology and Molecular Genetics

Saleem A. Khan, Ph.D., Professor, Microbiology and Molecular Genetics

Laura J. Niedernhofer, M.D., Ph.D., Associate Professor, Microbiology and Molecular Genetics

John L. Woolford, Jr. Ph.D., Professor, Biological Sciences

William S. Saunders, Ph.D., Major Thesis Advisor, Associate Professor, Biological Sciences

DISCOVERY AND CHARACTERIZATION OF THE INTERPHASE FUNCTION OF MITOTIC MOTORS IN PROTEIN SYNTHESIS

Kristen Marie Bartoli, PhD

University of Pittsburgh, 2010

Mitotic motors have gained considerable interest as anticancer targets given their often essential functions during mitosis. Furthermore, mitotic motors are thought to represent ideal targets because their functions are believed to be confined to mitosis; thus, only rapidly dividing cells would be susceptible to inhibitors of mitotic motors. The work presented herein challenges the concept of mitotic motors as specific targets of dividing cells by exploring the interphase function of three mitotic motors Kid, Eg5, and MKLP1. Our results demonstrate that all three motors associate with the nucleolus and with the ribosomal subunits. Furthermore, it is demonstrated Eg5 functions to increase the processivity of the ribosome, the first cellular factor to be characterized with that property. Additionally, as loss of Kid results in an increase in focal adhesion proteins throughout the cell and increased protein synthesis in its absence, our data are consistent with a role for Kid in mRNA silencing and transport of mRNAs for site-specific translation. Also, evidence is presented that suggests a role for Kid in ribosome biogenesis and/or ribosomal function, similar to nucleophosmin. Finally, both Kid and Eg5 participate in stress granule dynamics, with Kid and Eg5 functioning in stress granule formation, and Eg5 participating in stress granule coalescence, transport and dissolution. Collectively these findings demonstrate diverse interphase functions for these mitotic motors in nearly all phases of the ribosome's life cycle. These studies not only call into question the potential safety of mitotic

motor inhibitors for the treatment of cancer, but also open a new avenue of exploring polypeptide synthesis.

TABLE OF CONTENTS

LIST OF FIGURES

PREFACE

I would like to take the time to thank all of the following people listed below who not only believed in me, but had a large influence on my growth as a person, as a scientist, and in life. Thank you to all of you from the bottom of my heart.

I would like to start out by thanking my graduate thesis advisor Dr. William S. Saunders. I appreciate all the guidance and wisdom that he provided. Bill allowed me to follow my project no matter what direction the project went in and this allowed me to grow into an independent scientist. When we started the mitotic motors project, neither one of us knew what direction it would go (and we certainly never thought we would end up defining a role for mitotic motors in protein synthesis). I thank him for entrusting me to carry out this project that utilized skills completely outside the labs knowledge.

Next, I would like to thank all my committee members, past and present, Dr. Stefan Duensing, Dr. Laura Niedernhofer, Dr. Saleem Kahn, Dr. John Woolford, Dr. Rick Wood, and Dr. Susan Gilbert for overseeing my graduate research, for all of their guidance and valuable advice, and their encouragement over the last six years. It was greatly appreciated.

I would also like to take the time to thank all the past and present members of the Saunders lab that I met during my time here. The one thing about the Saunders Lab is that we are like a big family. Although we split and went our separate ways, we keep in touch and when we

do get to see each other, it is like we haven't missed a day together. They are all wonderful people. I will start by thanking past members Dr. Ceyda Acilian, who is a wonderful person, friend and scientist and I appreciate your friendship. Dr. Qian Wu, one of my dearest friends. I appreciate all of her helpful advice on life, inside and outside of lab. Dr. Fengfeng Xu, my best friend and my forever sister. Not only a wonderful person on the outside, but she has a heart of gold on the inside. Jennifer Glasser, at one time an undergraduate in the lab. I appreciate her help on my stress granule project and for always keeping the lab up and running. Finally, I would like to thank Ruta Sahasrabudhe. Thank you for all the advice you have given me and your friendship means so much.

I would like to thank the Biological Sciences Department for being a supportive working environment and Cathy Barr, Crystal Petrone, and Pat Dean, for keeping this department running and for all of their heart-warming conversations, encouragement, and friendship over the last few years. I also want to thank the School of Medicine, specifically Cindy Duffy and Dr. Horn for their help and funding during the difficult times. I appreciate all of you.

I express my sincerest gratitude and appreciation to our collaborators, Dr. John Woolford and Jelena Jakovljevic. I enjoyed all of our scientific and nonscientific discussions and valuable comments and feedback you have given to me. I am forever grateful to have such wonderful collaborators as you.

Lastly, I dedicate my thesis work to my beloved family. They are truly amazing. I have the most wonderful and loving parents and brother in the whole entire world. They have given me so much love, support and encouragement during my life, but especially these last six years; not to mention how hard they worked to allow me to fulfill my dreams of becoming a research scientist, undeniably they are the reason I am where I am today. The opportunities they allowed me to pursue and the sacrifices they made helped shape me into the person I am today. The determination that they instilled in me allowed me to push on to achieve my PhD and I am not sure what I would have done

without them. My doctoral research belongs to them as much as it belongs to me. Personally, I thank my mom for always being my best friend and for being there for me on the good and the bad days, always offering her love and her support and helping me split my cells even if she never touched a pipette in her entire life. I thank my dad for always encouraging me and getting me to enter my first science fair and teaching me how to conduct science. I always appreciate him stepping outside the box to help me to try and figure out why my experiments stopped working and what I can do to get it working. I also thank him for always giving me a different perspective and analysis of my data. He may not have gone to school or worked as a scientist, but he is a scientist at heart. All of your opinions and advice was/is extremely helpful. I thank my brother for helping me brush up on all my basic biology ☺ year after year in college and for being a wonderful and thoughtful brother. My brother and I are complete opposites, I was the smart one and he was the athletic one, but we both ended up succeeding in our career choices and we have our parents to thank for that. I want to thank my grandparents, the Chromeys and the Pepes…they were not able to see me finish my graduate work or defend my thesis, but I know they are always watching over me. My grandpa Chromey (a high school biology teacher) did get to see me begin my graduate work and I am sad he did not get to see me finish, but I appreciated all of his helpful discussions and his scientific questions during the first years. I miss all of you deeply!!! I want to thank Sparkle for keeping me on my toes and being an awesome roommate and never being afraid to tell me when I was ignoring her. And finally, I would love to thank my boyfriend Dr. Jason Thomas for all of his encouragement, scientific discussions and support during the last 6 years. He has always been there for me with helpful advice on the good and the bad days. I thank him for sticking by me on this journey and I look forward to spending the rest of our lives together. I love you ALL ☺

Kid nucleolar localization

1.0 INTRODUCTION

Mitotic microtubules motors have previously thought to only function in mitosis (Burris, Jones et al.) (Lad, Luo et al. 2008), however recently I have identified an interphase function for a select group of motors in protein synthesis. The outline of this thesis is as follows. First, the introductory Chapter 1 will provide the reader with detailed background information necessary to place our research findings in their proper context. In Chapter 2, our finding regarding the dynamic interphase nucleolar localization of three mitotic motors Kid, Eg5 and MKLP1 will be presented. Furthermore, the mechanism of nucleolar retention for Kid will be discussed. Chapter 3 delves further into the findings of Chapter 2 by examining (patho)physiological conditions which induce Kid to shuttle from the nucleolus to the nucleus. Chapter 3 concludes with hypothesizing the interphase function of Kid is to facilitate ribosome biogenesis. In Chapter 4, we eagerly present that the three motors that localize to the nucleolus during interphase also associate with mature ribosomal subunits. This Chapter focuses on the role of Eg5 and its ability to aid efficient translation by ensuring the processivity of the translating ribosome. In Chapter 5, we further extend our novel findings from Chapter 4 to examine the role of Kid and Eg5 in stress granule formation, coalescence, and dissolution. From this, Chapter 5 will demonstrate that both Kid and Eg5 participate in stress granule formation and that Eg5 participates in stress granule coalescence and dissolution. Finally, Chapter 6 examines some preliminary, but very exciting data examining the role of Kid in focal adhesion assembly. Specifically, we will provide data to

support the hypothesis that Kid functions to transport mRNAs for site-specific translation and in doing so serves as a translational repressor. The results are the collimation of a 6 year labor-of-love which has spanned many diverse fields, but is ultimately unified by a central theme: at least some mitotic motors have previously uncharacterized interphase functions.

1.1 PROTEIN TRANSLATION

The translation of proteins is an essential process. As many readers may be generally familiar with ribosome biogenesis and maturation, and the steps of protein translation (initiation, elongation, and termination), it may be advisable for such readers to skip section 1.1. This section contains material that is intended to provide a background for readers who may be less familiar with the aspects of protein translation.

Eukaryotic translation consists of a series of orchestrated events that produce large biological macromolecules that make up 44% of the human body's dry weight (Davidson S.D. 1973). Proteins are the workhorse of the cell, having numerous roles in structure, transport, catalysis, and regulation, amongst others. Much of the cells energy and resources are devoted to translation and the synthesis of components necessary to carry out translation such as the making of mRNAs, ribosomes (both rRNA and ribosomal protein components), tRNA's, enzymes, and proteins. The energetic commitment to translation can be seen all the way down to *Saccharomyces cerevisiae*, which when rapidly growing contain more than 200,000 ribosomes produced at ~2000 ribosome/min in the cytoplasm, occupying as much as 30-40% of the cytoplasm (Warner 1999).

1.1.1 Ribosome Biogenesis

Ribosome biogenesis begins in the nucleolus where ribosomal DNA (rDNA) is transcribed into rRNA, which is then packaged with associated proteins into pre-ribosomal subunits (Raska, Koberna et al. 2004; Olson and Dundr 2005). rDNA genes are compiled in tandem repeats within the fibrillar center of the nucleolus, also known as nucleolar organizing regions (NOR's) and consist of five different chromosomes, 13, 14, 15, 21, and 22 (Raska, Koberna et al. 2004; Olson and Dundr 2005). Ribosomal biogenesis is a linear process of moving ribosomes, where rDNA are transcribed into ~7000 nucleotide long pre-rRNAs, by RNA polymerase I (RNA pol I) occurring on the border of the fibrillar center and the dense fibrillar component (Raska, Koberna et al. 2004). Nonribosomal proteins and small nucleolar proteins (snoRNAs) associate with this nascent transcript during this process before the 5S rRNA is added. Next, the rRNA transcript is processed resulting in the 18S, 5.8S, and 28S rRNAs. These rRNAs are processed further to form the pre-40S and pre-60S complexes, while ribosomal proteins are added during the assembly process. These pre-ribosomes, with ribosomal proteins and nonribosomal proteins attached, are transported out of the granular component, through the nucleus and the nuclear pores, and into the cytoplasm (Olson and Dundr 2005; Zemp and Kutay 2007). In the cytoplasm it undergoes the maturation steps and specific splicing events, ultimately producing the mature ribosome, which then functions to translate mRNA into proteins.

1.1.2 Steps of Translation

For translation to occur, two ribosomal subunits, a small 40S subunit and a large 60S subunit must associate together along the mRNA to form the 80S ribosomal complex. When more than

two 80S complexes form on a given mRNA, the resulting complex is called a polysome or a translating complex. Each of these ribosomal subunits is made up of a distinct subset of RNAs and proteins; the small 40S subunits consists of a 18S RNA and ~33 proteins, whereas the large 60S subunit consists of three RNAs (5S, a 28S, and a 5.8S) and ~49 proteins in humans. The small 40S ribosomal subunit contains three different sites, the A-site, the P-site and the E-site, which will allow binding of different translational components during the synthesis of a protein.

The process of translation occurs in three different stages, the initiation phase, elongation phase, and the termination phase. Each phase is described below.

1.1.2.1 Translation Initiation: Cap-dependent

There are two types of translation initiation, cap-dependent, which will be discussed here, and cap-independent which will be discussed later.

Translation initiation is a highly orchestrated series of events. Initiation is the first step of translation and ultimately leads to the assembly of the 80S ribosome on the initiation site of mRNA. Cap-dependent translation initiation requires the 40S and 60S ribosomal subunits and at least 12 well-characterized initiation factors (eIFs) to aid in the process (Hinnebusch 2006). Phosphorylation of these initiation factors not only controls the rate of ribosomes binding to an mRNA, but it is also a key factor in affecting and regulating translation (Pierrat, Mikitova et al. 2007); these phosphorylation events are highly context-dependent as such events can either inhibit or facilitate translation (Kozak 1992; Gray and Wickens 1998).

Translation initiation begins when a ternary complex consisting of eIF2, GTP, and Met-$tRNA_i^{MET}$ (initiator tRNA) is recruited to the mRNA. The 43S pre-initiation complex, consisting of the 40S subunit and multiple initiation factors, is able to “scan” the mRNA in the 3’ direction

disrupting any mRNA secondary structure until it reaches the first start codon, AUG, at which time the pre-bound initiator tRNA basepairs with the first AUG.

1.1.2.2 Elongation

The elongation phase of translation consists of the addition of amino acids to the elongating polypeptide chain intended for the message that is being translated. The process of elongation is a time consuming process; as many as 20 different charged tRNA's can be tested on each codon prior to finding the correct match.

Initiation ends with the initiator tRNA in the P-site of the ribosome and the A-site awaiting the correct aminoacyl-tRNA, pertaining to the next codon on the mRNA, to enter and bind. The elongation phase is completed by a series of steps that are continuously repeated until the mRNA stop codon is reached. The steps involved are, binding of the correct aminoacyl-tRNA into the A-site of the ribosome, formation of the peptide bond, and translocation of the tRNA from either the A-site to the P-site or the P-site to the E-site in preparation for the next codon to be translated. Various elongation factors are used to complete these steps mentioned, including eEF-1, eEF-2, and most recently eIF5A (Saini, Eyler et al. 2009); each of these proteins requiring ATP and GTP to carry out their functions. In fact it is worth noting that almost all of the energy used during protein synthesis is exploited during the elongation step, as the addition of the new amino acid to the chain and the translocation step of the peptide utilize at least 7 ATPs/GTPs.

1.1.2.3 Termination

Translation elongation continues until one of the stop codons appears in the ribosome A-site, causing release of release factor proteins (RF) and terminating translation. To be accurate, stop codons are not read by a tRNA, rather they are recognized by RF proteins. There are two classes of RF proteins, the first class function in recognizing the stop codon (eRF1), whereas the second class of RF proteins functions as a GTPase (eRF2). The first stage of termination occurs when the eRF1 protein recognizes the stop codon. When eRF1 binds to the ribosome with the stop codon in the A-site, hydrolysis is induced at the peptidyl-tRNA bound to the completed protein in the P-site, allowing for immediate dissociation of the completed protein from the ribosome. The function of the second RF protein, eRF3, is to remove eRF1 from the ribosome after release of the completed polypeptide chain, but its exact and detailed function in eukaryotes termination remains obscure. In other systems, such as the eubacteria, a third class of RF factors have been found and aid in ribosome recycling, but to date no eukaryotic homolog has been found (Pavlov, Freistroffer et al. 1997; Pisarev, Skabkin et al. 2010).

1.1.2.4 Processivity

There exists a debate as to whether a translating ribosome exhibits processivity; processivity being defined as the distance a ribosome can travel before dropping-off its transcript. Processivity is a property used to describe attributes of DNA and RNA polymerases. One such example is the RNA polymerase in bacteria that has demonstrated to randomly release from the

DNA (von Hippel and Yager 1991). The debate centers on whether a ribosome exhibits any probability of dropping-off while actively translating. Arguing against processivity of a ribosome are a collection of articles which study the kinetics of translation on a specific transcript (Bretscher 1968; Bergmann and Lodish 1979). These studies found no evidence of ribosomal drop-off based on modeling studies derived from fitting experimental kinetic data. However inside a cell the picture of translation is far more complex because the ribosome is not asked to translate only one given transcript, but rather the entire transcriptome. Recent evidence examining translation in its native environment and has uncovered a propensity of a ribosome to exhibit drop-off while translating including treatment with elongation inhibitors (Chan, Khan et al. 2004), during conditions that decrease amino acid levels leading to slowed elongation (Caplan and Menninger 1979), or even by microRNAs which were shown to cause ribosome drop-off as a way of controlling protein synthesis (Petersen, Bordeleau et al. 2006). Each of these examples will be discussed further in Chapter 4.

If a ribosome exhibited any degree of drop-off during protein synthesis, one could envision the cell incorporating fail-safe mechanisms to inhibit the ribosome from falling-off the mRNA prematurely. As you will see, one such fail-safe mechanism is through association with mitotic motor Eg5 and the microtubules. As I will demonstrate, we believe the ribosome is anchored to microtubules via Eg5 and it is this arrangement that aids the ribosome in continued processivity during translation.

A central reason for this debate has been the lack of experiments, and thus methods, designed or intended to test processivity. In Chapter 4, we will present a simple, yet robust assay to measure processivity.

1.2 MECHANISMS OF TRANSLATIONAL CONTROL

1.2.1 mRNA

The central dogma of biology states that mRNA is transcribed from DNA and possesses the information required to make a protein. The life cycle of an mRNA begins with transcription and addition of a 5'-cap (RNA 7-methylguanosine m^7G cap) in the nucleus which is then edited and transported to the cytoplasm where it is spliced in the nucleus, translated, made into a protein, and eventually degraded. mRNA can form secondary and tertiary structures, based on its sequence, allowing for regulation of the mRNA for translation, silencing, etc. The extent of secondary and tertiary structure of the 5'-UTR is believed to confer an additional level of translational control as the extent of secondary structure can influence the efficiency of the initiation phase of translation (Hershey 1991; Kozak 1992; Pierrat, Mikitova et al. 2007). The 3'-UTR is thought to have sequences encoded in it that direct the mRNA for cytoplasmic localization and site-specific translation (Vuppalanchi, Coleman et al. ; Shestakova, Singer et al. 2001), as well as control the half-life of the mRNA (Ross 1996; Newbury 2006). The poly-A tail, at the end of the mRNA, aids in transport of the mRNA from the nucleus to the cytoplasm and protects the mRNA from degradation. Though, it should be noted, that not all mRNA's use their 5'-cap structure to begin translation, rather it has been shown that about 85 cellular mRNAs, as of 2006, are found to be regulated by internal ribosomal entry sequences (IRES) (Dani, Blanchard et al. 1984; Holcik 2004).

Every mRNA has a different half-life that can range from minutes to days (Aviv, Voloch et al. 1976; Dani, Blanchard et al. 1984). This stability of an mRNA determines how many proteins can be produced from the same mRNA. The cell controls the stability of the mRNA so

that it can rapidly change the translation status of a protein at any given time (Hershey 1991). There is a balance between the processes of translation and mRNA decay, and this balance is reflected in the size of processing bodies (P-bodies) (Balagopal and Parker 2009). P-bodies are structures where mRNA can be sequestered, or degraded, and consist of many different enzymes involved in mRNA turnover. Functions of P-bodies include: removing the 5' cap, degradation and/or storage of the mRNA, and translational repression.

1.2.1.1 Translation Initiation: Cap-independent

As mentioned previously, there are two types of translation initiation, the traditional cap-dependent and the untraditional cap-independent. Cap-dependent was discussed in section 1.1.2.1. Cap-independent translation initiation occurs through the use of an internal ribosome entry sites (IRES), where the 5'-UTR region of these mRNAs are shown to recruit ribosome binding as an alternate mechanism of initiating translation. Many viral mRNAs and some cellular mRNAs that encode proteins involved in apoptosis, growth control and differentiation, have conserved 5'-UTRs that are several hundred bases long (Holcik 2004; Baird, Turcotte et al. 2006); these regions appear to have secondary and tertiary structures, making it difficult for initiation factors to bind and to allow scanning by the 43S pre-initiation complex, therefore yielding poorly translated mRNAs.

Viruses contain most of the necessary components to amplify their genomes, however when it comes to translation, viruses are entirely dependent on the infected cell's native translation machinery to translate viral mRNAs. Thus, viruses use various techniques to co-opt the host cell's translational machinery for translation of their own mRNAs, while inhibiting translation of the host cell's mRNAs by cleavage and/or modifications of translation initiation

factors or phosphorylation of elongation factors. Poliovirus, a well studied cytoplasmic virus belonging to the Picornaviridae family, preferentially inhibits translation of the host mRNAs by cleavage and modifications of several translation initiation factors, while allowing its own viral mRNA to be translated. Analysis into how poliovirus was able to translate its protein while inhibiting its cell's host mRNA, revealed a 750 nucleotide 5'-UTR region containing various AUG codons and extensive secondary and tertiary structures (Lenk and Penman 1979). This lead to the discovery that viral mRNA does not contain a 5'-cap structure, rather they contain a 5'pU (polyuridine) sequence. This analysis suggested that viral mRNA must be translated in a cap-independent manner, independent of the cleaved and modified initiation factors. Confirmation that viruses use cap-independent translation came from studies utilizing bicistronic assays (Nie and Htun 2006), where an mRNA using cap-dependent translation is placed upstream of an mRNA thought to use cap-independent translation; if the viral mRNA is translated it would be in a cap-independent manner. Further studies inserting the 5'-UTRs of the poliovirus, as well as other viruses, into bicistronic plasmids demonstrated that the viral mRNA is able to be translated independent of the upstream sequence suggesting that viral mRNA translation occurs in a cap-independent mechanism, whereby the 5'-UTR can recruit the 80S ribosome binding independent of initiation factors and 5'-cap. Various RNA and DNA viruses have been found to use IRES elements to initiate translation, but the necessity for various host translation initiation factors differ from virus to virus.

1.2.2 Translational control by initiation factor eIF2

Translational control in protein synthesis is crucial to regulate gene expression. One of the most well-studied and highly controlled translational control mechanisms in eukaryotic cells is the

recruitment of translation initiation factor eIF2 to the mRNA (Sarre 1989; Perry and Meyuhas 1990; Hershey 1991; Proud 2002). This protein contains three different subunits, and each subunit has a specific function in translation ranging from formation of the initiator ternary complex, thereby beginning translation, to phosphorylation of its subunit and inhibition of translation.

1.2.2.1 Phosphorylation of eIF2α

The phosphorylation status of eIF2 α is a key regulatory event and is activated in response to various stresses and direct stimuli. The level of eIF2 α phosphorylation can lead to inhibition of protein synthesis. Phosphorylation of eIF2 α is a dynamic and regulated system, as various kinases and phosphatases for the eIF2 α system exist to control it.

1.2.3 Stress Granules

One such regulatory event that occurs after phosphorylation of eIF2 α is stress granule formation. Stress granules are dynamic cytoplasmic foci that rapidly aggregate in response to cellular stress and translational inhibition from heat shock, oxidative stress, viral infection, and UV irradiation (Kedersha and Anderson 2002; Kedersha and Anderson 2007). Stress granules are believed to be sites of mRNA triage, where mRNAs are stored, degraded, or inhibited from translation during stress. The ability to form stress granules in response to a given stimuli allows the cell to divert its resources to responding appropriately to the stimuli, while allowing the rapid resumption of translation and thus normal physiological process. These stress granules primarily

form in response to eIF2α phosphorylation (Anderson and Kedersha 2002). Stress granules consist of stalled 48S complexes (from disassembling polysomes), mRNA bound to initiation factors (eIF4E, eIF3, eIF4A, and eIF4G), small ribosomal subunits, RNA binding proteins, transcription factors, RNA helicases, nucleases, kinases, and other signaling regulatory proteins. More recently, stress granules have been shown to contain microRNAs, mRNA-editing proteins, enzymes (Anderson and Kedersha 2009), and as I will show in Chapter 5, mitotic motors. Most recently, it has been found that kinesin and dynein microtubule motor complexes participate in stress granule dynamics (Loschi, Leishman et al. 2009). The dynein-dynactin-binding protein Bicaudal-D1 (BICD1) was demonstrated to be required for stress granule assembly, while kinesin 1 was shown to be required for stress granule disassembly (Loschi, Leishman et al. 2009). The use for motor-based assembly and disassembly is intriguing, but the identification of motors functioning in stress granule assembly or disassembly is. Chapter 5 addresses this question by providing two new motors involved in stress granule dynamics.

1.2.4 Translation inhibition during mitosis

It is well known that translation is inhibited during mitosis when cell division occurs, however, the stage at which protein synthesis is inhibited (i.e., initiation, elongation, termination) continues to be investigated. In 1970, Fan and Penman published that the inhibition of translation occurred at the initiation stage (Fan and Penman 1970); however, most recently, Sivan, et al. demonstrated that translation inhibition in mitosis leads to a build-up of polysomes along the actively translating mRNA during mitosis, leading the authors to hypothesize that those transcripts arrested in mitosis are arrested in the elongation stage (Sivan, Kedersha et al. 2007). This satisfyingly explains how the cell is able to rapidly resume translation after the completion

of mitosis and save energy in the process. This inhibition of elongation during mitosis is shown to occur through phosphorylation of eEF2. This paper does not rule out that translation is not inhibited at the initiation stage, rather it provides evidence that global translation inhibition does not occur exclusively at the initiation stage during cell division.

As I will demonstrate in Chapter 4, the mitotic motor protein Eg5 functions not only during mitosis in bipolar spindle separation, but also during translation elongation in interphase. It is quite interesting to speculate that the cell has developed fail-proof quality control mechanisms to control protein synthesis at the elongation phase through the use of mitotic motors such as Eg5. This would suggest that during interphase Eg5 functions in translation, yet at the onset of mitosis when it becomes phosphorylated, Eg5's role as well as translation is inhibited so that Eg5 can complete its mitotic function.

1.2.5 Protein synthesis and cancer

Protein translation is a complex and extremely multifaceted process regulating molecular processes that control ribosome biogenesis and mRNA translation; one can foresee that deregulation of any or all of these processes or signaling pathways may lead to a physiologically dysfunctional cell. Regulation of protein synthesis could be predicted to have a great impact on cancer development and progression, as the pathways that are controlled on a translation level include mitogenic signal stimulation, cell growth and proliferation pathways, as well as responses to nutritional deprivation or cellular stresses. Protein synthesis has recently been found to be aberrantly regulated in cancer cells (Cuesta, Gupta et al. 2009), as cancer cells can easily exploit misregulation of translation at the level of mRNA and protein expression (Watkins and Norbury 2002). Various dysregulated components in cancer cells involving the translation

machinery exist including ribosome synthesis, ribosomal proteins, translational factors, tRNAs, regulatory proteins, and expression or translation of various mRNAs (Le Quesne, Spriggs et al. ; Brewer 2001; Watkins and Norbury 2002; Perkins and Barber 2004; Belin, Beghin et al. 2009). The effects of such abnormal regulation results in overexpression of proteins, up-regulation of protein synthesis, and selective translation of checkpoint proteins that are typically used to inhibit cells from dividing or proliferating if defects are found (Le Quesne, Spriggs et al. ; Watkins and Norbury 2002; Perkins and Barber 2004; Rice 2009).

1.3 PROTEIN SYNTHESIS IN VIVO

Most of the discussion of translation has been done so in the context of just the translational machinery. In fact, as discussed thus far, the sequence and events of translation can be reconstituted with in vitro purified enzymes. However, protein translation is significantly more complex in vivo. This section highlights the complex regulation of protein translation carried out by the cell in vivo.

1.3.1 Interactions during protein synthesis

Studies have demonstrated that polysomes, mRNA, aminoacyl-tRNA synthetases, initiation factors and elongation factors all associate with the cytoskeleton. Compartmentalization of mRNAs with the cytoskeleton has also been shown to occur, while the three major filament structures of the cytoskeleton have been demonstrated to be involved in mRNA targeting and transport.

1.3.2 Translation and the cytoskeleton

The cytoskeleton of eukaryotic cells during interphase has a high degree of organization which is required for its cellular functions. The cytoskeleton consists of three different filament structures: microtubules, intermediate filaments, and actin filaments (microfilaments), which function in cell movement, cell shape, organelle positioning, vesicle and RNA transport, as well as centrosome and chromosome segregation. As I will discuss, there exists a relationship between the cytoskeleton filaments, associated microtubule motors and translational components, but the exact motors involved and their function in translation is incompletely understood. Chapter 4 offers penetrating insight into this multifaceted relationship.

Although it has been previously thought that mRNAs are transported from the nucleus to the cytoplasm and become randomly distributed, recent evidence exists that disputes this conclusion. It is now believed that mRNAs are tightly associated with the cytoskeleton, although the fraction of associated mRNA or polysome complexes differs from 15-75%, depending on the cell type and experimental approach used (Jansen 1999) (Singer, Langevin et al. 1989; Taneja, Lifshitz et al. 1992; Hesketh 1996; Hovland, Hesketh et al. 1996).

The first line of evidence stems from the observation that the cytoskeleton fraction from cell lysates was found to be enriched in polysomes, translation initiation factors, elongation factors, and cellular mRNA (Jansen 1999). Importantly, these translational components remained associated with the cytoskeleton in the presence of high ionic conditions, implying strong physical binding rather than a weak association of RNA to the cytoskeleton.

The second line of evidence is derived from microscopy studies where it was observed that mRNA and polysomes are found quite close to cytoskeleton structures (Jansen 1999). From analysis of immunofluorescence experiments, ribosomes, initiation and elongation factors

demonstrated an intracellular distribution that resembles that of the microtubule and actin cytoskeleton.

Protein translation efficiency benefits from the close and spatial proximity for the association of all factors involved in translation, as actively translated mRNA is often found in cytoskeletal-associated polysomes. For examples, in sea urchin embryos, upon egg activation, polysomes were found to become attached to the cytoskeleton, at the same time when translation of messages was induced (Moon, Nicosia et al. 1983). Also, during viral infection host cell translation is shut down, however newly synthesized viral-RNA containing polysomes are found to be cytoskeletally-associated (Lenk and Penman 1979; van Venrooij, Sillekens et al. 1981; Bonneau, Darveau et al. 1985). Despite these provocative findings, little is known about the nature of the association between translational components and cytoskeletal elements. Without knowing which proteins mediate such interactions it is impossible to study the physiological consequences of the association between translational components and cytoskeletal elements. Chapter 2 identifies candidate proteins that mediate such interactions and Chapters 4 and 6 directly address the physiological functions of such interactions.

1.3.3 Microtubules and translation

Microtubules are long hollow cylindrical filamentous structures that carry out a number of intracellular functions including capture of chromosomes and transport during mitosis, provide for spatial organization and remodeling of the cytoskeleton, facilitate recruitment of organelle and membranous structures through their interaction with motors. The walls of the microtubule are composed of 13 protofilaments organized in alternating alpha and beta dimers in long chains. Microtubules are typically oriented so that their dynamic plus-ends are pointed towards the cell

periphery, and their minus-ends are anchored in the microtubule organizing center (MTOC). These microtubules serve as roadways for the microtubule motors to carry various cargoes.

There exists an interaction between microtubules and translational components. Since the late 1980's, microtubules (Suprenant 1993; Jansen 1999) have been implicated in mRNA targeting and cellular transport. Microtubule organization and distribution, dynamic instability, and microtubule motors all provide a highly-organized network for anchoring or distributing mRNA within cells; dynamic instability as defined as the constant growth and shrinkage at the microtubule ends.

1.3.3.1 mRNA localization with microtubules

Recent evidence within the last 20 years has demonstrated that specific mRNAs are localized and transported in a microtubule-dependent manner in oocytes and embryos of Xenopus (Yisraeli, Sokol et al. 1990), Drosophila (Pokrywka and Stephenson 1991), Zebrafish (Palacios and St Johnston 2001), and mammalian cells (Finch, Revankar et al. 1993; Hovland, Hesketh et al. 1996) . Vg1 RNA in Xenopus (Yisraeli, Sokol et al. 1990), cyclin B and bicoid mRNA in Drosophila (Pokrywka and Stephenson 1991), are just a few of the known mRNAs to be transported along microtubules (Jansen 1999). Several factors may determine which mRNAs are localized with the cytoskeleton such as specific localization signals known as the 'zip codes' found in the 3'-UTR region of mRNAs identified in Vg1, bicoid, and nanos transcripts (Kislauskis, Li et al. 1993). Additionally, interactions of other translational components, proteins, or even ribosomes with the mRNA may mediate the mRNA localization with the cytoskeleton (Hovland, Hesketh et al. 1996).

1.3.3.2 Microtubules and ribosomes

There are several examples demonstrating interactions between ribosomes and microtubules. In mammalian cells, ribosomes have been shown to be clustered around microtubules and attached to the microtubule walls by short filaments (Suprenant, Tempero et al. 1989; Hamill, Davis et al. 1994). In ovaries of the hemipteran insects, it has been shown that ribosomes move slowly at a speed of 20 μm/h through nutritive tubes from the anterior ovarioles to the developing oocyte toward the minus-ends of microtubules (Stebbings 1986). In the mitotic spindles, ribosome-like particles were shown to be linked to microtubules by filamentous arms (Turner and McIntosh 1977; Salmon 1982; Suprenant, Tempero et al. 1989). In sea urchin embryos, it has been shown that ribosomes associate with microtubules through a stalk-like structure, and association may be regulated, as polysomes, but not monosomes were shown to interact with microtubules (Suprenant and Rebhun 1983; Suprenant, Tempero et al. 1989; Suprenant 1993). Finally, in ovaries of Pyrrhocoris, newly synthesized RNA component has been found to move at both, slow (30 μm/h) and fast (200 μm/h) speeds, arguing against the bulk flow of ribosomes and favoring a microtubule based movement (Macgregor and Stebbings 1970).

1.3.3.3 Mitotic apparatus and ribosomes/RNA

The mitotic apparatus has been demonstrated to contain bound RNA and ribosomes in sea urchin embryos, suggesting that even in mitosis, an organization of microtubules and RNA/ribosomes exist (Mazia and Dan 1952; Suprenant 1993). In the presence and absence of detergent-extracted spindles, ribosomes have been shown to localize along microtubules in the centrosome complex

and on vesicle surfaces (Salmon 1982). Using quick-freeze, deep-etch electron microscopy, ribosomal particles were found to be tightly attached on the mitotic apparatus to the microtubule by fine filamentous arms, and can only be released in the presence of high salt (Hirokawa, Takemura et al. 1985).

1.3.3.4 RNA transport

Microtubules have also been demonstrated to be involved in RNA transport through the use of microtubule motors. mRNA transport is facilitated by the packaging of mRNAs into large ribonucleoprotein particles or granules. The motors that are used to transport the RNA will be discussed in section 1.42.

1.3.4 Microtubules and translational regulation

Not only do microtubules play a role in mRNA localization and transport, but there is significant evidence suggesting roles for microtubules in formation of cytoplasmic translation complexes. mRNA transport from the nucleus to the cytoplasm was shown to be inhibited by colchicine treatment in rat liver nuclei (Schumm and Webb 1982). Microtubules are also needed for the formation of membrane-bound polysomes in hepatectomized rats, as colchicine treatment caused dissociation of membrane-associated polysomes (Walker and Whitfield 1985). It was further determined that the mRNAs were released and degraded from the ribosomes, leaving the 80S ribosome intact and bound to the membrane (Walker and Whitfield 1985). Furthermore, loss of microtubules in the regenerating liver prevented ribosomal subunits from dissociating and reforming the initiation complexes.

1.3.5 Site-specific translation

mRNA localization is relevant in highly polarized cells like neurons, where the site of transcription can be distances away from the final location of the protein. Therefore, localized protein translation aids the problem of transporting proteins over long distances, which can sometimes take longer than the half-life of a protein (Campenot and Eng 2000). In neurons, site-specific protein translation has been shown to occur in dendrites, prominent compartments which account for most of the postsynaptic sites in the nervous system (Eberwine, Miyashiro et al. 2001; Tang and Schuman 2002; Wu, Zeng et al. 2007). Neurons are polarized cells where mRNAs move and are targeted to allow localized translation to take place. This polarized localization is essential for proper functioning of the neuron.

Using electron microscopy, a number of components of translation machinery have been found to localize near one another in the neuron (Martin ; Job and Eberwine 2001). Ribosomes have been found throughout the dendritic shafts, polysomes have been found in the necks of dendritic spines and beneath the spine synapses, endoplasmic reticulum/Nissl bodies and spine apparatus/Golgi apparatus all have been found in distal regions of the dendrites (Job and Eberwine 2001). Also, mRNAs have been shown to localize to the synaptic sites and to move in a microtubule-dependent manner (Roegiers 2003; Antar, Dictenberg et al. 2005). This active transport of mRNA and the presence of translational machinery in close proximity to one another indicate that dendrites can synthesize protein in a site-specific manner and independently of the main cell body.

1.4 MOLECULAR MOTORS

Molecular microtubule motors are proteins that transport intracellular cargoes within cells by moving along microtubules using ATP hydrolysis. They are referred to as motors because they convert chemical energy to mechanical energy, using the energy of ATP hydrolysis to carry cargo on microtubules. There are two different families of motor proteins, the kinesins and the dyneins. The kinesins typically carry cargo along the plus-end of the microtubule, whereas dyneins typically carry cargo along the minus-ends of microtubules. Microtubule motors can function in a variety of processes including cellular organization, organelle and vesicle transport, cell division, mRNA transport, and the motility of cilia and flagella. Intracellular transport by kinesins and dyneins has been shown to be essential and loss of these proteins can lead to deleterious effects.

1.4.1 Kinesins

There are approximately 45 different kinesins in humans (Ohsugi, Tokai-Nishizumi et al. 2003). Each of these is defined as containing a conserved motor domain. The kinesins can be separated into three different groups based on the location of their motor domain, which can be found on the N-terminus, the C-terminus, or in the middle of the protein. Of the 45 kinesins, three have the motor domains on the C-terminus and three have the motor domain in the middle of the protein. N-terminal kinesins walk toward the plus-end of the microtubule, near the cell periphery, those that have C-terminal motor domains walk along the minus-end of the microtubule, near the nucleus, whereas those that contain their motor domain in the middle of the protein typically function in depolymerization of microtubules. The kinesin family has become so expansive in

recent years, that a specific classification system has evolved classifying the kinesins into families designated by their function in mitosis. There are now 14 different kinesin families representing, making it easier to distinguish between identified kinesins and aiding in the identification and classification of new kinesins (Lawrence, Dawe et al. 2004).

1.4.1.1 Substructure of kinesins

In general, the structure of kinesins and microtubule motors consist of a motor domain, a head connected to a neck linker, and a common stalk leading to the tail domain. Each of these regions has a dedicated function. The motor domain is responsible for binding to the microtubule and nucleotide hydrolysis. The head that is connected to the neck linker is responsible for the directionality of the motor and undergoes nucleotide-dependent conformational changes creating a powerstroke by docking and undocking to the nucleotide sites, whereas the tail domain binds to the cargo which is being transported.

1.4.2 Motors and mRNA transport

1.4.2.1 Kinesin

Kinesin motors have also been implicated in the localization of Vg1 mRNA to the vegetal pole of Xenopus oocytes (Betley, Heinrich et al. 2004; Yoon and Mowry 2004) . Kinesin 1 was found to co-immunoprecipitate with Staufen protein, which localizes to the vegetal pole with Vg1 mRNA. Furthermore, oskar mRNA is found to require kinesins to localize to the posterior end of

the oocyte (Palacios and St Johnston 2001). However, there is still an open question whether kinesin is directly or indirectly, responsible for these movements.

1.4.2.2 Dynein and mRNA transport

High resolution time-lapse movies have captured the bidirectional transport of mRNA, as transcripts were demonstrated to undergo frequent directional reversal. Dynein is thought to transport mRNAs to the anterior end, while kinesin is thought to transport them to the posterior end of the oocyte, in Drosophila (Duncan and Warrior 2002). In these experiments, inhibition of dynein led to strong inhibition of transport in both directions, as anticipated given that transport by kinesin and dynein requires strong coordinated movements of dynein with kinesin. However, it should be noted that recently in mouse brains it was found that dynein is capable of bidirectional movement suggesting that the bidirectional movement observed may only be due to transport by dynein (Ross, Wallace et al. 2006).

Dynein has been implicated in the transport of numerous mRNAs including K10, bicoid, and gurken, although no RNA binding domain has been found for the dynein. However, recently two RNA binding proteins and dynein binding partners have been implicated in this role, Bicaudal-D (BicD) and egalitarian (EGL) (Dienstbier and Li 2009). These proteins are found in the same complexes with dynein and have been shown to be required for dynein mRNA transport, as mutations in dynein light chain that inhibits its binding to EGL impair dynein mediated transport of the mRNAs to the oocyte.

1.4.3 Mitotic Motors

Mitotic microtubule motor proteins are important for the carefully organized sequence of events that underlie mitosis. Motors not only help to assemble the mitotic spindle and to accurately segregate sister chromatids, but they provide the mechanical forces needed to drive mitosis. The cellular tasks accomplished by motors is not the result of one individual motor; rather, a combinatorial effort from many different motors functioning concurrently which underlie the diversity of their functions (Sharp, Rogers et al. 2000). There are a variety of motors during mitosis that are shown to have redundant or even antagonistic functions, all working together to produce the mitotic spindle and to accurately divide the sister chromatids. Mitotic motors drive mitosis by completing four distinct functions relating to cell division: bipolar spindle formation, congression of chromosomes, chromosome segregation, and separation of spindle poles prior to cytokinesis. They complete these functions by using one of three mechanisms, sliding adjacent microtubules relative to other microtubules or other structures, transporting specific mitotic cargos along the microtubules, or by regulating microtubule dynamics, such as growth and shrinkage along the microtubule ends. Perturbation of the dynamic balance between motors during mitosis can lead to segregational defects during cell division. Lagging chromosomes during metaphase and anaphase, and multipolar spindle formation can be the result of motor defects.

There are two microtubule motors, Kid and Eg5, whose novel interphase functions will be the focus of the research efforts presented later. However, these motors have known functions during mitosis.

1.4.4 Kid

Kinesin-like DNA binding protein (Kid), also known as Kif22, is an N-terminal, plus-end directed, chromokinesin motor which belongs to the Kinesin-10 family of proteins (Tokai, Fujimoto-Nishiyama et al. 1996; Yajima, Edamatsu et al. 2003). Kid has multiple functions during mitosis including maintaining metaphase spindle length, producing polar ejection force, and pushing chromosome arms away from spindle poles (Funabiki and Murray 2000; Levesque and Compton 2001; Tokai-Nishizumi, Ohsugi et al. 2005). The known movement of chromosomes parallels the mRNA transport function for Kid we will propose in this document in Chapter 6.

1.4.4.1 Kid localization

Localization of Kid during mitosis is primarily found on chromosomes and spindles; Kid has been found to localize with condensing chromosomes during prophase, associates with chromosomes and spindles during metaphase and anaphase, and primarily associates with chromosomes entering daughter cells during telophase (Tokai, Fujimoto-Nishiyama et al. 1996). As with other proteins involved in spindle formation and chromosome segregation, the localization of Kid to chromosomes and spindles seems to be dependent on phosphorylation. Two residues have been shown to be phosphorylated, Ser427 and Thr463, by Cdc2/cyclin B, a key regulator of G2/M progression (Ohsugi, Tokai-Nishizumi et al. 2003). More notably, phosphorylation of Thr463 was demonstrated to be essential for localization of Kid with chromosomes, as the T463A mutation was discovered to localize only with spindles.

1.4.4.2 Kid Structure

Characterization of Kid has revealed an ATP-binding site, a motor domain, two phosphorylation sites, a DNA binding domain, two microtubule-binding sites, and a coiled-coil domain. Sequence analysis suggests that Kid contains three nuclear localization sites that may account for the diffuse nuclear localization observed in many cell lines. Kid suppression by siRNA leads to lagging chromosomes and a shortening of metaphase spindle length, consistent with Kid function as a chromokinesin motor, a motor which binds to chromosomes.

1.4.5 Eg5

Eg5, also known as Kif11, is an N-terminal, plus-end directed kinesin motor that belongs to the kinesin-5, BimC protein family currently consisting of BimC (Aspergillus nidulans), Eg5(Xenopus laevis), KLP61F (Drosophila melanogaster), cut7 (Schizosaccharomyces pombe), CIN8 and KIP1 (Saccharomyces cerevesiae) and HsEg5 (human) (Sawin, LeGuellec et al. 1992; Kashina, Rogers et al. 1997; Drummond and Hagan 1998). Eg5 typically functions during mitosis as a homotetrameric complex in spindle assembly and maintenance in all organisms mentioned above. Specifically Eg5 functions to slide adjacent microtubules apart, crosslink antiparallel microtubules, and slide microtubules toward the centrosomes aiding in poleward flux (Kapoor and Mitchison 2001). Eg5 typically localizes on the spindle poles during mitosis, as with other some mitotic motors; the localization of Eg5 to the spindles seems to be dependent on its phosphorylation status (Blangy, Lane et al. 1995). Eg5 is phosphorylated at Thr-927 by Cdc2; mutation of this residue to T927A blocked Eg5 from localizing to the spindle (Blangy, Lane et al. 1995; Sawin and Mitchison 1995).

1.4.5.1 Eg5 characterization

The overall architecture of Eg5 comprises an ATP-binding domain, motor domain, region of predicted alpha-helices, and a nonhelical tail domain (Sawin and Mitchison 1995). In the tail domain, the BimC family of proteins have a 40 residue region that is partially conserved in all family members, except CIN8 and KIP1 (Kashina, Rogers et al. 1997). Within this region, contains the phosphorylation site which controls the localization of Eg5 and other sequences that may be phosphorylated by a proline-directed kinase or ERK-family kinase.

1.4.5.2 Loss of Eg5 in cultured cells

Loss of Eg5, by immunodepletion of extracts led to a phenotype of monopolar spindles. In human cells, microinjection of Eg5 antibody induced 80% of the cells to arrest with a prometaphase-like chromosome arrangement but no spindle pole separation (Walczak, Mitchison et al. 1996; Goshima and Vale 2005). Furthermore, loss of Eg5 by siRNA, led to monopolar spindles with two only slightly separated centrosomes. Therefore, loss of Eg5 inhibits centrosome separation and formation of the bipolar mitotic spindle leading to incomplete spindle assembly (Blangy, Lane et al. 1995; Goshima and Vale 2005)

Eg5 is essential and deletion of KLP61F, the Eg5 homolog in Drosophila, and deletion of both yeast homologs, Cin8 and KIP1, cause lethality (Roof, Meluh et al. 1992). When the mouse *knsl1* gene on chromosome 18 was deleted, it resulted in pre-implantation embryonic lethality phenotype in the mice homozygous for the Eg5 deletion (Castillo and Justice 2007). However female and male mice heterozygous for Eg5 deletion (Eg5 +/-) did not appear any different from

control mice homozygous for Eg5. These results suggest that Eg5 is essential in early developmental stages and its loss cannot be compensated by any other kinesin motor in single copy.

1.4.5.3 Monastrol

The use of small molecule inhibitors has been instrumental in our understanding of various proteins and complex processes. This is particularly true for Eg5, as numerous classes of inhibitors have been developed. The first identified small molecules inhibitor, monastrol, was reported by the Mitchison lab (Mayer, Kapoor et al. 1999; Kapoor, Mayer et al. 2000). Monastrol exerts its inhibitory effects on Eg5 by binding to its motor domain preventing Eg5 from walking along microtubules and causing cellular arrest of cells in M phase with monopolar spindles. Monastrol does not compete with ATP binding to Eg5, rather Monastrol appears to inhibit microtubule-stimulated ADP release. According to the crystal structure of Eg5-monastrol complex, monastrol seems to bind a hydrophobic induced-fit pocket, a region that is not conserved in kinesins (Maliga and Mitchison 2006; Maliga, Xing et al. 2006).

Since the discovery of monastrol, several new Eg5 inhibitors have been discovered, some of which are in clinical trials. Most of the newly discovered Eg5 inhibitors, bind in the same hydrophobic pocket as monastrol (Lad, Luo et al. 2008). Ispinesib, an inhibitor in stage II clinical trials, has been quite promising for treatment of non-small cell lung, ovarian, and breast cancer that have failed using other treatments (Lad, Luo et al. 2008; Lee, Belanger et al. 2008). Ispinesib has been demonstrated to inhibit Eg5 using the same mechanism as monastrol.

1.4.5.4 Overexpression of Eg5

Eg5 overexpression has been shown to cause genomic instability and segregational defects (Castillo, Morse et al. 2007), as overexpression disrupts the delicate balance of forces generated to form and maintain the mitotic spindle. When Eg5 was overexpressed in mice, abnormal spindle assembly, genomic instability, and a wide range of tumors including hematopoietic, adenoma/adenomacarcinomas, ovarian, sarcomas, as well as others, was observed (Castillo, Morse et al. 2007).

1.5 MITOTIC MOTORS MAY HAVE INTERPHASE FUNCTIONS

Over the last 20 years the primary focus of Eg5 and Kid motor function has been centered on their respective roles during mitosis, premised with the notion that mitotic motors only function in mitosis. This is a key rationale for choosing Eg5 as a target for inhibition of cancer.

However the uniqueness of mitotic motors as cancer targets is being challenged as recent examination of their functions during interphase is revealing functions outside of mitosis not only in postmitotic neurons, but also in dividing cells. Such interphase functions could render these once anti-cancer treatments problematic, as their inhibition may also cause uncharacteristic problems to healthy interphasic cells.

2.0 CHAPTER II : MITOTIC MICROTUBULE MOTOR KID LOCALIZES TO THE NUCLEOLUS DURING INTERPHASE IN A GTP-DEPENDENT MANNER

2.1 INTRODUCTION

The nucleolus constitutes the sole site of the early steps in ribosome biogenesis (Hernandez-Verdun 2006; Cmarko, Smigova et al. 2008). It is a nonmembranous, suborganelle of the nucleus that is divided into three different compartments. The nucleolus is subdivided into the fibrillar center, where the rDNA genes are located, the dense fibrillar component, where rDNA transcription takes place, and the granular component, where the pre-ribosome is packaged and moves through prior to being transported out of the nucleus and through the nuclear pores (Scheer and Hock 1999).

Up until the 1990s, it was thought that the nucleolus only had one function, and thus only contained proteins that had a role in ribosome biogenesis. However, the true identity of the nucleolus as a multitasking organelle with diverse cellular functions was unmasked by proteomic studies which revealed numerous proteins found in the nucleolus without any known function in ribosome biogenesis (Andersen, Lam et al. 2005; Olson and Dundr 2005). More than 700 proteins were identified, however the majority of these newly identified proteins do not maintain a permanent residence in the nucleolus; rather they are temporarily stored in the nucleolus until after they complete their function. The motors I will describe here, Kid, Eg5, and MKLP1, were

not found in this proteomic screen. This may be because they used cancer cells to characterize the nucleolus-localizing proteins.

In addition to the expansion of proteins known to localize to the nucleolus, the functional role of the nucleolus has similarly expanded. The nucleolus has been implicated in a wide array of processes such as regulation of tumor suppressors and oncogenes, cell cycle regulation, signal recognition particle (SRP) assembly, modification of small RNAs, control of aging, response to cellular stress and telomerase function (Olson, Dundr et al. 2000). This diversity of the nucleolus is relevant for our observations of Chapter 2, investigating the role of mitotic motors in the nucleolus.

2.2 RESULTS

2.2.1 Mitotic microtubule motors Kid, Eg5, and MKLP1 localized to the nucleolus during interphase

As previously published data from our lab demonstrated that the mitotic motor dynein was found mislocalized in cancer cells in comparison to normal cells, we pursued the investigation of the mitotic localization of other motors in noncancer versus cancer cells. Interestingly, we uncovered a previously undescribed localization of some of these motors during interphase. The interphase localization could be segregated into two groups: (1) those which displayed distinct nucleolar localization (Figure 2.1A) and (2) those which displayed more diffuse nuclear or cytoplasmic localization (Figure 2.1B). From the panel of nine mitotic motors examined CENP-E, MCAK,

Figure 2.1

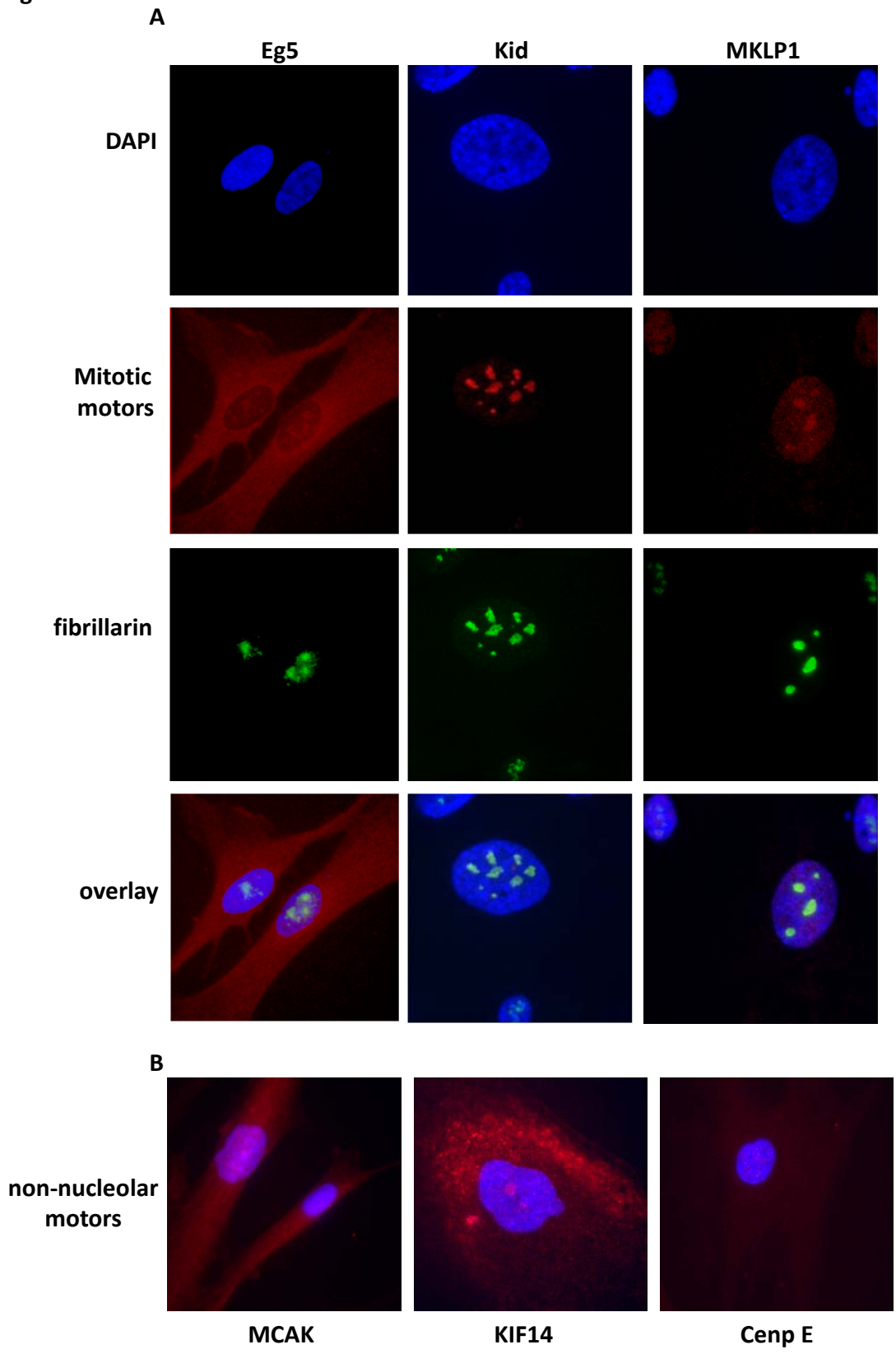
A
Eg5
Kid
MKLP1
DAPI
Mitotic motors
fibrillarin
overlay
B
non-nucleolar motors
MCAK
KIF14
Cenp E

Figure 2.1: Localization of mitotic motors during interphase.

(A) Kid, Eg5, and MKLP1 demonstrated nucleolar localization during interphase, as confirmed by nucleolar marker fibrillarin. Blue, DAPI; red, mitotic motor, green, fibrillarin. (B) Other mitotic motors, MCAK, CenpE, demonstrated diffuse nuclear or cytoplasmic localization during interphase. Kif14 did demonstrate nucleolar localization in this image, but was inconsistent during this analysis.

HSET, KIF14, KIF4, cytoplasmic dynein were characterized by diffuse nuclear or cytoplasmic localization, while Eg5, Kid and MKLP1, localized at least partially to the nucleolus.

2.2.2 The nucleolar-associating motors localized differently between noncancer and cancer cells during interphase

Quantification of the immunofluorescent localization of these motors between noncancer and cancer cells revealed that Kid localized to the nucleolus ~80% of the time in all noncancer cells lines tested, and to the nucleolus less than 35% of the time in cancer cell lines examined (Figure 2.2A). MKLP1 followed a similar trend, where MKLP1 localized to the nucleolus in noncancer cells greater than 60% and in cancer cells, less than 5% of the time, with the exception of UPCI:SCC103 cells which had ~80% nucleolar localization. However, analysis of Eg5 localization revealed opposite results in comparison to Kid and MKLP1 such that in the different cell lines, Eg5 was found to localize to the nucleolus in both normal and cancer cells ~60% of

the time, with the exception of UPCI:SCC103 cells, where it localized less than 25% of the time (Figures 2.2B,C). It is interestingly that the three nucleolar-associating motors localized differently between the noncancer and cancer cells, specifically it is important to note that in UPCI:SCC103 cells, Eg5 localization was found to be absent from the nucleolus, unlike in the other cancer cells, whereas MKLP1 was found to localize to the nucleolus in UPCI:SCC103 cells, unlike the other cancer cell lines. As of now, the reason for this difference is unclear, but as motors typically execute a dynamic balance of forces, this result may suggest disruption of the delicate balance between motors in this cell line, such that overexpression of MKLP1 causes Eg5 NoLS to be lost.

Figure 2.2

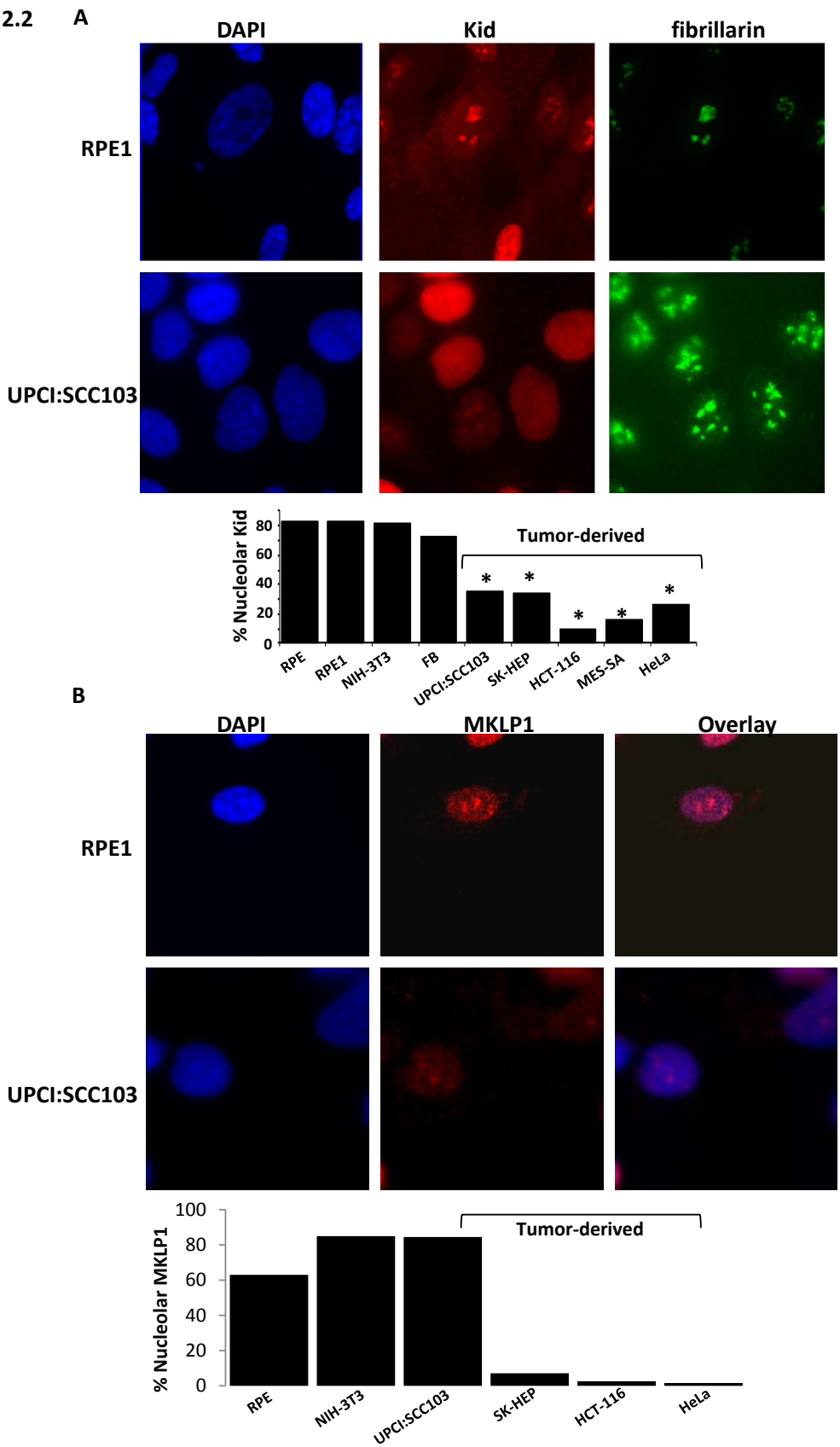
A
DAPI
Kid
fibrillarin
RPE1
UPCI:SCC103
% Nucleolar Kid
Tumor-derived
RPE
RPE1
NIH-3T3
FB
UPCI:SCC103
SK-HEP
HCT-116
MES-SA
HeLa
B
DAPI
MKLP1
Overlay
RPE1
UPCI:SCC103
% Nucleolar MKLP1
Tumor-derived
RPE
NIH-3T3
UPCI:SCC103
SK-HEP
HCT-116
HeLa

Figure 2.2

C

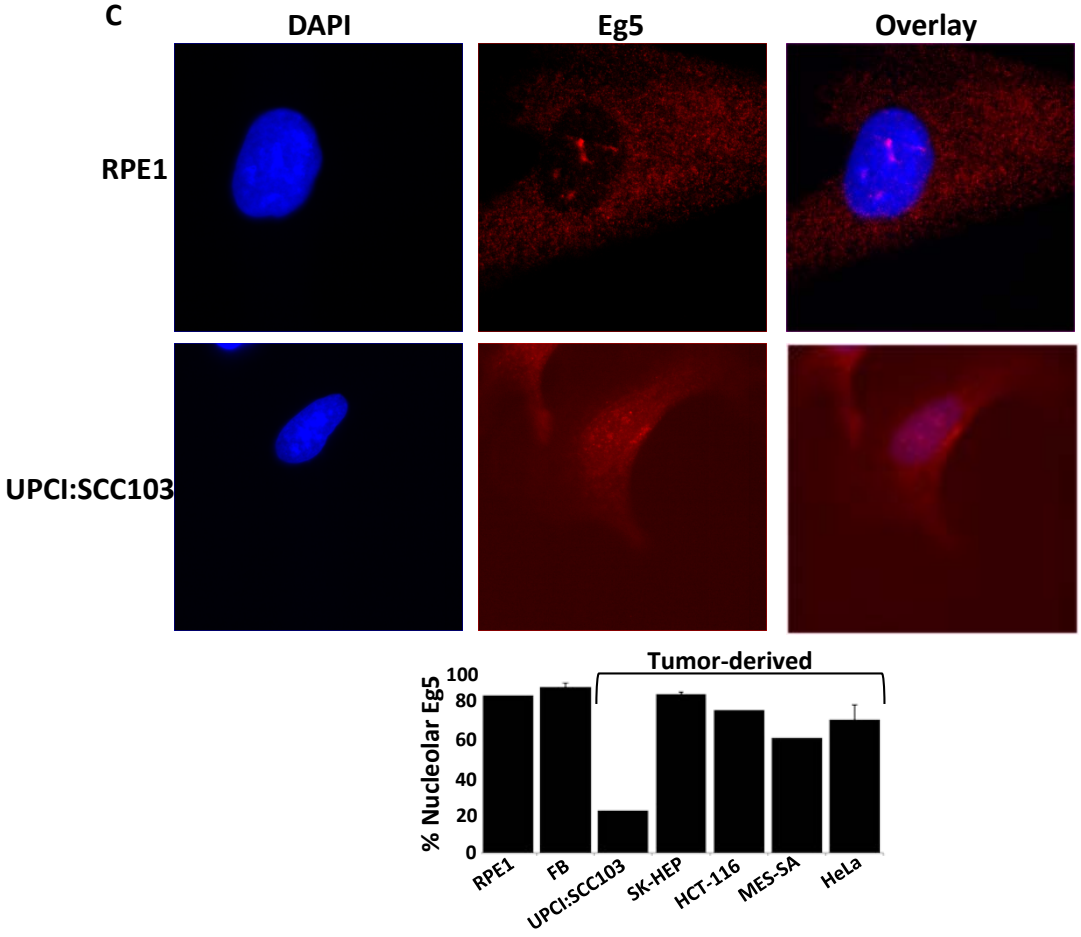

Figure 2.2: Localization of mitotic motors during interphase between noncancer and cancer cells.

(A) Top: Immunofluorescence analysis of Kid localization appeared to be different between noncancer RPE1 cells and cancer UPCI:SCC103. Bottom: Quantitation of immunofluorescence between noncancer and cancer cells. Red, Kid; Blue, DAPI; Green, fibrillarin. (B) Top: Immunofluorescence analysis of MKLP1 localization in noncancer and cancer cell lines. Red, MKLP1; Blue, DAPI Bottom: Quantitation of immunofluorescence analysis. (C) Top: Immunofluorescence analysis of Eg5 localization in noncancer and cancer cell lines. Red, Eg5; Blue, DAPI Bottom: Quantitation of immunofluorescence. *= p value <0.05.

Nucleolar localization of these motors were confirmed by co-staining with fibrillarin, a protein localizing to the dense fibrillar component (Figure 2.1A), and/or nucleophosmin (NPM) a protein localizing to the granular component (Figure 2.3). Furthermore, the nucleolar localization of the motors Kid and MKLP1 was validated in tissue by immunohistochemistry of cross-sections from frozen intestine of eight-week-old mice (Figure 2.4). The nucleolar localization of these motors is quite intriguing because an interphase function for these motors has not been investigated previously.

2.2.2.1 Kid localizes to the nucleolus in both noncancer and cancer cells

Additionally, the nucleolar localization of Kid was further confirmed by immunofluorescence of isolated nucleoli (Figure 2.5A), immunoblotting of nucleolar enrichment (Figure 5B) and cellular fractionation (Figure 2.5C), in collaboration with Maya Ashfag and Dr. Jason Weber. Nucleolar fractionation/enrichment was completed by gently lysing cells, separating the nuclear components using a sucrose gradient, and subsequent immunoblot analysis on the fractions. Although the immunofluorescence analysis in Figure 2.2A of Kid suggested a distinct localization pattern between noncancer and cancer cells, the biochemical fractionation revealed that Kid was present in the nucleolus of both noncancer, RPE1 cells, and cancer, UPCI:SCC103 cells. This biochemical fractionation experiment also demonstrated the specificity of the antibody verifying the immunofluorescence staining was not due to cross reactivity with another nucleolar protein.

Figure 2.3

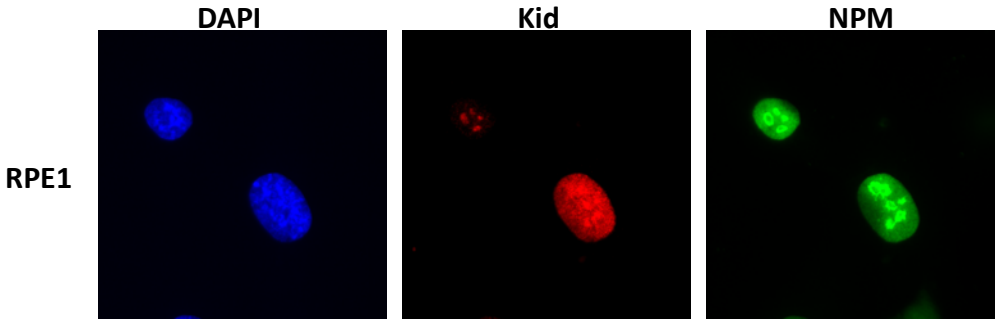

Figure 2.3: Kid completely co-localizes to the nucleolus similar to NPM, a nucleolar marker.

Untreated RPE1 cells were co-stained for Kid (red) and NPM (green) and DAPI (blue).

Figure 2.4

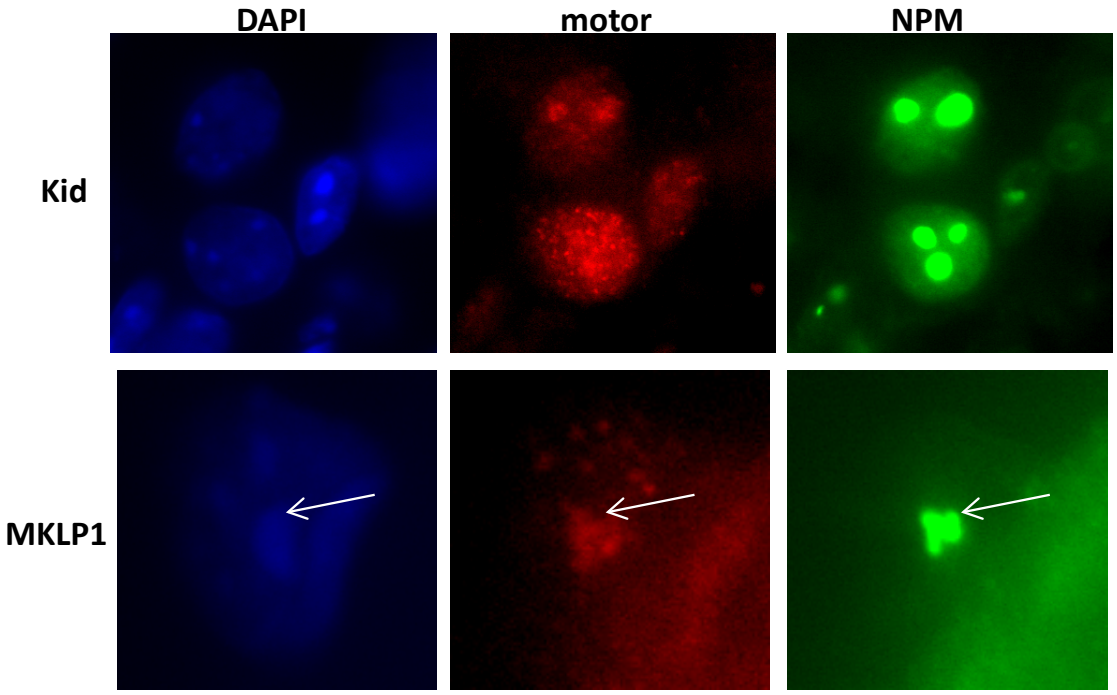

Figure 2.4 : Kid and MKLP1 localize to the nucleolus in tissue.

Eight- week-old frozen mouse intestine cryosectioned tissue was co-stained with antibodies to Kid or MKLP1 (in red) and NPM (in green), or DAPI representing the nucleus in blue. White arrow represents the cell demonstrating nucleolar localization of MKLP1.

Figure 2.5

A

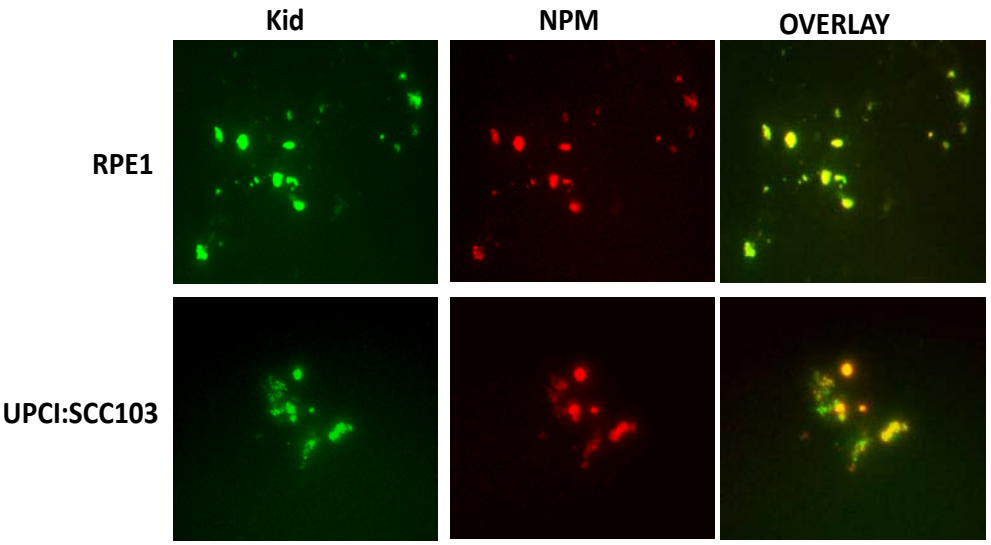

B

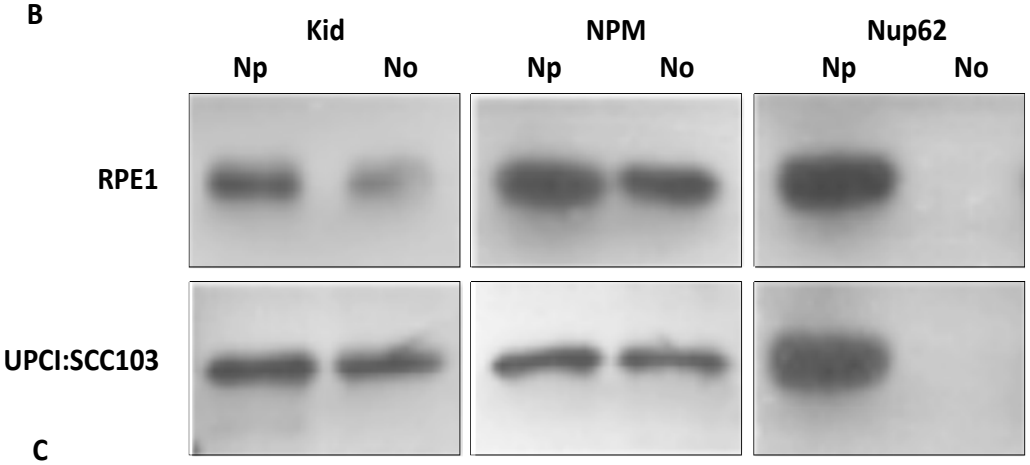

C

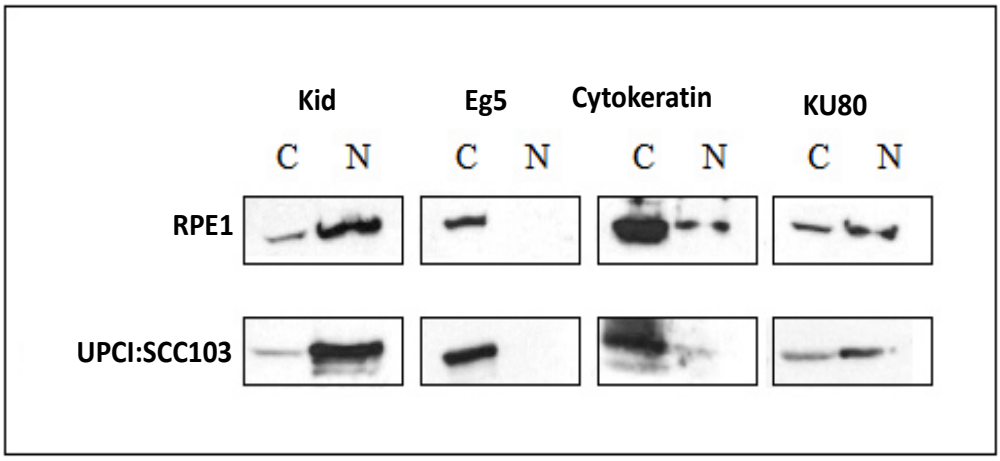

Figure 2.5: Kid is demonstrated to specifically localize to the nucleolus in both noncancer and cancer cells.

(A) Isolated nucleoli from RPE1 and UPCI:SCC103 cells demonstrate complete co-localization with NPM. Green, Kid; Red, NPM. (B) Biochemically fractionated nucleoli from RPE1 and UPCI:SCC103 demonstrated specificity of the Kid antibody and verified Kid localization to the nucleolus in both RPE1 and UPCI:SCC103 cells. NP=nucleoplasm, No=nucleolus, Nup62=nucleoporin. (C) Kid and Eg5 subcellular fractionation into cytosol (C) and nucleus (N) in RPE1 and UPCI:SCC103 cell lines. KU80=nuclear, cytokeratin=cytosolic markers.

The differences between the immunofluorescence and biochemical fraction data with regard to Kid in these two cell lines can be reconciled by noting the presence of bright nuclear staining, which likely obscured the nucleolar staining in the cancer cells. Typically, a nuclear protein that is excluded from the nucleolus exhibits a “spherical black hole” or “ghost” where the nucleolus is located and as the nucleolus exhibited no such “ghost” pattern in these UPCI:SCC103 cells, it was determined that the nucleus/nucleolus likely contained a continuous distribution of Kid (Armstrong, Franklin et al. 2001).

2.2.2.2 Kid is not overexpressed in cancer cells

As the staining of Kid during interphase seemed to be more intense and uniform in cancer cells as compared to noncancer cells, it suggested that the overall levels of Kid may be greater in

cancer cells. An elevated expression level of Kid in cancer cells could explain the differences in nucleolar/nuclear localization observed between cancer and noncancer cells. Initially, in noncycling cells the expression of Kid was determined to be elevated in some cancer cells in comparison to noncancer cells by immunoblot analysis (Figure 2.6A). However because the expression of Kid is known to increase during mitosis (Ohsugi, Tokai-Nishizumi et al. 2003), (Germani, Bruzzoni-Giovanelli et al. 2000) and cancer cells are known to have at least a 2-3-fold increase in the number of mitotic cells compared to RPE1 cells, the same experiment was repeated with noncancer and cancer cells arrested in mitosis. Under mitotic arrest, a difference in Kid expression in whole cell lysates was not observed between the various noncancer and cancer cell lines tested (Figure 2.6B). These results strongly suggest that the difference in nucleolar localization observed is not due to a difference in expression levels of Kid. At this point, we turned our attention towards the function of motors associated with the nucleolus, rather than furthering characterizing the differences between normal and cancer cells.

Figure 2.6

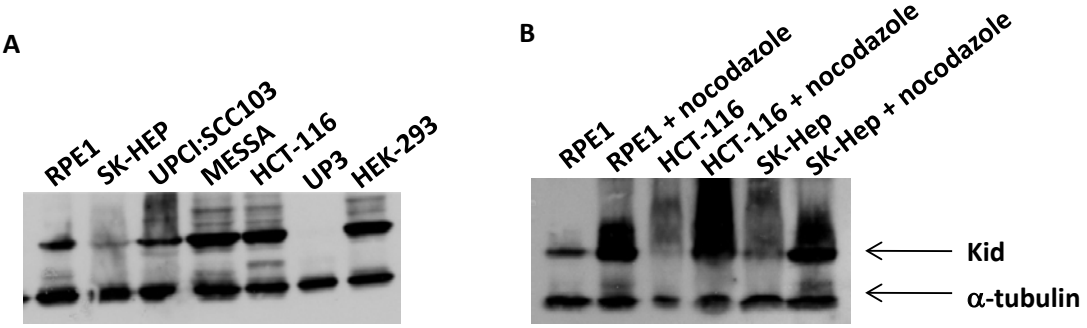

Figure 2.6: Kid is not overexpressed in cancer cells.

Various unsynchronized (A) or mitotically synchronized (B) noncancer and cancer cell lines were analyzed by immunoblotting for their protein expression of Kid. For synchronization, cells were treated with 0.003 mM nocodazole for 16 hrs, followed by an 8 hrs release, and the addition of 0.003 mM nocodazole for an additional 12 hrs. Cells were trypsinized, lysed, and subjected to SDS-PAGE and immunoblotting for the indicated antibodies. In either case, overexpression was not observed.

2.2.3 Mechanism of Kid localization to the nucleolus

As mentioned previously, the nucleolus has diverse functions. To begin to understand which nucleolar pathway involved motors, we first examined under what conditions the Kid motor localized to the nucleolus. Investigation of the literature revealed that proteins that localize to the nucleolus do so through one of two mechanisms. The first is by containing a nucleolar localization sequence (NoLS) (Lower, Turner et al. 2002; Song and Wu 2005), or secondly by

utilizing a GTP-dependent shuttling mechanism by use of its NoLS (Finch, Revankar et al. 1993; Tsai and McKay 2005).

2.2.3.1 Nucleolar-associating motors contain multiple NoLS's

Sequence comparison of the 700 proteins found to localize to the nucleolus failed to reveal a consensus NoLS; rather a general trend towards basic (arginine and lysine) amino acids of various length were observed (Armstrong, Franklin et al. 2001; Lower, Turner et al. 2002; Song and Wu 2005) (Figure 2.7). Besides basicity, proper folding has been proposed to be important to allow specific secondary structures to form and interact with proteins in the nucleolus. Upon examination of the motor sequences, Kid, Eg5, and MKLP1 were found to contain two, three, and five putative NoLSs, respectively (Figure 2.7). In order to test whether a putative NoLS-retention mechanism is responsible for the nucleolar localization of these motor proteins, mutagenesis and subsequent localization experiments were required. Kid was the ideal candidate motor to assay the NoLS-retention mechanism as Kid contained the least number of NoLSs of the three nucleolar motors. Each amino acid was mutated from an arginine or a lysine to an alanine, prior to transfection of this construct into RPE1 cells. Unfortunately, as we later learned, Kid was not able to be overexpressed in cells under the CMV promoter, as the cells that took up the plasmid would arrest and/or undergo apoptosis. Subsequent efforts led to cloning Kid under the eF1α promoter, a promoter that allowed Kid to be expressed at only 5-10 times greater than its endogenous promoter (Ohsugi, Tokai-Nishizumi et al. 2003). However, even under conditions of relatively mild overexpression cells which took up the plasmid arrested in interphase; thus future experiments involving the transfection of cells with Kid constructs were halted. However, this observation suggests a possible role for Kid in interphase as will be discussed in Chapter 6.

Figure 2.7

Figure 2.7: Nucleolar localization sequences observed in various proteins.

Kid, Eg5, and MKLP1 are demonstrated to have various putative nucleolar localization sequences, in comparison to the 7 proteins with known nucleolar localization sequences (MDM2, Coilin, Survivan-delta Exe, Hiv Tat, DEDD, p14Arf, PTHrP).

2.2.3.2 Nucleolar-associating motor Kid localizes to the nucleolus through a GTP-dependent shuttling mechanism

The second mechanism of nucleolar localization is a GTP-dependent shuttling mechanism. Previously published literature for other nucleolar proteins have shown that nearly 3% of the

total proteins with nucleolar localization retain a GTP binding sequence and localize to the nucleolus via a GTP-dependent mechanism (Misteli 2005). One such protein is nucleostemin which has previously been demonstrated to localize to the nucleolus based on a GTP-dependent cycling mechanism (Tsai and McKay 2005). Nucelostemin is found within the nucleolus when GTP levels are high using its NoLS to retain the protein within the nucleolus, and when the GTP levels decrease, its nucleolar localization sequence is released and nucleostemin shuttles out into the nucleus. In order to determine whether any of these nucleolar motors may also localize to the nucleolus based on a GTP-dependent mechanism, their sequences were searched for GTP-binding domains. There are at least five known GTP-binding consensus motifs, four of which were found within the region of the nucleolar motors: (1) the Walker A motif, or P-loop motif, consisting of the sequence GxxxxGKS is a known ATP/GTP binding sequence, 2) DxxG motif, 3) xKxD motif, and 4) ExSA motif. In addition to the variety of motifs identified each, nucleolar-localizing motor was found to contain a plurality of such motifs; Kid, Eg5, and MKLP1 were found to contain 6, 9, and 6 motifs, respectively (Figure 2.8A).

Figure 2.8

A

GTP Binding Sequences	KXXDL	GXXXXGK[S/T]	DXXG	EXSA
Nucleostemin	KSDL	GFPNVGKS		
KID GTP BS	KVLDL	GPTGAGKT	DLAG	EGSA
			DSLG	
			DCRG	
MKLP1 BS	KGDI	GVTGSGKT	DPVG	
			DADG	
			DLAG	
			DGEG	
Eg5 BS:	KRDL	GGTGTGKT	DLAG	
	KSDL		DSLG	
	KTDL		DVSG	
			DIFG	

B

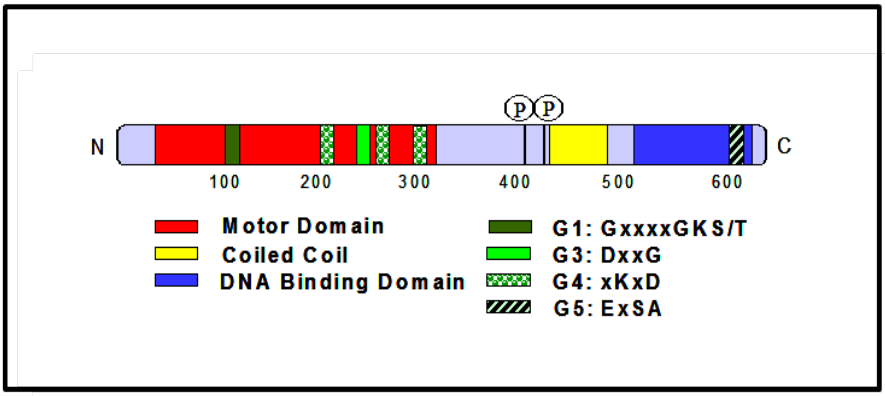

Figure 2.8: Putative GTP binding sequences in Kid, MKLP1,and Eg5 as well as the known protein Nucleostemin.

(A) Kid, MKLP1 and Eg5 are demonstrated to contain multiple GTP binding sequences. Armstrong, S.J., 2001. (B) Schematic demonstrating where the GTP binding sequences are found.

2.2.3.3 Kid shuttles out of the nucleolus when GTP levels are decreased

To begin to determine whether the nucleolar localization of Kid was regulated by a GTP-shuttling mechanism, we initially took advantage of mutational analysis of the GTP-binding motifs, but as overexpression of Kid was found to be toxic to cells when overexpressed, this approach proved unuseful. Fortunately, a number of distinct small molecule inhibitors are available that are known to decrease GTP levels within cells, as such we decided to treat cells with one of these inhibitors to determine if Kid would leave the nucleolus as a result of lower levels of GTP. Two different inhibitors, mycophenolic acid (MPA) and ribavirin, were used independently, each inhibiting the same enzyme inosine monophosphate dehydrogenase and resulting in decreased intercellular pools of GTP (Finch, Revankar et al. 1993; Tsai and McKay 2005). Treatment of RPE1 cells with 30 μM MPA followed by immunoflorescence resulted in ~80% of cells exhibiting Kid localization from the nucleolus to the nucleus (Figure 2.9A,B). This change in Kid localization by immunofluorescence analysis demonstrated that the nucleolus no longer contained Kid, as the nucleolus was unstained. However, as Kid changed localization from the nucleolus to the nucleus, it seemed as though the expression of Kid may also have changed. To examine this, cells were treated with varying amounts of MPA followed by cell lysis and immunoblotting. Kid expression was observed to increase when Kid localization changed from the nucleolus to the nucleus after treatment with MPA (Figure 2.9C). As MPA treatment is known to cause a decrease in RNA and DNA synthesis of ribosomal genes (Lowe, Brox et al. 1977), this change in Kid localization is likely reflective of loss of this decreased synthesis and may hint at Kids function as discussed in Chapter 6.

Treatment with ribavirin for four hours also resulted in a similar percentage of cells with Kid localization to the nucleus (Figure 2.9D, top two rows). These data suggest that the localization of Kid is regulated by a GTP-dependent shuttling mechanism. As a corollary to this proposed mechanism, if GTP levels could be restored with the addition of guanosine, Kid should relocalize to the nucleolus. Indeed, when cells were treated for four hours with 100 μM ribavirin, followed by the addition of 100 μM guanosine for four hours, Kid relocalized to the nucleolus (Figure 2.9C bottom row, 9E). Additionally, the shuttling could be blocked by adding ribavirin and guanosine at the same time. Therefore this demonstrates that Kid localization to the nucleolus requires a GTP-dependent shuttling mechanism.

Figure 2.9

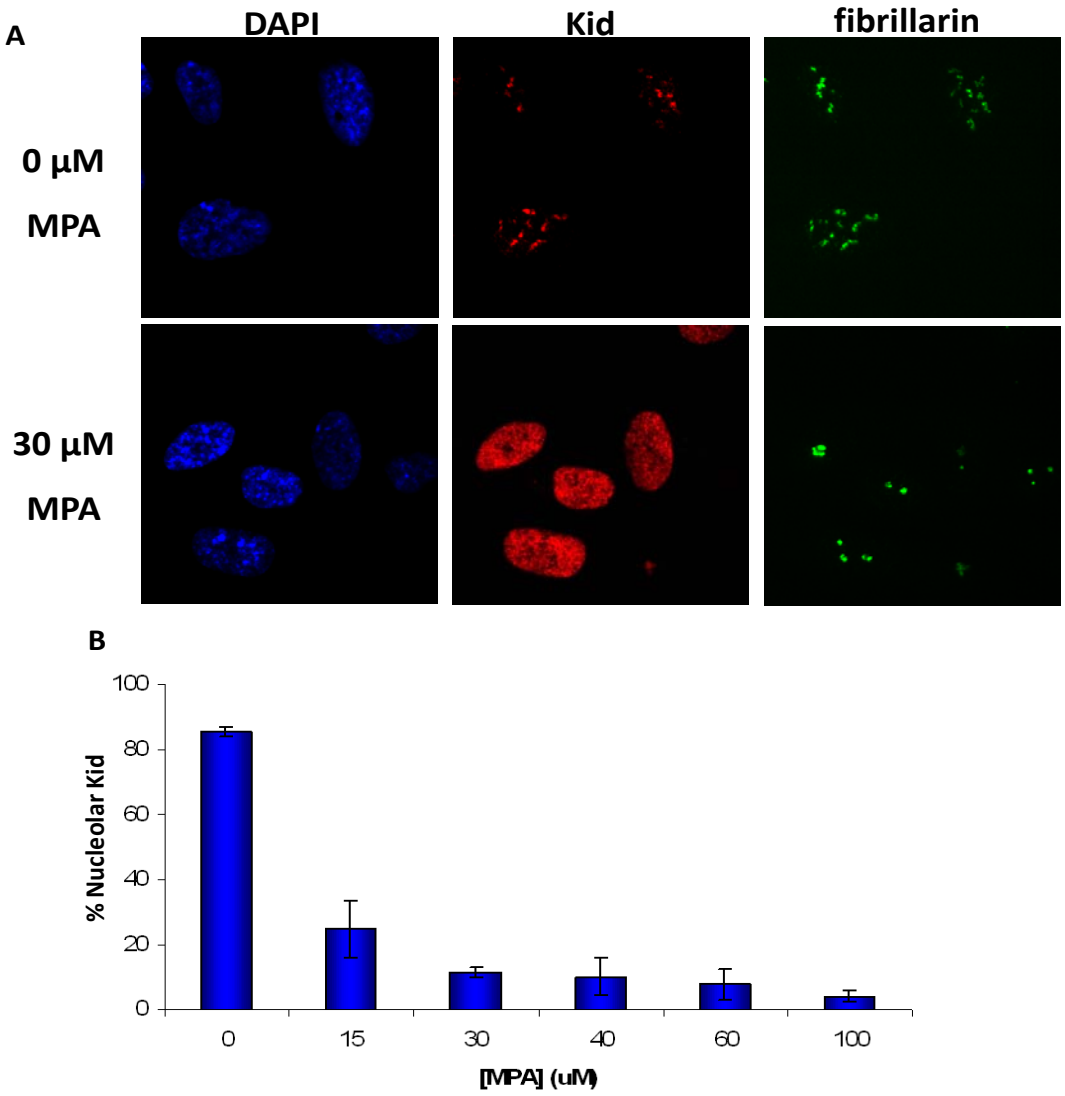
A
DAPI
Kid
fibrillarin
0 µM
MPA
30 µM
MPA
B
% Nucleolar Kid
100
80
60
40
20
0
0
15
30
40
60
100
[MPA] (uM)

Figure 2.9 continued

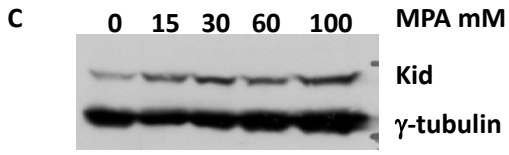

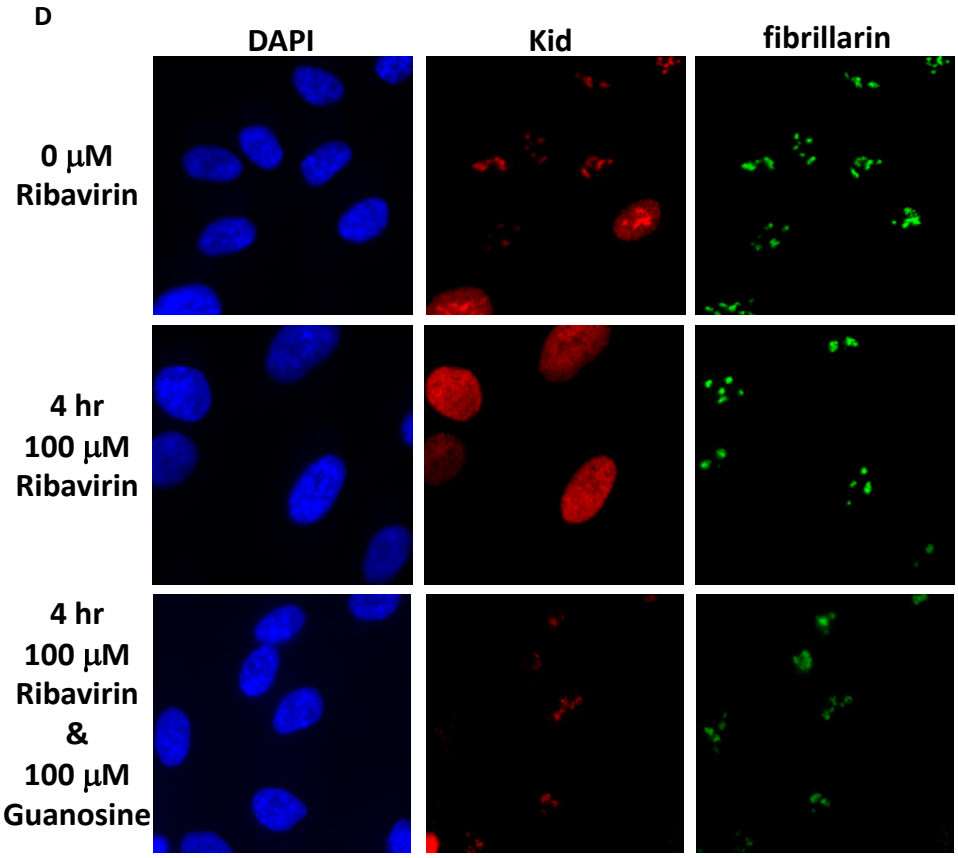

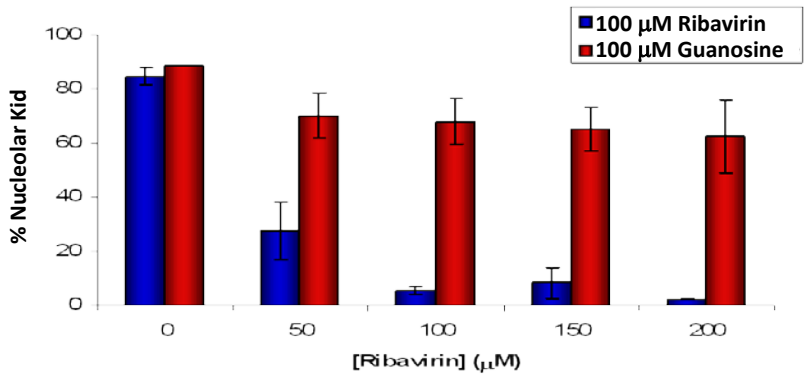

Figure 2.9: Kid translocates from the nucleolus to the nucleus based on a GTP-dependent shuttling mechanism in RPE1 cells.

(A) Immunofluorescence analysis of Kid localization before (top row) or after MPA treatment (bottom row). (B) Quantitation of Kid localization in the nucleolus after a 4 hr treatment with various concentrations of MPA. (C) Immunoblot of RPE1 cells treated with varying amounts of MPA. (D) Immunofluorescence analysis of Kid localization before treatment with ribavirin (top row), after treatment with ribavirin for 4 hrs (middle row), or after a 4 hr treatment with ribavirin followed by a 4 hr treatment with guanosine (bottom row). (E) Quantitation of Kid localization in the presence of various concentrations of ribavirin and/or guanosine. DAPI; Red, Kid. Green, fibrillarin.

2.2.3.4 MKLP1 does not localize to the nucleolus through a GTP-dependent shuttling mechanism

As Kid was observed to change localization in response to decreased GTP levels, we inquired whether another nucleolar motor MKLP1 could also change its localization in response to decreased GTP levels. When varying concentrations of MPA were added to cells for 4 hrs, a change in MKLP1 nucleolar localization was not observed (Figure 2.10). This suggests that not all nucleolar-associating motors require a GTP-dependent shuttling mechanism, even though GTP binding sequences were found within the MKLP1 sequence.

Figure 2.10

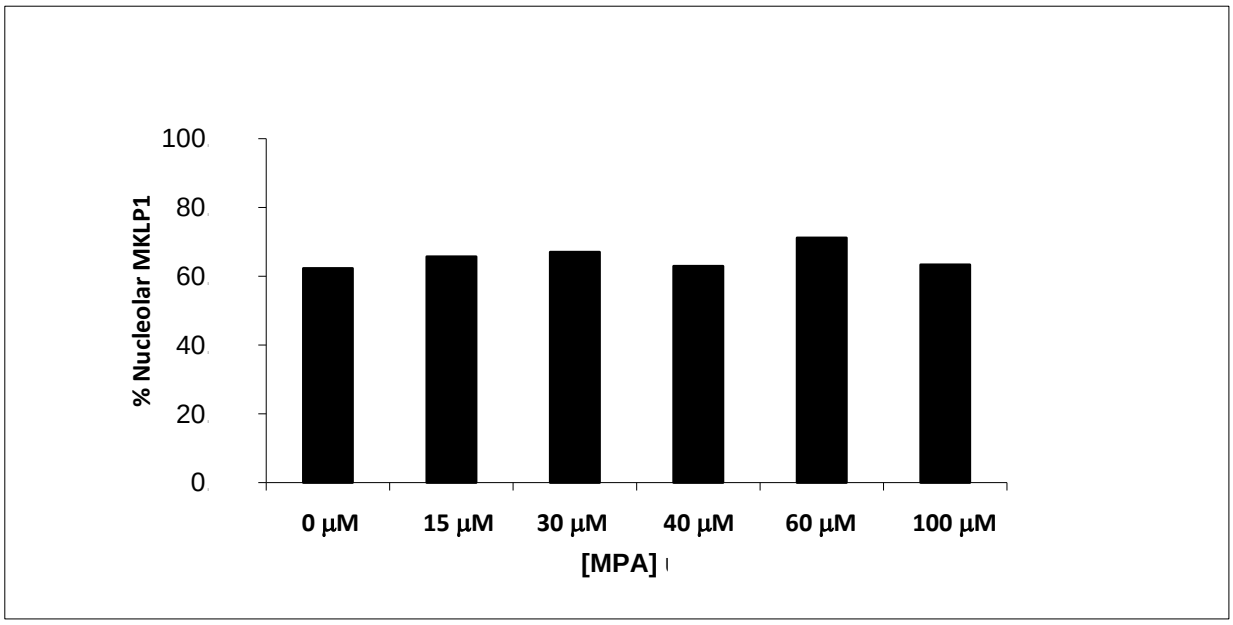

Figure 2.10: MKLP1 is not regulated by a GTP-dependent shuttling mechanism.

RPE1 cells were treated with various amounts of MPA, prior to fixation and staining. Quantitation of MKLP1 localization in RPE1 cells after various concentrations of MPA treatment demonstrated no change in localization.

2.2.3.5 In cancer cells, Kid also localizes to the nucleolus through a GTP-dependent shuttling mechanism

After treatment with MPA or ribavirin, the localization of Kid from the nucleolus to the nucleus appeared similar to the localization of Kid in cancer cells, UPCI:SCC103, as cancer cells contain high levels of nuclear Kid. We inquired whether the decreased localization of Kid to the nucleolus was due to reduced levels of GTP. To test this hypothesis, UPCI:SCC103 cells were

first treated with ribavirin for 4 hrs to cause the complete loss of nucleolar localization of Kid, followed by the addition of 300 μM of guanosine to cells for 4 hrs (Figure 2.11). This resulted in ~80% of cells relocalizing Kid to the nucleolus in the cancer cell population Next, cells were treated with varying concentrations of guanosine to determine whether Kid would relocalize to the nucleolus in the cancer cells without first decreasing GTP levels more than the endogenous levels. UPCI:SCC103 treated with varying concentrations of guanosine (50 μM-1000 μM) actually doubled the percentage of Kid cells containing nucleolar localization (Figure 2.12A,B). Although this redistribution of Kid is significant, it still falls short of the untreated noncancer cells. Thus, it appears that differences in GTP levels between cancer and noncancer cells can account for some of the observed differences in nucleolar localization; although, additional mechanisms are likely exerting their control as well.

Figure 2.11

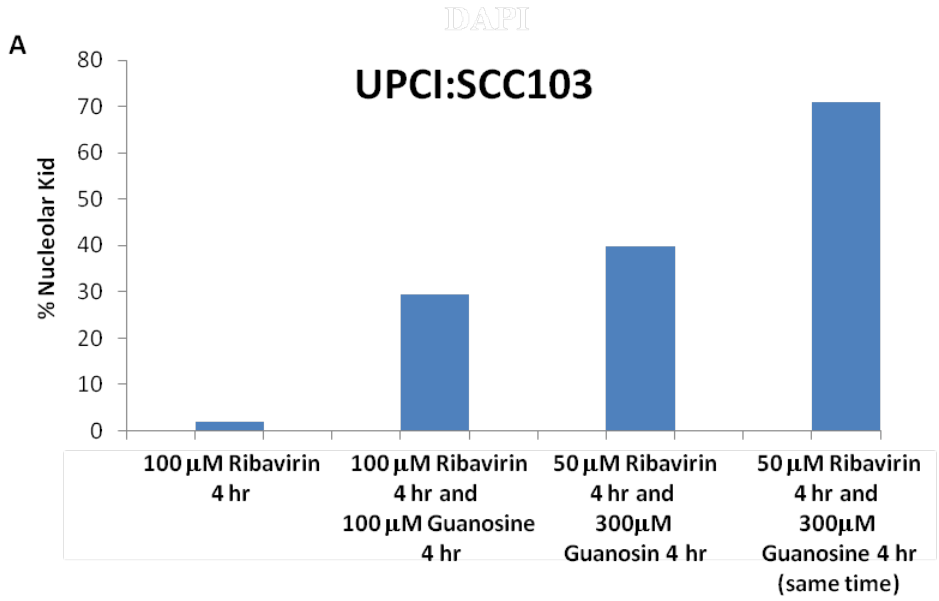

Figure 2.11: Kid localization to the nucleolus in UPCI:SCC103 cells increased after depletion of GTP levels and replenishment of GTP by guanosine.

Quantitation of UPCI:SCC103 localization after cells were treated with Ribavirin for 4 hrs (to deplete GTP levels in cells) and the re-addition of guanosine, at various concentrations (to increase GTP levels).

Figure 2.12

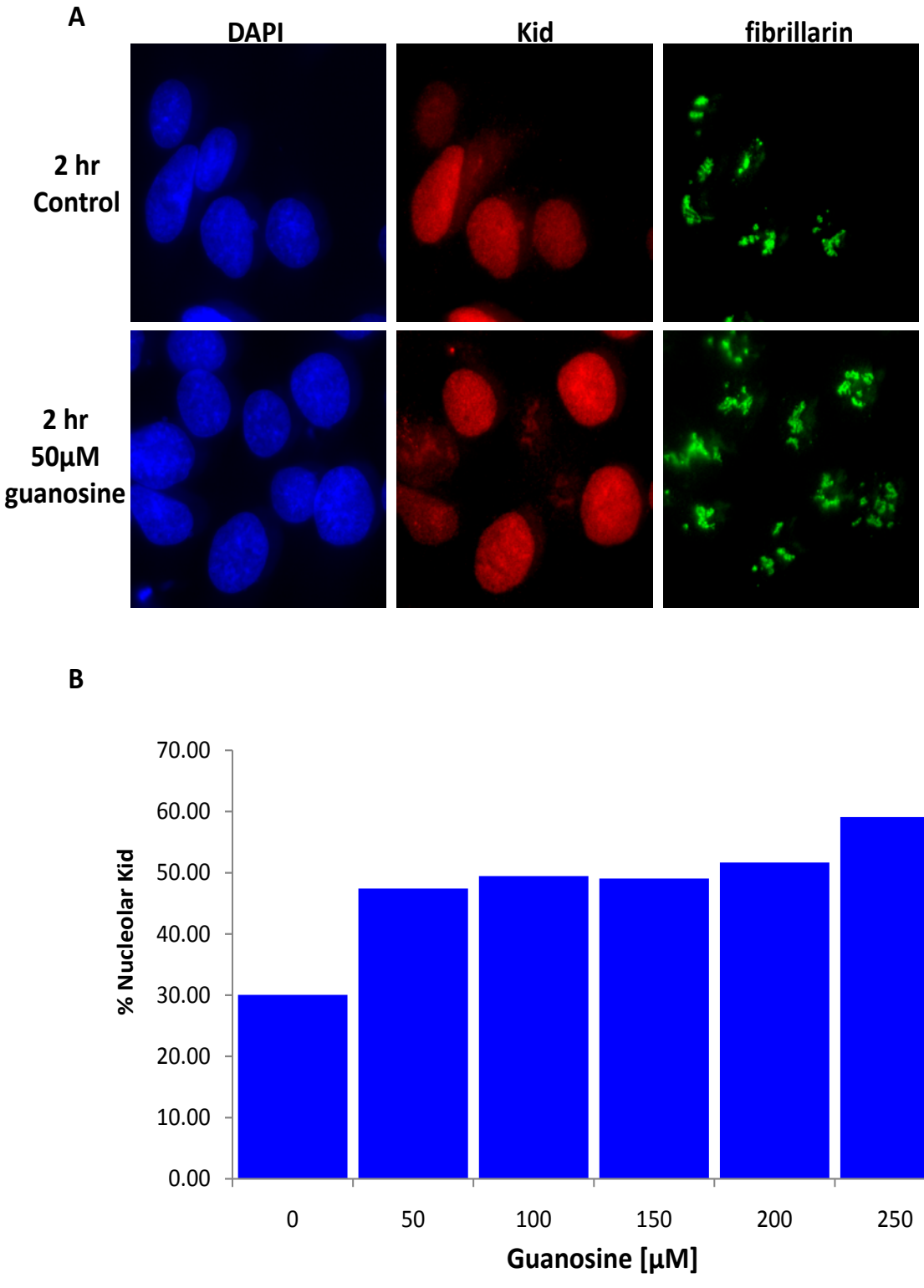
A
DAPI
Kid
fibrillarin
2 hr Control
2 hr 50µM guanosine
B
% Nucleolar Kid
70.00
60.00
50.00
40.00
30.00
20.00
10.00
0.00
0
50
100
150
200
250
Guanosine [µM]

Figure 2.12: UPCI:SCC103 cells increased localization to the nucleolus in the presence of guanosine.

(A) Immunofluorescence analysis of UPCI:SCC103 cells treated with guanosine. (B) Quantitation of Kid nucleolar localization after various concentrations of guanosine were added for 2 hrs. DAPI; Red, Kid; Green, fibrillarin

2.2.3.6 GTP-dependent shuttling mechanism of Kid extends to its mitotic function

Given our exciting and novel findings regarding the dynamic localization of Kid to the nucleolus and particularly the mechanism by which the cell is able to control the localization of Kid, we sought to determine whether differing GTP levels could account for the known Kid deficient phenotype. Loss of Kid during mitosis leads to lagging chromosomes, misalignment of chromosomes along the metaphase plate and even lagging chromosomes during anaphase, as Kid is responsible for the force that pushes chromosome arms away from spindle poles (Funabiki and Murray 2000; Zhu, Zhao et al. 2005). Specifically, we inquired whether the mitotic defects known to occur after loss of Kid observed in cancer cells could be due to decreased GTP levels. To examine this, the noncancer RPE1 cells were treated with MPA for 4 hr after which mitotic defects were examined. Although Kid localization shuttled from the nucleolus to the nucleus during interphase, this did not interrupt Kid localization during mitosis (Figure 2.13A). Additionally, MPA treatment resulted in a ~5-fold increase in metaphase and anaphase defects, suggesting that decreased intracellular GTP levels can lead to defects during mitosis (Figure 2.13B). Next, we sought to determine whether such defects observed in cancer cells could be corrected by elevating the intercellular GTP levels. UPCI:SCC103 cells treated with varying

concentrations of guanosine significantly decreased the metaphase mitotic defects; however, no difference was observed for anaphase defects (Figure 2.14). Furthermore, this decrease of metaphase defects was linearly concentration-dependent, rather the curative effects of guanine seemed to plateau around 60 μM. Interestingly, this data would suggest that our newly uncovered GTP-shuttling mechanism of Kid may extend to its traditional physiological mitotic function.

Figure 2.13

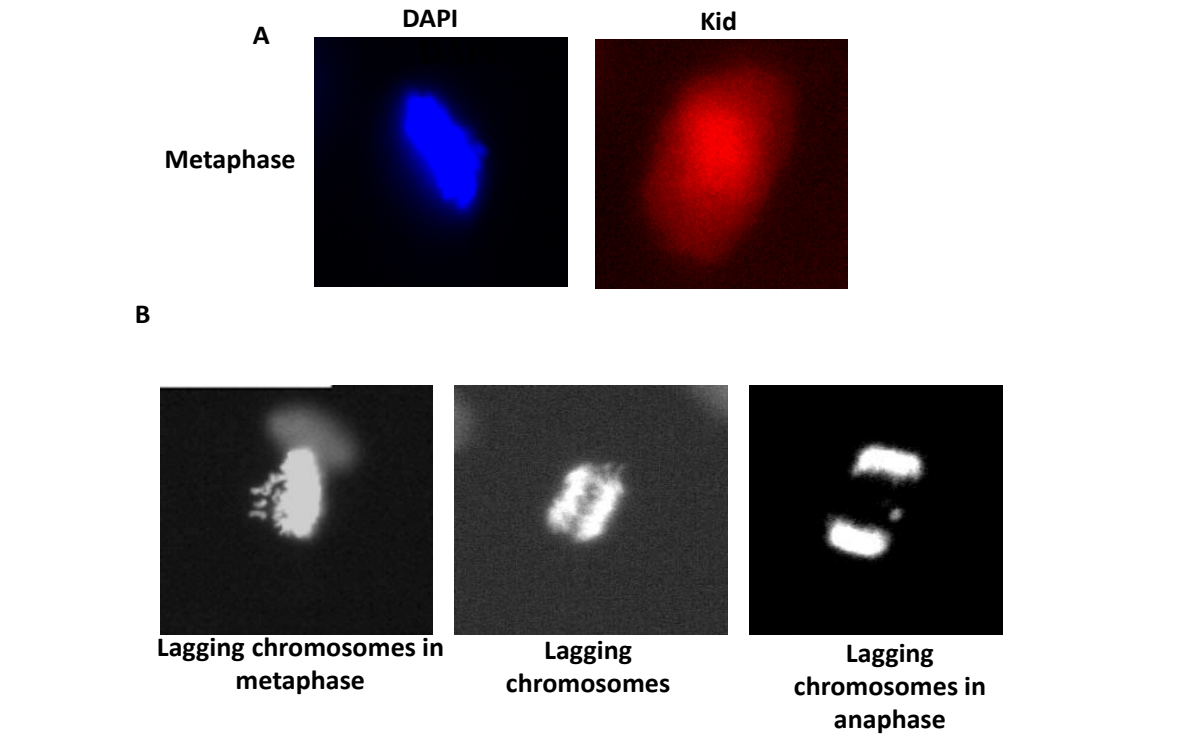
A
DAPI
Kid
Metaphase
B
Lagging chromosomes in metaphase
Lagging chromosomes
Lagging chromosomes in anaphase

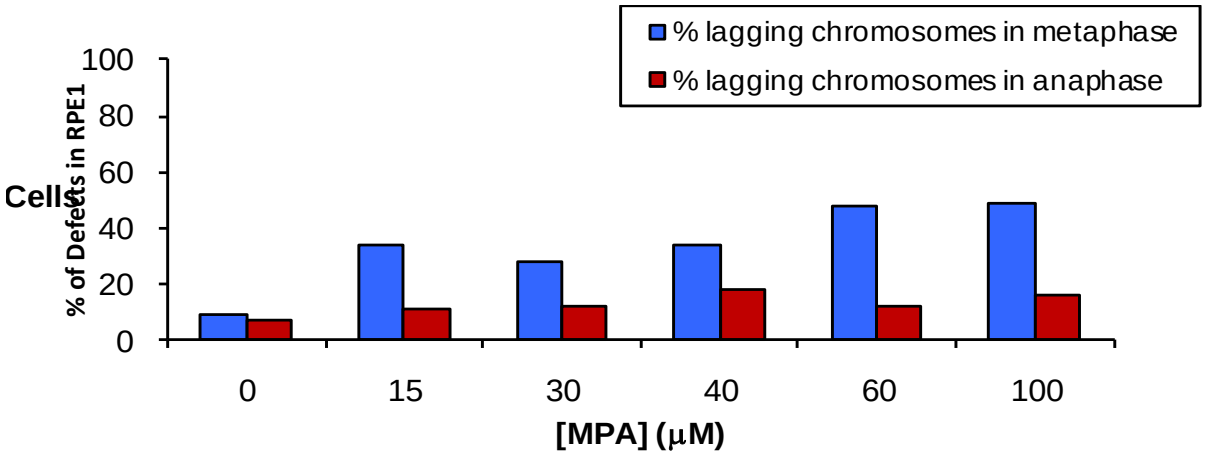
% lagging chromosomes in metaphase
% lagging chromosomes in anaphase
% of Defects in RPE1 Cells
100
80
60
40
20
0
0
15
30
40
60
100
[MPA] (μM)

Figure 2.13: Kid mislocalization in interphase leads to increased mitotic defects in RPE1 cells.

(A) Kid localizes correctly during mitosis even though Kid did not localize to the nucleolus during interphase. Blue, DAPI; Red, Kid. (B) Top: Immunofluorescence of mitotic defects observed during mitosis, consistent with Kid function, when Kid was mislocalized during interphase. Bottom: Quantitation of mitotic defects in RPE1 with various concentrations of MPA to cause Kid mislocalization during interphase.

Figure 2.14

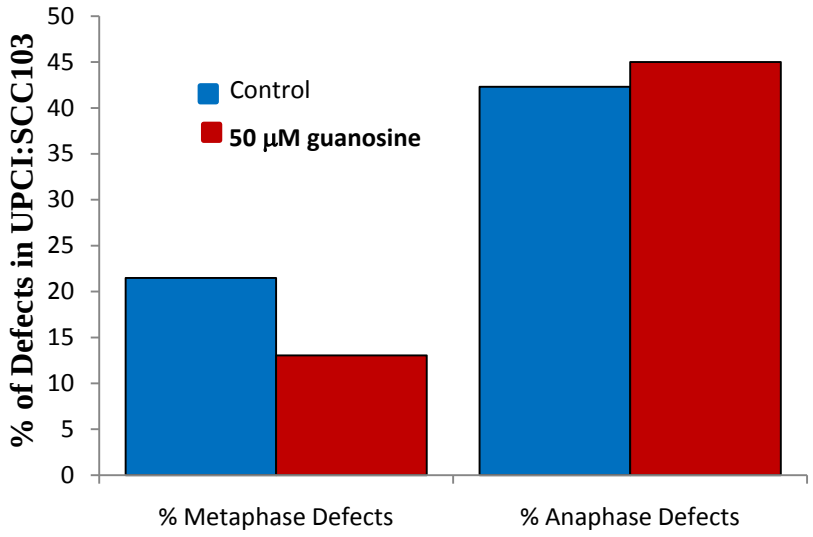

Figure 2.14: UPCI:SCC103 metaphase defects decreased with the addition of guanosine, while anaphase defects remained constant.

50 mM of guanosine was added UPCI:SCC103 cells and mitotic defects were examined. Interestingly, increased GTP levels corrected various metaphase defects typically observed in UPCI:SCC103 cells, but did not correct anaphase defects.

2.3 DISCUSSION

2.3.1 Why haven't these motors been identified as nucleolar proteins previously?

As there are over 700 proteins found to localization in the nucleolus (Andersen, Lam et al. 2005), it is not surprising that molecular motors, Kid, Eg5, and MKLP1, are also found to localize to the nucleolus. What is interesting though is that during the proteomic analysis of the nucleolus, these motors were not identified. This discrepancy can be explained by the fact that the proteomic profiling was completed in HeLa cells, which demonstrated very low percentages of Kid and MKLP1 in the nucleolus. Although Eg5 was found to localize to the nucleolus in HeLa cells >75% of the time, it is not surprising that Eg5 was not identified during the proteomic analysis. As I will discuss later in Chapter 4, Eg5 does not co-fractionate with pre-ribosomal subunits in the nucleolus, suggesting an unstable association with the nucleolus. Further evidence of a weak interaction by Eg5 was provided in Figure 2.5C, wherein Eg5 failed to cofractionate with the nucleus. An alternative interpretation of the data provided in Figure 2.5C is that association of Eg5 to the nucleolus may be highly sensitive to lysis conditions, resulting in loss of Eg5 association.

2.3.2 Kid has ATPase and GTPase activity

The GTP-dependent shuttling mechanism of Kid regulating the localization is quite intriguing because microtubule motors are generally thought to function using their ATPase properties. The observation of a motor functioning in response to GTP levels is unique. The Walker A motif, is commonly found in the P-loop which is capable of ATPase or GTPase activity and is known to

bind and hydrolyze nucleoside triphosphates (Galinier, Lavergne et al. 2002). Although not unexpected, the identification of Kid being able to function in response to GTP is unprecedented.

2.3.3 Kid shuttles from the nucleolus after treatment with clinical GTP inhibitors: implications in future studies

It is quite interesting that Kid translocates from the nucleolus to the nucleus when treated with inhibitors to inosine monophosphate dehydrogenase. As GTP is a precursor of nucleic acid synthesis and its depletion can cause a reduction of DNA and RNA synthesis, an important question would be if nucleic acid synthesis inhibition could cause Kid translocation from the nucleolus to the nucleus; experiments which have not been completed but would prove useful for future analysis.

Additionally, as these two drugs are used to decrease intracellular GTP levels in cells, they actually have clinically relevant uses for treatment of other diseases and disorders. MPA is typically used to inhibit organ transplant rejections as well as to manage autoimmune disorders such as systemic lupus, scleroderma, and pemphigus vulgaris (Surjushe and Saple 2008). Ribavirin is used as an antiviral drug to treat influenza, heptitus C infections, respiratory syncytial virus, as well as various other viral disorders (Chan-Tack, Murray et al. 2009). Thus, it would be of significant interest to study the change in Kid localization in response to either of these inhibitors in cell culture models of the above mentioned diseases.

2.3.4 Why does Kid not localize to the nucleolus in 100% of the cell population?

Kid had been found to localize to the nucleolus greater than 85% of the time and to the nucleus approximately 15% of the time which led us to question exactly why Kid does not localize to the nucleolus in 100% of the cells. During the end of G1 and S phase, various nucleolar proteins, such as nucleophosmin, have been found to localize to the nucleoplasm (nucleus) (Chou and Yung 1995). This nucleoplasm localization is common because it is known that rRNA processing occurs mostly during the G1 and S phases; as such, proteins like NPM have been found to be involved in rRNA processing and transport and shuttle during G1 and S phases (Chou and Yung 1995). It is also plausible that during these processes, GTP levels decrease sufficiently to allow these proteins to shuttle out of the nucleolus and into the nucleoplasm to aid in their interphase functions. Thus it is tempting to speculate that given the shared localization within the nucleolus and shared distribution pattern of NPM, Kid may also function in rRNA processing and/or biogenesis. The cell cycle specific localization of Kid, demonstrating its nucleoplasmic localization during S-phase, will be further discussed in Chapter 3 section 3.2.1.4.

2.3.5 Kid is observed to localize more to the nucleus in cancer cells because of upregulation of ribosome biogenesis

Furthermore, as the nucleolar localization of Kid in UPCI:SCC103 cells was found to be obscured during interphase we believe this can be explained by noting that cancer cells have been shown to exhibit upregulation of ribosome processing, biogenesis, and production which leads to tumor progression (Belin, Beghin et al. 2009). Certain oncogenes and tumor supressors have been demonstrated to regulate ribosome processing; loss of these regulatory mechanisms

leads to strong upregulation of proteins involved in ribosomal biogenesis and maturation. For example, c-myc oncogene has been shown to activate RNA pol II, as well as RNA pol I and III, and overexpression of c-myc leads to elevated ribosome biogenesis, processing, and mRNA in those cancers (Oskarsson and Trumpp 2005). Additionally, the dysregulation of major tumor suppressor proteins Rb and p53 in cancer cells have been shown to induce strong activation of ribosome biogenesis in cancer cells (Trere, Ceccarelli et al. 2004). Therefore, as cancer cells has been shown to upregulate ribosome biogenesis and processing, it seems that the obscured Kid nucleolar localization during interphase may be due to upregulation of these processes as Kid does play a role in ribosomal processing.

2.3.6 Overexpression of Kid leads to cellular arrest

Previously published data have demonstrated that in cancer cells ribosome assembly factors such as nucleophosmin are overexpressed (Ye 2005; Grisendi, Mecucci et al. 2006). This overexpression has been shown to increase cellular proliferation and inhibition of apoptosis leading to tumorigenesis. However, in normal cells, NPM overexpression has been shown to lead to cellular arrest (Ye 2005), very similar to what we observed after Kid overexpression.

Cellular arrest after Kid overexpression in RPE1, was surprising at first but in retrospect the cellular arrest observed was consistent with that observed of other ribosome assembly proteins which were overexpressed in noncancer cells. Therefore, in retrospect the overexpression of Kid plasmids should have been completed in cancer cells. Cancer cells were not chosen at first because it was thought that cancer and noncancer cells might have had different mechanisms of Kid localization. It was not until much later that it was demonstrated by the nucleolar fractionation data that the cancer and noncancer cells demonstrated nucleolar

localization of Kid because the diffuse localization of Kid in cancer cells obscured the nucleolar localization by immunofluorescence. Therefore, it would be quite interesting to revisit the overexpression studies of Kid in cancer cells, as they may be more tolerant of Kid overexpression. Additionally, we would hypothesize that Kid may function similar to other ribosomal proteins, such as NPM, and would increase cell proliferation, and lead to tumorigenesis but, this hypothesis requires further investigation.

2.3.7 Stable Transfection of Kid in RPE1 cells

After our overexpression studies were proved uninformative by means of transient transfections, we did try to stably overexpress Kid, in RPE1 cells using a Kid overexpression plasmid from Ohsugi, et al. (Ohsugi, Tokai-Nishizumi et al. 2003). Although 100% of the cells did take up the plasmid and did overexpress Kid approximately 10-15 times its endogenous level, we observed many phenotypes that we believed, at that time, cells were displaying atypical phenotypes. The phenotypes observed were:

1) Rounding up of the cells, rather than a flat fibroblastic appearance
2) Increase in cell proliferation
3) Increase in nucleoplasmic localization of Kid, rather than nucleolar

Because we did not have a control vector to compare our Kid overexpression cells to, we were unsure if overexpression of Kid resulted in the observed phenotypes or whether the stable transfection of the vector would cause these changes, as these changes we observed were

unexpected. However, after looking back and having more insight into the interphase function of Kid in ribosome biogenesis and translation, as will be discussed in Chapter 4 and 6, it is now very possible that the phenotypes observed were actually a result of overexpression of a ribosomal protein, Kid.

3.0 CHAPTER III: IDENTIFICATION OF KID FUNCTION IN RIBOSOME BIOLOGY

3.1 INTRODUCTION

As the nucleolus is the center of ribosome biogenesis and thus has to maintain ribosomal subunits to complete protein synthesis during the entire cell cycle, the nucleolus has evolved to respond to changes in cellular growth rate and metabolic activity (Boisvert, van Koningsbruggen et al. 2007). Any alteration to the cellular status (DNA damage, cellular stress, or even infection) will signal the nucleolus to inhibit ribosome biogenesis in order to focus the energy of the cell on repairing the designated problem (Rubbi and Milner 2003; Mayer and Grummt 2005). As we have demonstrated in chapter 2, Kid localizes dynamically to the nucleolus and thus experiments of this chapter were completed to identify how Kid responds to different types of stress. That is, does Kid remain in the nucleolus at all times when the nucleolus is intact, or does Kid shuttle from the nucleolus in response to stress or damage?

3.2 RESULTS

3.2.1 Changes in Kid localization

3.2.1.1 Kid translocates from the nucleolus to the nucleus after UV-C treatment

To begin to determine whether the nucleolar localization of Kid is altered in response to different cellular stresses, cells were first subjected to ultraviolet irradiation (UV). There are three different types of UV (UV-A, UV-B, and UV-C) and each subtype of UV corresponds to the specific wavelength range; UV-A (long wave) has a wavelength range of 400-315 nm, UV-B (medium wave) has a wavelength range of 300-200 nm, and UV-C (low wave) has a wavelength range of 280-100 nm. UV-C has been shown to induce significant cellular damage and produces DNA lesions, such as thymidine dimers, leading to single strand breaks (SSB) within the DNA duplex (Parrilla-Castellar, Arlander et al. 2004). RPE1 cells were exposed to varying amounts of UV-C, ranging from 10 Joules/meter^2 (J/m^2) to 100 J/m^2, and were allowed to recover from 1-24 hrs after treatment (Figure 3.1). Interestingly, Kid was observed to move out of the nucleolus within 1 hr after 10 J/m^2 of UV-C treatment, while the control nucleolar protein nucleophosmin (B23/NPM) remained within the nucleolus. As 1 J/m^2 of UV-C is sufficient to cause 40,000 lesions per cell, it was decided to test lower levels of UV-C treatment to determine if Kid may also change localization in response to these lower levels (BEIRV 1990). Therefore, a lower dose of UV-C treatments (1-8 J/m2) were employed and were sufficient to also induce an alteration of Kid localization from the nucleolus to the nucleus (Figure 3.2). However after further analysis, although a change in Kid localization was always observed, the percentage of Kid nucleolar

Figure 3.1

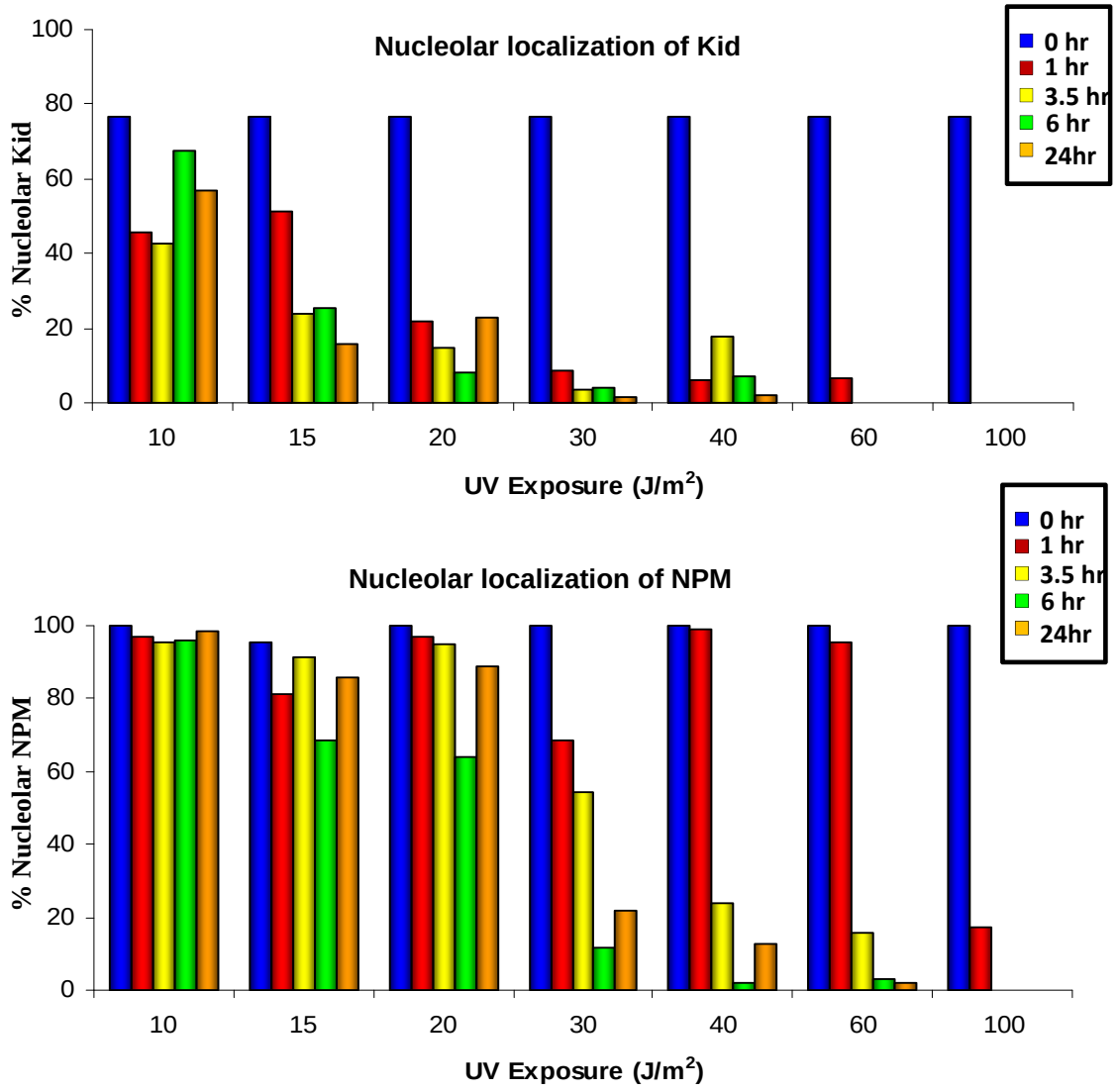

Figure 3.1: Kid moves out of the nucleolus prior to nucleolar breakdown or NPM. **RPE1 cells were subjected to various concentrations of UV-C treatment and were allowed to recover for 1-24 hrs during analysis. Top graph represents change in Kid localization and the bottom graph represents NPM change in localization after the different UV-C treatments. Additionally, NPM began to leave the nucleolus at around 40 J/m^2, consistent with the literature and when nucleolar breakdown is shown to occur.**

Figure 3.2

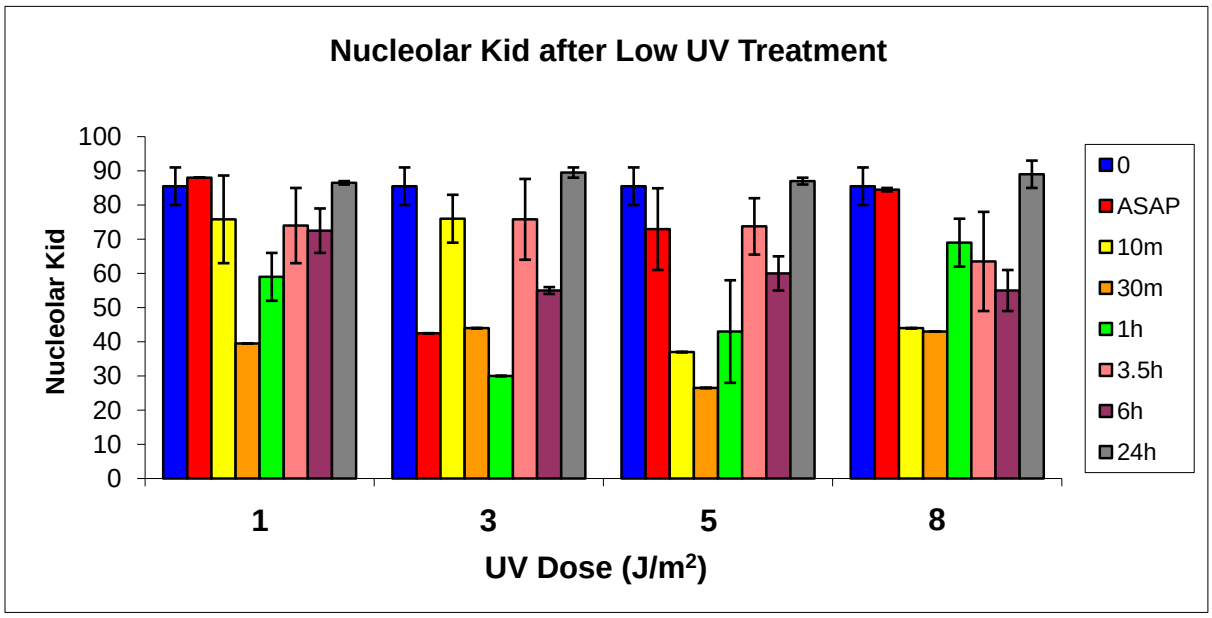

Figure 3.2: Kid localization after low amounts of UV-C treatment.

RPE1 cells were subjected to various concentrations of UV-C treatment (1-8 J/m^2) and were allowed to recover for 1-24 hrs during analysis. Kid change in localization after the low doses of UV-C treatment proved to be inconsistent.

As a change in Kid localization was observed after UV-C treatment and the damage exerted on the cells during the 10 J/m^2 UV-C treatment were causing approximately 400,000 lesions per cell, it was investigated whether the cell could recover from this damage and more importantly, whether Kid would relocalize to the nucleolus. Notably, the effects of UV-C damage on Kid nucleolar/nuclear localization was reversible, as Kid was found to completely relocalize to the nucleolus within 6 hrs after 10 J/m^2 of UV-C treatment (Figure 3.1, top). Furthermore, a time course analysis of Kid localization following UV-C treatment revealed that

as little as 5 min after UV-C damage, was sufficient for Kid translocation from the nucleolus to the nucleus; suggesting that Kid rapidly alters its localization in response to cellular stress (Figure 3.3).

Even at higher concentrations of UV-C treatment, such as 20 J/m^2, Kid was determined to change localization from the nucleolus to the nucleus, while NPM remained within the nucleolus and thus suggesting that the nucleolus was still intact (Figure 3.4). Previously published data, as well as analysis of my experiments, determined that NPM was able to leave the nucleolus after ~30-40 J/m^2 of UV-C treatment (Lee, Smith et al. 2005). Furthermore, this treatment of UV-C was shown to cause loss of Kid prior to nucleolar disruption in RPE1 cells.

Figure 3.3

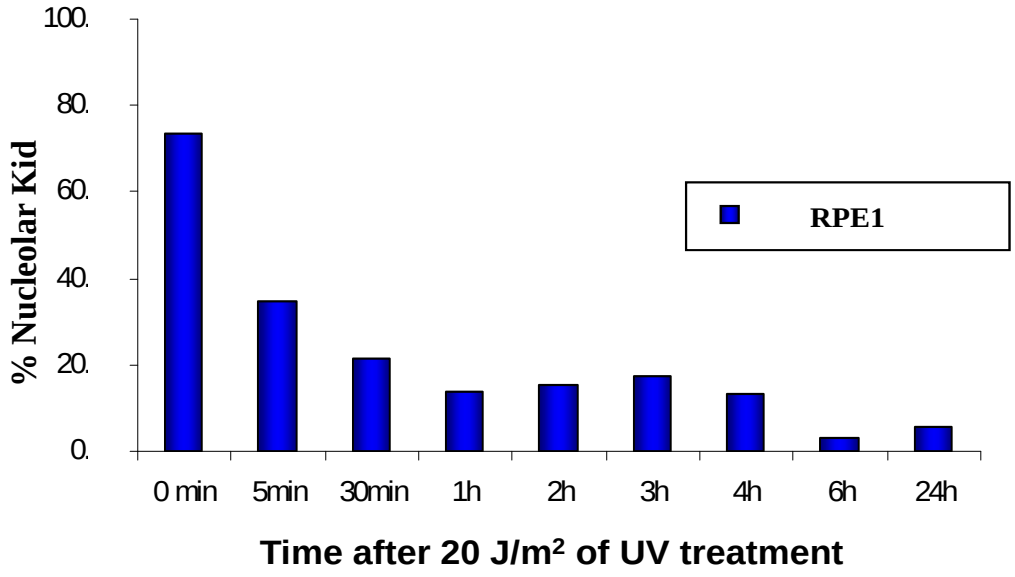

Figure 3.3: Kid changed localization from of the nucleolus within 5 min after UV-C treatment.

RPE1 cells were treated with 20 J/m^2 of UV-C and were allowed to recover for 5 min-24 hrs. Blue bars represent Kid nucleolar localization.

Figure 3.4

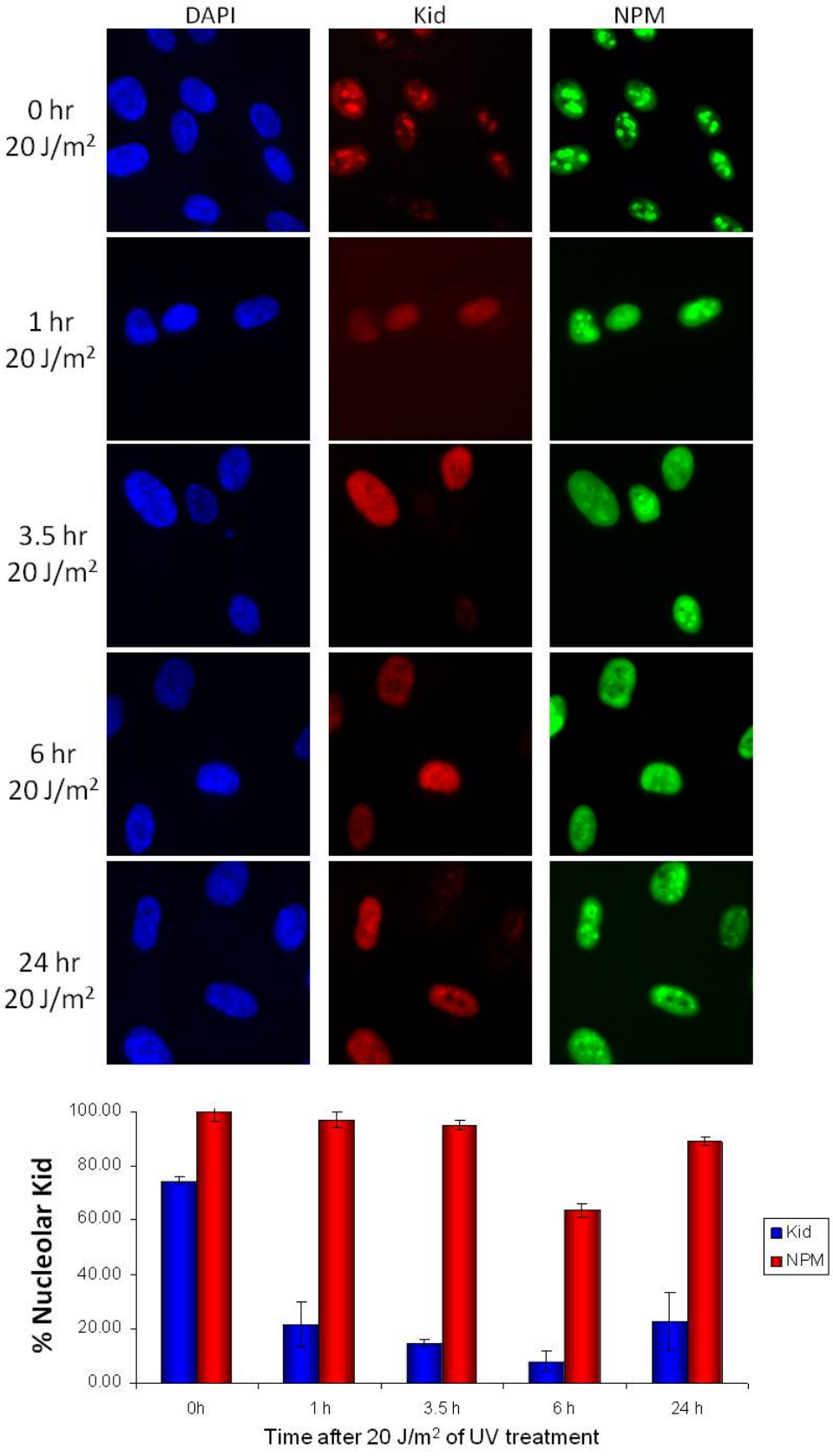
DAPI
Kid
NPM
0 hr
20 J/m2
1 hr
20 J/m2
3.5 hr
20 J/m2
6 hr
20 J/m2
24 hr
20 J/m2
% Nucleolar Kid
100.00
80.00
60.00
40.00
20.00
0.00
0h
1 h
3.5 h
6 h
24 h
Time after 20 J/m2 of UV treatment
Kid
NPM

Figure 3.4: Time course and immunofluorescence analysis after 20 J/m2 of UV-C.

Top: RPE1 cells were subjected to 20J/m^2 and were allowed to recover from 1-24 hrs.

Bottom: Quantitation of Kid and NPM shuttling from the nucleolus. Blue, DAPI; Red, Kid; Green, NPM. Kid was demonstrated to leave the nucleolus prior to NPM.

3.2.1.2 Kid translocates from the nucleolus to the nucleus after UV-C treatment in a microtubule-independent manner

Given the known motor function of Kid, we sought to address whether Kid alters its localization from the nucleolus to the nucleus by the use of microtubules. Cytoskeletal filaments, such as microtubules or actin, have never been found in the nucleus of mammalian cells, but their respective soluble components, β-tubulin and soluble actin, have been found within the nucleus. To determine whether the movement of Kid is dependent on the presence of microtubules, cells were treated with two different concentrations of nocodazole (0.1 μg/ml or 1 μg/ml) and were incubated for 1 hr prior to UV-C treatment (20 J/m^2) after which time cells were allowed to recover from the UV-C treatment with or without nocodazole. The results of this experiment demonstrate that the movement of Kid out of the nucleolus as well as the relocalization of Kid occurs through a microtubule-independent mechanism, as the absence of microtubules at any time did not alter the anticipated localization of Kid (Figure 3.5).

Figure 3.5

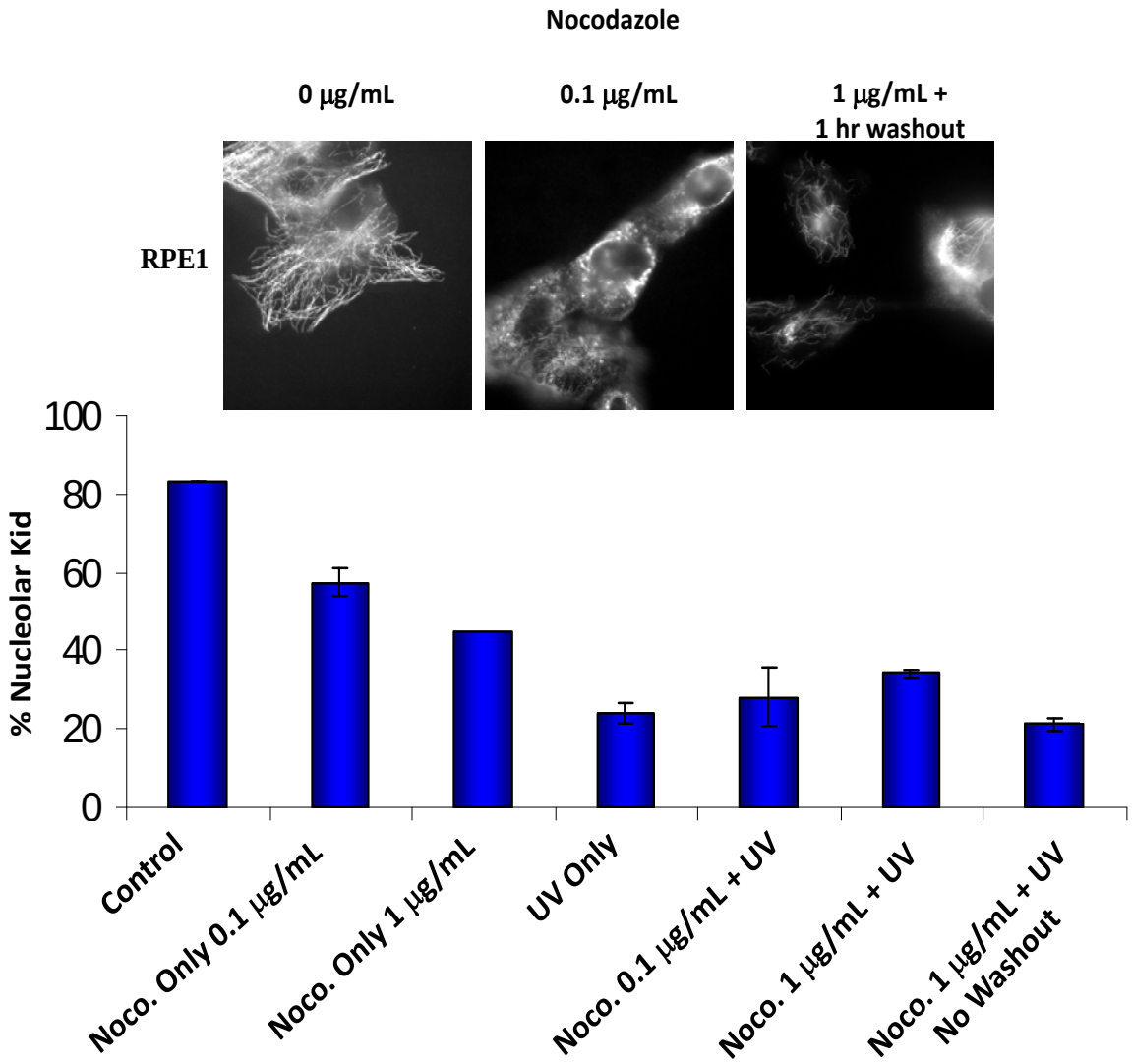

Figure 3.5: Kid staining decreases in the nucleolus after UV-C treatment in a microtubule-independent manner.

RPE1 cells were treated with or without nocodazole and/or 20 J/m^2 UV-C treatment. Immunofluorescence analysis (top) demonstrates microtubule depolymerization and quantitation (bottom) represents Kid localization after UV-C treatment. Noco=Nocodazole

3.2.1.3 Kid remains within the nucleolus after IR treatment

Given that Kid changes localization in response to UV-C treatment, we sought to determine the generality of this effect by challenging the cells with another form of cellular stress, ionizing radiation (IR). IR is a form of radiation that can cause DNA double-strand breaks (DSBs) (Zha, Alt et al. 2007). When RPE1 cells were treated with 0.1-1.2 Gy of IR and were allowed to recover for 24 hrs, Kid was found to remain within the nucleolus (Figure 3.6); interestingly, the nucleolar localization of Kid seemed to increase significantly. Similar results were also obtained for another cell line, UPCI:SCC103 cells, an oral squamous carcinoma cell line. Next, Kids recovery after IR treatment was examined using 0.4 Gy of IR, as this treatment was determined to give the lowest amount of DSBs, as assessed by immunoflorescence analysis of phospho-H2AX (Figure 3.7A). After 0.4 Gy of IR, Kid was found to remain within the nucleolus for all time points tested (5 min-24 hrs), thus demonstrating that Kid translocation is not triggered by all forms of DNA damage (Figure 3.7B,C). Additionally, Kid localization actually increased to the nucleolus after ionizing radiation in two different cell lines tested. This increase of nucleolar Kid localization is consistent across both, cancer and noncancer cell lines. Comparing the basal nucleolar Kid localization, one can anticipate that if this was a true physiological response that the cancer cells could be induced to localize Kid similar to noncancer RPE1 cells. Given that was not the case, the small increase is likely reflective of secondary effects caused by IR rather than changes in Kid activity.

Figure 3.6

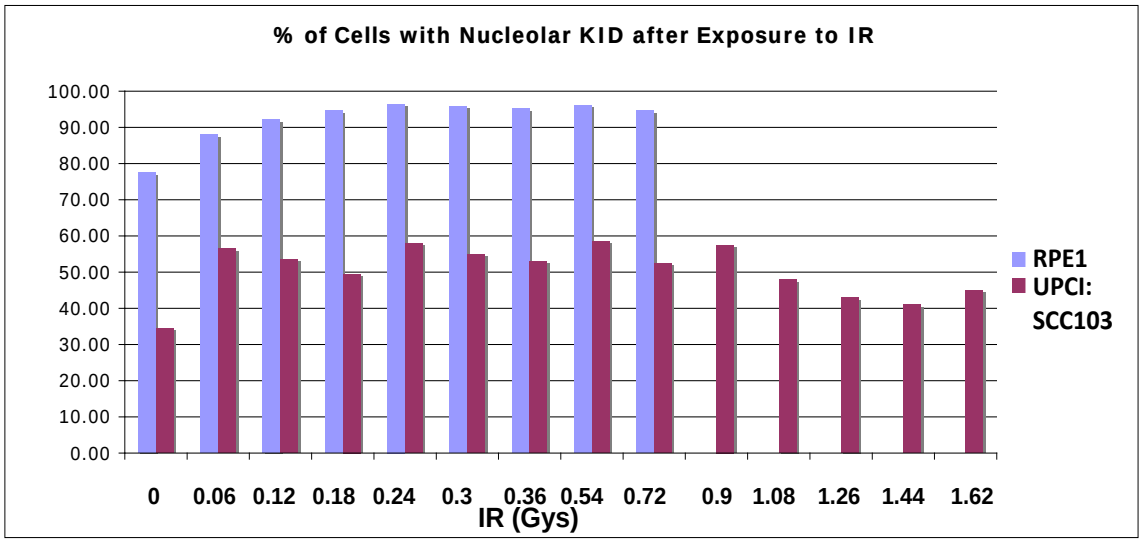

Figure 3.6: : Kid remains in the nucleolus after IR treatment.

RPE1 and UPCI:SCC103 cells were treated with varying doses of IR and were allowed to recover for 24 hrs prior to fixation and staining. No decrease in Kid staining was observed.

Figure 3.7

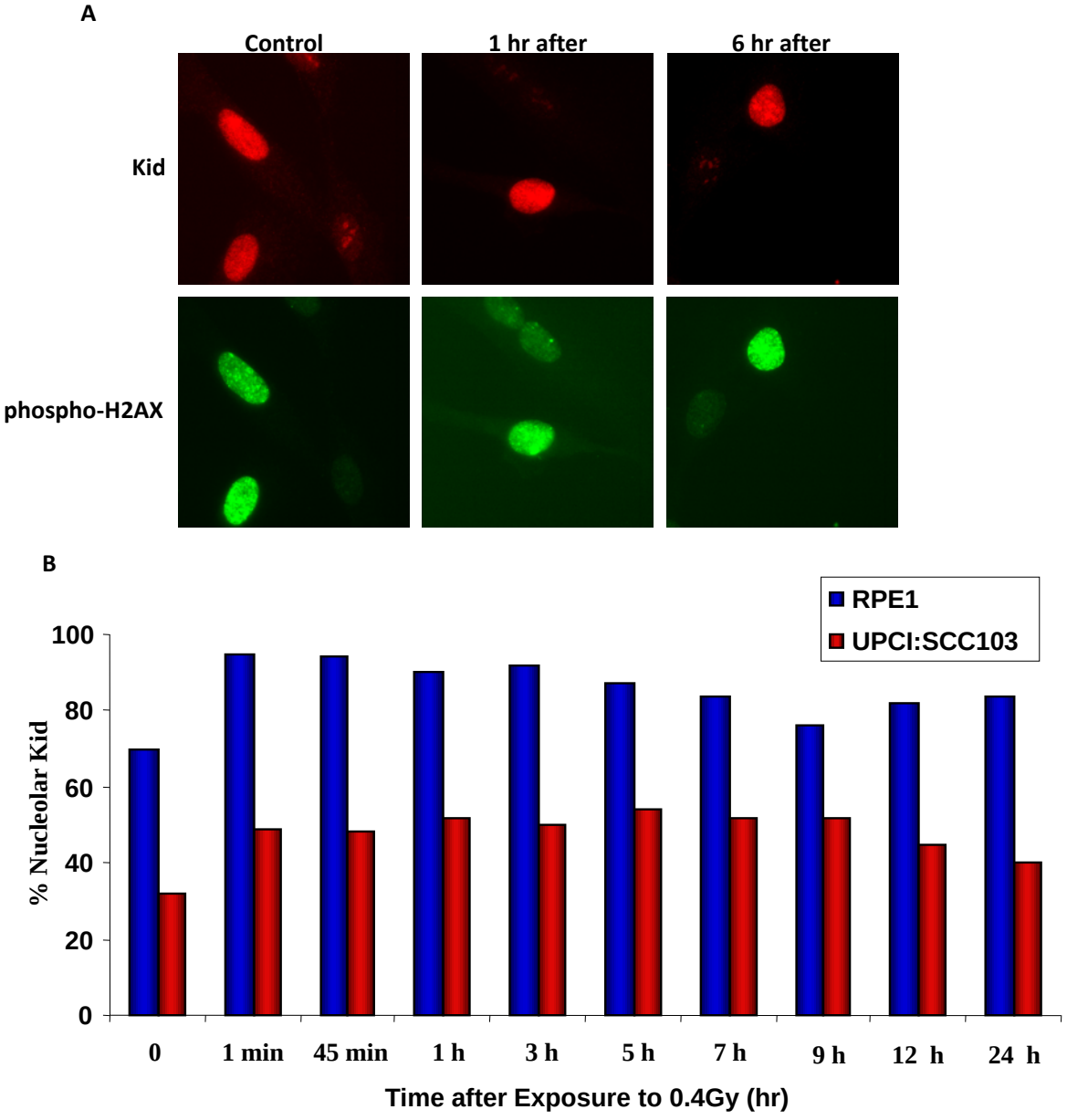
A
Control
1 hr after
6 hr after
Kid
phospho-H2AX
B
RPE1
UPCI:SCC103
% Nucleolar Kid
100
80
60
40
20
0
0
1 min
45 min
1 h
3 h
5 h
7 h
9 h
12 h
24 h
Time after Exposure to 0.4Gy (hr)

Figure 3.7 continued

C

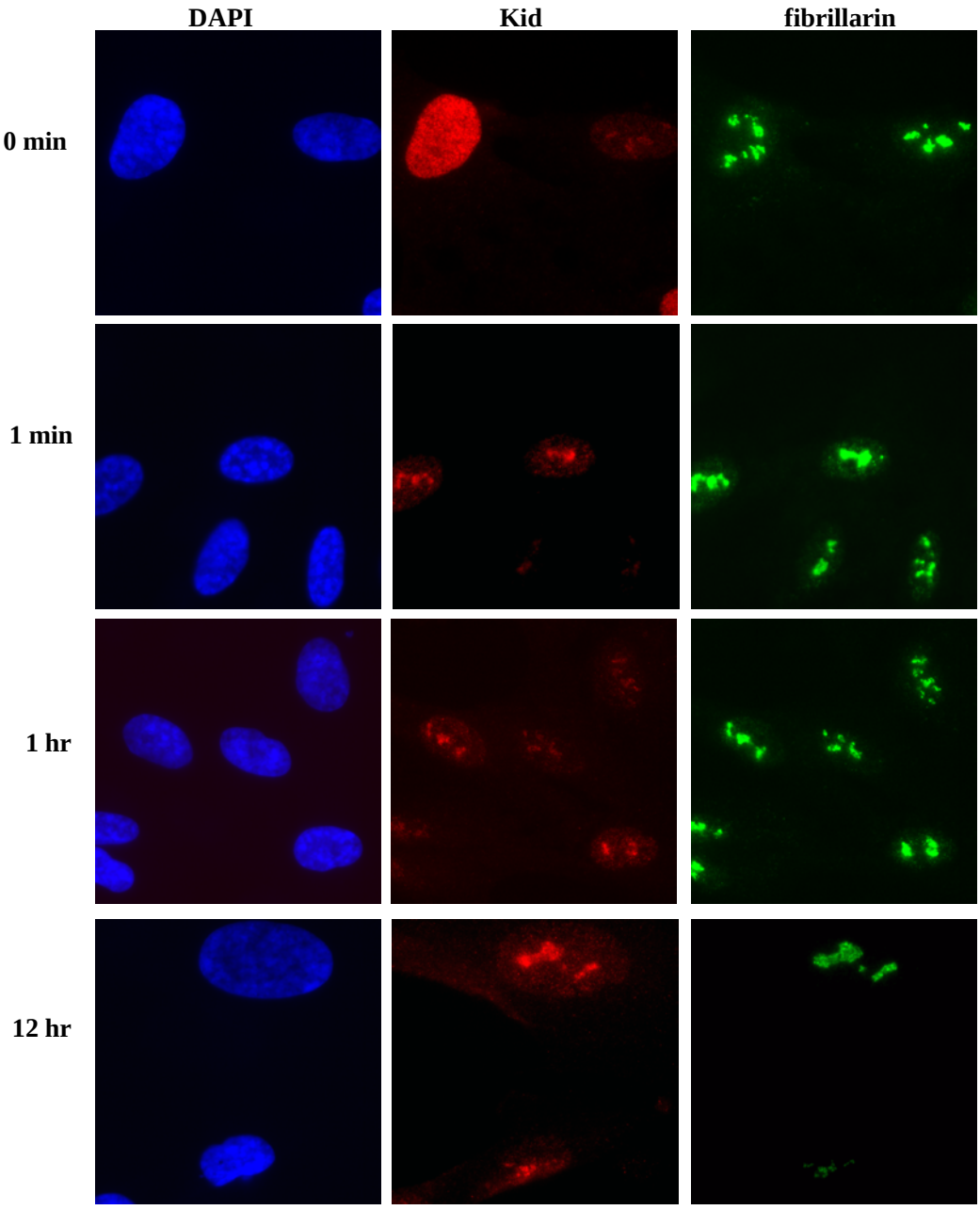

Figure 3.7: Kid localization after 0.4 Gy of IR.

(A)Immunofluorescence analysis of DSBs in RPE1, as demonstrated by phospho-H2AX foci, after 0.4 Gy of IR and the indicated recovery listed above images. Red, Kid; Green, phospho-H2AX. (B) Quantitation of Kid localization in RPE1 and UPCI:SCC103 cells after IR treatment. And recovery. (C) Immunofluorescence of RPE1 cells during recovery after 0.4 Gy of IR. Blue, DAPI; Red,Kid; Green, fibrillarin.

3.2.1.4 Kid localization inversely correlates with phospho-H2AX foci

Interestingly, in the previous experiment, upon examination of *untreated* control cells stained with phospho-H2AX, a DSB marker, an inverse correlation was observed between Kid nuclear localization and phospho-H2AX staining. In untreated cells that contain one or very few phospho-H2AX foci, Kid retained its localization to the nucleolus; however, in cells that contained an abundance of phospho-H2AX foci, Kid was found to translocate from the nucleolus to the nucleus (Figure 3.8). This correlation was observed in multiple cell lines suggesting a general phenomenon. Examination of the literature revealed that the presence of phospho-H2AX foci in *untreated* cells that are in S-phase for one of three possibilities: 1) as a result of stalled replication forks at sites of damage that occur during normal replication, 2) during a block in replication when DNA polymerase is stalled, resulting in a Y-shaped DNA structure (Takahashi and Ohnishi 2005). This structure is recognized by a nuclease that nicks the template strand DNA near the blocking lesion resulting in a DSB, which is recognized by phospho-H2AX. 3) phospho-H2AX may recognize multiple SSB in close proximity to each other as DSB and therefore become upregulated (Takahashi and Ohnishi 2005). In either of these cases, the

upregulation of phospho-H2AX during S-phase along with the inverse correlation of nuclear Kid localization, implied that the 15% cells containing nuclear Kid were probably a reflection of cells in S-phase, thus, the localization of Kid maybe cell cycle dependent.

Figure 3.8

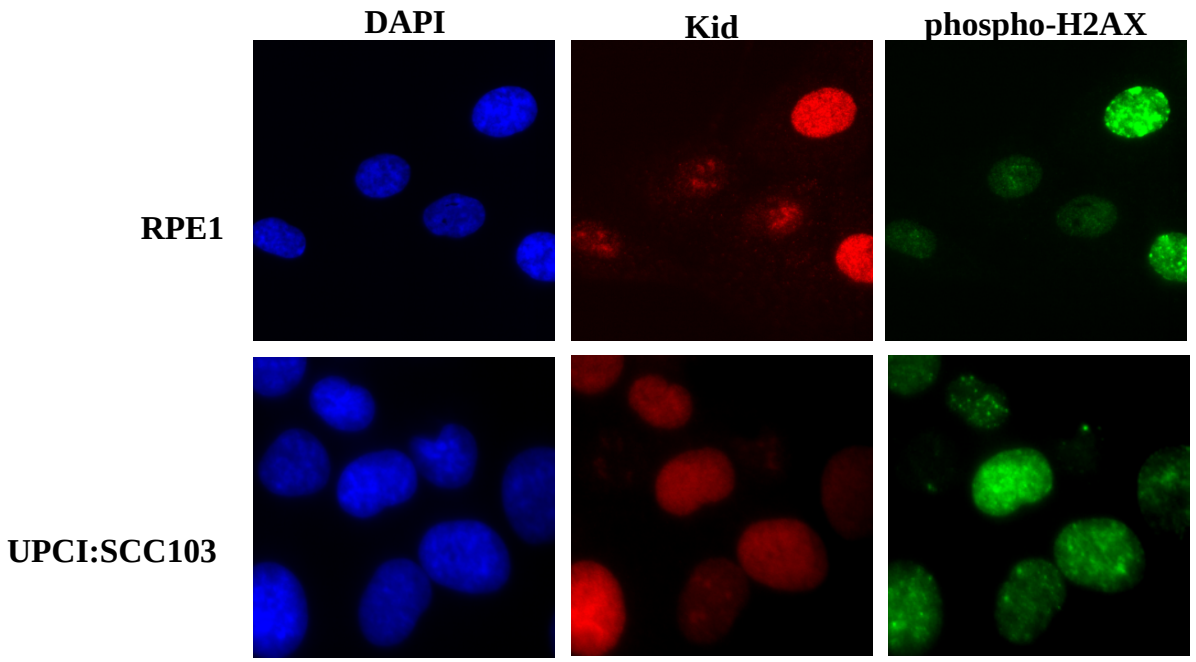

Figure 3.8: Inverse correlation between Kid localization and phospho-H2AX foci.

In untreated RPE1 and UPCI:SCC103 cells, an inverse correlation was observed between Kid localization and phospho-H2AX foci; nuclear Kid was found in cells containing phospho-H2AX foci, while nucleolar Kid was in cells containing little to no foci. Blue, DAPI; Red, Kid; Green, phospho-H2AX.

3.2.1.5 Differences between UV-C and IR treatment

As we observed opposite results for Kids response to the cellular stresses, UV-C and IR, we began to investigate the differences between these treatments. There are four known differences between IR- and UV-induced damage that may account for the differences observed in the experiments above: (1) UV damage causes SSB and is sensed through PARP-1 (poly (ADP-ribose)-1) (de Murcia, Niedergang et al. 1997) and responded to by ATR (ATM- and Rad3-related) (Garcia-Muse and Boulton 2005), while IR causes DSB is responded to by ATM (ataxia-telangiectasia mutated) (Shiloh 2001), (2) UV inhibits transcription, whereas IR does not, (3) sufficiently high exposure of UV causes disassembly of the nucleolus while IR appears to have no effect on the nucleolus, (4) damaged DNA is repaired rapidly in response to IR treatment, whereas DNA damage response is slower in UV treatment due to the formation of bulky adducts (Parrilla-Castellar, Arlander et al. 2004).

3.2.1.6 Kid remains within the nucleolus after H_2O_2 treatment to cause SSBs

To begin to dissect the differences in Kid localization, SSBs and DSBs were examined in more detail. As UV-C treatment causes SSB, resulting in a redistribution of Kid from the nucleolus to the nucleus, while IR causes DSBs and exerts no effect on the localization of Kid, we sought to determine if Kid is responding to the presence of SSB. Hydrogen peroxide (H_2O_2) treatment is known to cause SSBs at low doses (< 30 mM) and DSBs at high doses (>30 mM) leading to oxidative stress and DNA base damage (Dahm-Daphi, Sass et al. 2000; Karmakar and Bohr 2005). Therefore, cells were treated with low doses of 0.1 mM and 0.5 mM of H_2O_2 for 10 and 30 min, followed by a 1 hr recovery and immediate fixation. Interestingly, Kid localization

remained almost unchanged; a small 20% reduction was observed, but was not similar to the effect seen after UV-C treatment causing SSBs (Figure 3.9). Therefore, it seems as though Kid may be responding to a secondary effect of the UV-C treatment rather than directly localizing in response to the presence of SSBs.

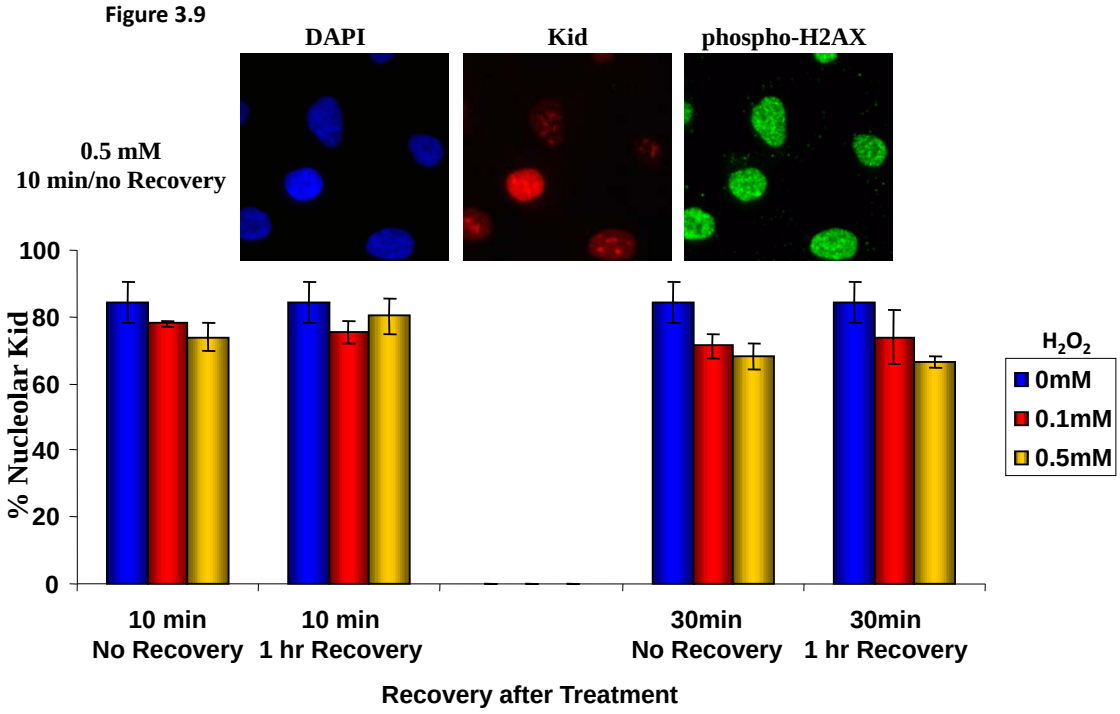

Figure 3.9: Kid localization in response to H2O2 treatment.

RPE1 cells were treated with either 0.1 or 0.5 mM of H_2O_2 for 10 min or 30 min, followed by a 1 hr recovery. Blue, DAPI; Red, Kid; Green, Phospho-H2AX. Immunofluorescent images are shown above and quantitation of Kid nucleolar localization is below. No change in Kid localization was observed after DNA breaks were induced by H_2O_2.

3.2.1.7 Kid does not localize to the site of DNA damage

We next determined if Kid may be localizing in response to sites of DNA damage. In these experiments, a filter containing an 8 μm pore membrane was placed on top of a coverslip containing cells and was exposed to UV-C. The size of the pores are so small that most of the cell will be covered by the membrane except for a small 8 μm area. If Kid was a DNA damage response protein, then in the presence of the damage, Kid would robustly localize to the area of the cell that was exposed to the damage in order to begin to repair the damage. The dosage of UV used varied from 10-80 J/m^2, and cells were allowed to recover from 5 min to 4 hrs, after which cells were fixed and stained with antibodies to Kid or cyclopyrimidine dimers (CPD), bulky adducts that form after UV treatment. First, we analyzed the localization of Kid in response to this treatment with cells that contained only one CPD lesion within the nucleus; in each of these cases, Kid did not to shuttle, move or localize to these sites of damage, therefore arguing against the interpretation that Kid may change localization in response to DNA damage only in the nucleolus. (Figure 3.10). We next investigated whether Kid may function as a general cellular stress sensor by examining cells with more than one lesion per nucleus. In each of the 300 cells examined, Kid retained localization within the CPD region unless, the CPD region was found to occur within the nucleolus. When a CPD dimer was found in the nucleolus, we found Kid to no longer localize there; hence, Kid may respond to this damage specifically in the nucleolus by reducing its presence in the nucleolus.

Figure 3.10

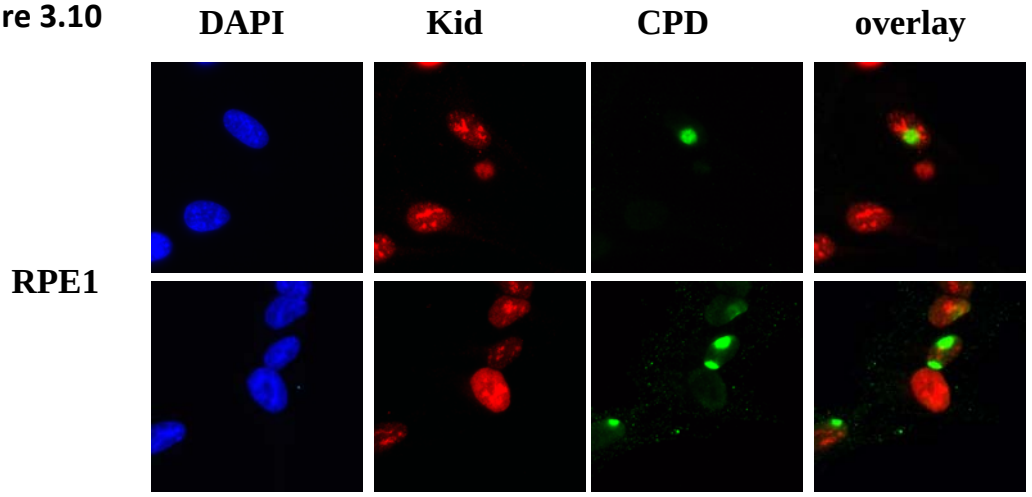

Figure 3.10: Kid does not localize to sites of DNA damage.

Localized UV-C damage experiments were conducted by placing an 8 micron pore membrane on top of a glass coverslip, prior to UV-C treatment. Cells were fixed 1 hr after UV-C. and were co-stained for Kid or CPD.

3.2.1.8 Cells are more sensitive to UV-C treatment after Kid knockdown

Next, we inquired whether cells may be more sensitive to UV-C treatment (i.e., DNA damage) after Kid knockdown. Cells were treated with siRNA constructs targeted against Kid for 72 hrs prior to being treated with 5-200 J/m^2 of UV-C, after which cells were allowed to recover for up to 24 hrs and an MTS cell proliferation assay was completed. Although general trends did emerge from this experiment such as at doses between 100-200 J/m^2 little to no change in viability is observed between siControl and siKid. Additionally, at lower doses of 5-80 J/m^2, a 20-50% reduction in cell proliferation was observed after Kid knockdown. However the results

of the experiments were difficult to interpret due to variability in Kid localization; this result can likely be attributed to cellular arrest due loss of Kid (Figure 3.11).

Figure 3.11

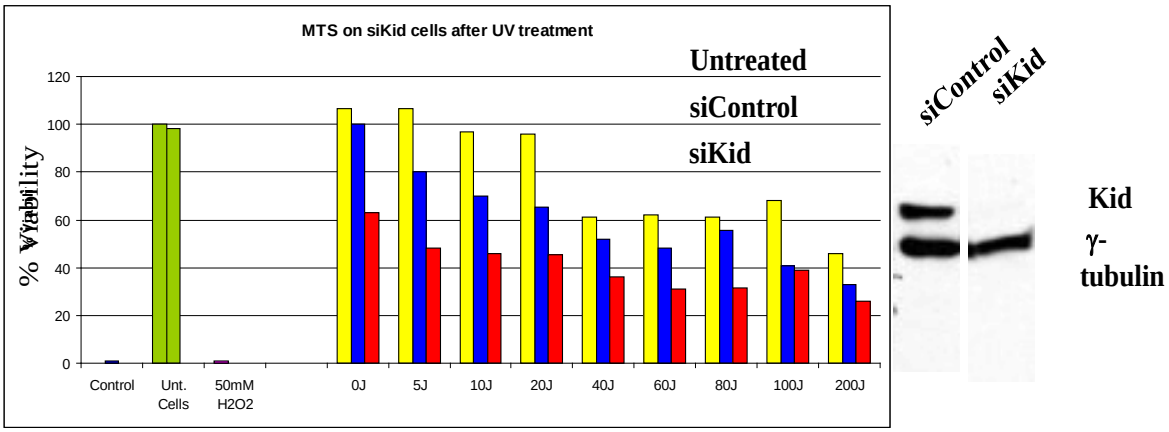

Figure 3.11: RPE1 cells are more sensitive to UV-C damage after Kid knockdown.

Left: Kid was knocked-down for 72 hrs in RPE1 cells prior to treatment with various doses of UV-C and completion of the MTS cell proliferation assay. Untreated cells and H2O2 treatment were used as positive controls for this experiment. Right: Immunoblotting demonstrating equal loading and Kid knockdown.

3.2.1.9 Kid translocated from the nucleolus after caffeine treatment

Next, another type of DNA damage treatment was used, caffeine when used at low concentrations is a known inhibitor of PI3K, which in turn inhibits ATM/ATR and the DNA damage response pathway, and at high concentrations to cause DNA strand breaks(Araya, Hirai

et al. 2005). Therefore, we inquired how Kid would respond to these DNA strand breaks. Cells were treated for 1 hr with 4 mM of caffeine, prior to fixation and staining. Interestingly, as observed with UV treatment, Kid changed localization from the nucleolus to the nucleus, suggesting that Kid localization to the nucleolus is quite sensitive to damage within the nucleolus (Figure 3.12).

Figure 3.12

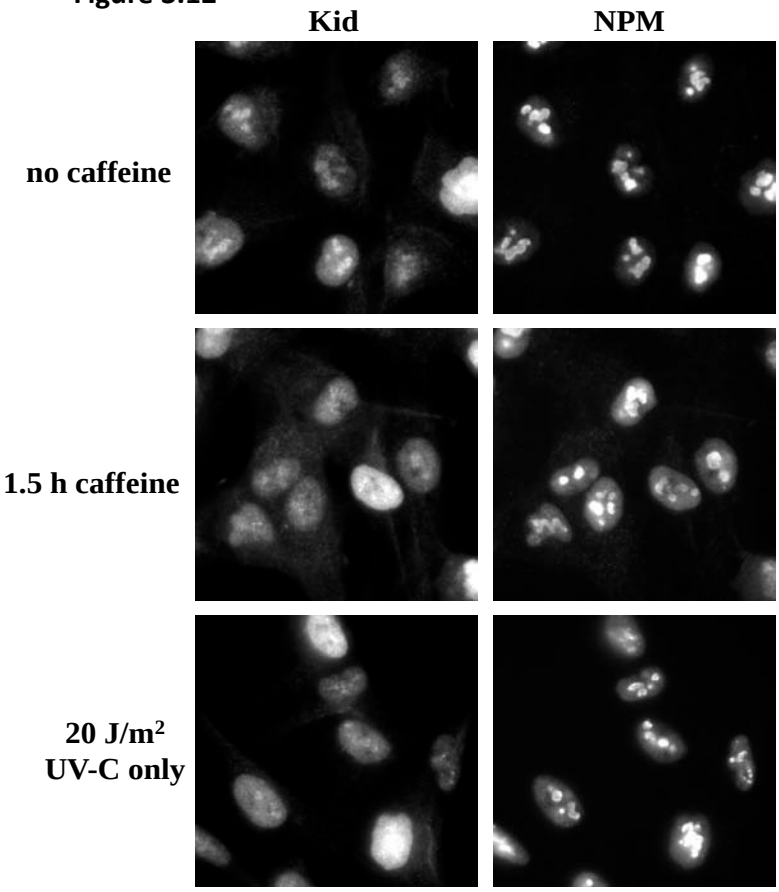

Figure 3.12: Caffeine treatment causes Kid to change localization.

RPE1 cells treated with or without 4 mM caffeine for 1.5 hrs , followed by fixation, staining, and quantitfication. Images demonstrate similar diffuse localization as UV-C treatment.

3.2.2 Kid translocates from the nucleolus in a p53-independent manner

As we have shown Kid localizes to the nucleolus >80% in normal cells, while in cancer cells Kid localizes to the nucleolus <35% of cells. As a common feature of a great majority of cancer cell lines is loss or mutated p53 (Collins, Jacks et al. 1997) especially within DNA binding sites, we first inquired whether Kid localization to the nucleolus was dependent on p53 and secondly, if Kid shuttling from the nucleolus to the nucleus after UV treatment was dependent on p53. To investigate the first question, we used mouse embryonic fibroblast cells, proficient or deficient in p53. Kid was found to localize to the nucleolus in both p53+/+ cells and p53-/- cells. There was a 15% decrease in the number of cells localizing to the nucleolus in p53-/- cells, but it was insignificant, therefore suggesting that Kid localizes to the nucleolus in a p53-independent manner and this cannot account for the difference observed in noncancer versus cancer cells (Figure 3.13).

Figure 3.13

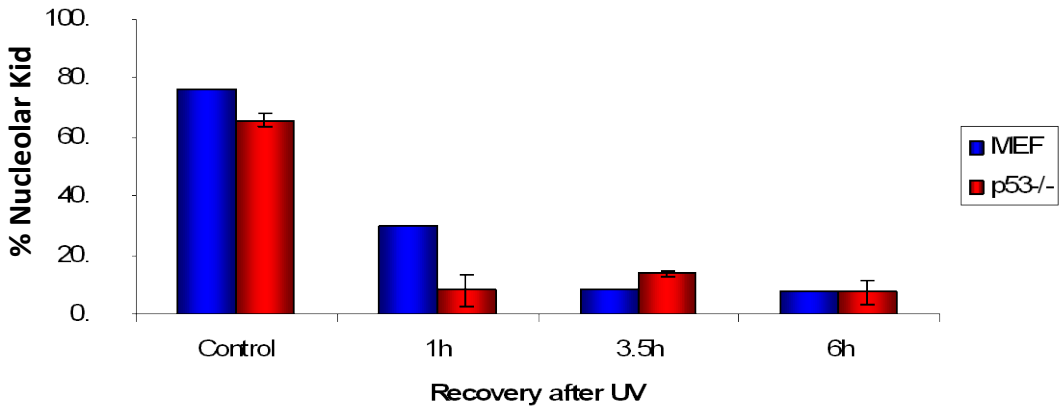

Figure 3.13: Kid localization to the nucleolus and Kid's shuttling ability after UV-C treatment is independent of p53.

Mouse embryonic fibroblasts proficient or deficient in p53 were subjected to UV-C treatment and allowed to recover for 1-6 hrs. Blue bars=MEF; Red Bars=p53 -/-.

3.2.3 Kid translocates from the nucleolus after RNA pol I inhibition

As we previously identified that Kid is not responding to a specific type of DNA damage, SSBs or DSBs, it is possible that Kid is responding to a secondary effect caused by the UV-C damage within the nucleolus. Therefore, we sought to investigate the hypothesis that Kid changes localization in response to transcriptional inhibition in the nucleolus. As mentioned previously, as a difference between UV-C and IR treatment is that UV-C inhibits transcription, whereas IR does not (Parrilla-Castellar, Arlander et al. 2004). Response to transcriptional inhibition within

the nucleolus finds support in the localized UV-C treatment experiments wherein Kid only altered its localization in response to damage with the nucleolus, while remaining within the CPD foci when the damage occurred in the nucleus. Consequently, we used two different transcriptional inhibitors to test this hypothesis. The first was actinomycin D which is an inhibitor of RNA polymerase I, the main polymerase that transcribes rRNA with the exception of the 5S rRNA (Shcherbik, Wang et al. 2010). The second is the RNA polymerase II inhibitor α-amanitin. RNA polymerase II transcribes all nonribosomal genes (Lindell, Weinberg et al. 1970). α -amanitin when used at concentrations lower than 1 μg/ml preferentially inhibits RNA polymerase II; however at high concentrations (>1 μg/ml) inhibition of RNA polymerase III is observed. RNA polymerase III is responsible for the transcription of 5S rRNA, tRNAs and other small RNAs.

3.2.3.1 Kid translocates from the nucleolus after actinomycin D treatment

Cells were treated with varying concentrations of actinomycin D, ranging from 0.01 to 1 μg/ml and as previously published data suggests, higher concentrations of actinomycin D will not only inhibit RNA polymerase I, but it will also lead to nucleolar breakdown, as once ribosomal RNA transcription is completely inhibited, the nucleolus will break apart (Misteli 2003). In RPE1 cells, nucleolar breakdown began to occur at concentrations above 0.5 μg/ml, as fibrillarin, the nucleolar control, began to relocalize with the granular component of the nucleolus rather than the fibrillar center. Such loss of localization is suggestive of loss of nucleolar integrity. Interestingly, while observing Kid localization in response to actinomycin D, with concentrations as low as 0.01 μg/ml, Kid was found to leave the nucleolus in response to RNA polymerase I inhibition, suggesting that inhibition of nucleolar transcription is a signal for Kid to leave the nucleolus (Figure 3.14).

Figure 3.14

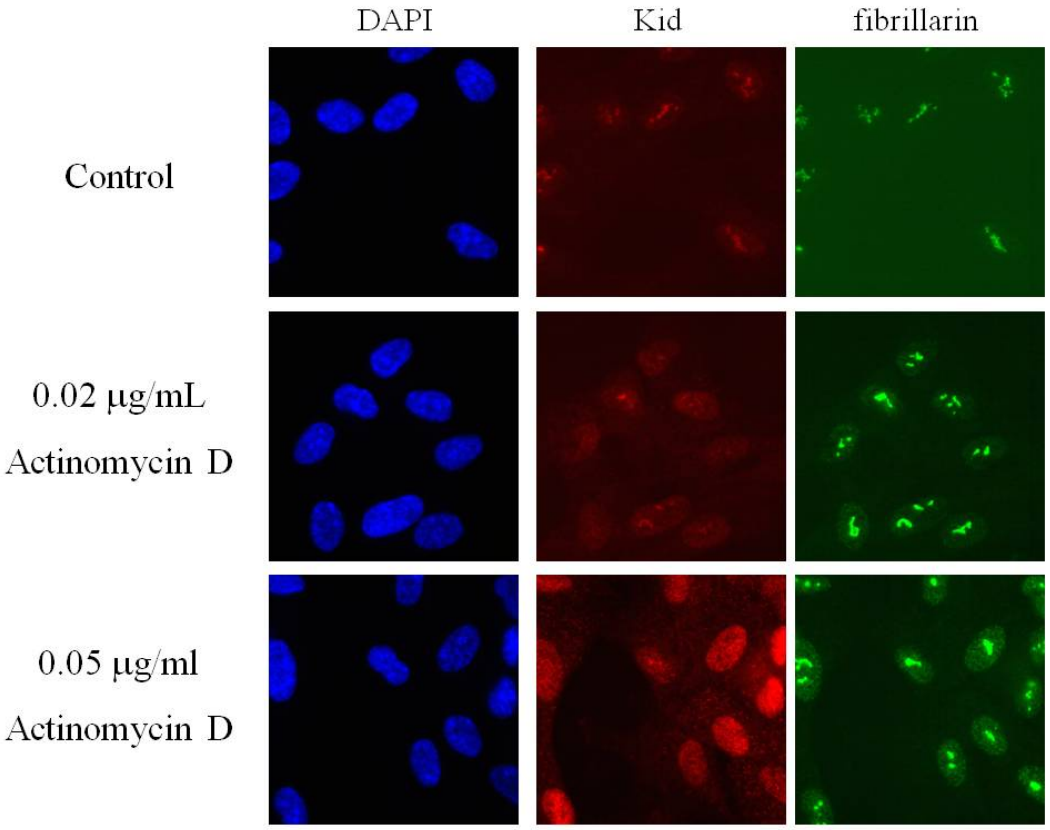
DAPI
Kid
fibrillarin
Control
0.02 µg/mL
Actinomycin D
0.05 µg/ml
Actinomycin D

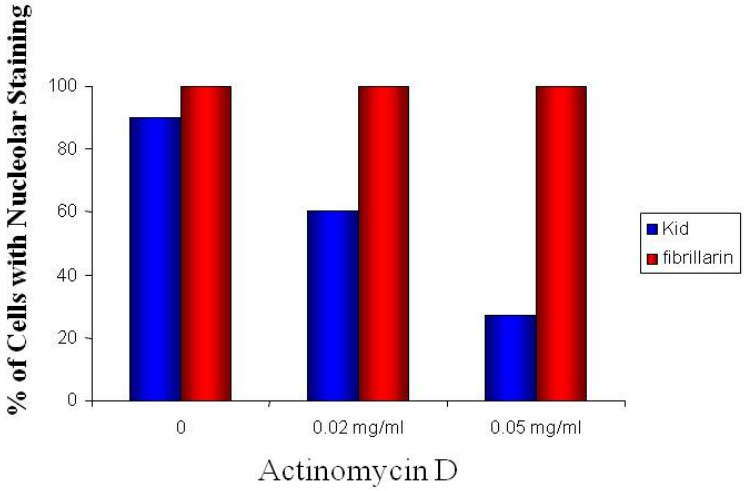
% of Cells with Nucleolar Staining
100
80
60
40
20
0
0
0.02 mg/ml
0.05 mg/ml
Actinomycin D
Kid
fibrillarin

Figure 3.14: Kid was no longer concentrated in the nucleolus after RNA pol I inhibition.

RPE1 cells were treated with actinomycin D, to inhibition RNA pol I. for 30 min, followed by fixation and staining. Top represent images after treatment, bottom represents quantification of Kid nucleolar localization (blue bars) or fibrillarin (red bars). Blue, DAPI; Red, Kid; Green, fibrillarin.

3.2.3.2 Kid remains within the nucleolus after α -amanitin treatment

We next investigated whether Kid also changes localization in response to α -amanitin treatment using three different concentrations and two different time points of 1 hr or 3 hrs of treatment. Interestingly, at concentrations known to preferentially inhibit RNA polymerase II (less than 1 μg/ml) (Lindell, Weinberg et al. 1970), Kid remained within the nucleolus. However, at concentrations greater than 1 μg/ml, we observed a 10-20% loss in Kid nucleolar localization (Figure 3.15). The known loss selectivity of α -amanitin at these concentrations could suggest that Kid is responding to inhibition of RNA pol III, the polymerase involved in rRNA synthesis of the 5S rRNA. Therefore these experiments are consistent with changes in Kid localization from the nucleolus to the nucleus in response to transcription inhibition of rRNA.

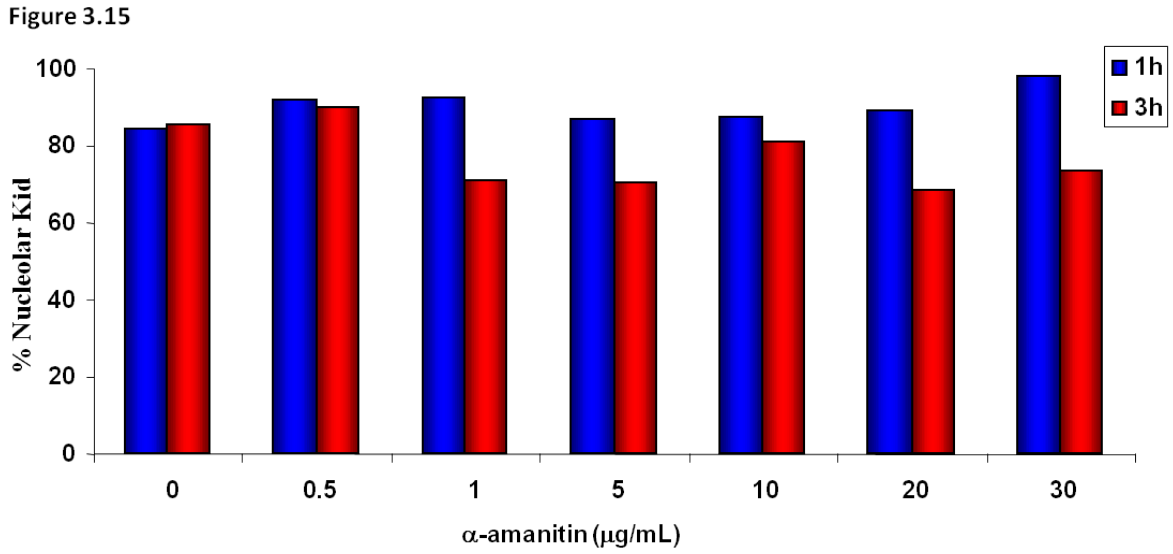

Figure 3.15: Kid remained within the nucleolus after RNA pol II inhibition.

Cells were treated with various amounts of alpha-amanitin for 1 or 3 hrs to inhibit RNA pol II or mRNA transcription. After treatment, cells were fixed and stained for Kid and fibrillarin.

3.2.4 Kid is dephosphorylated after UV-C treatment

Two-dimensional gel electrophoresis was used in the presence or absence of UV-C treatment in order to identify post-translational modifications of Kid that may occur under the same conditions which induced a change in nucleolar localization. Cells were treated with or without 20 J/m^2 of UV-C treatment, followed by a 1 hr recovery, prior to subjection to 2D gel electrophoresis and subsequent western blot analysis. Interestingly, in the absence of UV-C treatment, 3-5 different bands representing Kid were observed (Figure 3.16A). These bands ranged in pI from 3-10, suggesting that under normal homeostasis, Kid contains various post-

translational modifications. However, after the 20 J/m^2 of UV-C treatment, followed by a 1 hr recovery, the bands corresponding to Kid uniformly shifted to a pI of 10 representing basic or more negative post-translational modifications (Figure 3.16B). This shift in the pI of the protein occurs under conditions known to cause Kid translocation to the nucleus.

Next, as Kid is known to contain various sites for phosphorylation, we inquired whether this shift to a more negative state was due to phosphorylation of Kid after UV-C treatment. Therefore, cells were treated with and without shrimp alkaline phosphatase (SAP) in the presence and absence of UV-C treatment (Figure 3.16C). Interestingly, the changes observed in the presence of SAP indicated that the prominent form of Kid is dephosphorylated after UV-C treatment (corresponding to the band at a pI of 10). It is an open question as to whether this dephosphorylation event triggers the translocation of Kid or whether the Kid translocates to the nucleus and becomes dephosphorylated.

Figure 3.16

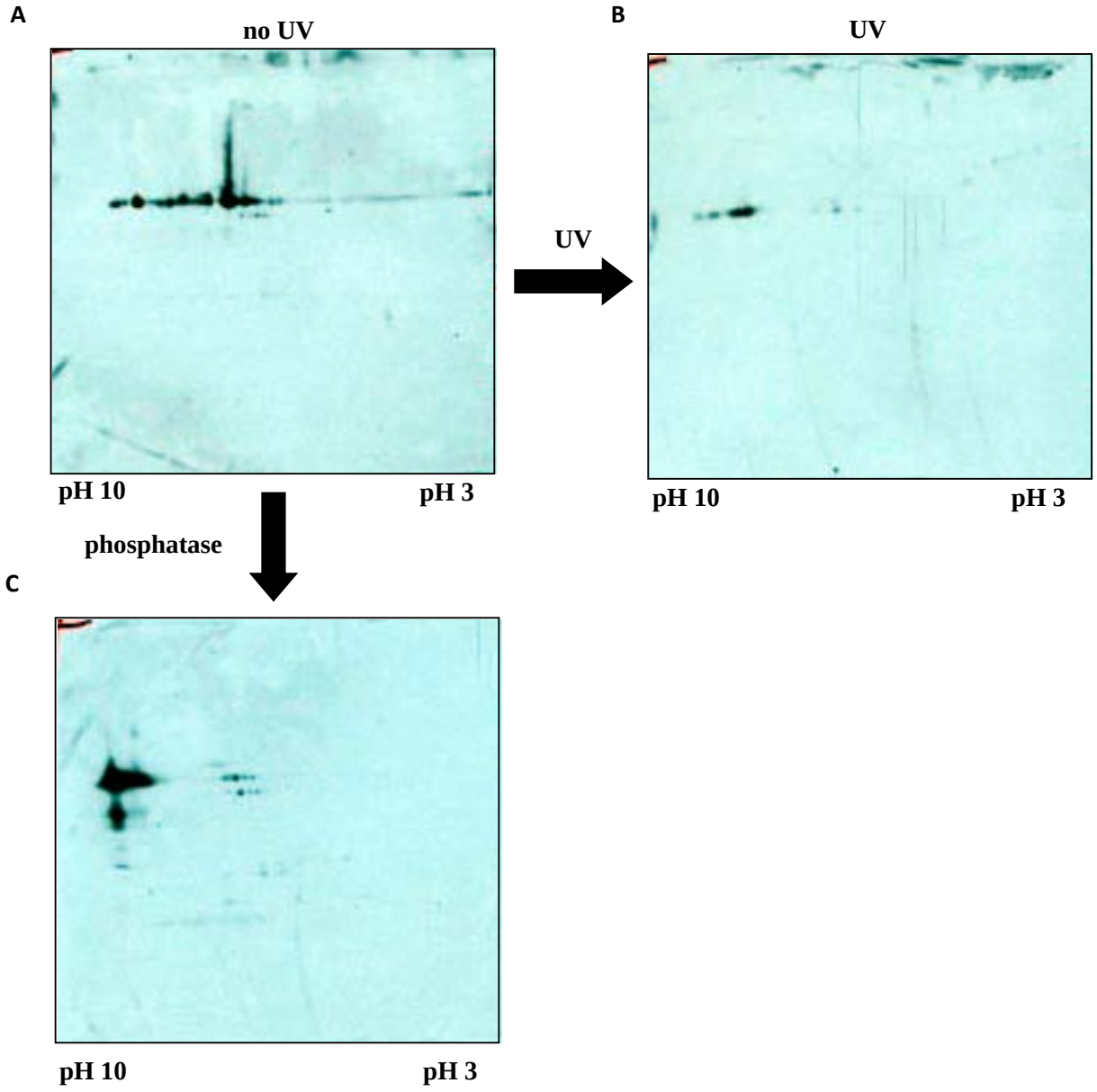

Figure 3.16: Kid is phosphorylated in the nucleolus.

2D gel electrophoresis before (A) or after(B) UV-C treatment or after phosphatases (C) treatment. B and C look similar suggesting that Kid is dephosphorylated after UV-C treatment, when it is found in the nucleus.

3.3 SUMMARY

Collectively the sum of this data demonstrates that Kid localizes to the nucleolus only during conditions of rRNA gene transcription. Therefore, suggests that Kid likely functions in the ribosome pathway, rather than DNA damage or other types of stress response.

3.4 DISCUSSION

3.4.1 Kid function in ribosomal biology

As this data demonstrate Kid changes localization in response to rRNA transcription, it is hypothesized that Kid may play a role in ribosome biogenesis, similarly to NPM (Lim and Wang 2006). As Kid does contain a nucleic acid-binding domain, which has been shown to bind DNA during mitosis (Tokai, Fujimoto-Nishiyama et al. 1996), it is very plausible that Kid can also bind RNA or pre-ribosomes during interphase, especially given that Kid is found to localize where rRNA transcription and processing takes place. The function of Kid is demonstrating to be quite similar to NPM is more ways than one, which was discussed in Chapter 2 and was further discussed in Chapter 3, and it is interesting that Kid may function in similar roles as NPM in ribosomal processing and even transport. The similarities between Kid and NPM include:

1) They localize to the same part of the nucleolus.
2) They both utilize a GTP-dependent shuttling mechanism.
3) Localization of both of these proteins are cell-cycle dependent, such that during S-phase they localize outside of the nucleolus.
4) They both co-fractionate with pre-ribosomes (as will be discussed in chapter 4).
5) Both localize to chromosome arms during mitosis (Okuwaki, Tsujimoto et al. 2002).
6) Both are required for congression of chromosomes and proper mitotic spindle formation (Amin, Matsunaga et al. 2008).
7) Both are phosphorylated by cdc2 at the onset of mitosis (Okuwaki, Tsujimoto et al. 2002).

As NPM is involved in ribosomal processing and even transport, it is very possible that Kid performs the same or very similar function as NPM.

Furthermore, as Kid is found to also localize to where the rRNA genes are located, future experiments using chromatin immunoprecipitation experiments would prove useful to identify if Kid may bind to the rRNA genes, similar to NPM.

3.4.2 Kid as a proliferation marker?

It is interesting to note that when cells are greater than 90% confluent, we have found that cells enter senescence, and during this time Kid becomes degraded (Figure 3.17). Senescence was determined by proliferation marker Ki67 and Kid by immunoblotting. Therefore experiments with Kid should always be completed with subconfluent populations of cells.

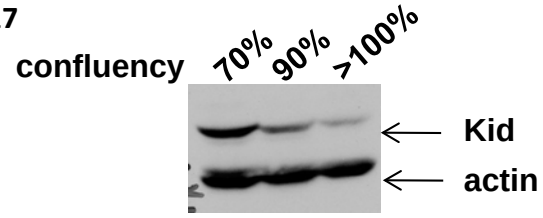

Figure 3.17: Kid levels decrease when cells are over confluent.

RPE1 cells were grown and lysed at 70%, 90% or over 100% confluency. These lysates were run on 10% SDS-PAGE gels and subjected to immunoblotting.

4.0 CHAPTER IV: IDENTIFICATION AND CHARACTERIZATION OF MICROTUBULE MOTOR EG5 FUNCTION IN SUPPORT OF THE RIBOSOMES PROCESSIVITY

4.1 INTRODUCTION

As discussed in chapter 3, the localization of Kid changes in response to DNA damage and inhibition of transcription in the nucleolus, thus it seems Kid's localization may depend on ribosome biogenesis. To determine whether Kid functions in this process, we began examining whether Kid, along with the other nucleolar-associating motors Eg5 and MKLP1, may associate with the pre-ribosomal subunits via fractionation of the nucleus.

4.2 RESULTS

4.2.1 Functional association of nucleolar-associating motors with various ribosomal subunits

4.2.1.1 Association of nucleolar-associating motors with pre- and/or mature ribosomes

Nuclear lysates from 30 million RPE1 cells were layed on a 10-25% sucrose gradient before being centrifuged and collected in one milliliter fractions with constant monitoring at an absorbance of 260 nm. Each fraction was TCA-precipitated and subjected to immunoblot analysis. In this assay, Kid was found to co-fractionate with both the pre-40S and pre-60S ribosomal subunits, as confirmed by co-localization with the ribosomal protein S7 (rpS7), which is part of the pre-40S ribosome, and NPM, which is a component of the pre-60S ribosome (Yu, Maggi et al. 2006) (Figure 4.1A); it should be noted that rpS7 was found co-fractionating with the pre-40S and pre-60S subunits, but this is not uncommon, as ribosomal proteins sequences are quite similar and antibody cross-reactivity between different subunits is frequently observed (Bartsch 1985). Under the same fractionation conditions, MKLP1 was found to co-fractionate with pre-60S, while Eg5 was not detected in the nuclear extracts. These results can be rationalized by noting the subnucleolar localization of each motor. Antibodies to both Kid and MKLP1 reacted strongly with the nucleolus, while antibodies to Eg5 bound less efficiently. Thus the absence of Eg5 from the pre-ribosomal subunits was not entirely unexpected.

As Kid and MKLP1 co-fractionated with pre-ribosomal subunits, we sought to determine if any of the nucleolar motors may also associate with mature cytoplasmic ribosomes, where translation occurs. Accordingly, whole cell lysates from 30 million RPE1 cells were layed on 10-25% sucrose gradients, centrifuged, fractions were collected, TCA-precipitated and immunoblotted as described above previously. After immunoblot analysis, Kid and Eg5 were found to co-fractionate with the 40S, 60S, 80S, and polysomal fractions, while MKLP1 was found to co-fractionate with the mature 60S ribosome Figure 4.1B); Eg5 co-fractionation with polysomes can be better observed in Figure 4.1C. In addition, all of the Eg5 protein was found to co-fractionate with the ribosomes, as none of the Eg5 was found in the discarded DNA pellet, (data not shown) while a majority of the Kid associated with both the ribosomes and the DNA pellet. This data demonstrates that these motors remain associated with the ribosomes during translation. We believe Eg5, MKLP1, and Kid are pioneering members of a new class of motors, the *ribosomal motors*. However it is important to note that not all proteins or motors co-fractionate with ribosomes, as two other proteins tested, cytoskeletal actin and the microtubule motor dynein, were found to not co-fractionate with ribosomes (Figure 4.1B).

Figure 4.1

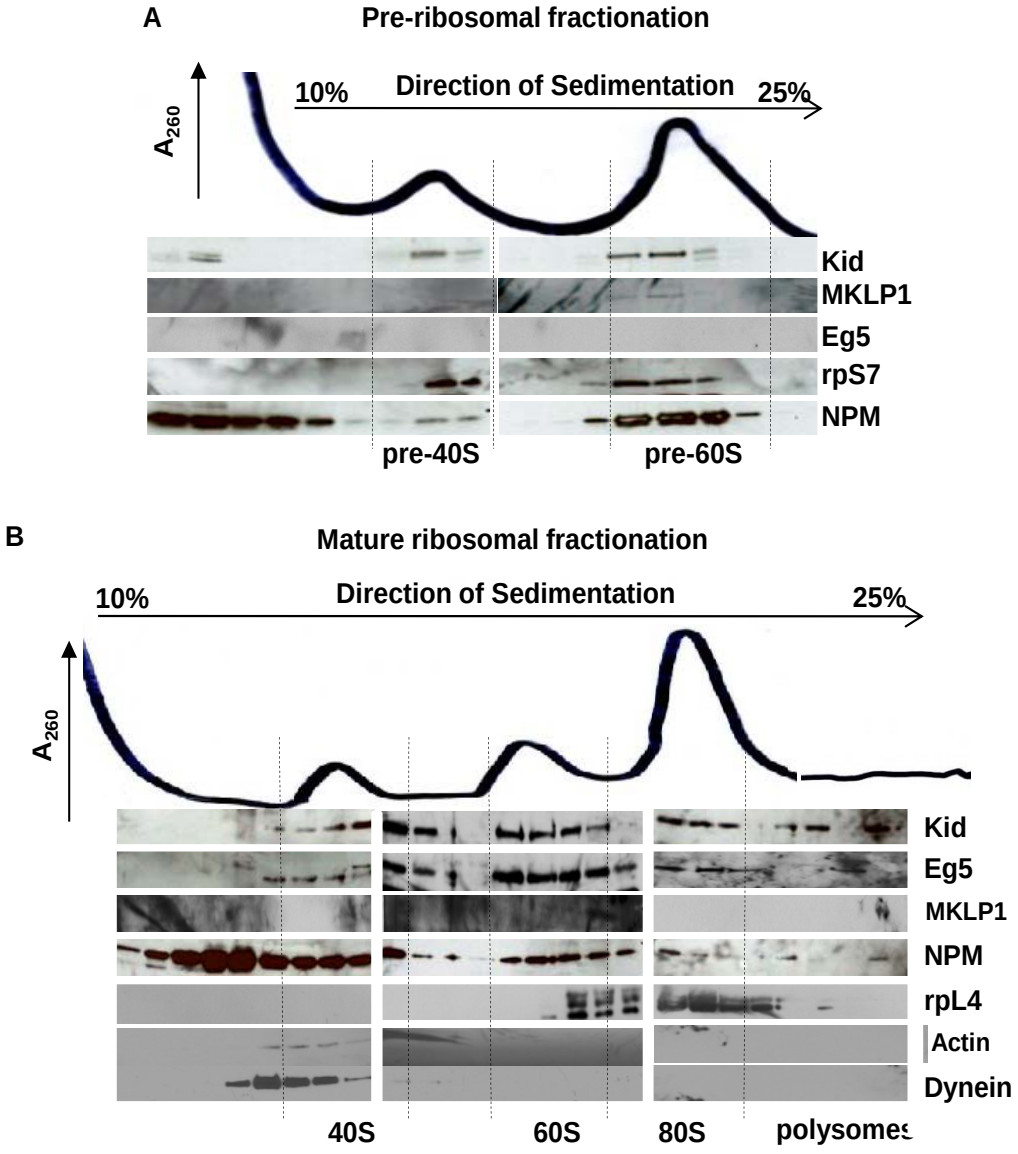
A
Pre-ribosomal fractionation
10%
Direction of Sedimentation
25%
A260
Kid
MKLP1
Eg5
rpS7
NPM
pre-40S
pre-60S
B
Mature ribosomal fractionation
10%
Direction of Sedimentation
25%
A260
Kid
Eg5
MKLP1
NPM
rpL4
Actin
Dynein
40S
60S
80S
polysomes

Figure 4.1 continued

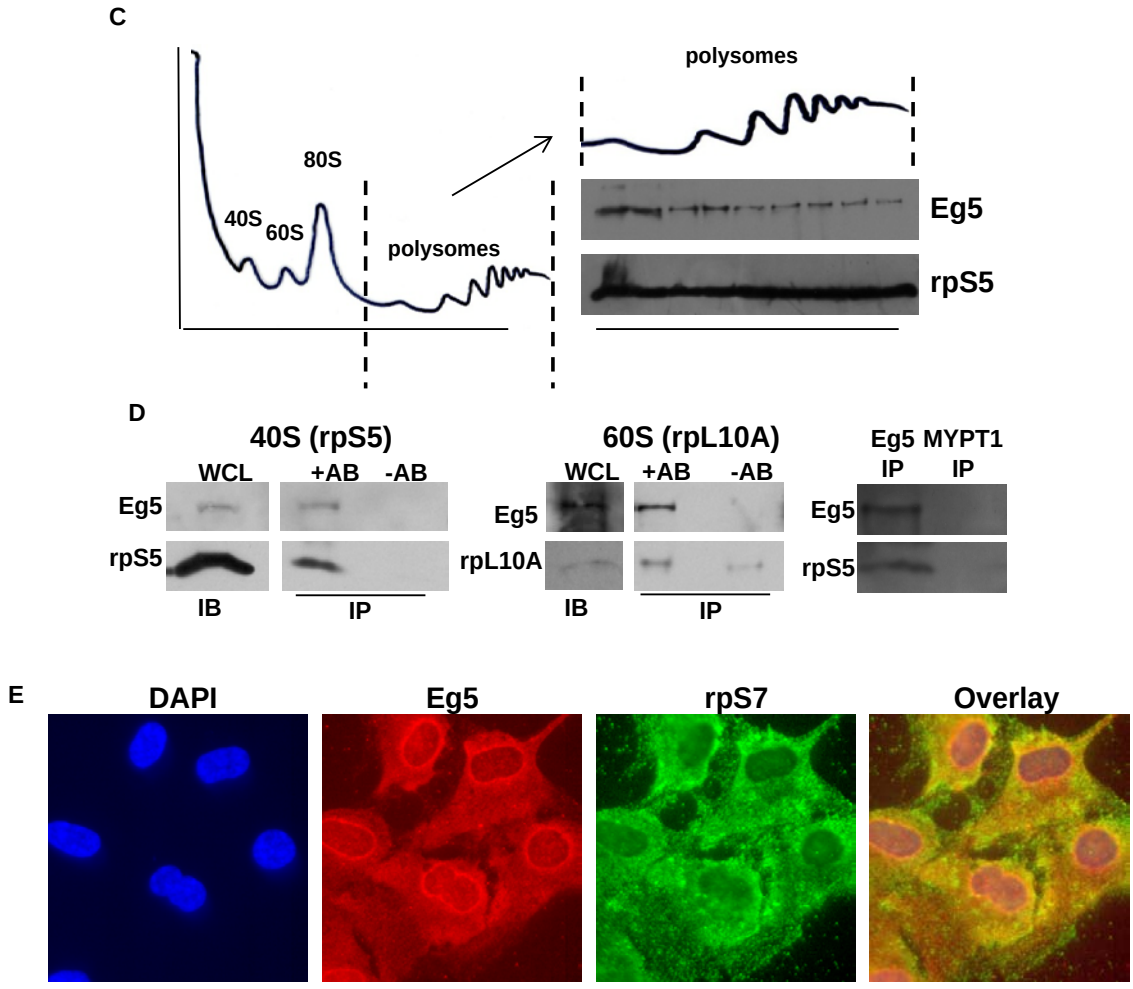

Figure 4.1: Eg5, Kid and MKLP1 co-fractionate with ribosomes.

(A) RPE1 nuclear fractions were layed on a 10-25% sucrose gradient, centrifuged, and 1 mL fractions were collected with constant monitoring at an absorbance of A260. RPS7, represents the pre-40S subunit, and NPM, represents the pre-60S subunit. (B) RPE1 whole cell lysates were layed on a 10-25% sucrose gradient, centrifuged, and 1 mL fractions were collected with constant monitoring at an absorbance of A260. rpL4 and NPM represents the 60S subunit; actin and dynein are negative controls. (C) Left:

Figure legend 4.1 continued: Polysome profile of control RPE1 cells. Right: Polysome fractions from polysome profile (on right) and immunoblot of Eg5 and rpS5 found in the polysomal fractions. D rpS5 (left), rpL10A (middle), co-immunoprecipitated with Eg5. Right: Eg5 IP demonstrating co-IP with rpS5, and a MYPT1 negative control did not co-fractionate with Eg5, lane two. E Immunofluorescence of co-localization between Eg5 (red), rpS7 (green), and DAPI (blue).

4.2.1.2 rpS5 and rpL10A co-immunoprecipitate with Eg5

To further confirm the association of Eg5 with the ribosomal subunits immunoprecipitation (IP) studies were conducted. IP-enrichment of Eg5 from whole cell lysates validated the association between Eg5 and the various mature ribosomal subunits, wherein rpS5 represents a marker for the 40S ribosome, and rpL10A represents a marker for the 60S ribosome (Figure 4.1D). This confirms the association of Eg5 with ribosomes in addition to the immunofluorescence analysis of co-localization between Eg5 and rpS7 (Figure 4.1E). Because of the availability of inhibitors and the well-studied view of this motor, from this point on, the majority of our studies for this chapter will be focused on the Eg5 ribosomal motor.

4.2.2 Protein synthesis is decreased after loss of Eg5

4.2.2.1 In vivo ^{35}S Met/Cys translation incorporation assays

4.2.2.2 Protein synthesis is decreased in whole cell lysates after loss of Eg5

As we observed that Eg5 associates with mature ribosomal subunits, we wanted to determine whether Eg5 participates in translation. To begin, ^{35}S methionine and cysteine (^{35}S Met/Cys) incorporation assays were employed to measure the rate of newly synthesized proteins in the presence or absence of Eg5. DMEM media without methionine and cysteine was added to the cells in the presence of 100 μCi of ^{35}S Met/Cys for 30 min, followed by the addition of cycloheximide to inhibit translation and by cell lysis in RIPA buffer, resulting in whole cell lysates (WCLs). Interestingly, 24 hrs after Eg5 knockdown with a siRNA targeting to the C-terminus of the Eg5 gene (siRNA #1), a 40% decrease in protein synthesis was observed (Figure 4.2A). In order to ensure that this decrease in protein synthesis after Eg5 knockdown was not due to off-target effect exerted on cells by the siRNA, a well-established Eg5 inhibitor, monastrol, was used. Monastrol is a chemical inhibitor of Eg5 that binds to the motor domain of Eg5 and inhibits the ATPase activity of Eg5, therefore preventing Eg5 from translocating on microtubules (Mayer, Kapoor et al. 1999; Kapoor, Mayer et al. 2000). Monastrol can arrest cells in mitosis at pro-metaphase resulting in monopolar spindles as early as 4 hrs after treatment. Therefore, ^{35}S Met/Cys incorporation assays were completed 4 hrs after monastrol treatment to inhibit Eg5's ATPase activity prior to significant mitotic arrest. Monastrol treatment resulted in a 60% decrease in newly synthesizing proteins in WCLs (Figure 4.2B). Additionally, when monastrol was washed out and cells were allowed to recover for an additional 4 hrs, protein synthesis

returned back to DMSO control levels. This data demonstrates that loss of Eg5, by inhibition or knockdown, results in decreased protein synthesis in RPE1 cells and it also reveals that the ATPase activity of Eg5 is needed for its function during translation.

Figure 4.2

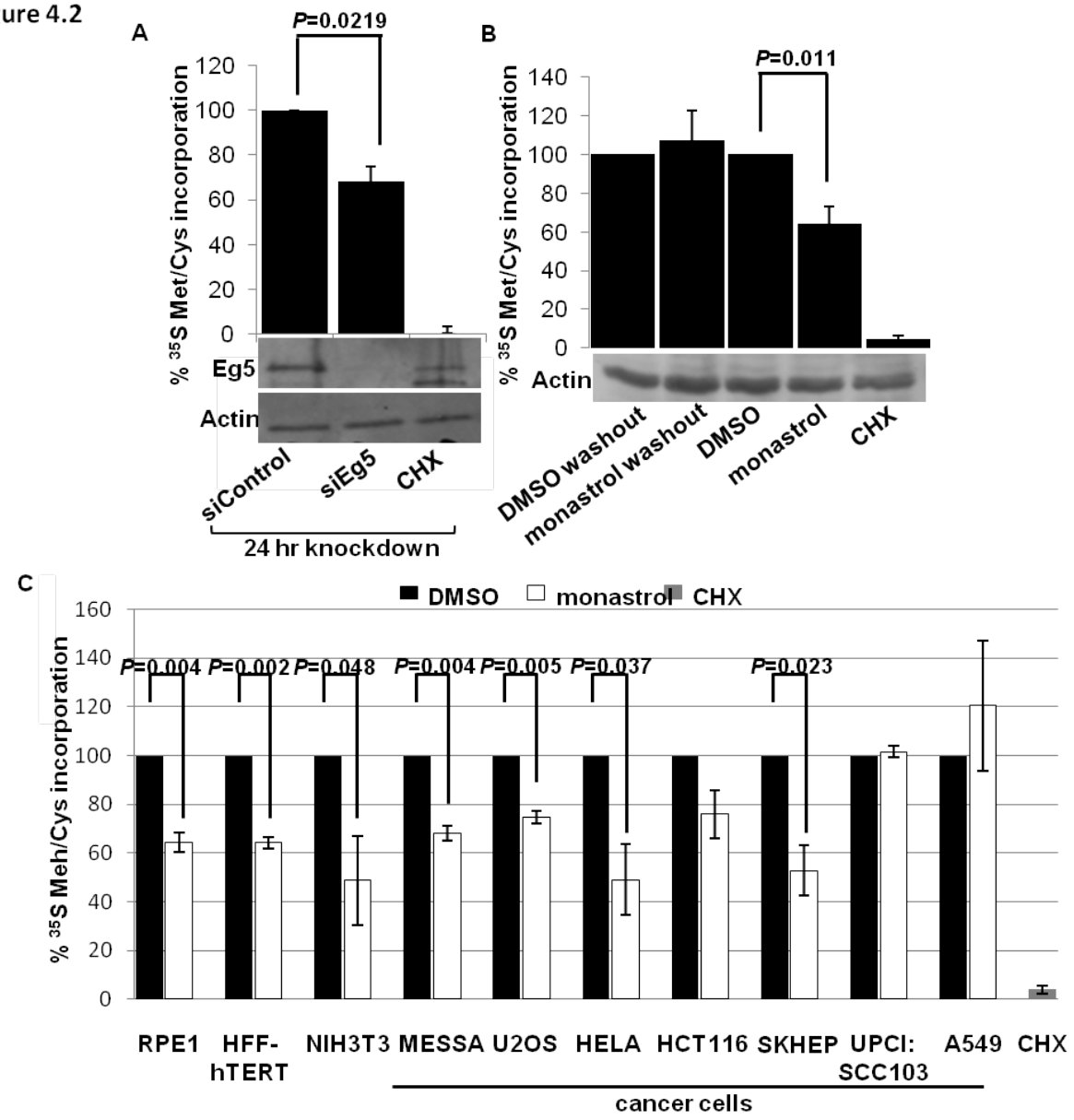

Figure 4.2: Loss of Eg5 causes a defect in protein synthesis of WCLs.

^{35}S Met/Cys incorporation assays completed after (A) a 24 hr knockdown of Eg5 in RPE1 cells, (B) after a 4 hr monastrol or 4 hr monastrol washout in RPE1 cells, (C) or after a 4 hr monastrol treatment in a variety of cell lines. Immunoblot shown below for knockdown and even loading. CHX, used as a positive control. Results are shown as mean ± s.d. and are representative of at least three independent experiments, *P* values represent students' t-test.

4.2.2.3 Decreased protein synthesis after loss of Eg5 is observed in multiple cell lines

We next inquired whether the observed decrease in translation efficiency after Eg5 inhibition was cell line specific or if it was a general effect observed in a variety of cell lines from different cellular backgrounds. Therefore, three different noncancer and seven different cancer cells were chosen for this analysis. After a 4 hr treatment with monastrol, ^{35}S Met/Cys was added to cells prior to cell lysis. Loss of Eg5 activity was found to decrease translation(~30-60%) in each of the noncancer and four out of the seven cancer cell lines (Figure 4.2C); thus, demonstrating that the function of Eg5 in translation is not a cell line or cell type specific phenomena. The cancer cells that were resistant to Eg5 inhibition will be discussed further in section 4.3.1.

4.2.2.4 Both membrane and cytosolic protein synthesis was decreased after loss of Eg5

The use of WCLs to measure the decrease of newly synthesizing proteins after inhibition of Eg5 ignores the fact that proteins can be translated in two different compartments. Thus, we inquired

whether Eg5 may facilitate translation of either cytosolic or membrane proteins, or both. Therefore 24 hrs after knockdown of Eg5, by siRNA #1, or after a 4 hr treatment with monastrol, ^{35}S Met/Cys was added to the cells prior to cell lysis; after cell lysis the cytosolic and membrane proteins were separated by centrifugation, and subjected to analysis. Interestingly, a significant 40-50% decrease in protein synthesis was observed in both the cytosolic and membrane proteins (Figure 4.3A,B). A second siRNA (#2) targeted to the N-terminus of the Eg5 gene resulted in a similar decrease in protein synthesis in both cytosolic and membrane proteins, thus confirming the findings that Eg5 facilitates translation of both cytosolic and membrane proteins (Figure 4.3C).

It is interesting to note that similar experiments were initially attempted with trypsinized cells left in suspension after knockdown of Eg5. Intriguingly, a marked reduction in newly synthesized proteins was observed, greater than 80%, but such a change was only observed in the cytosolic fraction (Figure 4.4). Although these results are interesting, we feel that the use of adherent cells is more likely to reflect the typical cellular physiology and thus have not pursued the detached translation assays any further.

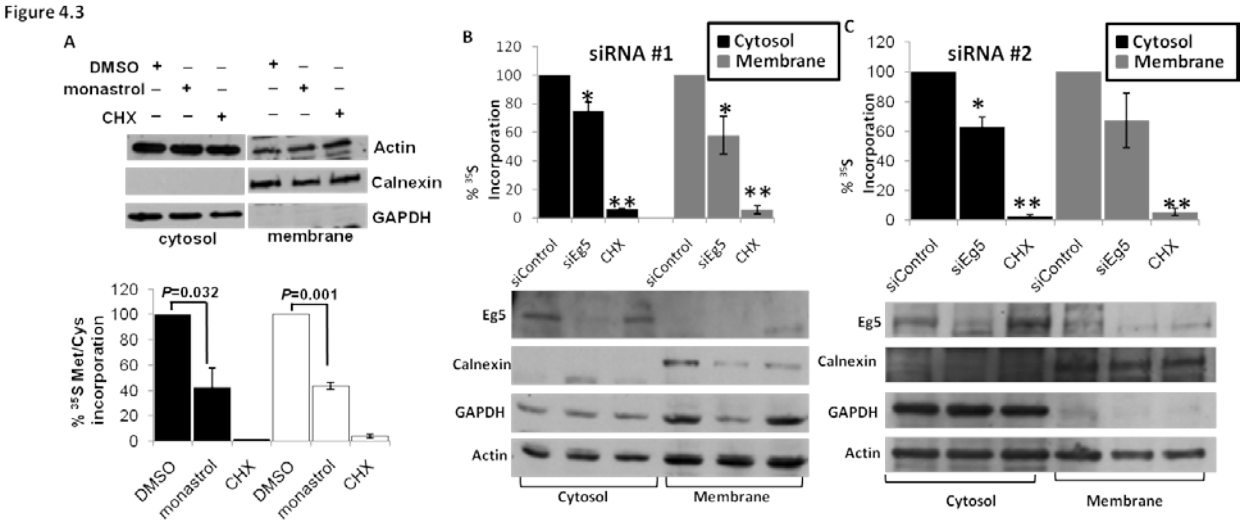

Figure 4.3: Protein synthesis of cytosolic and membrane proteins are reduced after Eg5 knockdown or inhibition.

^{35}S Met/Cys incorporation assays completed (A) after a 4 hr monastrol treatment or (B) 24 hr Eg5 knockdown with siRNA #1 or (C) siRNA #2 in RPE1 cells after fractionation into cytosolic and membrane proteins. Immunoblots are shown below for knockdown of Eg5, equal loading, and fractionation. Calnexin is a marker for ER proteins, and GAPDH is used as a marker for the cytosolic fraction. CHX was used as a positive control. Results are shown as mean ± s.d. and are representative of at least three independent experiments, *P* values represent students' t-test.

Figure 4.4

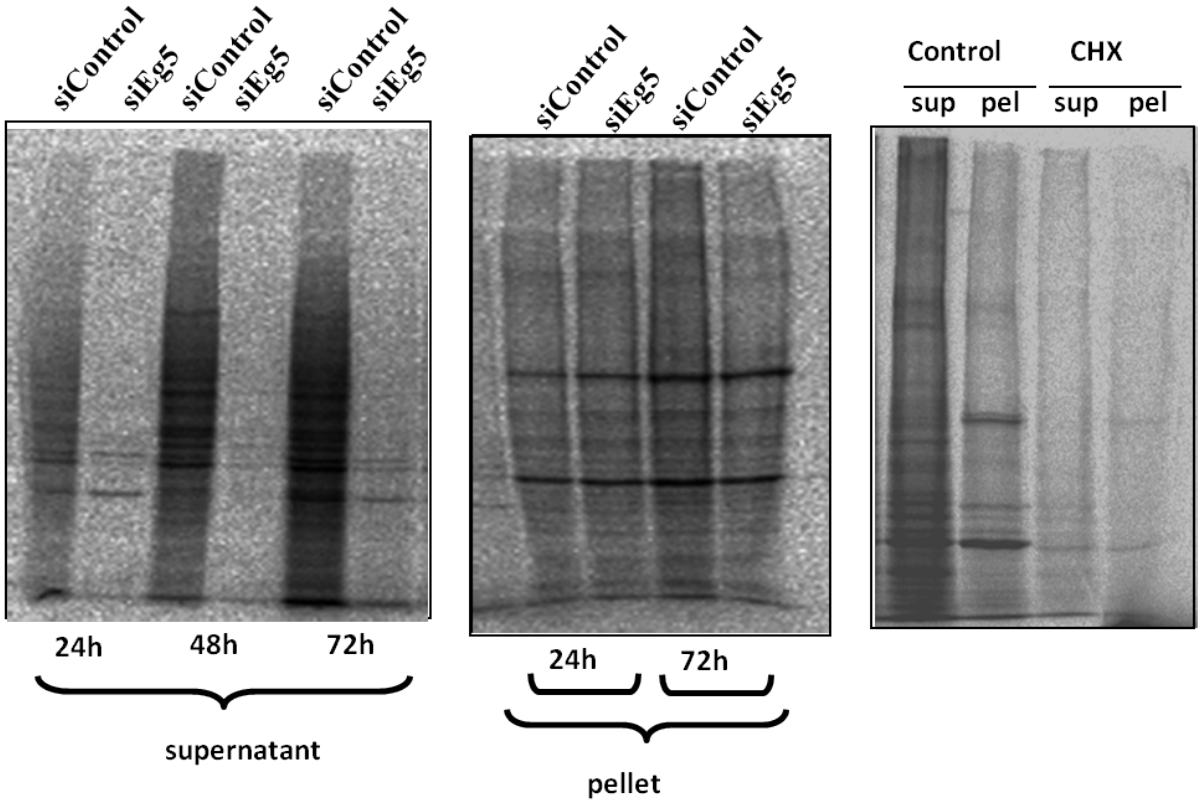

Figure 4.4: Reduction in protein synthesis of cytosolic, but not membrane proteins after Eg5 knckdown in suspended cells.

Left. ^{35}S Met/Cys incorporation assays completed in suspended cells after a 24, 48, or 72 hrs of Eg5. Supernatant fractions, representing the cytosolic proteins are shown on the left. Middle: The pellet fractions, Right: controls for the translation assays. CHX was used as a positive control.

4.2.3 Decrease in protein synthesis is specific to Eg5

Next to provide additional lines of evidence that the decrease in protein synthesis after Eg5 knockdown or treatment with monastrol was due to on-target effects, we performed the same ^{35}S Met/Cys experiment after a 24 hr Eg5 knockdown by siRNA #1 and followed it by treatment with monastrol for 4 hr. The rationale for this experiment is that if the decrease in protein synthesis observed after monostrol treatment is indeed specific to inhibiting Eg5, then one would anticipate that removing the target protein by siRNA knockdown of Eg5 would not exert any further decrease in translation efficiency. Gratifyingly, after knockdown of Eg5 and subsequent monastrol treatment no greater decrease in protein synthesis was observed in addition to the 60% caused by knockdown of Eg5 (Figure 4.5). From these results, as well as the decrease in translation after the use of two different siRNAs and a small molecule inhibitor to Eg5, demonstrate that the decrease in translation is specific to loss of Eg5 activity.

Previously published data has suggested that prolonged exposure to Eg5 inhibition (by small molecule inhibition or by knockdown) will result in an elevated mitotic index and apoptosis (Chin and Herbst 2006). If the knockdown and/or small molecule inhibition of Eg5 in our experiments were causing apoptosis/cell death or an elevated mitotic index, this would result in decreased protein synthesis as during either of these circumstances, protein synthesis seizes. Therefore, to test whether the decreased protein synthesis observed after Eg5 knockdown was a primary result of loss of Eg5 or a secondary effect of cell death or an elevated mitotic index, several assays were completed including MTS cell proliferation assay, mitotic index analyses, and immunoblotting for caspase 3 cleavage.

Figure 4.5

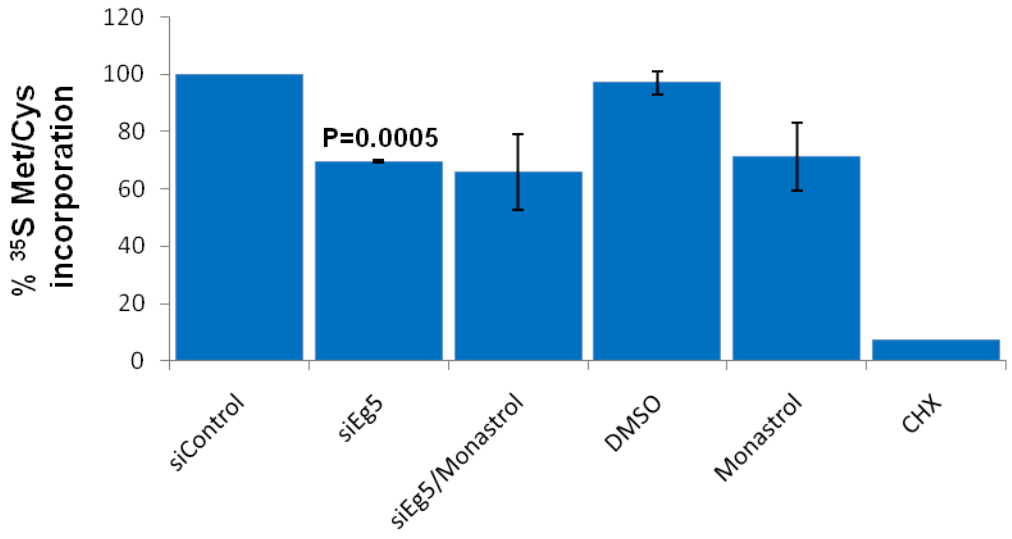

Figure 4.5: Reduction in protein synthesis after loss of Eg5 is not due to off target effects. **24 hrs after knockdown of Eg5, cells were treated with or without monastrol. No greater decrease in protein synthesis was observed after treatment with both, Eg5 knockdown or monastrol, in comparison to treatment with monastrol or knockdown of Eg5 independently. Results are shown as mean ± s.d. and are representative of at least three independent experiments, *P* values represent students' t-test.**

4.2.3.1 Mitotic index does not increase after loss of Eg5

First we investigated whether an increase in the mitotic index was observed after Eg5 knockdown or monastrol treatment and whether this could be responsible for the decrease in

protein synthesis. It is well-established that during mitosis protein synthesis is inhibited (Fan and Penman 1970; Sivan, Kedersha et al. 2007). Therefore, a time course analysis was completed after Eg5 knockdown with siRNA #1 where cells were fixed and stained with DAPI for visualization of nuclei and counted for the mitotic index at 24, 48, and 72 hrs after knockdown. 24 hrs after Eg5 knockdown, an increase in the mitotic index was not observed; time points at 48 or 72 hrs knockdown of Eg5 did cause a 50% increase in the mitotic index. Although this increase is consistent with previous literature precedent (Chin and Herbst 2006), these later time points are not a concern as the time point used for translational inhibition was 24 hrs (Figure 4.6A). Next, mitotic index was examined after a 24 hrs after Eg5 knockdown with siRNA #1 or siRNA #2 or after a 4 hr monastrol treatment. In these experiments an increase in the mitotic index was not observed after Eg5 knockdown by siRNA #1, as demonstrated above, or after monastrol treatment (Figure 4.6B). Although it should be noted that a slight increase of ~15% was observed in the mitotic index after Eg5 knockdown by siRNA #2, however this 15% increase could not account for ~40% decrease in protein translation that was observed; therefore an increase in the mitotic index after loss of Eg5 can likely be ruled out as a possible reason for the decrease in protein synthesis.

Figure 4.6

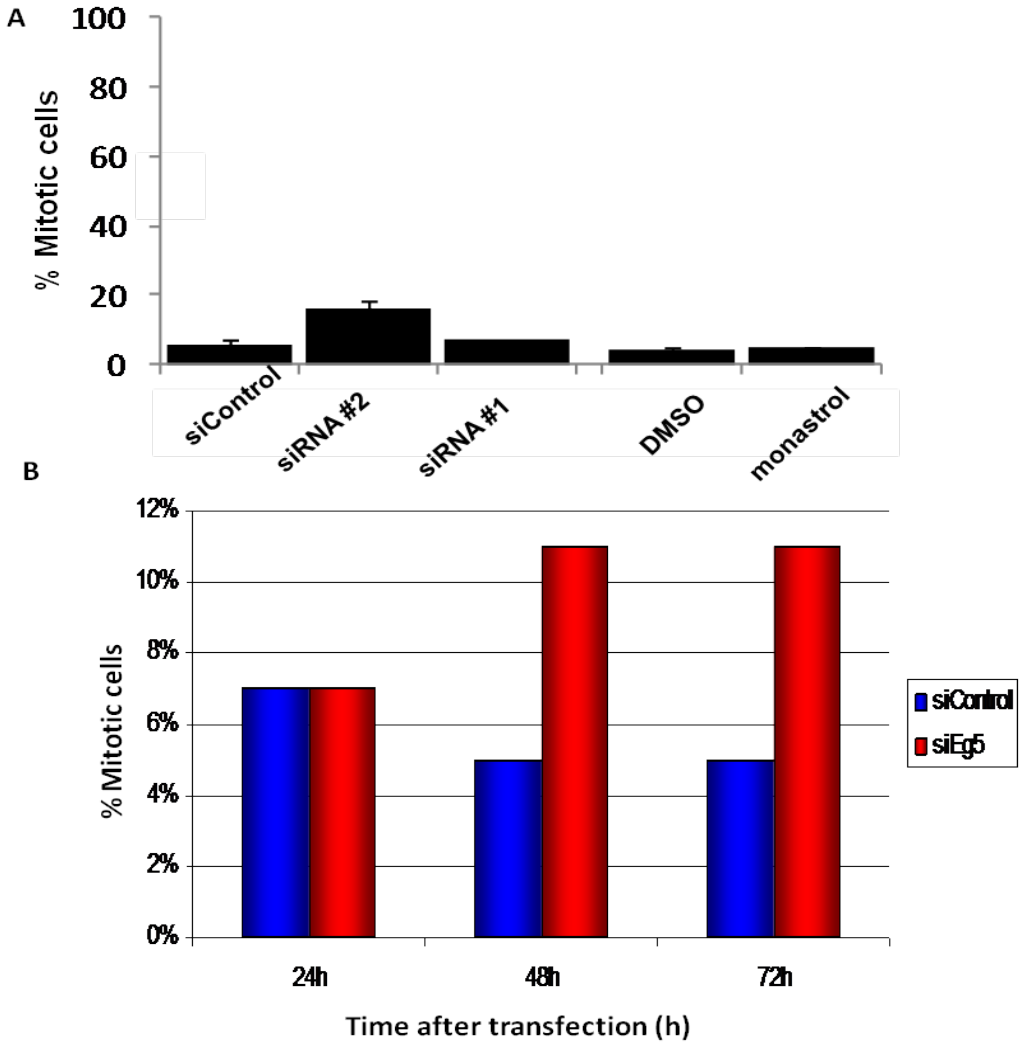

Figure 4.6: Reduction in protein synthesis after loss of Eg5 is not due to an increase in the mitotic index.

(A) 24 hrs after Eg5 knockdown by siRNA #1 or #2 or even monastrol treatment did not cause a large increase in the mitotic index. (B) Time course analysis of Eg5 knockdown in RPE1 cells 24, 48, or 72 hrs. Results are shown as mean ± s.d. and are representative of at least three independent experiments, *P* values represent students' t-test.

4.2.3.2 Cell proliferation does not decrease after loss of Eg5

Next, the MTS cell proliferation assay is a colorimetric assay wherein metabolically active cells convert reduced tetrazolium compounds to a soluble colored formazan product utilizing NADPH as a cofactor (Berridge, Herst et al. 2005). In order to identify if the decreased protein synthesis was due to decreased cell proliferation, cells were treated with siRNA #1 targeted to Eg5 for 24, 48 or 72 hrs (Figure 4.7A, B). At the time point of 24 hrs, which was the time used to complete the translation assays, a decrease in cell proliferation was not observed. However, we did observe an expected decrease in cell proliferation after the later time points following knockdown of Eg5. The later time point data is of a lesser concern because the translation assays were completed at 24 hr after knockdown which is a time when no decrease in cell proliferation is observed. Additionally, a second siRNA targeted to Eg5 was also employed and 24 hrs after Eg5 knockdown cell proliferation did not decrease (Figure 4.7B). Finally, monostrol treatment was also examined for a decrease in cell proliferation. In this case, 4 hrs after monastrol treatment, a 40% decrease in protein proliferation was initially observed, however after a 4 hr washout, cell proliferation recovered and returned to similar levels as control cells. This suggests that although there was a reduction in cell proliferation after an acute monastrol treatment, the decrease was not due to cell death as the cells recovered. Rather it is likely that after monastrol treatment, a reduction in cellular metabolism was observed similar to what is expected when translation is inhibited.

Figure 4.7

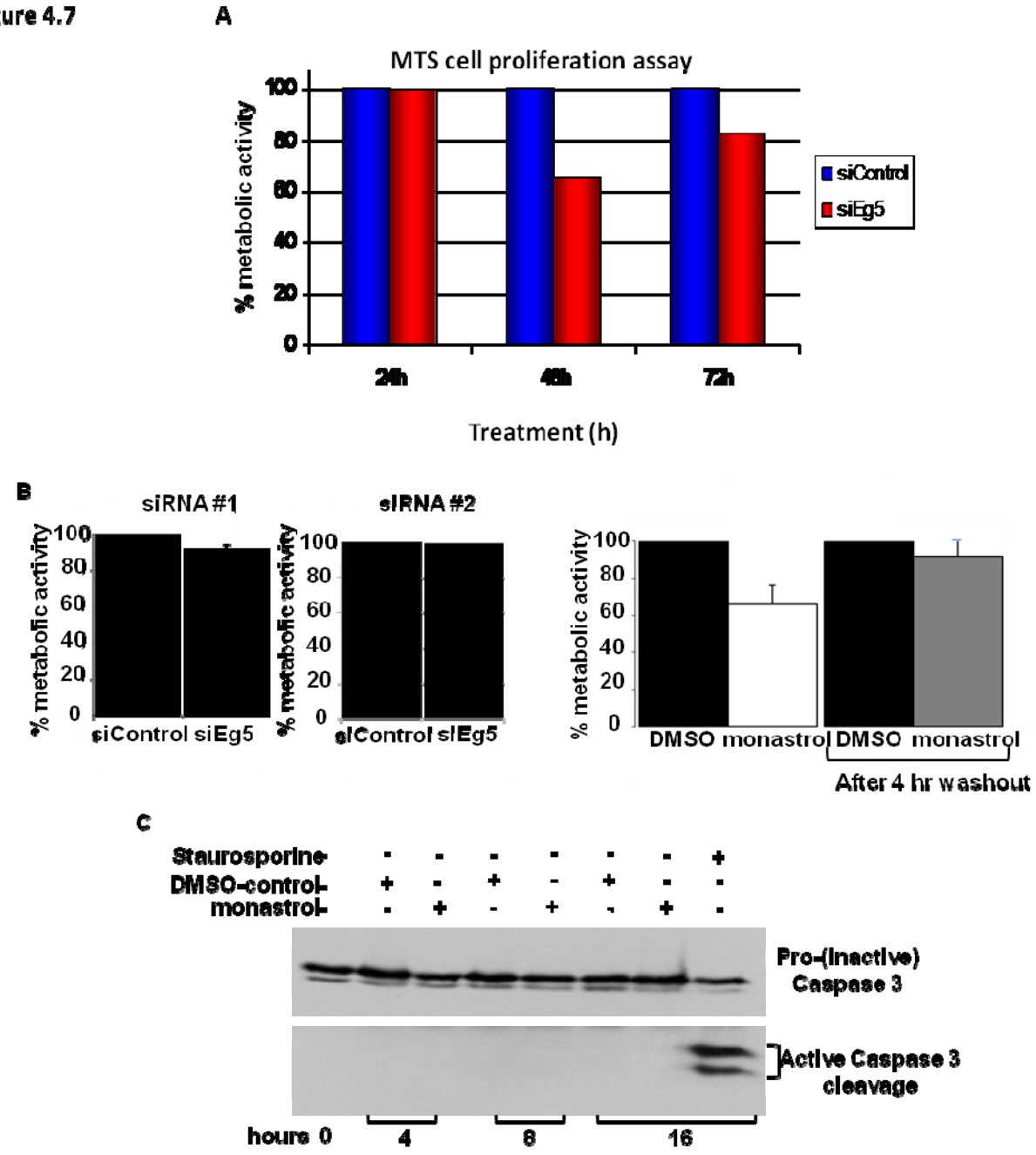
A
MTS cell proliferation assay
% metabolic activity
100
80
60
40
20
0
siControl
siEg5
24h
48h
72h
Treatment (h)
B
siRNA #1
siRNA #2
% metabolic activity
siControl siEg5
DMSO monastrol DMSO monastrol
After 4 hr washout
C
Staurosporine
DMSO-control
monastrol
Pro-(Inactive) Caspase 3
Active Caspase 3 cleavage
hours 0
4
8
16

Figure 4.7: Reduction in protein synthesis after loss of Eg5 was not due to a decrease in cell proliferation or apoptosis.

(A) MTS cell proliferation assay was completed after a 24 hr, 48 hr, or 72 hr knockdown of Eg5. (B) MTS cell proliferation assays after a 24 hr knockdown of Eg5 by siRNA #1 or siRNA #2 or after a 4 hr monastrol treatment. (C) RPE1 cells were treated 130 mM of monastrol and various time points were taken to examine apoptosis induction, via caspase 3 cleavage. Staurosporine was used as a positive control. Results are shown as mean ± s.d. and are representative of at least three independent experiments, *P* values represent Students' t-test.

4.2.3.3 Cell death does not occur after Eg5 inhibition

Finally, we examined whether the decrease in translation of newly synthesizing proteins was due to cell death after monastrol treatment. RPE1 cells were treated with monastrol for varying periods of time, ranging from 4-16 hrs, followed by subjection to immunoblotting for caspase-3 cleavage, a hallmark of apoptosis. At all time points, caspase-3 was not cleaved in the monastrol-treated cells suggesting that the decrease (Belmokhtar, Hillion et al. 2001) in protein synthesis was not due to apoptosis (Figure 4.7C). Staurosporine, a highly promiscuous kinase inhibitor known to induce apoptosis was used as a positive control in these experiments wherein caspase-3 cleavage was observed.

From these controls, it was determined that the decrease in protein synthesis was due to loss of Eg5 and not due to decreased cell proliferation, an increase in the mitotic index or due to cell death.

4.2.4 Ribosomes associate with microtubules through Eg5

4.2.4.1 Microtubules are also needed for protein synthesis

As Eg5 is a molecular motor and few motors have ever been identified to function without the use of microtubules and given that previously it has been shown that the cytoskeleton is quite important for multiple processes leading up to translation (Jansen 1999), we turned our attention to the role of microtubules in the Eg5-mediated translation efficiency. To begin to examine the role of microtubules in translation, ^{35}S Met/Cys incorporation assays were completed after 2 hr microtubule depolymerization by either nocodazole or colecimid. As anticipated, a significant 20% reduction of protein synthesis was observed after microtubule inhibition, consistent with a role for motors in protein synthesis (Figure 4.8A). As a decrease in translation was observed and previous published data has suggested that prolonged nocodazole treatment can lead to apoptosis, cells were treated with varying concentrations of nocodazole for 2-16 hrs prior to cell lysis and immunoblotting for caspase-3 cleavage (Figure 4.8B). At all times tested, caspase-3 was not cleaved therefore demonstrating that the decrease in translation was specific to microtubule inhibition and not apoptosis.

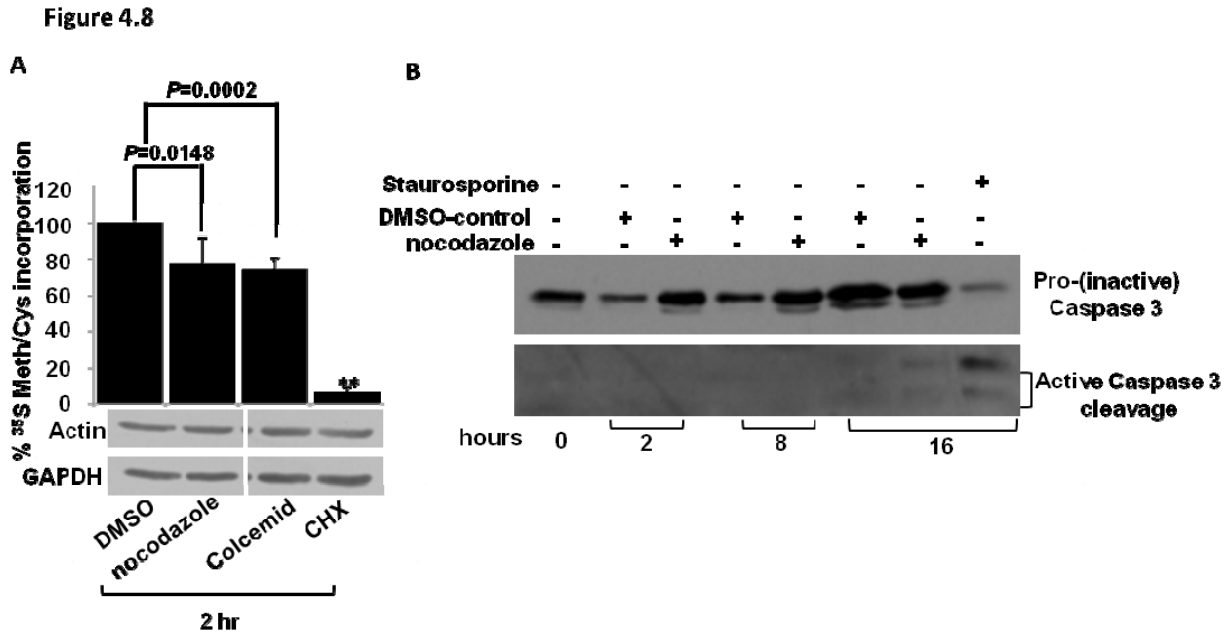

Figure 4.8: Reduction in protein synthesis was observed after microtubule inhibition. **(A) RPE1 cells were treated with nocodazole or colcemid for 2 hrs prior to ^{35}S Met/Cys incorporation assays. Immunoblots are shown below representing equal loading. (B) Apoptosis was investigated after nocodazole treatment for various time points. Staurosporine was used as a positive control for caspase 3 cleavage. Results are shown as mean ± s.d. and are representative of at least three independent experiments, *P* values represent students' t-test.**

4.2.4.2 40S ribosomal subunit and the 80S ribosome is bound to microtubules through Eg5

Identification as to how microtubules are involved in translation lead us to hypothesize that in mammalian cells ribosomes may associate with microtubules, similar to that seen in sea urchin embryos, and that this association may be microtubule motor-dependent (Suprenant, Tempero et

al. 1989). Therefore, to investigate this, in vivo WCL microtubule binding assays were completed in the presence or absence of Eg5 and/or microtubules. To complete these assays, whole cells were lysed, the DNA pellet was omitted, and cells were either treated under conditions to polymerize microtubules (37˚C + taxol) or to depolymerize microtubules (4˚C + nocodazole). Cells were then incubated in a binding reaction for 30 min prior to centrifugation, three washes of microtubule pellet, and immunoblotting. In the presence of microtubules, ribosomes, as demonstrated by the antibody to rpL4, were found to pellet in the presence of microtubule stabilizing conditions, but not under microtubule depolymerizing conditions; therefore suggesting that ribosomes associate to microtubules in a microtubule-dependent manner (Figure 4.9A). Next, we investigated whether Eg5 may be mediating the interaction of ribosome association to microtubules. Therefore, the exact assay was completed again, but in absence of Eg5. Notably, after Eg5 knockdown, the association of ribosomes with microtubules was significantly reduced by 42%, suggesting that Eg5 may act as a linker between ribosomes and microtubules in vivo.

Subsequently, we inquired exactly which ribosomal subunits (40S or 60S) and or ribosomes (80S complex) associate to microtubules via Eg5 in mammalian cells. In vitro microtubule binding reaction were performed where ribosomal subunits and ribosomes were first isolated through sucrose gradient fractionation and each ribosomal fraction (as determined by continuous monitoring at an absorbance of 260) from each ribosome/ribosomal subunits were pooled together and incubated in a binding reaction, either with the addition of polymerized microtubules (from purified α -tubulin) or without microtubules. These reactions were incubated for 45 min, centrifuged, providing a supernatant and a pellet, washed to rid of nonspecific binding, and subjected to immunoblotting. The supernatant is interpreted to contain non-

microtubule binding proteins, while the pellet contains microtubules and microtubule-bound proteins. Interestingly, the 40S ribosomal subunit and the 80S ribosome, but not the 60S ribosomal subunit, were found to pellet only in the presence of microtubules, and not in the absence of microtubules, confirming that ribosomal subunits and ribosomes associate to microtubules (Figure 4.9B). Additionally, the same experiment was completed after Eg5 knockdown, and we observed the 40S ribosomal subunit and the 80S ribosome no longer associating to microtubules in the absence of Eg5. These data are highly suggestive of a role for Eg5 as a linker protein between the 40S ribosomal subunit and the 80S ribosome. It is interesting to note that the association between Eg5 and the mature ribosomes is not microtubule dependent as polysome fractionation studies completed after microtubule depolymerization with nocodazole for 2 hrs prior to cell lysis revealed that Eg5 continued to cofractionate with ribosomes in the absence of microtubules (Figure 4.9C). Additionally, polysomes were not mentioned above because they were found to pellet independent of microtubules, even at 4°C, therefore suggesting nonspecific pelleting and thus could not be used for further analysis.

Figure 4.9

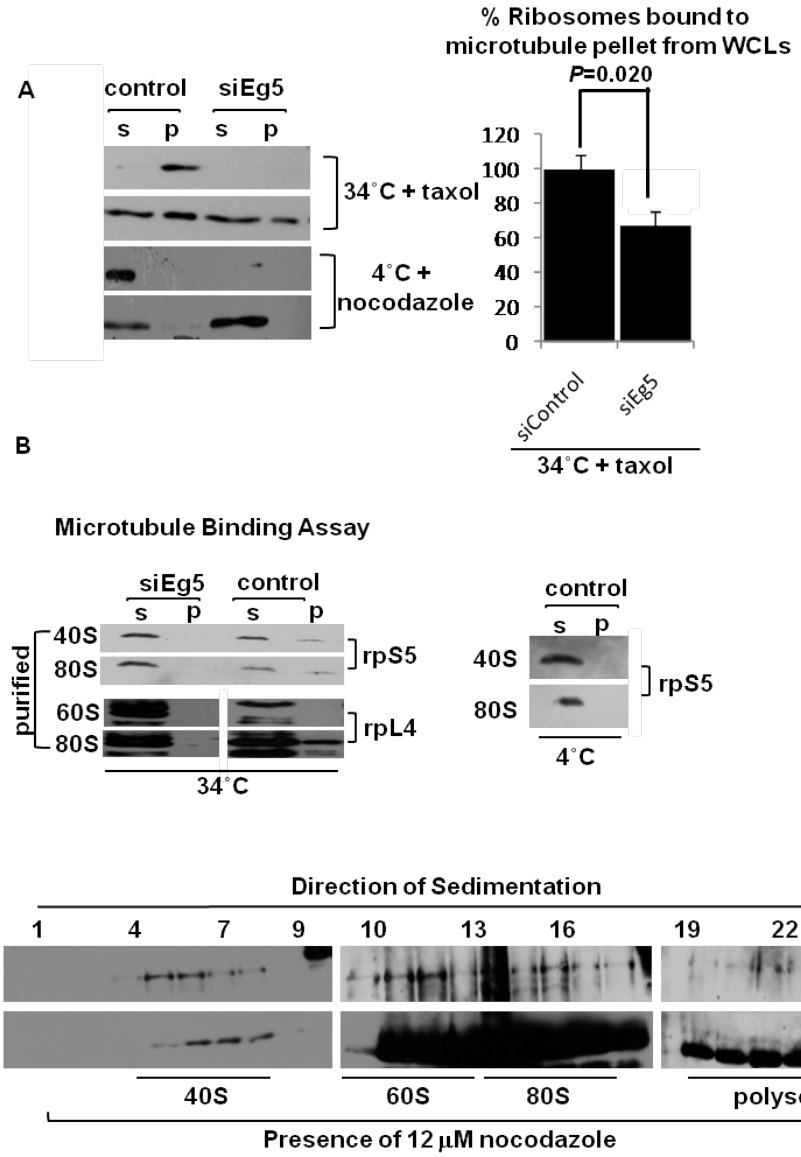
A
control
siEg5
s p s p
34˚C + taxol
4˚C + nocodazole
% Ribosomes bound to microtubule pellet from WCLs
P=0.020
120
100
80
60
40
20
0
siControl
siEg5
34˚C + taxol
B
Microtubule Binding Assay
siEg5
control
s p s p
purified
40S
80S
60S
80S
rpS5
rpL4
34˚C
control
s p
40S
80S
rpS5
4˚C
C
Direction of Sedimentation
1 4 7 9 10 13 16 19 22 26
Eg5
rpL4
40S
60S
80S
polysomes
Presence of 12 μM nocodazole

Figure 4.9: Ribosomes are bound to microtubule through Eg5.

(A) In vivo microtubule binding assays were completed in the presence and absence of Eg5 and microtubules. WCLs were lysed under conditions to either polymerize microtubules (34°C+taxol) or depolymerized microtubules (nocodazole+4 ° C). Left: immunoblot analysis of rpL4. Right: Graph representing quantification of immunoblots. (B) In vitro microtubule binding assays. Ribosomes or ribosomal subunits from each fraction after polysome profiling, in the presence or absence of Eg5, were pulled together and incubated in the presence of absence of microtubules. Left: Immunoblotting for designated proteins. Right: Control completed at 4 °C in the absence of microtubules. (C) Polysome profiling completed in the absence of microtubules, 2 hrs after nocodazole treatment. Immunoblots are shown from TCA-precipitations of the indicated fractions. Results are shown as mean ± s.d. and are representative of at least two independent experiments, *P* values represent Students' t-test.nocodazole treatment. Immunoblots are shown from TCA-precipitations of the indicated fractions. Results are shown as mean ± s.d. and are representative of at least two independent experiments, *P* values represent Students' t-test.

4.2.5 Which step in protein synthesis requires Eg5 function?

4.2.5.1 Polysome profiling after loss of Eg5

As loss of Eg5 causes a decrease in protein synthesis, the exact step in translation in which Eg5 functions was next investigated. There are three independent steps in translation, which I

discussed previously in section 1.1.2 (Chan, Khan et al. 2004) of the introduction, initiation, elongation and termination. To begin to dissect at which step in translation Eg5 functions, we began by completing sucrose gradient fractionation and polysome profiling analysis to examine the ribosome distribution in the absence of Eg5; examining the ribosomal distribution profiles in comparison to known translation inhibitors will help to aid the identification in which step of translation Eg5 is functioning 24 hrs after Eg5 knockdown a ~40% increase in the 80S ribosome was observed when compared to control cells (Figure 4.10). This increase in the 80S ribosome was further confirmed after a 4hr monastrol treatment (Figure 4.11A). Additionally 2 hr nocodazole resulted in a more subtle, but similar increase in the 80S ribosome (Figure 4.11B).

Typically, an initiation defect is coupled with an increase in the 80S ribosome. This is observed with arsenite treatment, a known translation initiation inhibitor (Li, Ohn et al. 2010), which yielded an increase in the 80S and a decrease in polysomes (Figure 4.12B). However this increase in the 80S and corresponding decrease in the polysomes was not seen with Eg5 inhibition, where instead polysome abundance remained stable. The Eg5 inhibited polysome profiles could be reproduced with low levels of puromycin, a known translation elongation inhibitor which causes premature termination of the polypeptide chain (Figure 4.11C) (Chan, Khan et al. 2004). Although it should be noted that experiments using high concentrations of puromycin resulted in a ~90% increase in the 80S and loss of polysomes due to its ability to cause premature termination of the polypeptide chain (Figure 4.12C). As the polysomes remained stable after loss of Eg5, it suggests that Eg5 may be involved in the elongation step of protein synthesis.

Figure 4.10

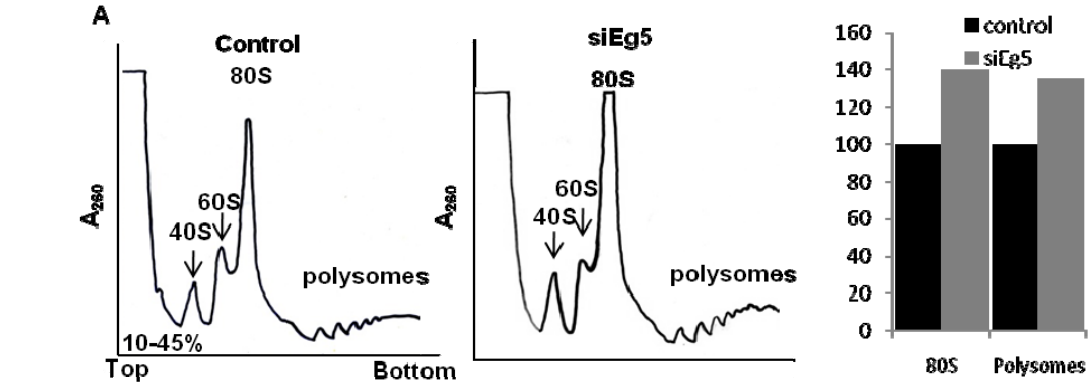

Figure 4.10: Polysome profiling after Eg5 knockdown causes an increase in 80S ribosomes and stabilization of polysomes.

Polysome profiling of 30 million cells was completed after a 24 hr knockdown of Eg5 using 10-45% sucrose gradients. Quantitation of the area under the peaks for the 80S and polysome fractions are demonstrated on the right. CHX was added 10 min before cell lysis in all samples above.

Figure 4.11

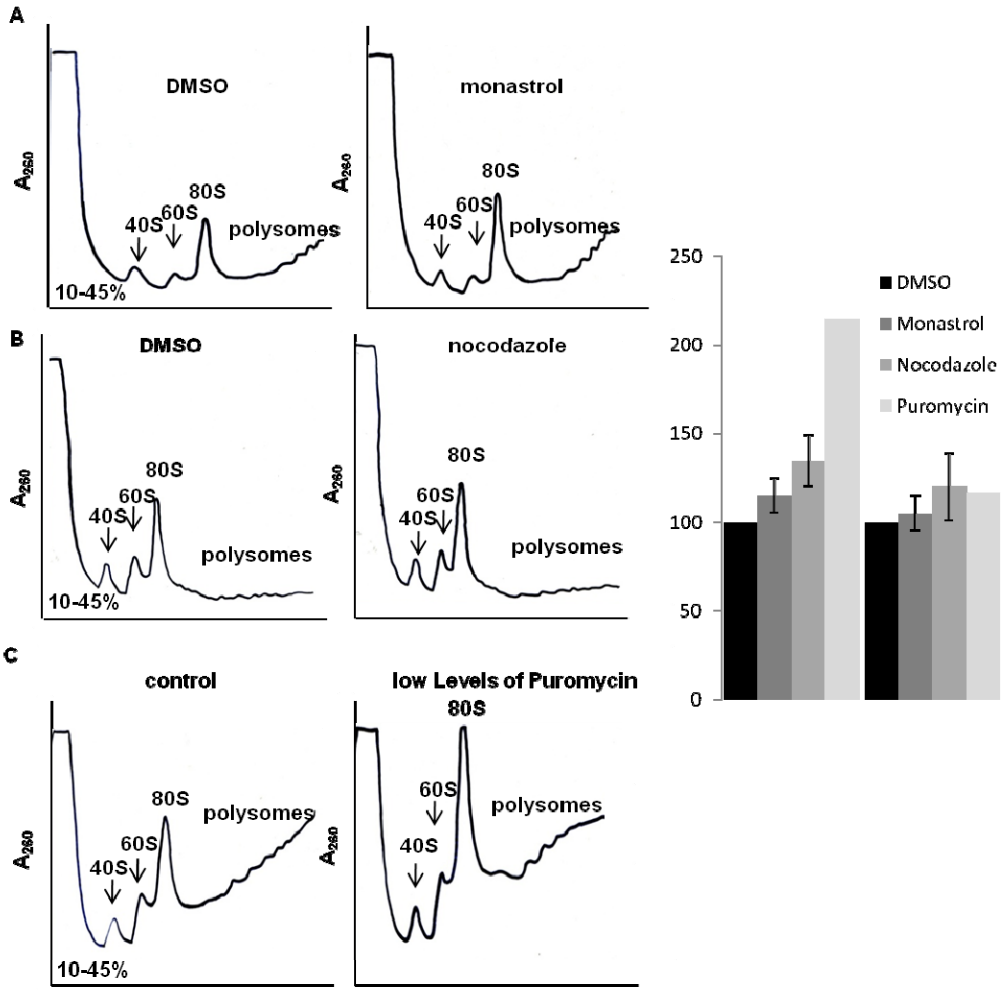

Figure 4.11: Polysome profiling after Eg5 inhibition, microtubule depolymerization or low levels of puromycin leads to an increase in 80S and stabilization of polysomes.

Polysome profiling of 30 million cells was completed after a 4 hr monastrol treatment (A), 2 hr nocodazole treatment to depolymerize microtubules (B), or low levels of puromycin (C), a elongation inhibitor. Samples were centrifuged on 10-45% sucrose gradients. Quantitation of the area under the peaks for the 80S and polysome fractions are demonstrated on the right. CHX was added 10 min before cell lysis in all samples above.

Figure 4.12

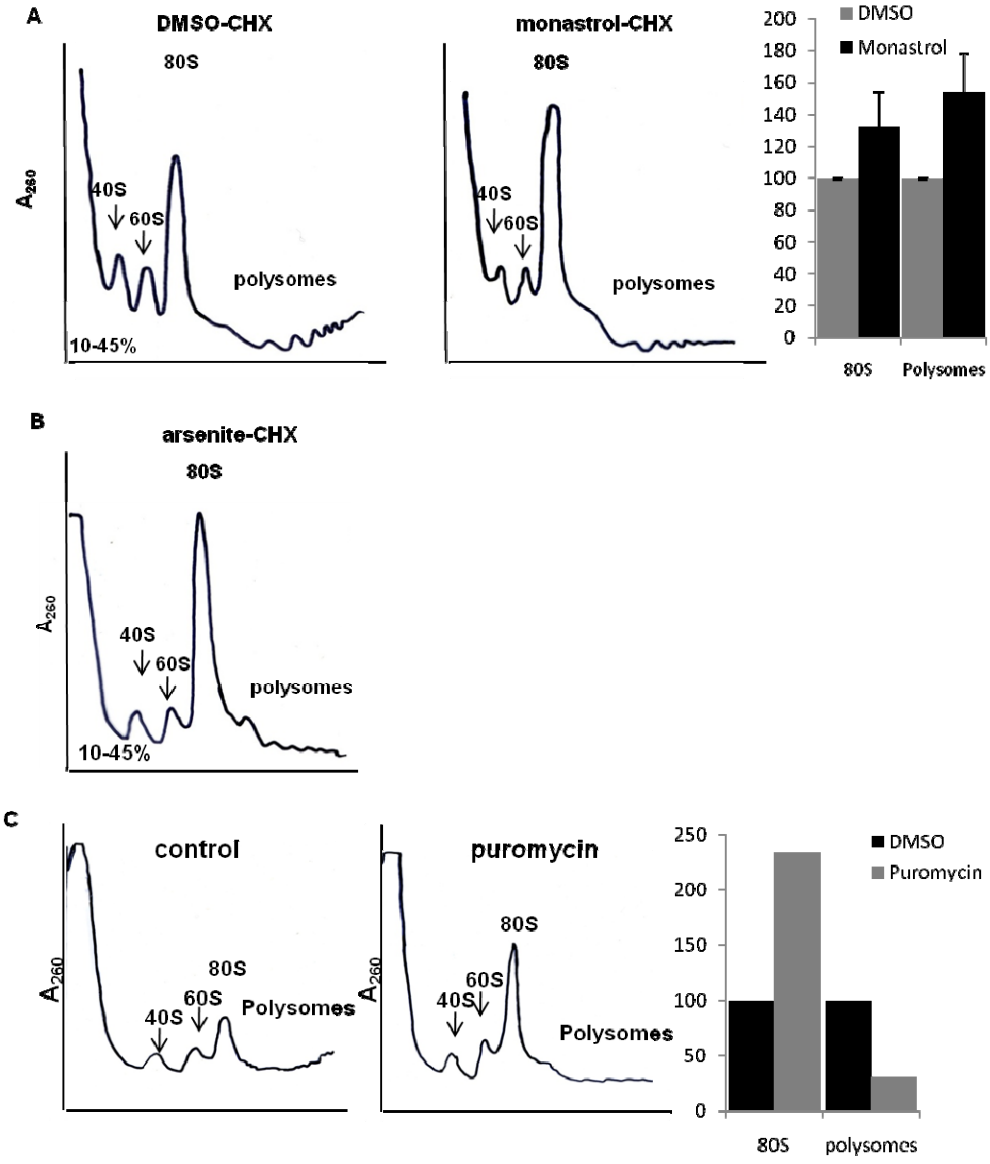
A
DMSO-CHX
80S
40S
60S
polysomes
10-45%
A260
monastrol-CHX
80S
40S
60S
polysomes
DMSO
Monastrol
200
180
160
140
120
100
80
60
40
20
0
80S
Polysomes
B
arsenite-CHX
80S
40S
60S
polysomes
10-45%
A260
C
control
80S
60S
40S
Polysomes
A260
puromycin
80S
60S
40S
Polysomes
A260
250
200
150
100
50
0
DMSO
Puromycin
80S
polysomes

Figure 4.12: Polysome profiling in the absence of CHX still leads to an increase in the 80S ribosomes and polysome stabilization after Eg5 inhibition.

Polysome profiling of 30 million cells was completed after a 4 hr monastrol treatment (A), 1 hr arsenite treatment (a translation initiation inhibitor) (B), or high levels of puromycin (C). Samples were centrifuged on 10-45% sucrose gradients. Quantitation of the area under the peaks for the 80S and polysome fractions are demonstrated on the right. CHX was omitted from experiments in samples A and B, but added 10 min before cell lysis in Figure C.

4.2.5.2 Polysome profiling without the addition of cycloheximide

As mentioned previously, the standard literature protocol for polysome profiles entails the addition of cycloheximide to halt translating ribosomes on the mRNA, thus preventing actively translating ribosomes from "running-off". Given this, one would hypothesize that if Eg5 participated during the initiation phase of translation, the polysomes would decrease in response to Eg5 inhibition and furthermore leaving cycloheximide out of the same experiment would magnify the decreased polysomes, as ribosomes would be able to "run-off" the mRNA, but not initiate new translational complexes. To test this hypothesis, the same experiment was completed in the presence or absence of monastrol and the presence or absence of cycloheximide. Interestingly, stabilization of polysomes was observed after a 4 hr monastrol treatment and in the absence of cycloheximide (Figure 4.12A). This is in stark contrast to DMSO-treated and arsenite-treated polysome profiles wherein a further loss of polysomes was

observed in both cases; recall arsenite is a translation initiation inhibitor. Therefore, from this data, we hypothesize that Eg5 is playing a role in translation after the initiation step.

4.2.5.3 Increase in 80S ribosome and stabilization of polysomes is not due to an increase in mitotic index or cellular stress

Next, polysome profiling was used to confirm that the translational phenotype of Eg5 inhibition was not due to mitotic arrest or cellular stress. To test this, a double thymidine block and release experiment was completed wherein ~18% of cells were captured in mitosis; this percentage of cells in mitosis is reflective of the levels typically observed in noncancer cells (Figure 4.13A). Also, this percentage of cells captured in mitosis is 3.4-fold higher than control cells and similar to the mitotic index observed after Eg5 knockdown by siRNA #2. When these cells were subjected to polysome profiling, we in fact observed a *decrease* in the 80S ribosomes. These data are entirely consistent with previously published data which supports the observation of an increase in mitosis leading to diminished levels of translating ribosome complexes (Sivan, Kedersha et al. 2007). Furthermore, to confirm that the increase in the 80S complex was not due to cellular stress, we mimicked cellular stress using serum starvation, which is also known to inhibit translation (Seal, Temperley et al. 2005). Cells were serum starved for 32 hours prior to polysome profiling, and again we also observed a *decrease* in the 80S ribosome and polysomes by a striking 80%; these data suggest that the increase in the 80S ribosome is specific to loss of Eg5 function and not a generic response to an increase in mitotic cells or cellular stress (Figure 4.13B).

Figure 4.13

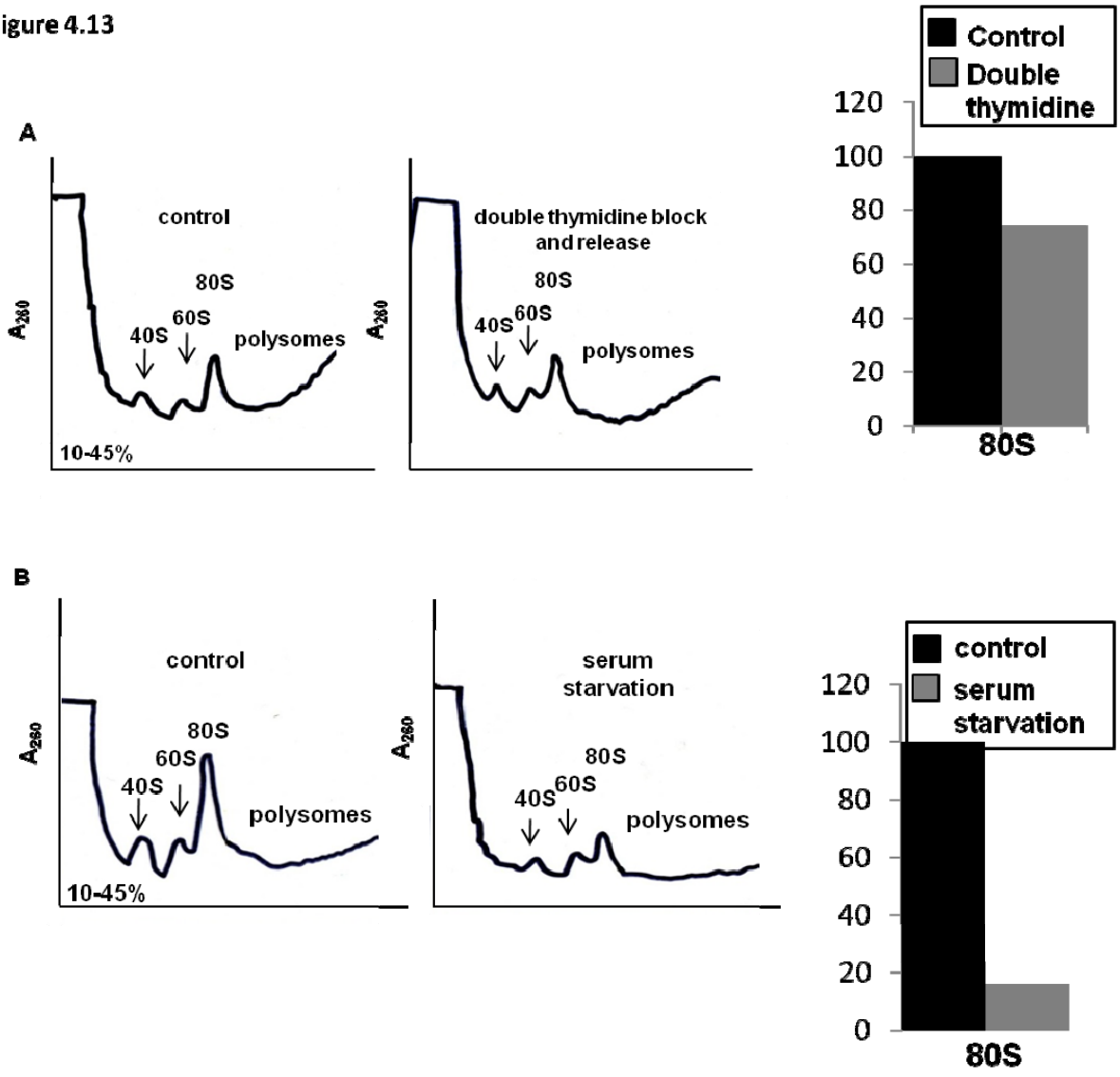

Figure 4.13: Polysome profiling after mitotic arrest or cellular stress does not cause an increase in the 80S ribosome, rather causes a decrease.

Polysome profiling of 30 million cells was completed after a double thymidine block arresting ~18% of cells in mitosis in RPE1 cells (A), or cellular stress through a 32 hr serum starvation (B). Quantitation of the area under the peaks for the 80S. CHX was added 10 min before cell lysis.

4.2.5.4 Eg5 knockdown causes a decrease in both cap-dependent and cap-independent translation

To further support the hypothesis that Eg5 facilitates translation after the initiation step, a bicistronic vector was used, which can differentiate between cap-dependent and cap-independent translation (Nie and Htun 2006). Cap-dependent translation on this plasmid occurs through the CMV promoter and leads to expression of YFP, while cap-independent translation occurs via internal ribosome entry site (IRES) and allows for expression of CFP. This bicistronic construction allows one to differentiate between defects in translation initiation and translation elongation because the IRES element recruits the 80S complex directly, thus bypassing the traditional initiation phase entirely (Nie and Htun 2006). Thus if Eg5 participated during initiation, then inhibition of Eg5 would selectively decrease YFP. However, if Eg5 functions during elongation, than a decrease in both YFP and CFP would be expected. Interestingly, 36 hrs after Eg5 knockdown in U2OS cells (chosen because of their high transfection efficiency), and 24 hrs after bicistronic plasmid transfection, a significant 55% and 52% reduction in YFP and CFP protein, respectively was observed (Figure 4.14). This decrease could not be due to mitotic arrest, as only a 14% increase in the mitotic index was observed after a 36 hr knockdown of Eg5 in U2OS cells. The decrease under cap-dependent and cap-independent translation strongly suggests that loss of Eg5 effects translation after the initiation step and confirms the data from polysome profiling which indicates that Eg5 plays some role during elongation.

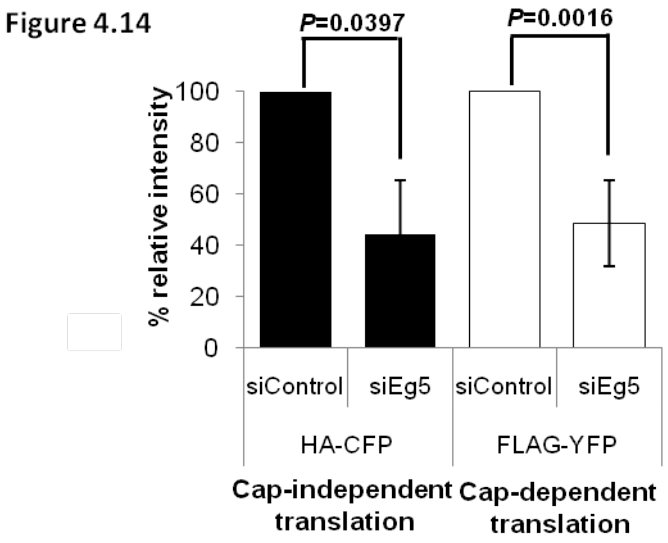

Figure 4.14: Reduced cap-dependent and cap-independent translation is observed after Eg5 knockdown.

U2OS cells were first knockdown with Eg5 for a total of 36 hrs and were transfected with the bicistronic promotor plasmid for a total for 24 hrs. Data is representative of 5 independent experiments; graph represents quantitation of immunoblotting. Results are shown as mean ± s.d. , *P* values represent students' t-test.

4.2.5.5 Ribosome half-transit time increases after loss of Eg5

Thus far we have accumulated a wealth of data which indicates that Eg5 facilitates translation elongation; however, much of the data has been indirect evidence supported by inference. Thus to conclusively demonstrate a role for Eg5 during translation elongation the half-transit time of the ribosome were investigated. The half-transit time of a ribosome refers to the time it takes for one ribosome to traverse an average sized mRNA (Sivan, Kedersha et al. 2007). In these

experiments, cells were treated with monastrol for 4 hr, followed by 10 μCi/ml of ^{35}S Met/Cys, and every 2 min, time points were taken by adding cycloheximide, cells were lysed, and DNA pellet was omitted. Half of the cell lysate was removed which contained total proteins (post mitochondrial supernatant), those proteins that completed protein synthesis as well as those still attached to the ribosome, while the other half was layed on a 20-60% stepwise sucrose gradient and subjected to ultra-centrifugation, pelleting out those nascent proteins still attached to the ribosome and removing the completed proteins (post ribosomal supernatant). Each of these fractions was then TCA precipitated on GF/C filters and subjected to scintillation counting, followed by linear regression analysis. In the control cells, ribosome half-transit time was calculated to be 59.3 seconds, while after monostrol treatment the half-transit time increased ~3-fold to 145.7 seconds (Figure 4.15A). Puromycin was used as our positive control in this experiment and exhibited a 2-fold increase in the ribosome half-transit assay (Figure 4.15B). This provides direct evidence that the decreased protein synthesis observed after loss of Eg5 resulted from decreased peptide chain elongation.

4.2.5.6 Rate of protein synthesis after loss of Eg5

The rate of protein synthesis was also investigated after Eg5 knockdown or monastrol treatment. For this assay, ^{35}S Met/Cys incorporation assay was preformed, with the exception that two time points were taken and the protein concentration was taken into consideration. After a 24 hr knockdown of Eg5, a 2.2-fold decrease in the rate of protein synthesis was observed, whereas after Eg5 inhibition by monastrol, a 1.5 fold-decrease in the rate of protein synthesis was observed (Figure 4.15C). Intriguingly, knockdown of Eg5 actually effects the rate of protein synthesis more than inhibition with a small molecule. However, this data are not surprising as

monastrol locks Eg5 onto the microtubule, therefore Eg5 is actually still present and may aid in retaining the ribosomes on mRNA. This data suggest that protein-protein interactions mediated by Eg5 as well as its ATPase activity are essential for the function of Eg5 during translation.

Figure 4.15

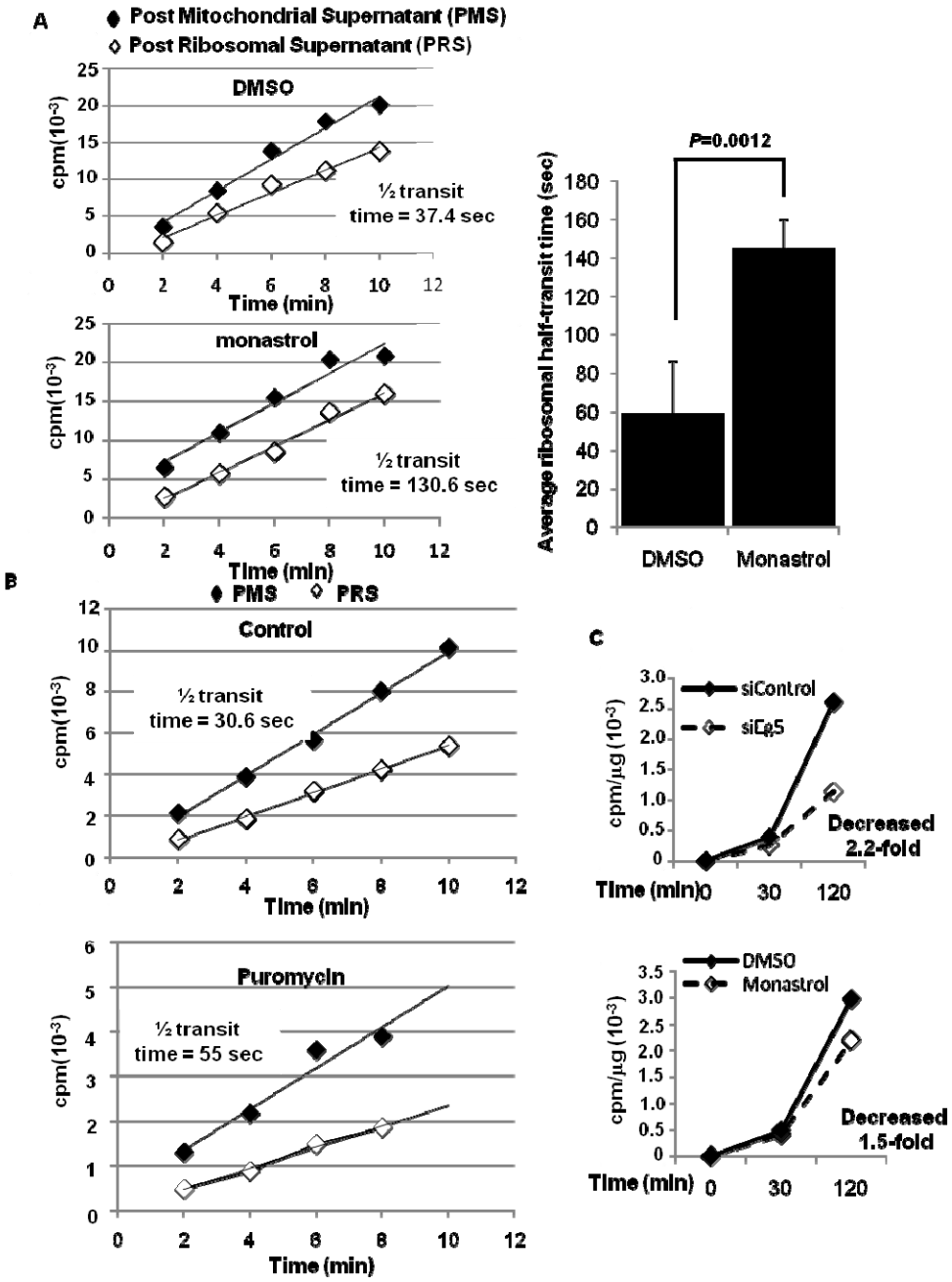

Figure 4.15: A 3-fold increase is observed in the ribosome half-transit time after Eg5 inhibition.

Ribosome half-transit time (A) after a 4 hr monastrol treatment or (B) after a 1 hr puromycin treatment. Graph in A represents analysis of four independent experiments after Eg5 inhibition. Incorporation of ^{35}S Met/Cys into total proteins or completed proteins released from the ribosome. The transit time was calculated as the difference in time between the two lines and was obtained by linear regression analysis. C Rate of protein synthesis assays after Eg5 knockdown (top) or after monastrol treatment (bottom). The transit time was calculated as the difference in time between the two lines and was obtained by linear regression analysis. C Rate of protein synthesis assays after Eg5 knockdown (top) or after monastrol treatment (bottom).

4.2.6 Eg5 functions to aid the ribosomes processivity

As the data so far suggests that Eg5 functions during elongation, it is interesting that after Eg5 inhibition an increase in the 80S is observed, which is typically thought of as an initiation defect. Initiation defects usually result in an increase in the 80S complex and a loss of polysomes (Li, Ohn et al. 2010), because 80S complexes are forming on the mRNA but never leave the initiation site and actively translating ribosomes continue to translate resulting in decreased polysomes. An elongation defect typically leads to a decrease in the 80S and an increase in polysomes resulting from hindered elongation and no new 80S complex formation (Sivan, Kedersha et al. 2007). So the question of how loss of Eg5 slows elongation and causes an increase in 80S ribosomes at the same time is quite intriguing. The sum of all the data collected thus far leads us to hypothesize

that after loss of Eg5 the translating 80S complexes are “falling-off” the mRNA; therefore the function of Eg5 is to hold/stabilize the 80S ribosome onto the mRNA.

Previous quantitative models have stated that the 80S does not fall off the mRNA, (Bretscher 1968; Bergmann and Lodish 1979) but recent data has since demonstrated that the 80S ribosome can actually fall-off or drop-off the mRNA during translation for a variety of reasons, a few of which I will discuss. The first is when cells, prokaryotes as well as eukaryotes, have been treated with elongation inhibitors such as puromycin or phyllanthoside and nagilactone C (Chan, Khan et al. 2004). Each of these inhibitors cause premature termination of protein synthesis at the elongation step and it has been demonstrated through polysome profiling analysis that the 80S ribosomes have been shown to fall-off the mRNA in a stop-codon independent manner. A second example occurs under diminished amino acid levels, which leads to slowed elongation and ribosomal drop-off leading to decreased protein synthesis (Caplan and Menninger 1979; Goldman 1982). Finally, a third example comes from microRNAs which have been demonstrated to be cause ribosomes to drop-off prematurely as a way of controlling protein synthesis (Petersen, Bordeleau et al. 2006). Given these precedents it is quite conceivable that Eg5 functions in such a way as to stabilize the mRNA/ribosomes, aiding the ribosome to prevent them from dropping-off the mRNA during translation and thus enhancing the ribosomes’ processivity. If Eg5 is functioning to aid in processivity during translation, then upon loss of Eg5 or its motor activity the ribosome has an increased probability of dropping-off the mRNA, leading to an increase in the 80S ribosomes. As a direct corollary, fewer proteins would be fully translated, and loss of Eg5 would lead to decreased elongation and increased ribosome half-transit time, which is exactly what we find after Eg5 knockdown.

The relevance of the above example of microRNAs bears further explanation. The prevailing notion of the translating ribosome is analogous to a moving locomotive. Defects in translation are generally thought to occur during the initiation phase or just as the ribosome begins translating, but once the ribosome begins moving nothing except reaching a stop codon will prevent the ribosome from translating. The ability of microRNAs to bind to a coding region in order to inhibit translation deflates the notion that a translating ribosome as an unstoppable molecular machine. One could argue that the ribosome is so susceptible to 'dropping-off' that the cell has evolved ways to exploit this tendency by targeting microRNAs to coding regions in order to inhibit translation. Given this apparent tendency for 'dropping-off', it seems reasonable that the cell would also have evolved fail-safe mechanisms to prevent termination of translation in codon-independent manner. Collectively our data suggests that Eg5 perform this exact function; that is, ensure processivity of the ribosome.

4.2.6.1 Eg5 knockdown affects protein synthesis of longer polypeptides more than shorter polypeptides

Therefore to test the hypothesis that Eg5 facilitates the ribosomes processivity, we developed a processivity assay to look at newly synthesizing proteins in the presence or absence of Eg5. In developing this assay, we argued that if Eg5 functioned to aid the ribosomes' processivity, then loss of Eg5 would be expected to impact larger proteins more than smaller proteins. This would be anticipated as the longer the mRNA the greater the probability a ribosome could drop-off due to the increased drag of the protein on the ribosome and the greater the processivity required to complete protein synthesis of longer proteins. For this assay, proteins were classified into two

groups, high molecular weight proteins, pertaining to proteins greater than 37 kDa in size (as determined by a molecular weight marker) and low molecular weight proteins, those proteins that are less than 37 kDa. As a positive control in developing this assay, low concentrations of puromycin was used; recall that low concentrations of puromycin produced polysome profiles very similar to monastrol-treated or siEg5-treated cells. Furthermore, puromycin is known to cause premature termination of the polypeptide chain, thus simulating decreased processivity. After 1 hr of 0.1 mg/ml of puromycin treatment, 100 μCi/mL of ^{35}S Met/Cys was added to cells, prior to cell lysis, followed by gel electrophoresis, and scintillation counting. Indeed treatment of low levels of puromycin caused a decrease in translation of larger molecular weight proteins relative to proteins less than 37 kDa. (Figure 4.16A)

In order to determine whether Eg5 facilitates the processivity of translating ribosomes cells were subjected to 24 hr Eg5 knockdown prior to completing the processivity assay. The results from this assay confirm the hypothesis the Eg5 aids in the ribosomes processivity, as loss of Eg5 caused the translation of proteins greater than 37 kDa to be decrease significantly as compared to proteins lower than 37 kDa (Figure 4.16B). This is precisely what is to be expected if Eg5 was functioning in stabilizing ribosome/mRNA interaction and aiding the ribosomes' processivity.

Figure 4.16

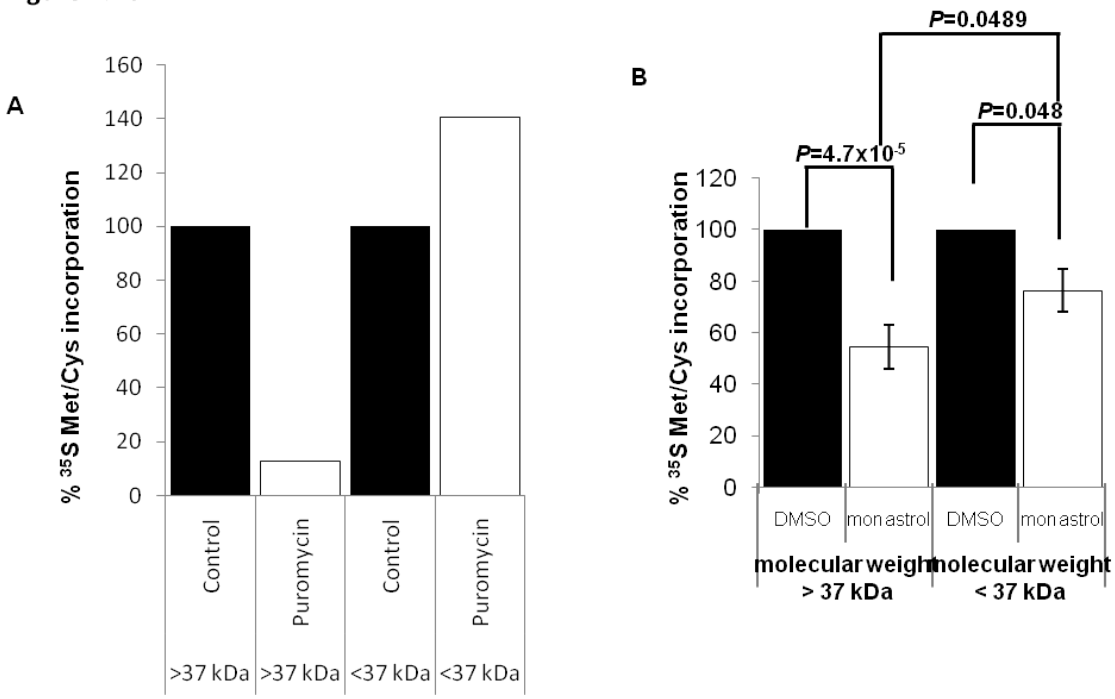

Figure 4.16: Decreased processivity of longer proteins more than shorter proteins is observed after Eg5 inhibition or puromycin treatment.

^{35}S Met/Cys incorporation assays were completed (A) after Eg5 inhibition or (B) after puromycin treatment, proteins separated by SDS-PAGE, and subjected to scintillation counting based on the proteins MW. Results are shown as mean ± s.d. and are representative of at least three independent experiments, *P* values represent students' t-test.

4.2.6.2 Difference between puromycin and Eg5 knockdown during the processivity assay

Additionally, our developed processivity assay reveals differences between Eg5 inhibition and low levels of puromycin treatment that we feel are reflective of the differences in the underlying Eg5 mechanism. In addition to inhibiting translation of larger molecular weight proteins, low levels of puromycin treatment causes an increase in lower molecular weight proteins. This is in contrast to Eg5 inhibition where a decrease is observed for both high and low molecular weight proteins. This difference can likely be explained by noting that part of the mechanism of puromycin is to cause the release of nascent growing polypeptides from the ribosome. Thus, treatment of puromycin not only prevents the translation of higher molecular weight proteins, but causes an apparent increase in lower molecular weight proteins by releasing the nascent peptide. Conversely, our processivity model for Eg5 would lead to decreased translation of higher molecular weight proteins without an increase in lower molecular weight proteins because loss of Eg5 is not expected to induce dissociation of the nascent polypeptide. That is, although larger molecular weight proteins are more affected by loss of Eg5, larger and lower molecular weight proteins are affected because the ribosome 'drops-off' without release of the nascent polypeptide.

Therefore, this data would suggest the ribosome have acquired other mechanisms to aid in protein translation outside of those known. These mechanisms include anchoring itself via Eg5 to non-translating structures (i.e., microtubules) while Eg5 binds to the ribosome, stabilizing the ribosome/mRNA interaction and aiding the processivity of the ribosome.

4.2.6.3 Increase in the 80S ribosome after loss of Eg5 requires ongoing translation

To further demonstrate that Eg5 functions in the processivity of ribosomes, we envisioned that if we could physically block translation concurrently with Eg5 inhibition, then the 80S ribosome should not be able to fall-off and should remain bound to the mRNA, if the increase in the 80S ribosome was due to ribosome drop-off in the absence of Eg5 function. To test this, cells were treated in the presence or absence of CHX and/or monastrol for 4 hrs, followed by cell lysis and polysome profiling; CHX was added concurrently with the treatment of monastrol to block the 80S ribosome drop-off caused by the monastrol treatment (Figure 4.17A,B). In the absence of CHX and the presence of monastrol, we observed an increase in the 80S ribosome; however when CHX and monastrol were added simultaneously to cells for 4 hrs, polysome profiles looked identical to control cells, therefore demonstrating that ongoing translation was required to cause the 80S ribosome to drop-off the mRNA in the absence of Eg5. This result was opposite of what we observed when cells were treated with CHX and arsenite, a translation initiation inhibitor. In this case, the 80S increased even in the presence of CHX.

In order to demonstrate that the increase in the 80S after monastrol inhibition was due to ongoing translation, cells were treated with or without monastrol and CHX was simultaneously added for 4 hrs, followed by a washout of the CHX and the re-addition of either DMSO, for control cells, or monastrol. In this experiment, after washout of CHX, the 80S ribosome fraction increased as compared to control. This experiment further confirmed that the increase in the 80S is due to ribosomal drop-off after Eg5 inhibition in mammalian cells (Figure 5.18 Model).

Figure 4.17

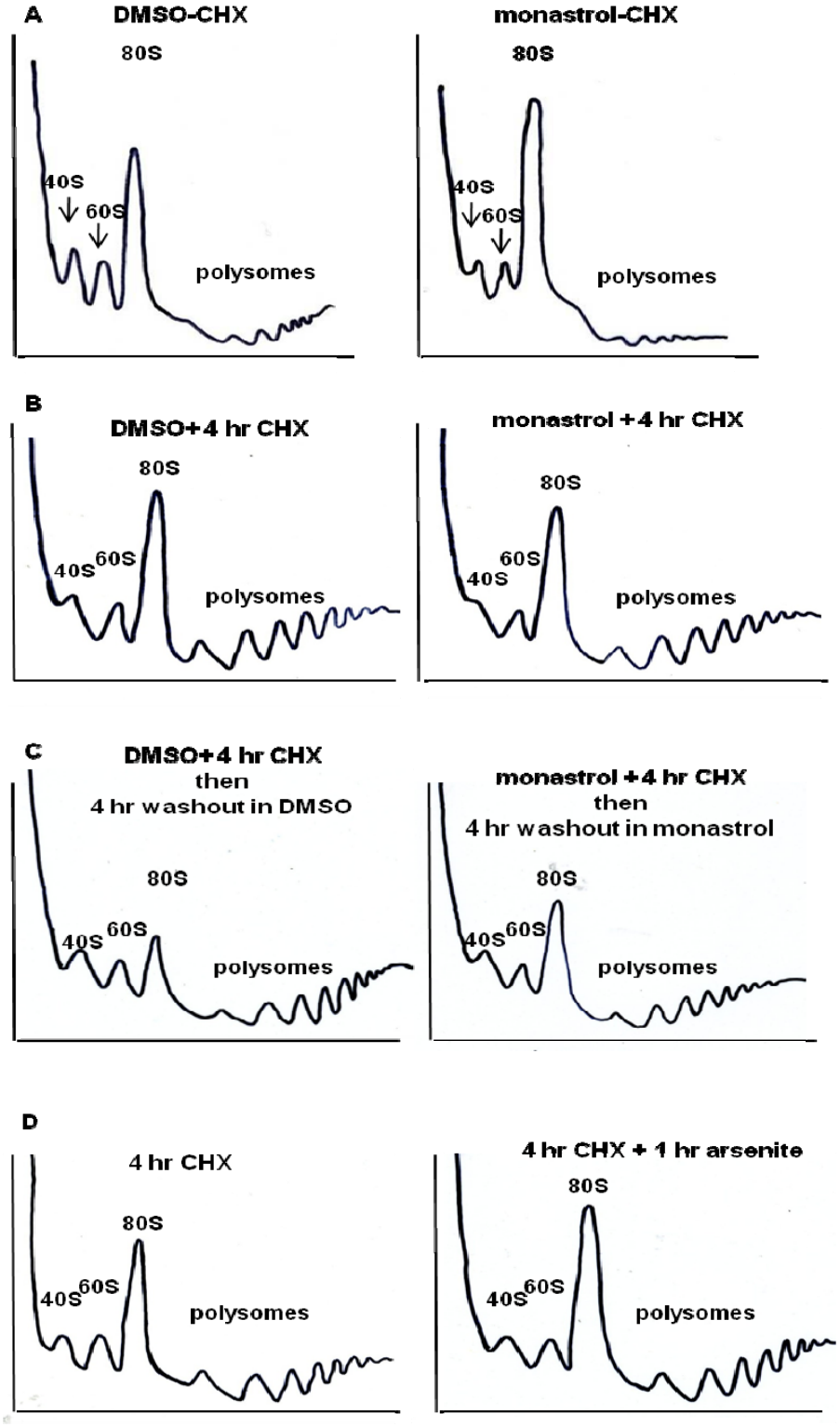
A
DMSO-CHX
80S
40S
60S
polysomes
monastrol-CHX
80S
40S
60S
polysomes
B
DMSO+4 hr CHX
80S
40S
60S
polysomes
monastrol +4 hr CHX
80S
60S
40S
polysomes
C
DMSO+4 hr CHX
then
4 hr washout in DMSO
80S
40S
60S
polysomes
monastrol +4 hr CHX
then
4 hr washout in monastrol
80S
40S
60S
polysomes
D
4 hr CHX
80S
40S
60S
polysomes
4 hr CHX + 1 hr arsenite
80S
40S
60S
polysomes

Figure 4.17: Increase in 80S ribosome after loss of Eg5 is due to ongoing translation. **Polysome profiling of 30 million cells in the (A) presence and absence of monastrol and (B) after a 4 hr CHX treatment in the presence and absence of monastrol, (C) In the presence or absence of monastrol with a 4 hr CHX treatment followed by a 4 hr washout and re-addition of monastrol or DMSO, or (D) in the presence or absence of arsenite, with a 4 hr CHX addition. The 4 hr of CHX in each case was used to block ongoing translation.**

Figure 4.18 Eg5 Model

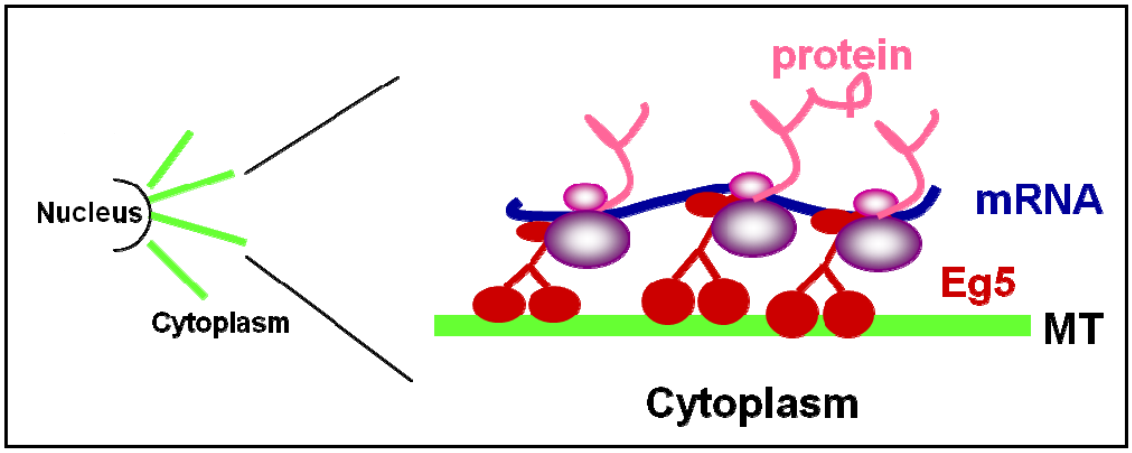

With Eg5: During protein translation, we believe ribosomes are associated with MTs through Eg5 and that Eg5 is not required for translation but increases the processivity of the ribosome.

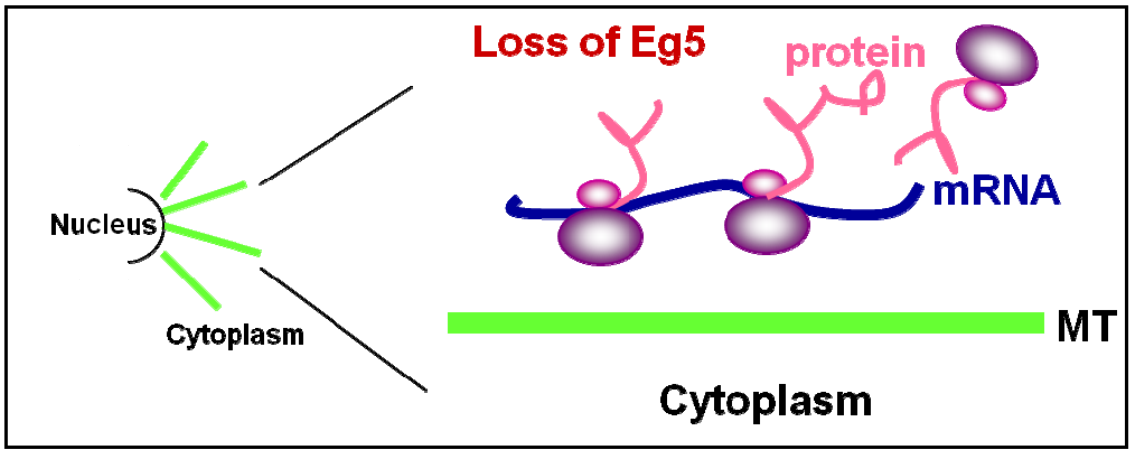

Without Eg5, the ribosome can still translate, but its processivity is reduced causing a decrease in protein synthesis and in particular polypeptides with high molecular weights.

Figure 4.18: Model of Eg5 functioning in translation elongation.

4.3 DISCUSSION

4.3.1 Inhibition of Eg5 causes a decrease in most but not all cell lines tested

As mentioned previously in section 4.2.2.2 monastrol treatment caused a decrease in translation in the majority of cell lines tested. However, in two of the ten different cell lines tested, translation did not decrease upon monastrol treatment. The cells lines were UPCI:SCC103 and an oral squamous and A549, a lung cancer cell line. Although there are many common hallmarks of cancer, there are also many differences making it very difficult, if not impossible, to *a priori* predict why these cell lines were resistant to monastrol-induced inhibition of translation. Some possible scenarios are that Eg5 may be overexpressed in these cell lines, thus lowering the effective concentration of monastrol, or it could be due to cell permeability issues, or due to an off-target protein that binds to monastrol that is present in those cell lines, or even due to multi-drug efflux pumps. Future experiments will be needed to directly pinpoint their resistance to monastrol treatment.

It has previously been demonstrated in clinical trials of small lung carcinoma cells, the Eg5 clinical inhibitor, Ispinesib, does not work effectively to inhibit or decrease tumor formation unless it is used in combination with radiotherapy (Saijo, Ishii et al. 2006). Therefore, the defects that are observed in these small lung carcinoma tumors and even A549 cells, may represent a defect such that monastrol does not efficiently inhibit Eg5 tumors or cells lines originating from the lung. Accordingly, future experiments examining translation in these cell lines should be completed with Eg5 knockdown, which may be more effective that monastrol.

4.3.2 Ribosome half-transit time reveals further evidence for Eg5's function in elongation

During analysis of the half-transit time of the ribosome after Eg5 inhibition, we observed a 3-fold increase. However, close examination of the data reveals Eg5 does not follow the same pattern of ^{35}S Met/Cys incorporation as a typical elongation inhibitor does during the half-transit assay. Usually elongation inhibitors have a decreased rate of incorporation in this assay, such that in control cells, the first time point is typically 1,000 cpm and the last time point is ~20,000 cpm (for both PMS and PRS), but for elongation inhibitors, the amount of incorporation is such that the first time point is generally 500 cpm and the last around 10,000 cpm (see puromycin ribosome half-transit time in figure 4.12B for example). That is, elongation inhibitors generally cause a decrease by ~50% throughout the entire time course. This is due to the decreased incorporation of ^{35}S Met/Cys because of the slowed/inhibited elongation. However, in similar experiments after Eg5 inhibition, the first and the last time points (of the PMS and PRS) both in control and monastrol–treated, were remarkably consistent. This suggested that Eg5 is clearly not functioning as a traditional elongation inhibitor. In fact, if one calculates the number of ribosomes with attached nascent proteins after Eg5 inhibition (by subtracting PMS values from PRS values); in this analysis, it yields approximately 1-2 more ribosomes with attached nascent polypeptides than control cells, suggesting ribosomal drop-off and retention of the polypeptide. This is in contrast to canonical elongation inhibitors, in this case puromycin, where there is 1-2 *less* nascent polypeptides bound to each ribosome because elongation is stalled but not dissociated. That is, ribosomes stalled during elongation prevent other ribosomes from initiating translation. From this data, it is suggesting that Eg5 is functioning in elongation different from the traditional elongation inhibitors such that Eg5 aids in mRNA/ribosome interactions and/or

processivity. One could anticipate observing more ribosomes bound to nascent proteins after Eg5 inhibition for two reasons:

1) In order for Eg5 to aid in processivity its ATPase activity is required. Thus one could hypothesize that the ribosome is exploiting a conformational change that takes place as Eg5 cycles between ATP-bound and ADP-bound forms. This cycle of conformational changes may be needed to ensure the association of Eg5 with various ribosomal subunits or to stabilize the translating complex with its transcript. Inhibition of Eg5 with monastrol would block the cycling of conformations and thus, loss of the ATPase activity of Eg5 would increase ribosome 'drop-off' rate by destabilizing the translating complex.

2) Even though the ribosome is hindered by the locked Eg5, one can imagine that the Eg5 is exerting a "pull" on the ribosome because it wants to keep translating but as it is not able to move efficiently. It is possible that the ribosome may pull to try and translate the protein, thus breaking its interaction with Eg5 and eventually "dropping-off" the mRNA, because Eg5 is no longer aiding in the stabilization.

4.3.3 Revisiting Eg5 as an ideal drug target

After decades of cancer therapies which entailed treating patients generally with cytotoxic compounds (i.e., etoposide, cisplatin, etc.), pharmaceutical companies have made a push to selectively target cancer cells over their healthy normal counterparts. Although proteins which are only present in cancer cells represent the ideal proteins (i.e, the BCR-ABL kinase), the

strategies to target other proteins in rapidly dividing cells are gaining momentum (Burris, Jones et al.) (Lad, Luo et al. 2008). Eg5 has emerged as promising drug target because its inhibition prevents dividing cells from completing mitosis. Inhibitors of Eg5 are in stages I and II of clinical trials with the assumption that Eg5 function only during mitosis, however the data presented here argues that Eg5 also functions during interphase in protein synthesis. This interphase function is likely a vital process that not only is needed in dividing cells, but in resting cells as well. Future studies examining Eg5 as a potential anticancer target will need to take into consideration this interphase function in translation as well.

4.3.4 Mitotic and interphase functions of Eg5

Additionally, inhibiting Eg5 for prolonged periods of time does lead to mitotic arrest and monopolar spindles, but whether mitotic and interphase roles are different or one in the same is yet to be answered. It is tempting to speculate that the mitotic and interphase roles of Eg5 are not different functions for the same protein; during mitosis it is known that protein translation is inhibited at the elongation stage, and it is during this time Eg5 is phosphorylated and begins to complete its mitotic function. The inhibition of elongation has been determined to occur by phosphorylation of eEF2, but it is possible that inhibition of translation during mitosis may still be linked to Eg5, at least in part, and only future experiments would fully determine if Eg5 phosphorylation also inhibits translation elongation.

5.0 CHAPTER V: IDENTIFICATION AND CHARACTERIZATION OF EG5 AND KID MOTORS IN STRESS GRANULE FORMATION

5.1 INTRODUCTION

During the examination of the interphase localization of Kid after high levels of UV-C treatment, Kid was found to localize to circular punctuate structures in the cytoplasm. Upon examination of the literature, I found that during conditions of translational inhibition or oxidative stress, such as the UV-C treatment, cells form structures called stress granules (Kedersha and Anderson 2002; Kedersha and Anderson 2007). Stress granules, as mentioned previously in the introduction section 1.2.3, are induced by eIF2α phosphorylation triggering inhibition of translation and leading to abortive initiation complexes. Stress granules harbor silenced mRNP complexes and are an assessment center for untranslated mRNAs. When these punctuate structures begin to form, they are small, but over times they coalesce to form large structures. When untranslated mRNAs localize to stress granules the mRNAs have three different fates: 1) reinitiate translation, 2) become degraded, or 3) remain within the stress granule for storage (Balagopal and Parker 2009).

5.2 RESULTS

5.2.1 Localization of nucleolar-associating motors to stress granules

5.2.1.1 Kid localizes to stress granules

In order to determine whether the cytoplasmic foci of Kid represented the localization of Kid to stress granules, co-localization studies with the stress granule marker eIF4E were conducted. Indeed, these studies confirmed the distinct cytoplasmic foci as stress granules. Furthermore, Kid was found to localize to stress granules when cells were induced to form stress granules by the typical dual puromycin- and arsenite-treatment (Figure 5.1A). Puromycin, causes premature termination of the polypeptide chain and enhances stress granule formation by increasing the formation of both pre-initiation complexes and availability of free 40S subunits, while arsenite treatment causes oxidative damage leading to phosphorylation of eIF2alpha (Roybal, Hunsaker et al. 2005). Thus, after treatment Kid was found to localize to stress granules under translational stress conditions. Future experiments will be conducted with arsenite treatment alone, as more recently published data demonstrated that arsenite alone is sufficient to induce stress granules and are more physiologically relevant (Roybal, Hunsaker et al. 2005).

Figure 5.1

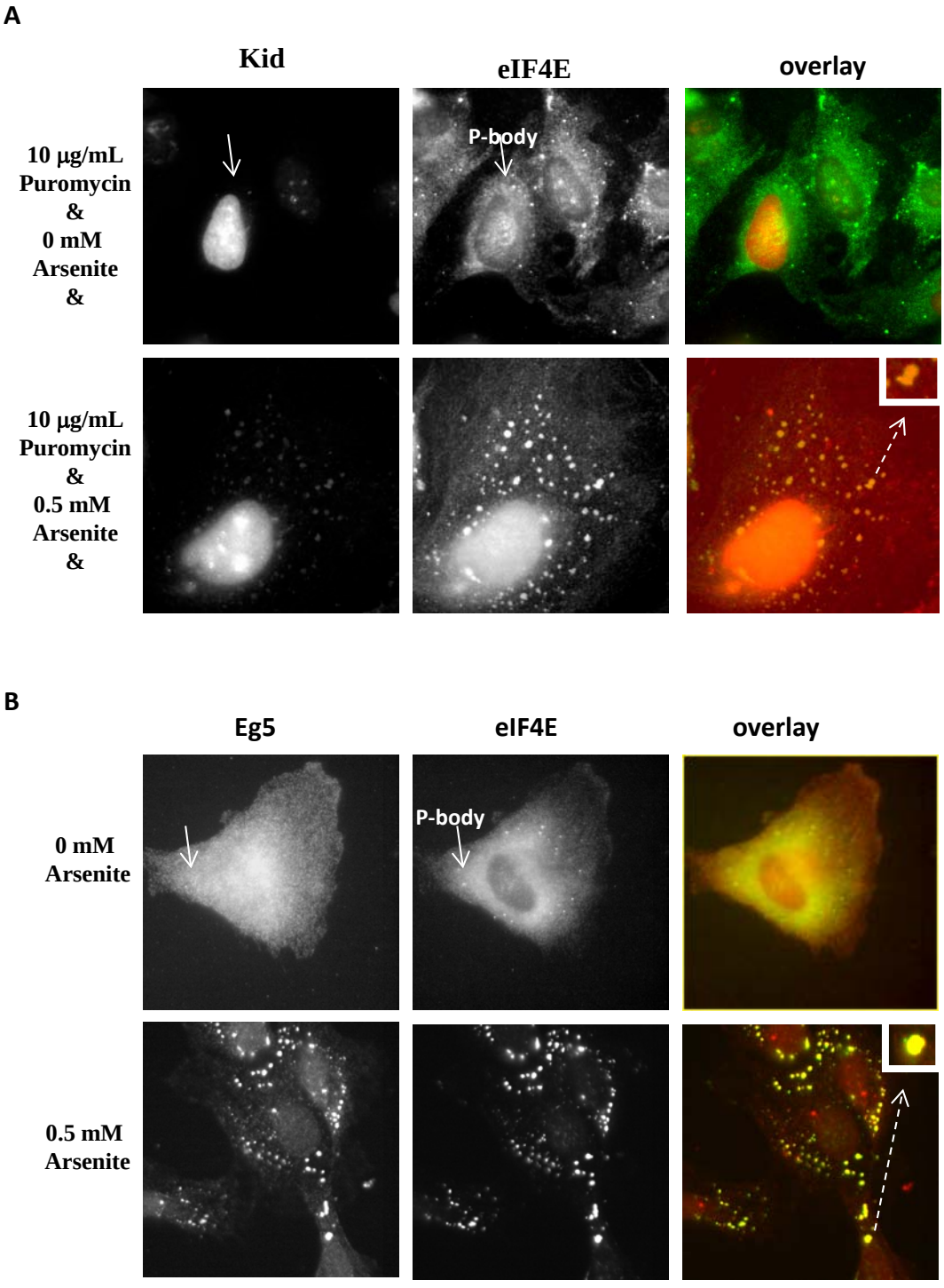
A
Kid
eIF4E
overlay
10 µg/mL Puromycin & 0 mM Arsenite &
P-body
10 µg/mL Puromycin & 0.5 mM Arsenite &
B
Eg5
eIF4E
overlay
0 mM Arsenite
P-body
0.5 mM Arsenite

Figure 5.1 Continued

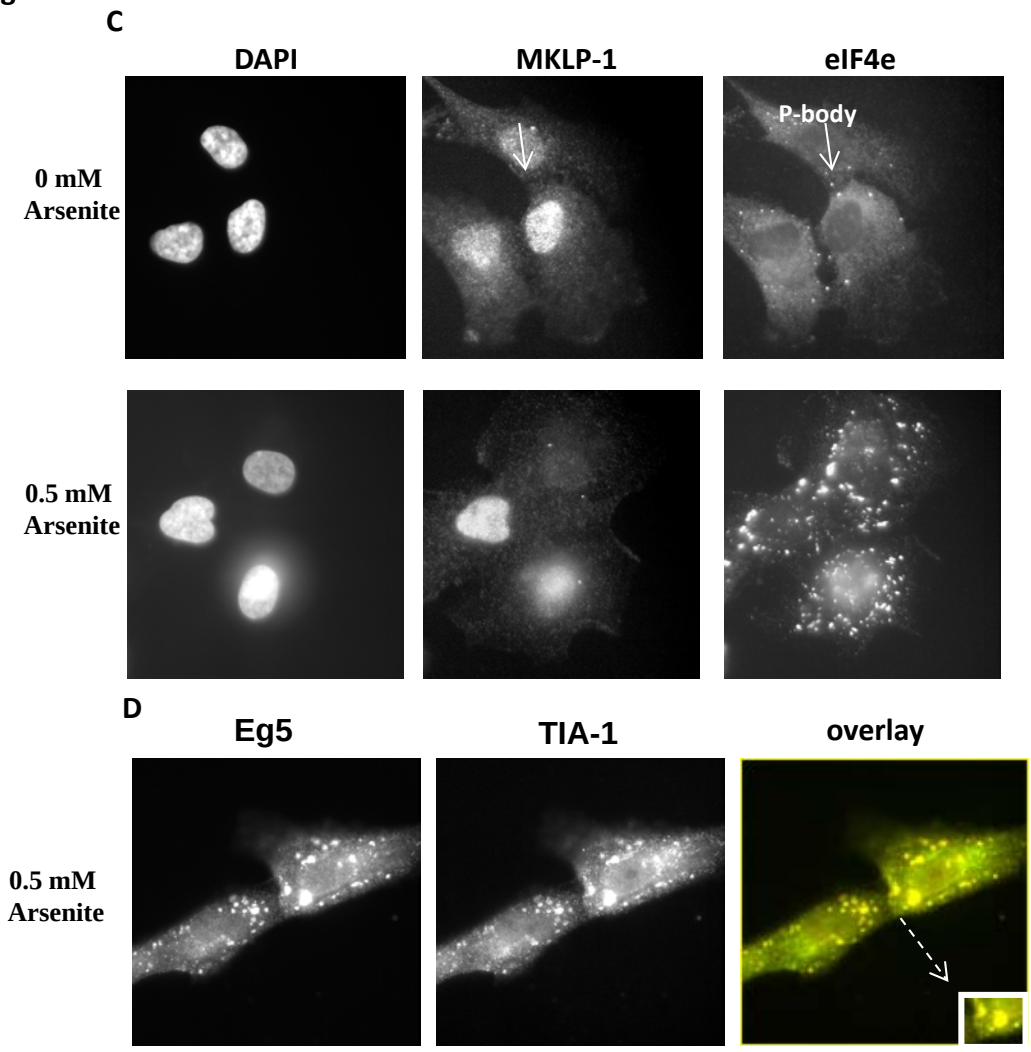

Figure 5.1: Kid and Eg5 localized to stress granules, but not P-bodies.

(A) RPE1 cells were treated with either puromycin and arsenite and stained for Kid and eIF4E, a stress granule marker. (B) RPE1 cells were treated with 0.5 mM arsenite and co-stained for Eg5 and eIF4E or (C) MKLP1 and eIF4E, or (D) Eg5 and TIA-1. Solid arrows represent p-bodies; insets shown stress granules co-localization.

5.2.1.2 Kid, Eg5, but not MKLP1, localizes to stress granules

As Kid was found to localize to stress granules, we next inquired whether the other ribosomal motors Eg5 or MKLP1 associated with stress granules. After 0.5 mM arsenite treatment, Eg5 but not MKLP1 robustly localized to stress granules (Figure 5.1B, C), as determined by co-localization with eIF4E and/or TIA-1, an RNA binding protein and structural component of stress granules (Figure 5.1D) (Kedersha, Gupta et al. 1999).

5.2.2 Kid, Eg5, and MKLP1 do not localize to P-bodies

As eIF4E is a marker not only for stress granules but for P-bodies, the localization of Eg5, MKLP1 and Kid to P-bodies was also investigated. P-bodies are distinct foci that are found in unstressed and stressed cells that contain mRNA as well as enzymes involved in mRNA turnover (Kedersha, Stoecklin et al. 2005). Stressed and unstressed cells were co-stained for Eg5, MKLP1 or Kid motor and eIF4E; in all cases the motor failed to localize to P-bodies (Figure 5.1A-C, as indicated by white solid arrows). This data would suggest that Kid and Eg5 are not associating with mRNA but rather associating with components of the translation complexes, consistent with our previous conclusions derived from polysome profiling.

5.2.3 Kid and Eg5 participate in stress granule dynamics

5.2.3.1 Kid knockdown causes a reduction in stress granule formation

As mentioned in section 1.2.3, recently published data has demonstrated roles for the anterograde transport of kinesin-1 and the retrograde transport of dynein heavy chain 1 in stress granule dissolution and formation, respectively (Loschi, Leishman et al. 2009). Consequently, we inquired whether Kid or Eg5 kinesin motors may also be involved in stress granule formation. Accordingly, Kid was knocked-down for 48 or 72 hrs, treated with or without arsenite treatment, after which stress granule formation was examined. After Kid knockdown and in the absence of arsenite, no induction of stress granules was observed; however, stress granule formation in the absence of Kid and presence of arsenite yielded a 20% decrease in the number of cells which formed stress granules (Figure 5.2). It should be noted that although a decrease in stress granule formation was observed, there was no striking difference in stress granule size between siKid and siControl cells when stress granules were present. This suggests a role for Kid in the formation or stability of stress granules.

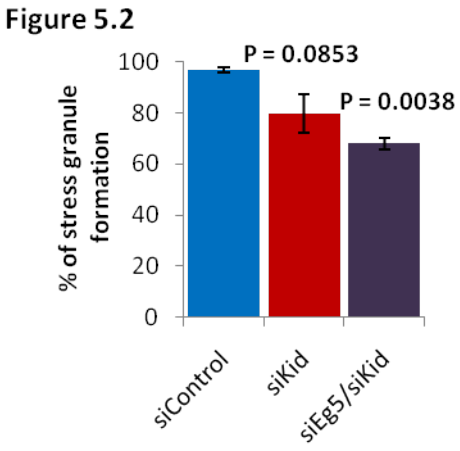

Figure 5.2: After knockdown of Kid, a small reduction in stress granule formation is observed.

Kid was knocked-down for 48 hrs prior to arsenite treatment. Additionally, Kid and Eg5 were simultaneously knocked-down for 48 hrs prior to arsenite treatment, fixation, and quantitation of stress granule formation. Results are shown as mean ± s.d. and are representative of at least two independent experiments, *P* values represent Students' t-test.

5.2.3.2 Eg5 knockdown causes a decrease in stress granule formation and coalescence

As Kid was found to contribute to stress granule formation, we next investigated whether Eg5 may also be important during stress granule assembly. Thus, 48 hrs after Eg5 knockdown, stress granule formation was investigated. In the absence of arsenite treatment, knockdown of Eg5 alone did not cause stress granule formation; however, in the presence of arsenite a nearly 40%

reduction was observed the number of cells which formed stress granules (Figure 5.3A, B). Additionally, of those cells which did form stress granules the size of the stress granules were significantly smaller and much greater in number than those of the siControl cells. Typically in control cells, stress granules are known to coalesce together in order to form large stress granules, however after Eg5 knockdown the stress granules did not appear to coalesce. Therefore, the reduction of cells exhibiting stress granules, as well as the smaller size and greater number observed suggests that Eg5 may be involved in stress granule formation, transport or the movement of stress granules to the center of the cell and/or coalescence, the joining of stress granules.

5.2.3.3 Live cell imaging reveals a loss in stress granule transport, formation, and coalescence after Eg5 knockdown

To examine the role of Eg5 in stress granule physiology, live cell imaging of stress granules in RPE1 cells was employed. RPE1 cells were transiently transfected with G3BP-GFP protein, a C-terminal GFP tagged variant of RasGAP-associated endoribonuclease, which is a component of stress granules and is involved in their assembly (Deigendesch, Koch-Nolte et al. 2006). Cells were treated with siEg5 and transiently transfected with G3BP-GFP for 48 hrs prior to live cell imaging. At time zero, arsenite treatment was added, and within 30 seconds stress granules began to form. However, in the absence of Eg5 the cells that did form stress granules took at least 4 times longer (up to 2 min) to initiate formation (Figure 5.4). Additionally, of the cells that did form stress granules (66%) the stress granules were smaller in size and more abundant in number (n=15), similar to the changes observed in fixed cells (Figure 5.3C). These small stress

granules were also found to be less motile and failed to coalesce as frequently. This data confirm that Eg5 is needed for stress granule formation/assembly, transport, and/or coalescence.

Figure 5.3

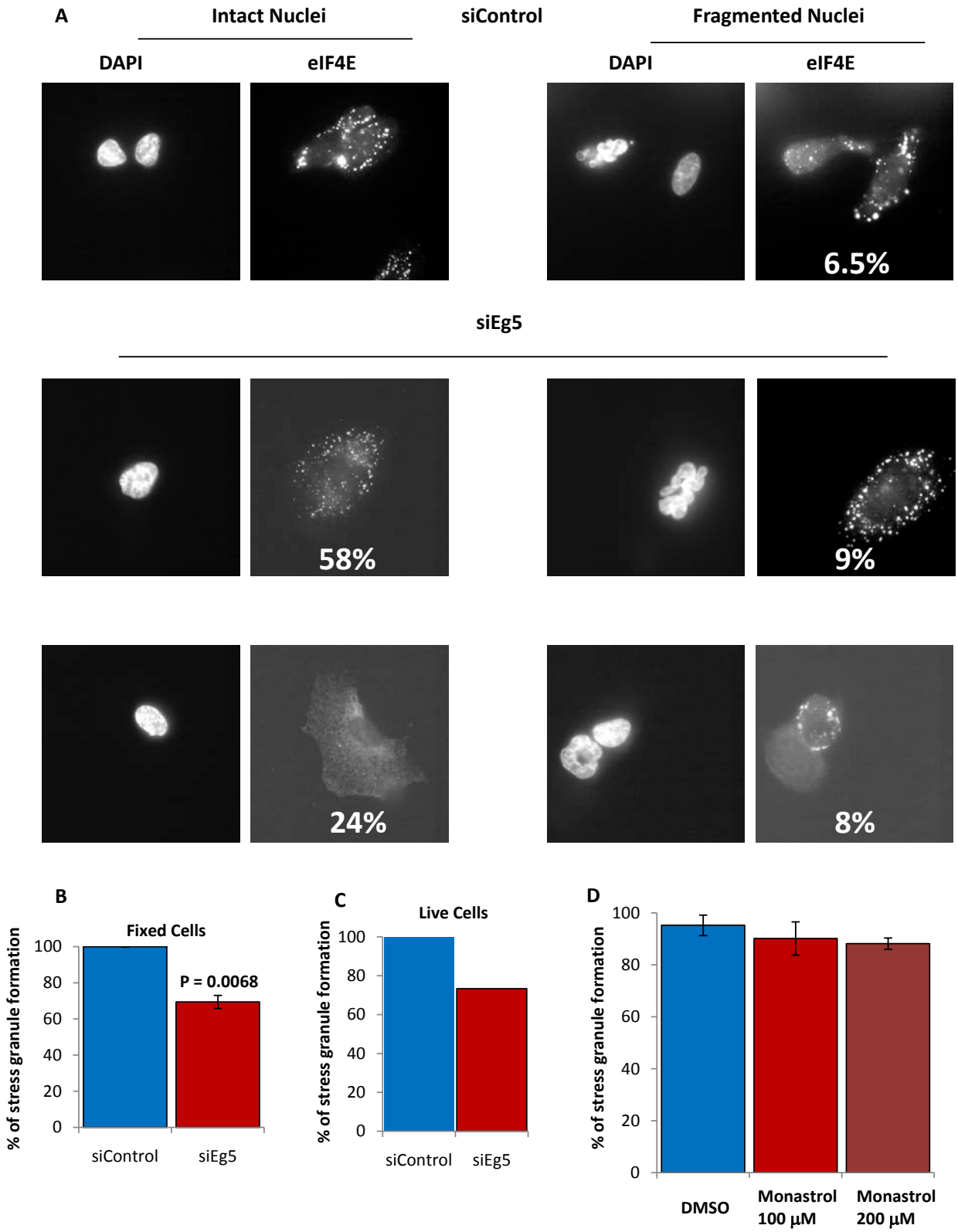
A
Intact Nuclei
siControl
Fragmented Nuclei
DAPI
eIF4E
DAPI
eIF4E
6.5%
siEg5
58%
9%
24%
8%
B
Fixed Cells
P = 0.0068
% of stress granule formation
100
80
60
40
20
0
siControl
siEg5
C
Live Cells
% of stress granule formation
100
80
60
40
20
0
siControl
siEg5
D
% of stress granule formation
100
80
60
40
20
0
DMSO
Monastrol 100 µM
Monastrol 200 µM

Figure 5.3: Reduction of stress granule formation and size after Eg5 knockdown.

(A) 48 hrs after Eg5 knockdown, cells were treated with 0.5 mM arsenite, fixed, and co-stained for Eg5 and eIF4E. Percentages represent quantitation of the number of cells with that phenotype. (B) Quantitation of fixed cells after Eg5 knockdown. (C) Quantitation of stress granule formation after Eg5 knockdown by live cell imaging. (D) Quantification of stress granule formation after Eg5 inhibition by monastrol. Results are shown as mean ± s.d. and are representative of at least two independent experiments, *P* values represent Students' t-test.

Furthermore, the reduction in stress granule formation after Eg5 knockdown is consistent with the role of Eg5 in translational elongation, as knockdown of elongation proteins does not cause stress granule formation in the absence of stress, but is known to cause a loss of granule formation under stressed condition. This is in contrast to translation initiation factors where knockdown alone is sufficient to cause stress granule formation, even in the absence of stress.

5.2.3.4 Eg5 and Kid function redundantly in stress granule formation

As a 20% reduction is stress granule formation was observed after siKid and a 32% reduction after Eg5 knockdown, we next inquired whether simultaneous knockdown of both motors would lead to synergistic effect on stress granules. After knockdown of both of these motors, stress granule formation did not decrease more than Eg5 knockdown alone (Figure 5.2). Therefore it

seems as though the mechanism by which these motors induce stress granule assembly is balanced or may be redundant.

5.2.3.5 Loss of Eg5 causes a small percentage of cells to undergo apoptosis

As prolonged exposure of Eg5 knockdown is known to cause mitotic arrest, cell death and apoptosis, we investigated whether the decrease in stress granule formation after Eg5 knockdown was the result of these well-known side-effects of loss of Eg5. Therefore, we first determined the percentage of cells found to be arrested in mitosis. After 48 hrs knockdown of Eg5, a 9% increase in the mitotic index was observed in RPE1 cells. However, it should be noted that the percentage of cells which were arrested in mitosis were not included in our analysis, as previously published data has demonstrated that mitotic cells do not contain stress granules. Next, we examined apoptosis by looking for fragmented nuclei by DAPI staining. In the control cells, 2% and 5.7% of cells contained fragmented nuclei before or after stress granule formation, respectively. In the case of Eg5 knockdown, of the 33% of cells that did not contain stress granules, 8% were found to contain fragmented nuclei, and of the 68% that contained small stress granules, 9% were found to have fragmented nuclei. Although the knockdown of Eg5 did increase the percentage of cells exhibiting fragmented nuclei, this percentage was the same between cells which did not form stress granules. Thus, the presence of fragmented nuclei could not be contributing to the decreased stress granule formation. (Figure 5.3A, right).

5.2.3.6 The ATPase activity of Eg5 is not required for stress granule formation, transport or coalescence

As knockdown of Eg5 exhibited a decrease in stress granule assembly, we inquired whether this is the result of the motor activity of Eg5 or the ability to Eg5 to form complexes through its cargo domain. Accordingly, when cells were treated with either 100 μM or 200 μM monastrol for 4 hrs, only a 6% decrease in stress granule formation/assembly was observed (Figure 5.3D). This strongly suggests that the binding of Eg5 to specific cargo, rather than its ATPase activity, is necessary for the role of Eg5 in stress granule formation/assembly.

Figure 5.4

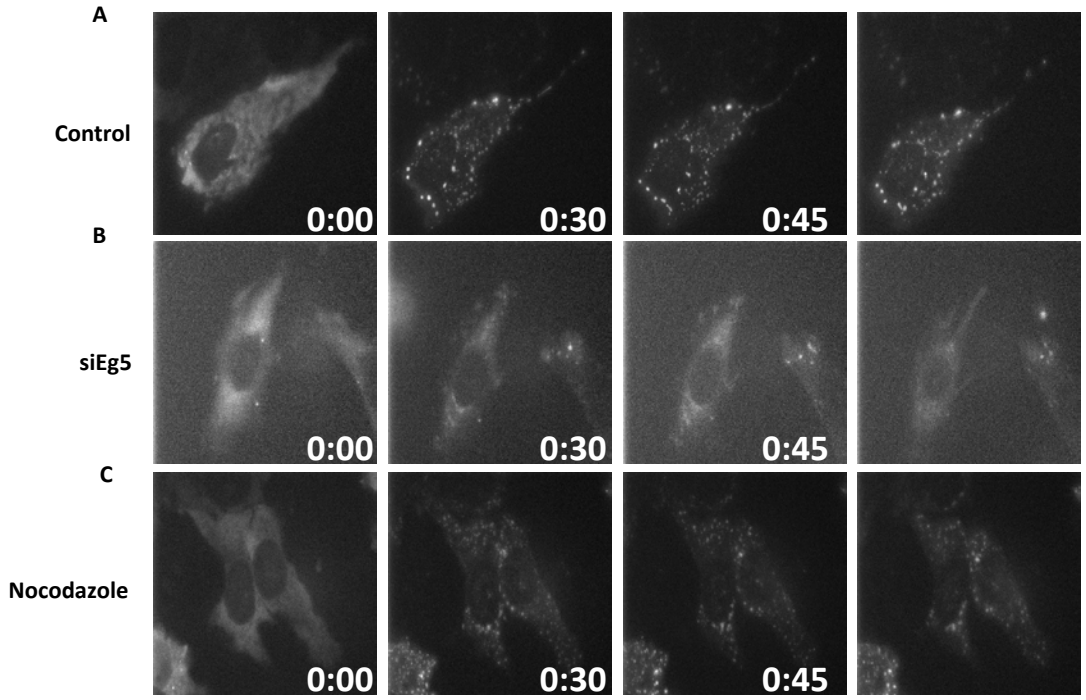

Figure 5.4: .Live cell imaging stills after Eg5 knockdown or microtubule depolymerization. Time stamp indicated hr:min. A) siControl, B) siEg5, or C) nocodazole treated.

5.2.3.7 Eg5 functions in stress granule dissolution

Given the role of Eg5 in stress granule formation and coalescence, we next inquired whether Eg5 may play a role in stress granule recovery or dissolution. Cells were treated with monastrol for 4 hrs prior to 1 hr arsenite treatment, followed by washout, and recovery. During recovery, various time points were taken every 20-30 min. Up until the 50 min time point, siControl and siEg5 cells showed no difference in stress granule dissolution (Figure 5.5A). However, a change in

stress granule dissolution was observed during a 30 min time period from 50-80 min, whereby monastrol-treated cells significantly persisted with ~40% of cells containing stress granules. However by the end of 90 min, stress granules had almost completely dissolved similar to control cells. This demonstrates that the ATPase activity of Eg5 may be needed during stress granule dissolution. Similar experiments were completed after knockdown of Eg5 and analogous results were observed, however 10-15% of cells retained stress granule formation even after siControl cells (Figure 5.5B). It should be noted that at the initial time point of 0 min, there was no loss of stress granule formation in this experiment; therefore this results will need to be repeated.

Figure 5.5

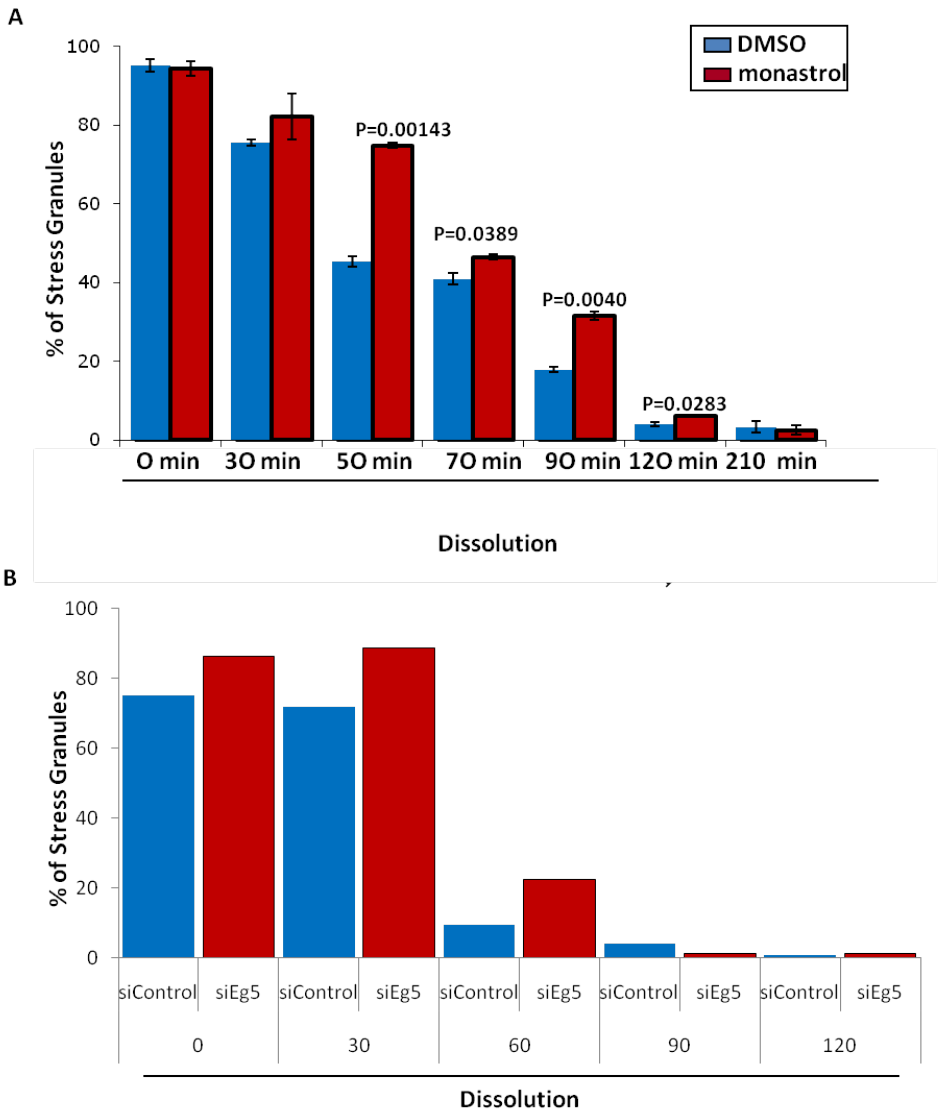

Figure 5.5: Eg5 inhibition and knockdown delays stress granule dissolution.

(A) 4 hr after monastrol treatment or (B) 48 hrs after Eg5 knockdown cells were treated with arsenite, washed-out and released, prior to time points every 20-30 min. Results are shown as mean ± s.d. and are representative of at least two independent experiments, *P* values represent Students' t-test.

5.2.4 Microtubules are also required for stress granule formation, transport and dissolution in RPE1 cells

5.2.4.1 Microtubules are needed for stress granule formation

Previously published data in COS-7 cells demonstrated that microtubules are required for stress granule formation (Ivanov, Chudinova et al. 2003). We tested this conclusion in RPE1 cells, using 12 μM nocodazole for 2 hrs prior to arsenite treatment, but only a ~30% loss of stress granules was observed (Figure 5.6). Similar to Eg5 knockdown, stress granules were smaller in size and greater in number as compared to control cells. This conclusion was confirmed by live cell imaging: 80% of cells examined formed stress granules (n=12), but were both significantly greater in number and smaller in size as compared to control cells (Figure 5.4). Additionally, even though control cells began to form stress granules within 30 seconds, in nocodazole treated cells stress granules assembly began around 5 min after arsenite exposure. This apparent loss of coalescence of stress granules suggests that microtubule inhibition causes a similar phenotype as that observed in the absence of Eg5, consistent with a role for microtubule motors like Eg5 and Kid in stress granule formation.

Figure 5.6

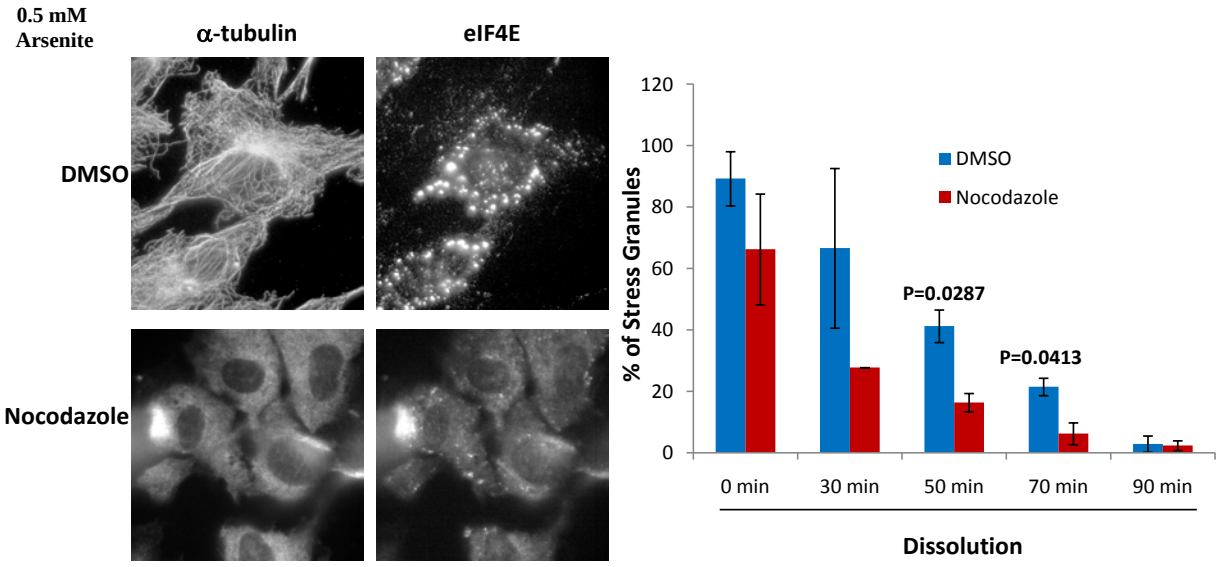

Figure 5.6: Microtubules are needed for stress granule formation.

Top: Immunofluorescence of a-tubulin or eIF4e in the presence or absence of microtubules. Bottom: Quantitation of stress granule dissolution after a 2 hr treatment with nocodazole followed by a 0.5 mM arsenite treatment, fixation, and quantitation. Results are shown as mean ± s.d. and are representative of at least two independent experiments, *P* values represent Students' t-test.

5.2.4.2 Live cell imaging reveals microtubules are needed for stress granule transport

Finally, during live cell imaging when cells were treated with nocodazole and arsenite at the same time, stress granules formed at similar sizes as in control cells, however, they did not move

towards the cell nucleus, rather they stayed at the edges of the cells. This suggests that in order for stress granules to move and localize around the cell nucleus, microtubules are required.

5.2.4.3 Microtubules are required for control of stress granule dissolution

Additionally, stress granule dissolution was also investigated after microtubule depolymerization. Cells were treated for 2 hrs with nocodazole, followed by a 1 hr arsenite treatment, and time points were taken every 20-30 min after arsenite washout. Interestingly, of the cells that formed stress granules, dissolution actually occurred faster in the absence of microtubules, than in the presence of microtubules (Figure 5.6). This result was quite interesting, as it would suggest that microtubules actually hinder the dissolution process.

5.3 SUMMARY

In summary, Eg5 is demonstrated to be required for the formation of stress granules, the coalescence of smaller stress granules into larger ones, dissolution of stress granules after arsenite washout and even transport towards the center of the cell. From these studies, the Kid motor was demonstrated to be needed for stress granule formation, but not transport or coalescence; however whether Kid may be needed for stress granule dissolution has yet to be examined (Figure 5.7). In the case of microtubules, they seem to mirror Eg5s' function in stress granules, but importantly, it seems to be mostly required for dissolution as loss of microtubules allowed stress granules to dissolve quicker which can lead to many detrimental effects on the cell, as discussed below.

Figure 5.7

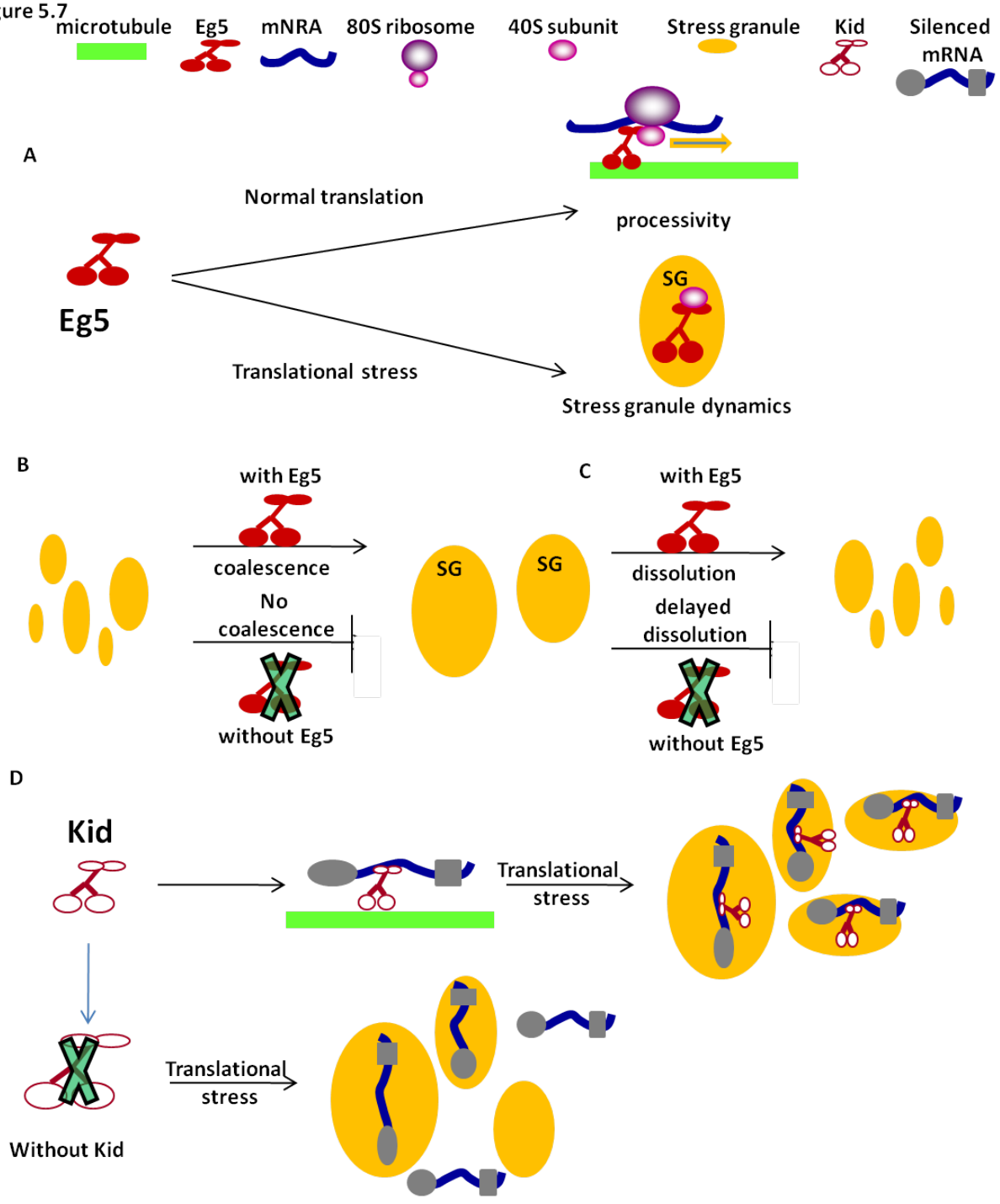
microtubule
Eg5
mNRA
80S ribosome
40S subunit
Stress granule
Kid
Silenced mRNA
A
Normal translation
processivity
Eg5
SG
Translational stress
Stress granule dynamics
B
with Eg5
coalescence
No coalescence
without Eg5
SG
SG
C
with Eg5
dissolution
delayed dissolution
without Eg5
D
Kid
Translational stress
Translational stress
Without Kid

Figure 5.7: Stress granule model.

(A) Eg5 has independent roles in ribosome processivity and stress granule formation. Under translational stress, Eg5 aids the 40S ribosome into the stress granule complex. However, in the absence of Eg5 (B) stress granule formation is decreased and coalescence is also inhibited. (C) Additionally, in the absence of Eg5, stress granule dissolution is delayed. (D) In the presence of Kid and under translational stress, Kid aids silenced mRNA into the stress granule complex, however in the absence of Kid, a loss in stress granule formation is observed and less mRNAs are transported into the stress granules during translational stress repair.

5.4 DISCUSSION

5.4.1 Eg5 makes use of protein-protein interactions, rather than its ATPase domain for stress granule formation and coalescence

The identification of Eg5, Kid and microtubules in stress granule assembly, transport, coalescence, and even dissolution is generally consistent and supportive with my previous conclusions of Eg5 participating in protein translation. As motors typically are known to transport cargo along microtubules, our findings suggest that under translational stress, Eg5 plays a role in transport of stress granules to aid in stress granule assembly, transport and coalescence, whereas Kid may participate only in stress granule assembly. Furthermore, the ATPase activity of Eg5 is dispensable for stress granule formation and coalescence, but is needed for its function

is dissolution. These data suggest that Eg5 ability to aid in stress granule coalescence is likely dependent on protein-protein interactions, rather than its actual motor activity.

5.4.2 Microtubules are required to control the dissolution of stress granules

Microtubules were also demonstrated to be important for stress granule formation as well as dissolution. Stress granule formation in the absence of microtubules revealed identical results as observed after Eg5 knockdown which may actually reflect the loss of Eg5, as motors typically use microtubules to carry out their function. However, what was interesting is that during stress granule dissolution, an increase rate of dissolution was observed, suggesting that microtubules may typically hinder the process. Although microtubules may hinder the process, the cell may have evolved for a slower dissolution rate because stress granules should only dissolve once the damage has been fixed or the stress conditions removed. If the stress granules dissolve faster than the damage is resolved, it could lead to translation of damaged mRNA and decrease the resource of the cell. Therefore, hindering stress granule dissolution in the presence of microtubules may actually be a safety mechanism for the cell.

5.4.3 Why do Eg5 and Kid behave differently?

Eg5 and Kid motors are both plus-end directed kinesins, but our studies are revealing that their function in stress granule dynamics is already demonstrating to be different. Eg5 plays a role in the coalescence of stress granules and in formation and transport, whereas Kid is only observed to function in stress granule formation. These differences in stress granule dynamics are consistent with the interphase function of each of these proteins. As discussed in Chapter 4, Eg5

directly participates in protein synthesis by directly associating with various ribosomal components. Also, as will be discussed in Chapter 6, loss of Kid leads to an increase in protein synthesis and loss of localized protein expression; as such, the dominant function of Kid appears in mRNA transport or transport of mRNP complexes.

The stress granule dynamics after loss of Eg5 parallels the interphase function of Eg5. The ability of Eg5 to participate in every phase of stress granule dynamics is likely through Eg5's association with various ribosomal subunits and consistent with this is the fact that the 40S ribosomes and the 43S translation complexes also associate with stress granules throughout the entire process (Kimball, Horetsky et al. 2003). Therefore, under stress conditions Eg5 likely functions in the transport of the 40S ribosome/43S translational complex to the stress granule prior to facilitating stress granule formation. While Kid's ability to participate in only stress granule assembly is consistent with other proteins involved in mRNA transport which have been shown to effect stress granule assembly and not stress granule coalescence or transport.

5.4.4 Is Eg5 function in protein synthesis and stress granule formation one in the same?

As Eg5 is demonstrated to aid in the processivity of the ribosome, one must inquire whether Eg5’s function in stress granule formation is a result of low processivity or if stress granule formation causes low processivity or if Eg5 is functioning in these two processes independently. There is no reason to speculate that stress granule formation causes low processivity especially because stress granule formation occurs after protein translation inhibition. Additionally, the decreased processivity after loss of Eg5 does not cause stress granule formation, as treatment with siEg5 alone does not induce stress granule formation. Therefore, this leads us to conclude that Eg5's function in stress granules and processivity are independent functions for this motor.

These separate and distinct functions could be exploited by the cell to uniquely position Eg5 to switch between both functions. Under normal conditions Eg5 functions to aid in ribosomal processivity, while under conditions of translational stress Eg5 can aid in the transport of the 40S ribosome to the stress granule prior to facilitate stress granule formation. Furthermore, once the translational stress is removed Eg5 functions to dissolve stress granules and resume its function in processivity. However, this cycle has yet to be formally tested.

6.0 CHAPTER VI: IDENTIFICATION OF KID IN TRANSPORT OF FOCAL ADHESION PROTEINS

6.1 INTRODUCTION

Recently, localized translation has been found to occur in a variety of organisms for embryonic patterning during embryogenesis (King, Messitt et al. 2005), memory formation (Sanchez-Carbente Mdel and Desgroseillers 2008) and neuronal development (Kindler, Wang et al. 2005). In mammalian cells, it has been proposed that localized translation occurs at focal adhesions (Hervy, Hoffman et al. 2006). Focal adhesions are anchoring junctions containing clusters of diverse adhesion proteins, which mechanically link the actin cytoskeleton to the extracellular matrix. This connection provides the cell with structural anchorage as well as signaling information regarding association with the extracellular environment.

6.2 RESULTS

6.2.1 Kid, Eg5, and MKLP1 localize to focal adhesions

Interestingly, we have identified that Kid, Eg5 and MKLP1, associate with focal adhesions in RPE1 cells, colocalizing with vinculin, a known focal adhesion protein (Turner, Glenney et al.

1990) and in a variety of cells lines including HeLa, fibroblasts, and NIH3T3 cells (Figure 6.1A, B). We chose to focus our efforts on characterizing the function of Kid at sites of focal adhesions. siRNA knockdown of siKid for 72 hrs yielded an increase in focal adhesions not only at the edges of the cells, but also at multiple foci throughout the entire cell (Figure 6.2A). In addition, after Kid knockdown a thinning of the cellular processes was observed, such that they cells became extremely long and flat (Figure 6.2B).

Figure 6.1

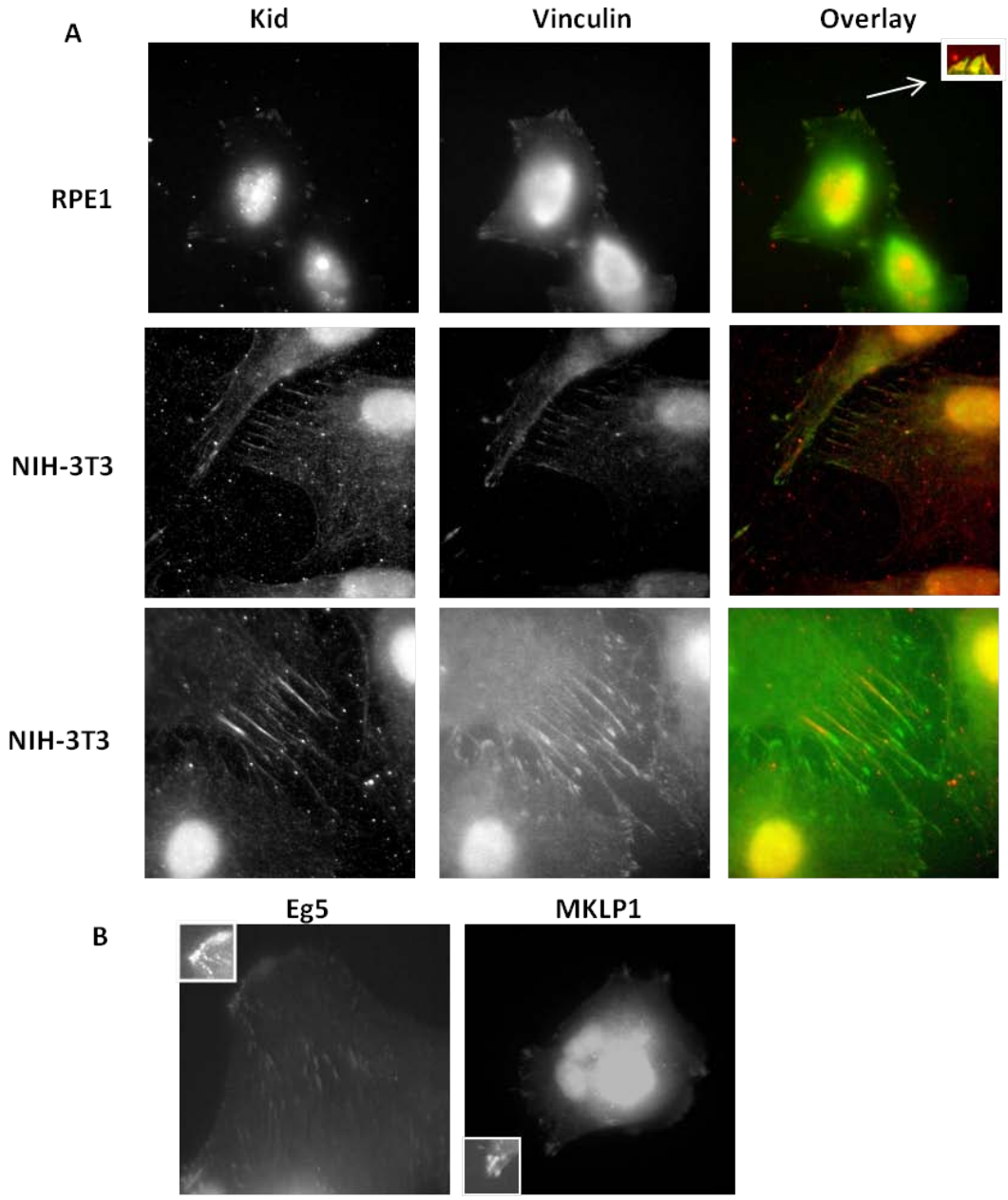

Figure 6.1: Kid, Eg5, and MKLP1 localize to foal adhesions.

(A) RPE1 or NIH3T3 cells were fixed and co-stained for Kid and vinculin, a focal adhesion protein. (B) Eg5 and MKLP1 immunofluorescence demonstrate similar staining to focal adhesions in RPE1 cells.

Figure 6.2

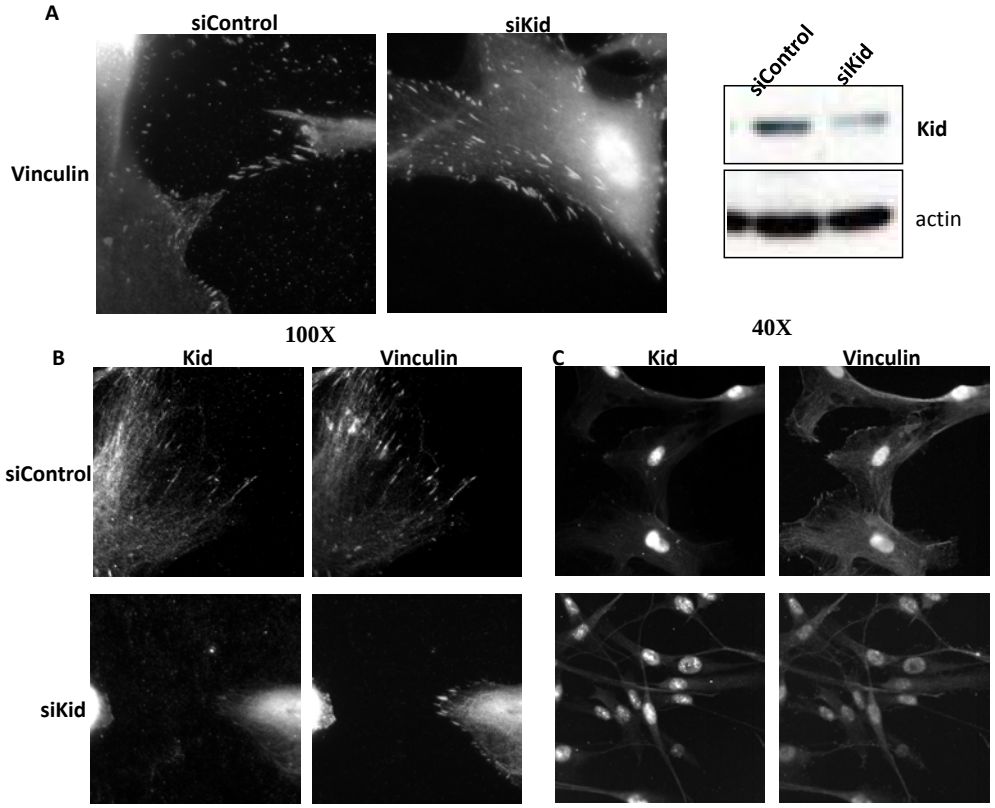

Figure 6.2: Knockdown of Kid causes an increase in focal adhesions and a change in cell morphology.

(A) Immunofluorescence analysis of RPE1 cells with Kid knockdown and stained for vinculin (left). Immunoblot demonstrating Kid knockdown (right). (B) Immunofluorescence analysis of Kid and vinculin, 72 hrs after Kid knockdown under 100X (B) or 40X (C).

6.2.2 Loss of Kid causes an increase in focal adhesions randomly distributed throughout the cell

As an increase in focal adhesions was observed after Kid knockdown and focal adhesions were identified proximally in the cell, we hypothesized that Kid may be involved in focal adhesion mRNA transport. That is, in the absence of Kid the vinculin mRNA may not be properly transported and instead distributed and translated inappropriately at interior points of the cell.

6.2.3 Kid localizes to the ends of microtubules

This phenotype may be consistent with Kid functioning as a motor. If Kid were to participate in transport of focal adhesion components, then one would expect Kid to localize along microtubules and concentrate at the edges of microtubules where microtubules meet focal adhesions. Accordingly, cells were co-stained for Kid and microtubules and as anticipated Kid was found to localize to the ends of microtubules, exactly where focal adhesions begin to form (Figure 6.3). Consistent with our model Kid may localize focal adhesion assembly to the distal portions of the cell.

Figure 6.3

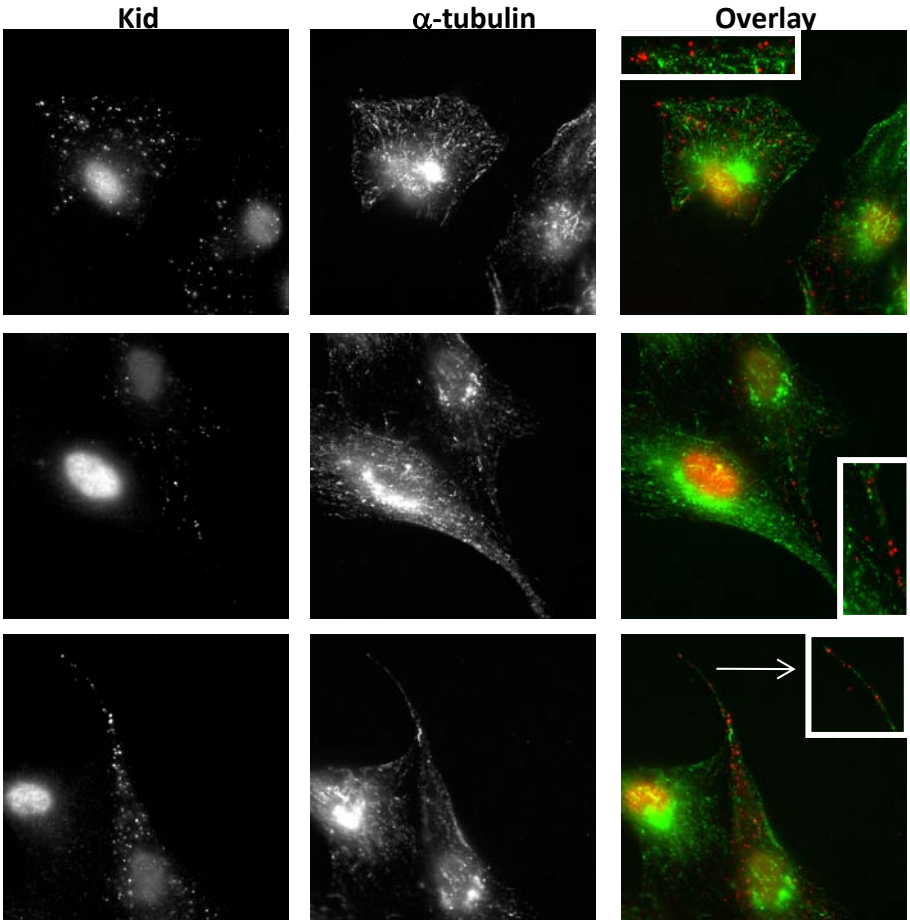

Figure 6.3: Kid localizes to ends of microtubules.

RPE1 cells were fixed to observe partial a-tubulin staining and Kid. Insets demonstrate blown-up images.

6.2.4 Kid knockdown causes an increase in protein synthesis

Additionally, after Kid knockdown, immunofluorescence analysis demonstrated an increase in the number of focal adhesion. Given that Kid was found to associate with ribosomes, we

inquired whether Kid may be involved in suppressing focal adhesions protein synthesis until the mRNA reached the ends of the microtubules. To begin to investigate this, we began by first examining the efficiency of translation in the absence of Kid, similar to Eg5. Accordingly, 24, 48, and 72 hrs after Kid knockdown, a significant 50% *increase* in protein translation was observed (Figure 6.4A). This *increase* in protein translation is precisely the opposite effect that was observed after Eg5 knockdown and lends support to the hypothesis that Kid may play a role in suppression of translation of specific proteins like focal adhesion components. This increase in translation is not due to an increase in the mitotic index (Figure 6.5B).

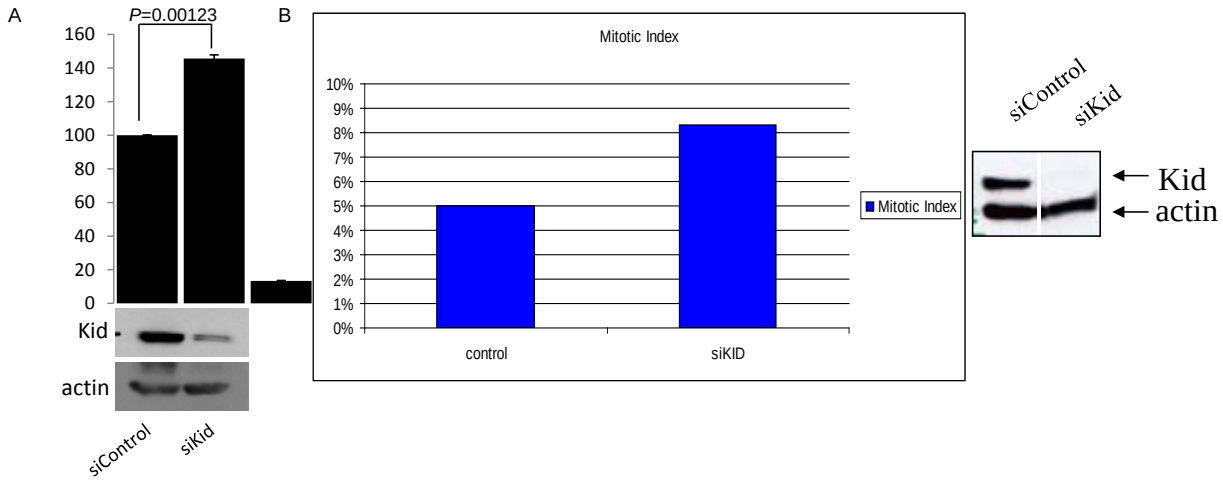

Figure 6.4: Translation increase after Kid knockdown.

(A) ^{35}S Met/Cys incorporation assays were completed after a 48 hr Kid knockdown. (B) Mitotic index analysis after a 48 hr Kid knockdown. Results are shown as mean ± s.d. and are representative of at least two independent experiments, *P* values represent students' t-test.

6.3 SUMMARY

Typically, an increase in translation after the knockdown of a given protein is suggestive of a translational repressor function for that given protein. Generally, translation repressors act by binding to the mRNA and blocking its translation (Vessey, Vaccani et al. 2006). Such proteins are typically found as part of the mRNP complexes. mRNP complexes contain silenced mRNAs and are typically assembled in the nucleus, transported into the cytoplasm, and carried to their final destination to be translated (di Penta, Mercaldo et al. 2009). Kid immunoblotting is very robust in the nucleolus, consistent with this model. Based on this data and previous data (Chapter 2-4), we hypothesize that Kid may act as a translational repressor and may be a part of the mRNP complexes assembled within the nucleus (Figure 6.5).

Figure 6.5. Kid Model.

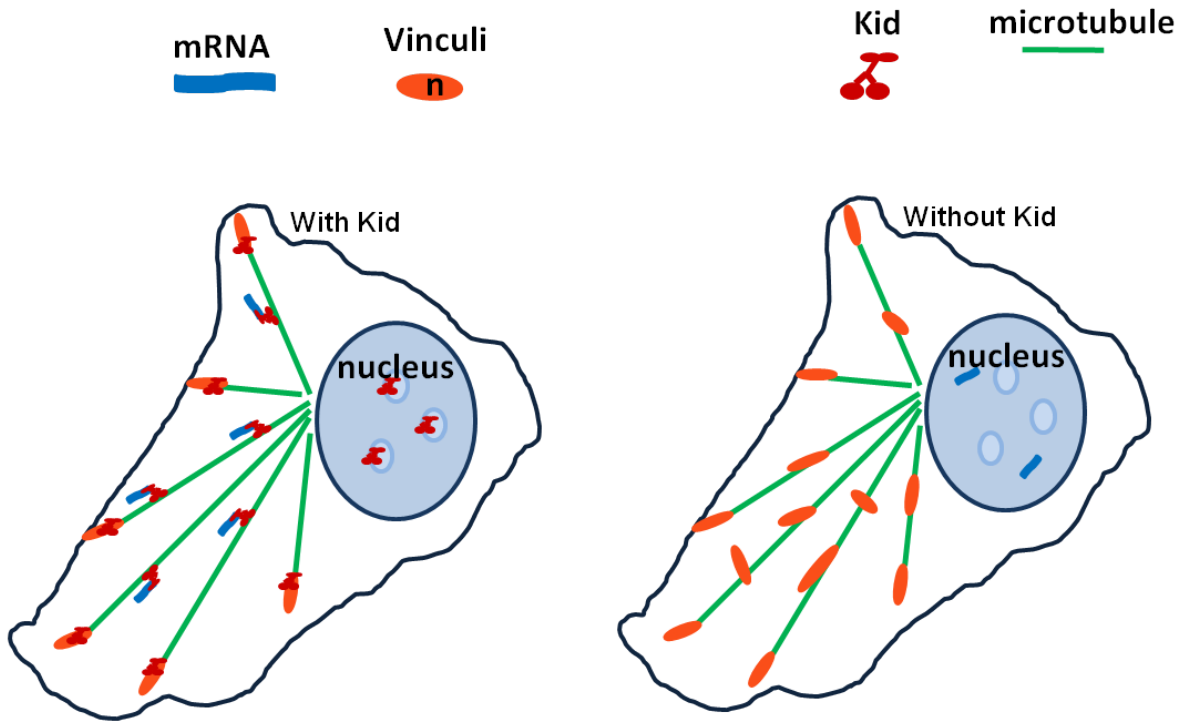

Figure 6.5: Focal adhesion model.

Left: With Kid : We propose that Kid may function as a translational repressor, silencing mRNA (vinculin) in the nucleus, transporting it through the cytoplasm, until it reaches its destination (the edge of the cell) for translation. Right: However without Kid, focal adhesions are found to be distributed movre randomly in the cytoplasm and are found in different orientations, suggesting that vinculin mRNA is not silenced and when it enters the cytoplasm, translation occurs prematurely before focal adhesion mRNA reaches the edge of the cell.

6.4 DISCUSSION

After Kid knockdown, an increase in focal adhesions was observed throughout the cell, which is consistent with the 50% increase in protein translation observed after siKid treatment. Even though an increase in focal adhesions was observed after Kid knockdown, this single protein could not account for the 50% increase in protein translation. Therefore, there are likely other unidentified mRNAs that are silenced and transported for translation by Kid. These data hint at the possibility that Kid may function as a translational repressor and may mediate the transport of multiple mRNAs. Further evidence regarding the role of Kid as a translational repressor could be provided by identifying an association of Kid with specific mRNP complexes.

6.4.1 Kid localization at the ends of microtubules

Kid localization to the ends of microtubules is not surprising, as other motors with a role in transport of cargoes/organelles have also been shown to localize to the ends of microtubules. Additionally, this localization is consistent with Kid function in focal adhesion component transport. At the end of microtubules, focal adhesions begin to form (Wehrle-Haller and Imhof 2003), thus it is logical that Kid is found at the ends of microtubules because it is transporting those focal adhesion components there to be translated.

6.4.2 Kid silencing mRNA

Furthermore, as focal adhesion proteins are needed in the distal parts of the cell and not the proximal, the transport and silencing function of Kid explains how focal adhesion proteins are

selectively and site-specifically translated. We believe Kid is able to silence focal adhesion proteins because Kid has a nucleic acid binding sequence. Our initial studies have provided the first physiological relevance of the RNA-binding function of Kid. A working model for the function of Kid in mRNA silencing and transport is as follows: Kid associates and silences the mRNA for focal adhesions early on in the nucleus and transports them into the cytoplasm where Kid uses microtubules to transport the focal adhesion protein to the end of the microtubule. Once the Kid-bound focal adhesion component cargo reaches the end of the microtubules, the complex becomes unsilenced and the focal adhesion protein can be translated. However, when Kid is not present, the focal adhesion proteins are not silenced and instead are translated immediately after leaving the nucleus without being transported, ending up within the proximal regions of the cell. Furthermore, given the significant increase in protein synthesis after knockdown of Kid suggests that Kid is likely important for silencing more mRNAs other than focal adhesions mRNAs.

7.0 CHAPTER VII: FINAL DISCUSSION

Until this study, interphase functions for mitotic motors were uninvestigated and were thought to be nonexistent. Accordingly, the identification of interphase functions for the motor proteins Eg5 and Kid is quite intriguing as before this discovery, mitotic motors were only thought to function in mitosis. This finding is critical and needs to be taken into consideration when mitotic motors are being considered as drug targets. Not only have these two proteins been identified as ribosomal motors, but they function in protein synthesis which occurs throughout the entire cell cycle. Inhibition of these essential interphase functions may outweigh the potential therapeutic benefit derived from inhibiting their mitotic functions.

Microtubule motors are known to possess not only redundant functions but they are also well known to function in a balance of forces (Sharp, Rogers et al. 2000); that is, antagonize each other's movements in order produce the correct amount of force to achieve the desired result. Furthermore, disruption of this dynamic balance can lead to pleiotropic effects on cells (Sharp, Rogers et al. 2000). In this study, the two motors, Eg5 and Kid, were found to function in protein translation. Interestingly, the antagonizing nature of mitotic motors is even reflected in our newly discovered interphase functions, as loss of Eg5 causes a decrease in protein synthesis which suggests that Eg5 acts as a translational activator, whereas loss of Kid causes an increase in protein synthesis which suggests Kid acts as a translational repressor. The reciprocal relationship of these proteins was conserved all the way down to knockdown of Eg5 resulting in

an increase in Kid expression, while Kid knockdown caused an increase in Eg5 expression (Figure 7.1). This suggests that Kid and Eg5 function uniquely to ensure efficient and proper translation, and altering this balance disrupts translation.

Figure 7.1.

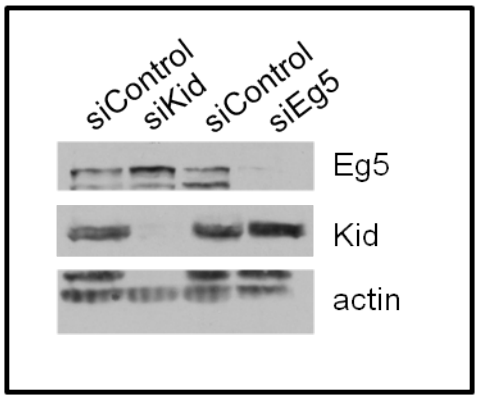

Figure 7.1: Recipical relationship of Kid and Eg5s balance of forces is demonstrated by immunoblotting of indicated proteins after knockdown.

Cells were knocked –down for 24 hrs in each case for Kid and Eg5.

The microtubule motor Kid was found to be associated with the nucleolus through a GTP-dependent shuttling mechanism. This shuttling mechanism was similar to NPM, a protein that functions prominently in ribosome biogenesis (Finch, Revankar et al. 1993). More importantly, Kid and NPM share many distinct similarities including cell cycle-dependent localization, co-fractionation with pre- and mature ribosomes, their localization during mitosis, and their phosphorylation by the same kinase at the onset of mitosis. Given these similarities, it

seems very likely that in addition to participating in stress granule formation, mRNA transport and silencing, Kid may function similarly to NPM in participating in ribosome biogenesis.

Previous quantitative models of protein synthesis assumed that ribosomes do not fall off the mRNA during translation, however our analysis and the analysis of others disputes this claim (Chan, Khan et al. 2004) (Caplan and Menninger 1979; Goldman 1982) (Vuppalanchi, Coleman et al.). Loss of Eg5 causes an increase in the 80S subunit and stabilization of polysomes, and this increase in the 80S ribosome requires ongoing translation. Additionally, our newly developed processivity assay demonstrates that after loss of Eg5, longer polypeptides were less frequently translated than shorter polypeptides. From this we conclude that Eg5 functions to aid the ribosomes processivity and provides a fail-safe mechanism against unwanted ribosomal drop-off. Recently published literature has shown that certain microtubule motors were found to function in stress granule formation and/or dissolution. Dynein was involved in stress granule formation, while kinesin was involved in stress granule dissolution (Loschi, Leishman et al. 2009). Therefore, we investigated whether Eg5, Kid or MKLP1 were involved in stress granule dynamics. Under translational stress Eg5 and Kid were found to co-localize to stress granules, while MKLP1 did not. Additionally, it was determined that Eg5, Kid, and microtubules were required for stress granule formation, while Eg5 was also needed for stress granule transport, coalescence and dissolution. Our studies add to the existing body of literature by expanding the number of motor proteins known to be involved in stress granule dynamics. Interestingly, although the defects observed after loss of Eg5 are not as dramatic as those seen after loss of dynein or kinesin alone, Eg5 is able to perform the function of both of these motors simultaneously.

7.1 FUTURE DIRECTIONS

MKLP1 was found to associate with both pre-ribosomes and mature ribosomes, but during this analysis we did not investigate the function of MKLP1 in protein synthesis. It is likely, considering MKLP1 associates with ribosomes similarly to Eg5 and Kid, which MKLP1 may function in protein synthesis as well.

MKLP1 was not included during our investigations with Eg5 and Kid for two main reasons. The first is that the expression level of MKLP1 is barely detectable and the second reason is that the antibodies available for MKLP1 are of poor quality. Given the need to reliably detect and measure MKLP1 levels in our studies investigating MKLP1 would have proven difficult, if not intractable.

Now that we have the proper assay conditions in place from our studies with Kid and Eg5, it may be possible to examine the function of MKLP1 in these same assays by using siRNAs against MKLP1 and validating knockdown by RT-PCR. Once successfully knocked-down, MKLP1 function in protein synthesis, through polysome profiling and ^{35}S Met/Cys incorporation assays can be investigated in order to determine if MKLP1 does function in protein synthesis. Alternatively, MKLP1 can be tagged and transiently transfected into cells. Increasing the expression of MKLP1 may enhance our ability to reliably detect it; additionally, tagging MKLP1 would allow us to use quality antibodies which would greatly facilitate our studies. Although the prolonged overexpression may lead to cytokinesis defects, looking at short time points may prove to be useful. Finally, we may need to develop a quality antibody in-house with the help of an antibody production facility by bacterial overexpression and eliciting an immune response in a model animal. This might prove useful, as the commercially available antibodies purchased far lack the desired specificity needed for our studies.

Finally, if after the completion of these initial studies no change in protein translation is observed, it will be worth conducting these same studies in absence of Kid, Eg5, or both Kid and Eg5. It may be possible that both Kid and Eg5 are the dominant motor proteins effecting translation; thus, in order to determine the role of MKLP1 in translation we may need to remove these more dominant proteins.

8.0 CHAPTER VIII: MATERIALS AND METHODS

8.1 METHODS USED THROUGHOUT

8.1.1 Cell culturing

Most cell lines were obtained from the American Type Culture Collection (ATCC), with the exception of UPCI cell lines which were a gracious gift from Susan M. Gollin (University of Pittsburgh). RPE1 (human retinal pigmented epithelial cells stably transfected with human telomerase reverse transcriptase (hTERT)) cells were cultured in Dulbecco's Modified Eagle Medium plus F-12, (#D6421, DMEM-F12), supplemented with 10% Fetal Bovine Serum (FBS) (#511150, Atlanta Biologicals). UPCI:SCC103, A549, and SKHEP cells were cultured in minimal essential medium (M4655, MEM) supplemented with 10% FBS, 2 mM L-Glutamine, and 1% MEM non-essential amino acids (Invitrogen). HFF-hTERT, NIH-3T3, FB and HeLa, were maintained in DMEM supplemented with 10% FBS and 2 mM L-Glutamine. MESSA, U2OS, and HCT116 cells were maintained in McCoy's media (#16600082, Invitrogen) supplemented with 10% FBS. All cultures were grown at 37°C with 5% CO_2. All culture media and supplements were purchased from Sigma, unless otherwise stated.

8.1.2 Antibodies

The following antibodies were used in this study: Kid – rabbit anti-Kid (AKIN12), Eg5 – rabbit anti-Eg5 (AKIN03), Mklp1 – rabbit anti-MKLP1 (AKIN06), Actin – rabbit anti-Actin (AAN01) (Cytoskeleton); Eg5 – mouse anti-Eg5 (#627802, Biolegend); RPS7 – mouse anti-RPS7, (#H00006201-M03, Abnova); RPS5 – mouse anti-RPS5 (#AB58345), RPL10A mouse anti-RPL10A (#Ab55544), Fibrillarin – mouse anti-fibrillarin (#AB18380) (Abcam); RPL4 – rabbit anti-RPL4 (#11302-1-AP, Protein Tech Group); Dynein Intermediate Chain (#MAB1618, Chemicon); Nucleophosmin - mouse anti-nucleophosmin (# 32-5200, Zymed); GAPDH – rabbit anti-GAPDH (14C10) #2118 (Cell Signaling); Calnexin; Caspase-3 – rabbit anti-caspase 3 (8G10) #9665 (Cell Signaling); FLAG – mouse anti-FLAG #4049 (Sigma); HA – mouse anti-HA # 1 583 816 (Roche), eIF4E – mouse anti-eIF4E (#SC-9976, Santa Cruz).

8.2 CHAPTER 2 METHODS

8.2.1 Microscopy analysis:

All cells were analyzed on an Olympus BX60 epifluorescence microscope with 100x oil immersion objectives, unless specified. Hamamatsu Argus-20 CCD camera was used to capture images.

8.2.2 Immunofluorescence

For Kid, MKLP1, MCAK, Kif14, and Cenp E staining, cells were fixed for 45 min in 4% paraformaldehyde followed by either 1 min Methanol or 15 min extraction in 0.2% triton X-100. Cells were blocked in 1.5% BSA in PBST (PBS plus 0.1% Tween 20), treated with primary antibodies, washed, treated with secondary antibodies, and finally 4',6-Diamidino-2-phenylindole (DAPI) for DNA staining. For Eg5 staining, cells were fixed in either a 5 min -20˚C Metanol or a 1:1 ratio of -20˚C Metanol:acetone for 1 min, followed by the same procedure stated above. All antibodies were diluted 1:500, unless otherwise noted. Primary antibodies used were: Kid, MKLP1, Eg5, MCAK, Kif14, Cenp E, NPM and fibrillarin.

8.2.3 Fixation and immunofluorescence of 8-week old frozen mouse intestine tissue

Intestine tissue from 8-week old mice were harvested in O.C.T. medium and placed on dry ice. Tissue was cryo-sectioned at a thickness of 5-10 μm and mounted on slides. Frozen tissues were fixed in 2% paraformaldehyde for 10 min at room temperature followed by three washes in 0.2% triton-X-100 for 5 min each. Tissues were blocked in blocking buffer (1.5% BSA, 0.1% Tween-20 in PBS) and incubated in anti-Kid and anti-nucleophosmin (1:250) antibodies for 30 min. Cells were washed three times in PBS, incubated in secondary for 30 min, washed three more times in PBS, and incubated in DAPI for 3 min before being mounted. Slides were analyzed and viewed by Olympus BX60 epifluorescence microscope with 100x oil immersion objectives. Hamamatsu Argus-20 CCD camera was used to capture images.

8.2.4 Subcellular fractionation of RPE1 cells

Nuclear and cytoplasmic fractions from RPE1 cells were isolated using the PARIS kit (#AM1921M, Ambion) following the manufactures' protocol. Samples were run on 10% SDS-PAGE gels and analyzed for Kid, Eg5, KU80 (nuclear control), and cytokeratin (cytoplasmic control).

8.2.5 Synchronization of noncancer and cancer cells

Equal numbers of cells were treated with 3 μM of nocodazole for 16 hrs, followed by an 8 hr release, and then treatment again with 3 mM of nocodazole for 12 hrs, prior to trypsinization, cell were lysed in RIPA buffer (150 mM NaCl, 50 mM Tris pH 7.2, and 1% NP40). Lysates were run on 10% SDS-PAGE gels and the mitotic index was counted.

8.2.6 MPA and Ribavirin treatments

Cells were treated with varying concentrations of MPA or Ribavirin for 4 hrs. For specific experiments, cells were also released from MPA or Ribavirin (washed times in FBS) for an additional 2-4 hrs in guanosine or guanosine was added in the presence of MPA or ribavirin to block GTP-shuttling from the nucleolus or guanosine alone. Cells were fixed and stained, with antibodies to Kid, MKLP1, or fibrillarin, as mentioned above or were trypsinized, and subjected to immunoblotting.

8.2.7 Quantitation of mitotic defects or mitotic indexes

Cells were fixed in 4% paraformaldehyde plus 0.02% triton X 100 for 15 min, prior to the addition of DAPI. A minimum of 300 cells were counted per trial. All reagents were purchased from Sigma unless specified.

8.3 CHAPTER 3 METHODS

8.3.1 Microscopy analysis

All cells were analyzed on an Olympus BX60 epifluorescence microscope with 100x oil immersion objectives, unless specified. Hamamatsu Argus-20 CCD camera was used to capture images.

8.3.2 UV-C treatment

RPE1 cells were subjected to various amounts of UV-C treatment. The amount of UV-C treatment was quantitated with the use of a UVP radiometer; for the most part the UV bulb emitted approximately 0.3 $J/m^2/s$, therefore for 20 J/m^2 experiments, cells were subjected to UV-C light for about 69 sec. After UV-C treatment, cells were allowed to recover anywhere from 5 min to 24 hrs, followed by immediate fixation, immunofluorescence staining of Kid, fibrillarin, or NPM, mounted, and analyzed. MEF proficient or deficient in p53 were also used in the above experiment.

8.3.3 Microtubule inhibition

Cells were treated with or without 0.1 μg/ml or 1 μg/ml, and in some cases followed by washout and/or UV-C treatment. Cells were then fixed and stained as mentioned above.

8.3.4 IR

RPE1 or UPCI:SCC103 cells were treated with various Grays (Grys) of IR treatment and allowed to recover for times ranging from 5 min – 24 hrs. At these times, cells were fixed, and co-stained for the indicated antibodies: Kid, phospho-H2AX, or fibrillarin. Cells were analyzed by microscopy.

RPE1 or UPCI:SCC103 cells were treated with 0.1 or 0.5 mM of hydrogen peroxide for either 10 min or 30 min, with or without recovery. Cells were then fixed and stained with the indicated antibodies.

8.3.5 Localized UV-C studies

For micropore UV irradiation, cells grown on glass coverslips were covered with an 8 μm filter, irradiated with 10 J/m^2 – 100 J/m^2 of UV-C radiation, and allowed to recover for 1.5 hrs. Cells were then fixed in 2% paraformaldehyde for 15 min at room temperature, washed in 0.2% Triton, blocked for 20 min in 5% BSA, and DNA was denatured with 0.4M NaOH at room temperature for 4 min. Primary antibodies were diluted in antibody dilution buffer consisting of 0.2% Glycine, 0.5% BSA in PBS and cells were incubated for 90 min. Cells were then washed three times prior to a 60 min incubation in secondary, followed by three washes in PBS, and a 5

min incubation with DAPI. For Figure 3.10, cells were treated with 40 J/m2 of UV-C and were allowed to recover for 1 hr prior to fixation.

8.3.6 MTS cell proliferation assay

Kid was knocked-down for 72 hrs, treated with varying amounts of UV-C, and followed by a MTS cell proliferation assay. MTS assay was conducted according to the manufactures protocol. Control was media alone, negative control was untreated cells, and positive control was H_2O_2 treated cells.

8.3.7 Caffeine treatment

RPE1 cells were treated with or without 4 mM caffeine for 1.5 hrs prior to fixation and staining. UV-C treatment was used as a control. Antibodies used are indicated.

8.3.8 Actinomycin-D (AD) treatment

RPE1 cells were treated with 0.01-0.5 mg/ml of (AD) for 30 min, prior to fixation and immunofluorescence staining with the indicated antibodies.

8.3.9 α-amanitin treatment

RPE 1 cells were treated with various concentrations ranging from 0.5-30 μg/ml of alpha-amanitin for 1 or 3 hrs, followed by fixation, staining, and analysis.

8.3.10 2-D gel electrophoresis

2D gel electrophoresis was conducted in collaboration with Dr. Jason White in Dr. Chris Bakkenists Lab. Briefly, prior to 1D and 2D gel electrophoresis, RPE1 cells were treated with or without UV, followed by subcellular fractionation under low salt conditions to isolate nuclei.

8.4 CHAPTER 4 METHODS

8.4.1 Inhibitor treatments

For treatments with inhibitors, the following times and concentrations were used unless otherwise specified: 4 hr monastrol at 130 μM, 2 hr nocodazole at 12 μM, 2 hr Colecimid at 0.002 mg/mL, 30 min of low levels of puromycin treatment at 100 μg/mL, cycloheximide at0.1 mg/mL, 1 mg/ml high levels of puromycin. All reagents were purchased from Sigma.

8.4.2 Transfections

8.4.2.1 siRNA transfections

Cells were reverse-transfected with 1.5 μg/60mm tissue culture plate of siRNA against Eg5 using HiPerfect transfection reagent following the manufactures' protocol and incubated 24 hrs prior to immunoblot analysis or further experimental procedures. Fluorescently labeled scrambled siRNA was used (cat# 1022563) as the control for all siRNA experiments. Briefly, 1.5 μg siRNA was mixed with 100 μL of opti-mem (#31985, Invitrogen) and 20 μL of HiPerfect,

prior to 5 min incubation. Following this incubation, the transfection mixture was placed in the 60 mm plate, the cells were added to this mixture, and opti-mem was added to a final volume of 2 mL. Cells were grown for 8 hrs in opti-mem plus transfection mixture, prior to the addition of full medium for the remainder of the time. All reagents were purchased from Qiagen unless specified. siRNA #1 (SI02653770) and siRNA #2 (s7904)(Ambion).

8.4.2.2 Plasmids

Bicistronic plasmid transfection (Addgene plasmid 18673) into U2OS cells was completed using FuGene6 (#1814443, Roche) transfection reagent for 24 hrs (following the manufactures' protocol), after a 12 hr knockdown of Eg5. Antibodies used were FLAG for cap-dependent translation or HA for cap-independent translation.

8.4.3 Pre-ribosome fractionation

20 million cells were trypsinized, washed twice in PBS, and nuclear fractions from RPE1 cells were isolated using the PARIS kit (#AM1921M, Ambion) following the manufactures' protocol. The nuclear fractions were placed on a continuous 10-25% (wt/wt) sucrose gradients (25 mM Tris (pH 7.5), 100 mM KCl, 1 mM DTT, 2 mM EDTA). Gradients were centrifuged at 27,000xg for 4 hrs at 4°C using a Beckman L7 Ultracentrifuge (Model L7 -65) in a Sorval AH629 rotor, after which gradients were fractionated by upward displacement through a ISCO UA-5 with constant UV monitoring at an absorbance of 260 nm and one milliliter fractions were collected. Fractions were precipitated using 10% final concentration of trichloroacetic acid for immunoblot analysis.

8.4.4 Polysome profiling

20-30 million RPE1 cells were trypsinized and incubated in the presence or the absence of 0.1 mg/mL of cycloheximide (CHX) for 10 min, prior to cell lysis. Cells were lysed in lysis buffer (20 mM Tris-HCl (pH 7.2), 130 mM KCl, 30 mM $MgCl_2$, 2.5 mM DTT, 0.2% NP-40, 0.5% sodium deoxycholate, 10 mg/mL of cycloheximide, 0.2 mg/mL of heparin, 1 mM PMSF), and incubated on ice for 10 min; to rid of DNA pellet, samples were centrifuged in a tabletop centrifuge for 10 min at 10,000 rpm. The supernatants were incubated at 4˚C before being placed on top of a 10-45% (wt/wt) sucrose gradients (10 mM Tris-HCl (pH 7.2), 60 mM KCl, 10 mM MgCl, 1 mM DTT, 0.1 mg/mL of heparin), unless otherwise specified. Samples were collected, and precipitated as mentioned previously for immunoblot analysis. For analysis of Eg5 in the absence of microtubules, cells were treated with 12 μM of nocodazole prior to polysome profiling.

For polysome profiling in the presence of a 4 hr cycloheximide treatment to block ongoing translation, cells were treated for 4 hrs in addition to other treatments or washout out for 4 hrs to allow cells to recover prior to polysome profiling protocol, as listed above.

For quantitation of polysome peaks, the polysome profile was mechanically amplified on a Xerox copy machine, and the lower point on the graph was used as the baseline. Each peak was carefully cut out in triplicate, and weighed on an analytical balance.

8.4.5 Immunoprecipitation

10 million cells were trypsinized, pelleted, lysed in lysis buffer (50 mM Hepes [pH 7.5], 150 mM NaCl, 0.1% Triton X-100, 1mM EDTA, 2.5 mM Glycerol, 1 mM NaF, 0.1 mM Na3VO4, 10

mM Beta-glycerophosphate, 1 mM PMSF), and incubated on ice for 10 min prior to a 10 min centrifuge spin at 10,000 rpm on a table top centrifuge, for removal of DNA pellet. Supernatant was placed in a new tube, 10% was saved for whole cell lysate (WCL) analysis, while the other 90% was pre-cleared for 1 hr at 4°C with protein A beads, to rid of nonspecific protein binding, (#17078001, GE Healthcare), centrifuged at 2,000 rpm for 2 min, before partitioning equal portions of the supernatant into two tubes. Each tube received either 2 μg of rabbit anti-Eg5 antibody or 4 μL of 30% glycerol, (Eg5 antibody was originally diluted in 30% glycerol), was incubated for 1.5 hrs at 4°C with constant rotation, after which protein A beads were added, and incubated at 4°C with constant rotation for an additional 1.5 hrs. Tubes were removed from 4°C, centrifuged briefly for 2 min at 2,000 rpm, and the supernatant was removed. The pelleted beads were then washed with lysis buffer, centrifuged for 1 min at 2,000 rpm, and supernatant was removed. This procedure was repeated three times, prior to the addition of 1X SDS dye to pellet, and boiling the sample for 10 min before loading the sample of a 12% SDS PAGE gel. Each sample loaded on the gel represented 50% of the total IP pellet except for the WCL lane which contained 10% of the total initial sample. MYPT1 was used as a negative control, to demonstrate the specificity of Eg5 association with ribosomes; IP procedure was completed as mentioned above, except with the addition of 2.5 μg of antibody.

8.4.6 In vitro microtubule binding assays

Purified tubulin (isolated from the brains of bovine) was thawed on ice on 15 min with the addition of an equal volume of 1X PM (10 mM PIPES (pH 7.0), 5 mM Mg Acetate, and 1 mM EGTA (pH 7.0)) buffer and 2 mM GTP added, incubated on ice for 30 min, followed by a 30 min centrifugation at 13,000 rpm at 4°C in a table top centrifuge. Supernatant was removed, and

grow buffer (1X PM buffer, 0.1 mM Taxol (Sigma), 5 mM GTP (final volume of 200 µL)) was added to it in a 4:1 ratio (tubulin : grow buffer), followed by a 15 min incubation at 37°C with constant rotation. Each fraction for each ribosomal subunit from the polysome profiling was pulled together, inverted and split: half of which received the binding reaction (5X PM buffer, 100 mM NaCl, 0.04 mM Taxol, 1 mM GTP) plus 12% tubulin and was incubated at 34°C for 45 min with constant rotation, while the other half received the binding reaction without tubulin, Taxol, or GTP and remained at 4°C with constant rotation for 45 min. After the binding reaction, lysates were centrifuged for 30 min at 34°C or 4°C at 13,000 rpm. The supernatant was removed (containing non-microtubule bound proteins), pellets were briefly washed in PBS, re-centrifuged for 5 min, and the supernatant was discarded. The pellet contained microtubules and anything that bound to the microtubules. 2X SDS loading dye was added to each sample, boiled for 5 min, prior to loading 20% of the supernatant and 50% of the pellet on 12% gels.

8.4.7 In vivo microtubule binding assays

10 million RPE1 cells were lysed in polysome profiling cell lysis buffer, incubated on ice for 10 min and DNA pellet was omitted by centrifugation for 10 min at 10,000 rpm. The supernatant was removed and split: half of which received a final concentration of 0.1 mM Taxol and 5 mM GTP and was incubated for 45 min at 34°C with constant rotation, while the other half received 12 µM of nocodazole followed by incubation at 4°C for 45 min with constant rotation. After the 45 min incubation, binding buffer was added; Taxol-stabilized tubulin received binding buffer with 0.04 mM Taxol and 1 mM GTP, whereas the nocodazole-depolymerized tubulin did not. Samples where then reincubated for 45 min at either 4°C or 34°C, prior to a 30 min centrifugation at 13,000 rpm. Supernatants were removed and pellets were washed once in PBS,

prior to repelleting, and resuspending the pellet in 2X SDS dye. 50% of supernatant and 50% of pellet was loaded on 12% SDS PAGE gels.

8.4.8 ^{35}S Met/Cys incorporation assays

Cells were grown in 60 mm plates and media was changed to DMEM without methionine and cystine (#D0244, Sigma) plus 5% dialyzed FBS (#F0392, Sigma) and 2 mM L-glutamine for 30 min at 37C, prior to the addition of 100 μCi/60 mm plate of ^{35}S Metionine and ^{35}S cystine (#NEG072007MC, Perkin Elmer). To stop reactions, 0.1 mg/mL of CHX was added, cells were trypsinized, and washed in PBS prior to cell lysis in RIPA buffer (150 mM NaCl, 50 mM Tris [pH 8.0], 1% NP40). The Lowry assay was used to normalize samples prior to splitting the samples in half and subjecting them to scintillation counting or immunoblot analysis. For scintillation counting, duplicate samples of each lysate was placed on GF/C filters (#28497-743, VWR), washed three times with 10% TCA, once with 100% ethanol, and dried before scintillation counting. The duplicate samples were separated on 12% SDS PAGE gels, for visualization of equal loading or confirmation of Eg5 knockdown.

For fractionation of cell lysates into cytosolic and membrane fractions, a digitonin fractionation protocol was used. Briefly, cells were trypsinized, washed, and the cell membrane was broke open by pipetting 25x's with a cut-pipette tip in digitionin buffer solution (10 mM Pipes [pH 6.8], 300 mM Sucrose, 3 mM $MgCl_2$, 5 mM EDTA, 0.01% Digitonin, 1 mM PMSF). Lysates were incubated for 8 min on ice, centrifuged at 5,000 rpm for 4 min, and the cytosolic fraction was removed. Pellet was washed once in PBS, centrifuged and resuspended in RIPA buffer to retain the membrane fraction.

8.4.9 ^{35}S Met/Cys translation incorporation assay in suspended cells

RPE1 cells were trypsinized and incubated for 30 min with 100 μCi of ^{35}S at 37°C. Cells were then centrifuged for 3 min at 0.6xg and washed once with PBS. Next, cells were lysed in lysis buffer and incubated on ice for 15 min, after which time cells were centrifuged again at 9000xg for 10 min, yielding a supernatant and a pellet. The supernatant was subjected to acetone precipitation prior to running samples on a 10% SDS PAGE gel. Gel was fixed in 25% isopropanol and 10% acetic acid for 20 min, dried for 1 h, and exposed to phosphoimager for 18-24 h.

8.4.10 Rate of protein synthesis assay

Assay was completed similar to the ^{35}S Met/Cys incorporation assay above, except two different time points were taken, one at 30 min and one at 120 min.

8.4.11 Ribosome ½ transit time assay

30 million cells were trypsinized, washed, and resuspended in Basal Medium Eagle (BME) (#B1522, Sigma) plus 10% dialyzed FBS and 2 mM L-glutamine prior to the addition of 10 μCi/ml of ^{35}S Met/Cys. Samples remained in a 37C water bath, until the time point was taken. At each time point, 500 μL of cells were removed, placed in an ice cold tube, and 500 μg/mL of CHX was added, inverted, and placed on an ice/water bath for at least 10 min. At this time, cells were centrifuged at 5,000 rpm for 5 min on a tabletop centrifuge, washed with ice cold PBS containing 250 μg/mL CHX, recentrifuged and lysed (0.02 M Tris [pH 7.2], 130 mM KCl, 30

mM $MgCl_2$, 1% NP40, 0.05% Sodium deoxycholate, 0.2 mg/mL Heparin, 0.25 mg/mL CHX, 1 mM DTT, 1 mM PMSF, RNAsin Inhibitor (Promega)). The lysed cells were then centrifuged for 10 min at 10,000 rpm to remove DNA pellet, prior to splitting the lysates in half: 500 μL of the lysate was placed in a new tube and labeled PMS fraction, containing total proteins, while the other 500 μL was placed on top of a stepwise 20% sucrose buffer (10 mM Tris-HCl [pH 7.2], 60 mM KCl, 10 mM $MgCl_2$, 0.1 mg/mL Heparin, 1 mM DTT) and 60% sucrose cushion. Samples were then centrifuged in a S100-AT5 ultra-centrifuge rotor at 55,000xg for 27 min, after which 500 μL of the sample was removed (PRS) containing completed proteins released from the ribosomes. The PMS and PRS fractions were then TCA-precipitated on GF/C filters and subjected to scintillation counting. Transit times were calculated by comparing the incorporation of radioactivity into total proteins (PMS) and completed proteins (PRS) released from the ribosomes.

8.4.12 Mitotic Index analyses

Cells were fixed in 4% paraformaldehyde plus 0.02% triton X 100 for 15 min, prior to the addition of DAPI. A minimum of 300 cells were counted per trial. All reagents were purchased from Sigma unless specified.

8.4.13 Apoptosis assay

Cells were treated with monastrol for 4-16 hrs or nocodazole for 2–16 hrs prior to lysing cells and running samples on a 12% SDS page gel. Caspase-3 antibody (1:500 dilution) was used to

determine apoptosis. As a positive control, cells were treated with 1 μM staurosporine (Sigma) for 16 hrs to demonstrate caspase-3 cleavage.

8.4.14 MTS assay

Cell proliferation assays were performed according to the manufactures' protocol (Promega).

8.4.15 Processivity Assay

^{35}S Met/Cys incorporation assay was preformed as described above with the following exceptions, 10 million cells were used and ^{35}S Met/Cys was added to the cells for 1 hr, prior to the addition of CHX. Cells were trypsinized, washed, lysed in RIPA buffer, and the Lowry assay was completed to equalize protein levels. 100 μg of protein was loaded on 15% SDS PAGE gels, with the addition of 5 μL of Bio-Rad broad range marker (#161-0318, Bio-Rad); gels were divided into 4 equal sections, based on size; section 1 – stacking, section 2 – above 37 kDa, section 3 – below 37 kDa, section 4 – the bottom 2 cm of the gel. Sections 1 and 4 were omitted from analysis, while the two other sections were placed in scintillation vials, and were subjected to scintillation counting.

8.5 CHAPTER 5 METHODS

8.5.1 siRNA transfections

Protocol is as described above with the following changes: Kid was knocked-down for 72 hrs using siRNA from Qiagen (Kif22-7), Eg5 was knocked-down for 48 hrs, or both proteins were knocked-down together for 48 hrs.

8.5.2 Small molecule inhibitions

RPE1 cells were treated with the following concentrations: 100 or 200 μM Monastrol for 4 hr, 0.01 mg/ml nocodazole for 2 hrs.

8.5.3 Microscopy analysis

All cells were analyzed on an Olympus BX60 epifluorescence microscope with 100x oil immersion objectives, unless specified. Hamamatsu Argus-20 CCD camera was used to capture images.

8.5.4 Stress granules formation assays

RPE1 cells were treated with or without either 0.01 mg/ml puromycin for 30 min followed by a 0.5 mM arsenite treatment for 1 hr or with 0.5 mM arsenite only for 1 hr. Cells were fixed for 20 min in a 2% or 4% paraformaldehyde/0.2% Triton-X-100 solution at 4°C, followed by a 30 min

incubation in blocking buffer (1.5% BSA, 0.1% Tween-20 in PBS). Cells were then incubated overnight at 4°C in primary antibodies Kid (1:500) and eIF4E (1:500). Cells were washed three times in PBS, incubated for 30 min in secondary, followed by PBS washes, and DAPI staining.

8.5.5 Live cell imaging

Cells were seeded with a density of $2x10^5$ on 35 mm glass-bottom Petri dishes (AmtTek Corp) and viewed after siRNA or DNA transfections. Cells were maintained at 37°C with a moisturized-warm air microscope chamber (Life Imaging Services, Reinach, Switzerland). Epifluorescence microscopy was performed on a Nikon TE2000-U inverted microscope with a Coolsnap HQ digital camera (Roper Scientific Photometrics). Images were taken by MetaMorph (Molecular Devices) and converted to TIFF format and exported to Adobe Photoshop.

8.5.6 Stress granule dissolution assays

RPE1 cells were treated with 0.5 mM arsenite for 1 hr, followed by 3 washes in fresh media, and were allowed to recover. Time points were taken every 20-30 min. Cells were fixed, stained and quantitation was completed.

8.6 CHAPTER 6 METHODS

8.6.1 Immunofluorescence

Cells were fixed in 4% paraformaldehyde plus 0.1% triton for 30 min at 4˚C, followed by blocking and staining as mentioned in Chapter 2. Antibodies are used an indicated.

8.6.2 siRNA transfection

RPE1 cells were transfected as mentioned above, except Kid was knocked-down for 72 hrs prior to fixation, staining and analysis.

8.6.3 ^{35}S Met/Cys incorporation assays

Assays were performed as described in chapter 4.

8.6.4 Mitotic index analysis

Cells were fixed in 4% paraformaldehyde plus 0.02% triton X 100 for 15 min, prior to the addition of DAPI. A minimum of 300 cells were counted per trial. All reagents were purchased from Sigma unless specified.

8.7 CHAPTER 7 METHODS

8.7.1 siRNA transfection

RPE1 cells were treated with siKid or siEg5 24 hrs, according to protocol listed in Chapter 4, followed by samples being resolved on 12% SDS-PAGE and immunoblotting with indicated antibodies.

BIBLIOGRAPHY

Amin, M. A., S. Matsunaga, et al. (2008). "Nucleophosmin is required for chromosome congression, proper mitotic spindle formation, and kinetochore-microtubule attachment in HeLa cells." FEBS Lett **582**(27): 3839-3844.

Andersen, J. S., Y. W. Lam, et al. (2005). "Nucleolar proteome dynamics." Nature **433**(7021): 77-83.

Anderson, P. and N. Kedersha (2002). "Visibly stressed: the role of eIF2, TIA-1, and stress granules in protein translation." Cell Stress Chaperones **7**(2): 213-221.

Anderson, P. and N. Kedersha (2009). "Stress granules." Curr Biol **19**(10): R397-398.

Antar, L. N., J. B. Dictenberg, et al. (2005). "Localization of FMRP-associated mRNA granules and requirement of microtubules for activity-dependent trafficking in hippocampal neurons." Genes Brain Behav **4**(6): 350-359.

Araya, R., I. Hirai, et al. (2005). "Loss of RPA1 induces Chk2 phosphorylation through a caffeine-sensitive pathway." FEBS Lett **579**(1): 157-161.

Armstrong, S. J., F. C. Franklin, et al. (2001). "Nucleolus-associated telomere clustering and pairing precede meiotic chromosome synapsis in Arabidopsis thaliana." J Cell Sci **114**(Pt 23): 4207-4217.

Aviv, H., Z. Voloch, et al. (1976). "Biosynthesis and stability of globin mRNA in cultured erythroleukemic Friend cells." Cell **8**(4): 495-503.

Baird, S. D., M. Turcotte, et al. (2006). "Searching for IRES." RNA **12**(10): 1755-1785.

Balagopal, V. and R. Parker (2009). "Polysomes, P bodies and stress granules: states and fates of eukaryotic mRNAs." Curr Opin Cell Biol **21**(3): 403-408.

Bartsch, M. (1985). "Correlation of chloroplast and bacterial ribosomal proteins by cross-reactions of antibodies specific to purified Escherichia coli ribosomal proteins." J Biol Chem **260**(1): 237-241.

BEIRV (1990). "Health Effects of Exposure to Low Levels of Ionizing Radiation." BEIR Report V National Academy of Science.

Belin, S., A. Beghin, et al. (2009). "Dysregulation of ribosome biogenesis and translational capacity is associated with tumor progression of human breast cancer cells." PLoS One **4**(9): e7147.

Belmokhtar, C. A., J. Hillion, et al. (2001). "Staurosporine induces apoptosis through both caspase-dependent and caspase-independent mechanisms." Oncogene **20**(26): 3354-3362.

Bergmann, J. E. and H. F. Lodish (1979). "A kinetic model of protein synthesis. Application to hemoglobin synthesis and translational control." J Biol Chem **254**(23): 11927-11937.

Berridge, M. V., P. M. Herst, et al. (2005). "Tetrazolium dyes as tools in cell biology: new insights into their cellular reduction." Biotechnol Annu Rev **11**: 127-152.

Betley, J. N., B. Heinrich, et al. (2004). "Kinesin II mediates Vg1 mRNA transport in Xenopus oocytes." Curr Biol **14**(3): 219-224.

Blangy, A., H. A. Lane, et al. (1995). "Phosphorylation by p34cdc2 regulates spindle association of human Eg5, a kinesin-related motor essential for bipolar spindle formation in vivo." Cell **83**(7): 1159-1169.

Boisvert, F. M., S. van Koningsbruggen, et al. (2007). "The multifunctional nucleolus." Nat Rev Mol Cell Biol **8**(7): 574-585.

Bonneau, A. M., A. Darveau, et al. (1985). "Effect of viral infection on host protein synthesis and mRNA association with the cytoplasmic cytoskeletal structure." J Cell Biol **100**(4): 1209-1218.

Bretscher, M. S. (1968). "Polypeptide chain termination: an active process." J Mol Biol **34**(1): 131-136.

Brewer, G. (2001). "Misregulated posttranscriptional checkpoints: inflammation and tumorigenesis." J Exp Med **193**(2): F1-4.

Burris, H. A., 3rd, S. F. Jones, et al. "A phase I study of ispinesib, a kinesin spindle protein inhibitor, administered weekly for three consecutive weeks of a 28-day cycle in patients with solid tumors." Invest New Drugs.

Campenot, R. B. and H. Eng (2000). "Protein synthesis in axons and its possible functions." J Neurocytol **29**(11-12): 793-798.

Caplan, A. B. and J. R. Menninger (1979). "Tests of the ribosomal editing hypothesis: amino acid starvation differentially enhances the dissociation of peptidyl-tRNA from the ribosome." J Mol Biol **134**(3): 621-637.

Castillo, A. and M. J. Justice (2007). "The kinesin related motor protein, Eg5, is essential for maintenance of pre-implantation embryogenesis." Biochem Biophys Res Commun **357**(3): 694-699.

Castillo, A., H. C. Morse, 3rd, et al. (2007). "Overexpression of Eg5 causes genomic instability and tumor formation in mice." Cancer Res **67**(21): 10138-10147.

Chan-Tack, K. M., J. S. Murray, et al. (2009). "Use of ribavirin to treat influenza." N Engl J Med **361**(17): 1713-1714.

Chan, J., S. N. Khan, et al. (2004). "Eukaryotic protein synthesis inhibitors identified by comparison of cytotoxicity profiles." RNA **10**(3): 528-543.

Chin, G. M. and R. Herbst (2006). "Induction of apoptosis by monastrol, an inhibitor of the mitotic kinesin Eg5, is independent of the spindle checkpoint." Mol Cancer Ther **5**(10): 2580-2591.

Chou, Y. H. and B. Y. Yung (1995). "Cell cycle phase-dependent changes of localization and oligomerization states of nucleophosmin / B23." Biochem Biophys Res Commun **217**(1): 313-325.

Cmarko, D., J. Smigova, et al. (2008). "Nucleolus: the ribosome factory." Histol Histopathol **23**(10): 1291-1298.

Collins, K., T. Jacks, et al. (1997). "The cell cycle and cancer." Proc Natl Acad Sci U S A **94**(7): 2776-2778.

Cuesta, R., M. Gupta, et al. (2009). "Chapter 7 The Regulation of Protein Synthesis in Cancer." Prog Mol Biol Transl Sci **90C**: 255-292.

Dahm-Daphi, J., C. Sass, et al. (2000). "Comparison of biological effects of DNA damage induced by ionizing radiation and hydrogen peroxide in CHO cells." Int J Radiat Biol **76**(1): 67-75.

Dani, C., J. M. Blanchard, et al. (1984). "Extreme instability of myc mRNA in normal and transformed human cells." Proc Natl Acad Sci U S A **81**(22): 7046-7050.

Davidson S.D., P. R., and Brock J.F. , Ed. (1973). Human nutrition and dietetics
London, United Kingdom, Churchill Livingstone

de Murcia, J. M., C. Niedergang, et al. (1997). "Requirement of poly(ADP-ribose) polymerase in recovery from DNA damage in mice and in cells." Proc Natl Acad Sci U S A **94**(14): 7303-7307.

Deigendesch, N., F. Koch-Nolte, et al. (2006). "ZBP1 subcellular localization and association with stress granules is controlled by its Z-DNA binding domains." Nucleic Acids Res **34**(18): 5007-5020.

di Penta, A., V. Mercaldo, et al. (2009). "Dendritic LSm1/CBP80-mRNPs mark the early steps of transport commitment and translational control." J Cell Biol **184**(3): 423-435.

Dienstbier, M. and X. Li (2009). "Bicaudal-D and its role in cargo sorting by microtubule-based motors." Biochem Soc Trans **37**(Pt 5): 1066-1071.

Drummond, D. R. and I. M. Hagan (1998). "Mutations in the bimC box of Cut7 indicate divergence of regulation within the bimC family of kinesin related proteins." J Cell Sci **111 (Pt 7)**: 853-865.

Duncan, J. E. and R. Warrior (2002). "The cytoplasmic dynein and kinesin motors have interdependent roles in patterning the Drosophila oocyte." Curr Biol **12**(23): 1982-1991.

Eberwine, J., K. Miyashiro, et al. (2001). "Local translation of classes of mRNAs that are targeted to neuronal dendrites." Proc Natl Acad Sci U S A **98**(13): 7080-7085.

Fan, H. and S. Penman (1970). "Regulation of protein synthesis in mammalian cells. II. Inhibition of protein synthesis at the level of initiation during mitosis." J Mol Biol **50**(3): 655-670.

Finch, R. A., G. R. Revankar, et al. (1993). "Nucleolar localization of nucleophosmin/B23 requires GTP." J Biol Chem **268**(8): 5823-5827.

Funabiki, H. and A. W. Murray (2000). "The Xenopus chromokinesin Xkid is essential for metaphase chromosome alignment and must be degraded to allow anaphase chromosome movement." Cell **102**(4): 411-424.

Galinier, A., J. P. Lavergne, et al. (2002). "A new family of phosphotransferases with a P-loop motif." J Biol Chem **277**(13): 11362-11367.

Garcia-Muse, T. and S. J. Boulton (2005). "Distinct modes of ATR activation after replication stress and DNA double-strand breaks in Caenorhabditis elegans." EMBO J **24**(24): 4345-4355.

Germani, A., H. Bruzzoni-Giovanelli, et al. (2000). "SIAH-1 interacts with alpha-tubulin and degrades the kinesin Kid by the proteasome pathway during mitosis." Oncogene **19**(52): 5997-6006.

Goldman, E. (1982). "Effect of rate-limiting elongation on bacteriophage MS2 RNA-directed protein synthesis in extracts of Escherichia coli." J Mol Biol **158**(4): 619-636.

Goshima, G. and R. D. Vale (2005). "Cell cycle-dependent dynamics and regulation of mitotic kinesins in Drosophila S2 cells." Mol Biol Cell **16**(8): 3896-3907.

Gray, N. K. and M. Wickens (1998). "Control of translation initiation in animals." Annu Rev Cell Dev Biol **14**: 399-458.

Grisendi, S., C. Mecucci, et al. (2006). "Nucleophosmin and cancer." Nat Rev Cancer **6**(7): 493-505.

Hamill, D., J. Davis, et al. (1994). "Polyribosome targeting to microtubules: enrichment of specific mRNAs in a reconstituted microtubule preparation from sea urchin embryos." J Cell Biol **127**(4): 973-984.

Hernandez-Verdun, D. (2006). "Nucleolus: from structure to dynamics." Histochem Cell Biol **125**(1-2): 127-137.

Hershey, J. W. (1991). "Translational control in mammalian cells." Annu Rev Biochem **60**: 717-755.

Hervy, M., L. Hoffman, et al. (2006). "From the membrane to the nucleus and back again: bifunctional focal adhesion proteins." Curr Opin Cell Biol **18**(5): 524-532.

Hesketh, J. E. (1996). "Sorting of messenger RNAs in the cytoplasm: mRNA localization and the cytoskeleton." Exp Cell Res **225**(2): 219-236.

Hinnebusch, A. G. (2006). "eIF3: a versatile scaffold for translation initiation complexes." Trends Biochem Sci **31**(10): 553-562.

Hirokawa, N., R. Takemura, et al. (1985). "Cytoskeletal architecture of isolated mitotic spindle with special reference to microtubule-associated proteins and cytoplasmic dynein." J Cell Biol **101**(5 Pt 1): 1858-1870.

Holcik, M. (2004). "Targeting translation for treatment of cancer--a novel role for IRES?" Curr Cancer Drug Targets **4**(3): 299-311.

Hovland, R., J. E. Hesketh, et al. (1996). "The compartmentalization of protein synthesis: importance of cytoskeleton and role in mRNA targeting." Int J Biochem Cell Biol **28**(10): 1089-1105.

Ivanov, P. A., E. M. Chudinova, et al. (2003). "Disruption of microtubules inhibits cytoplasmic ribonucleoprotein stress granule formation." Exp Cell Res **290**(2): 227-233.

Jansen, R. P. (1999). "RNA-cytoskeletal associations." FASEB J **13**(3): 455-466.

Job, C. and J. Eberwine (2001). "Localization and translation of mRNA in dendrites and axons." Nat Rev Neurosci **2**(12): 889-898.

Kapoor, T. M., T. U. Mayer, et al. (2000). "Probing spindle assembly mechanisms with monastrol, a small molecule inhibitor of the mitotic kinesin, Eg5." J Cell Biol **150**(5): 975-988.

Kapoor, T. M. and T. J. Mitchison (2001). "Eg5 is static in bipolar spindles relative to tubulin: evidence for a static spindle matrix." J Cell Biol **154**(6): 1125-1133.

Karmakar, P. and V. A. Bohr (2005). "Cellular dynamics and modulation of WRN protein is DNA damage specific." Mech Ageing Dev **126**(11): 1146-1158.

Kashina, A. S., G. C. Rogers, et al. (1997). "The bimC family of kinesins: essential bipolar mitotic motors driving centrosome separation." Biochim Biophys Acta **1357**(3): 257-271.

Kedersha, N. and P. Anderson (2002). "Stress granules: sites of mRNA triage that regulate mRNA stability and translatability." Biochem Soc Trans **30**(Pt 6): 963-969.

Kedersha, N. and P. Anderson (2007). "Mammalian stress granules and processing bodies." Methods Enzymol **431**: 61-81.

Kedersha, N., G. Stoecklin, et al. (2005). "Stress granules and processing bodies are dynamically linked sites of mRNP remodeling." J Cell Biol **169**(6): 871-884.

Kedersha, N. L., M. Gupta, et al. (1999). "RNA-binding proteins TIA-1 and TIAR link the phosphorylation of eIF-2 alpha to the assembly of mammalian stress granules." J Cell Biol **147**(7): 1431-1442.

Kimball, S. R., R. L. Horetsky, et al. (2003). "Mammalian stress granules represent sites of accumulation of stalled translation initiation complexes." Am J Physiol Cell Physiol **284**(2): C273-284.

Kindler, S., H. Wang, et al. (2005). "RNA transport and local control of translation." Annu Rev Cell Dev Biol **21**: 223-245.

King, M. L., T. J. Messitt, et al. (2005). "Putting RNAs in the right place at the right time: RNA localization in the frog oocyte." Biol Cell **97**(1): 19-33.

Kislauskis, E. H., Z. Li, et al. (1993). "Isoform-specific 3'-untranslated sequences sort alpha-cardiac and beta-cytoplasmic actin messenger RNAs to different cytoplasmic compartments." J Cell Biol **123**(1): 165-172.

Kozak, M. (1992). "Regulation of translation in eukaryotic systems." Annu Rev Cell Biol **8**: 197-225.

Lad, L., L. Luo, et al. (2008). "Mechanism of inhibition of human KSP by ispinesib." Biochemistry **47**(11): 3576-3585.

Lawrence, C. J., R. K. Dawe, et al. (2004). "A standardized kinesin nomenclature." J Cell Biol **167**(1): 19-22.

Le Quesne, J. P., K. A. Spriggs, et al. "Dysregulation of protein synthesis and disease." J Pathol **220**(2): 140-151.

Lee, C., B. A. Smith, et al. (2005). "DNA damage disrupts the p14ARF-B23(nucleophosmin) interaction and triggers a transient subnuclear redistribution of p14ARF." Cancer Res **65**(21): 9834-9842.

Lee, C. W., K. Belanger, et al. (2008). "A phase II study of ispinesib (SB-715992) in patients with metastatic or recurrent malignant melanoma: a National Cancer Institute of Canada Clinical Trials Group trial." Invest New Drugs **26**(3): 249-255.

Lenk, R. and S. Penman (1979). "The cytoskeletal framework and poliovirus metabolism." Cell **16**(2): 289 301.

Levesque, A. A. and D. A. Compton (2001). "The chromokinesin Kid is necessary for chromosome arm orientation and oscillation, but not congression, on mitotic spindles." J Cell Biol **154**(6): 1135-1146.

Li, C. H., T. Ohn, et al. (2010). "eIF5A promotes translation elongation, polysome disassembly and stress granule assembly." PLoS One **5**(4): e9942.

Lim, M. J. and X. W. Wang (2006). "Nucleophosmin and human cancer." Cancer Detect Prev **30**(6): 481-490.

Lindell, T. J., F. Weinberg, et al. (1970). "Specific inhibition of nuclear RNA polymerase II by alpha-amanitin." Science **170**(956): 447-449.

Loschi, M., C. C. Leishman, et al. (2009). "Dynein and kinesin regulate stress-granule and P-body dynamics." J Cell Sci **122**(Pt 21): 3973-3982.

Lowe, J. K., L. Brox, et al. (1977). "Consequences of inhibition of guanine nucleotide synthesis by mycophenolic acid and virazole." Cancer Res **37**(3): 736-743.

Lower, K. M., G. Turner, et al. (2002). "Mutations in PHF6 are associated with Borjeson-Forssman-Lehmann syndrome." Nat Genet **32**(4): 661-665.

Macgregor, H. C. and H. Stebbings (1970). "A massive system of microtubules associated with cytoplasmic movement in telotrophic ovarioles." J Cell Sci **6**(2): 431-449.

Maliga, Z. and T. J. Mitchison (2006). "Small-molecule and mutational analysis of allosteric Eg5 inhibition by monastrol." BMC Chem Biol **6**: 2.

Maliga, Z., J. Xing, et al. (2006). "A pathway of structural changes produced by monastrol binding to Eg5." J Biol Chem **281**(12): 7977-7982.

Martin, K. C. "Anchoring local translation in neurons." Cell **141**(4): 566-568.

Mayer, C. and I. Grummt (2005). "Cellular stress and nucleolar function." Cell Cycle **4**(8): 1036-1038.

Mayer, T. U., T. M. Kapoor, et al. (1999). "Small molecule inhibitor of mitotic spindle bipolarity identified in a phenotype-based screen." Science **286**(5441): 971-974.

Mazia, D. and K. Dan (1952). "The Isolation and Biochemical Characterization of the Mitotic Apparatus of Dividing Cells." Proc Natl Acad Sci U S A **38**(9): 826-838.

Misteli, T. (2003). "A nucleolar disappearing act in somatic cloning." Nat Cell Biol **5**(3): 183-184.

Misteli, T. (2005). "Going in GTP cycles in the nucleolus." J Cell Biol **168**(2): 177-178.

Moon, R. T., R. F. Nicosia, et al. (1983). "The cytoskeletal framework of sea urchin eggs and embryos: developmental changes in the association of messenger RNA." Dev Biol **95**(2): 447-458.

Newbury, S. F. (2006). "Control of mRNA stability in eukaryotes." Biochem Soc Trans **34**(Pt 1): 30-34.

Nie, M. and H. Htun (2006). "Different modes and potencies of translational repression by sequence-specific RNA-protein interaction at the 5'-UTR." Nucleic Acids Res **34**(19): 5528-5540.

Ohsugi, M., N. Tokai-Nishizumi, et al. (2003). "Cdc2-mediated phosphorylation of Kid controls its distribution to spindle and chromosomes." EMBO J **22**(9): 2091-2103.

Okuwaki, M., M. Tsujimoto, et al. (2002). "The RNA binding activity of a ribosome biogenesis factor, nucleophosmin/B23, is modulated by phosphorylation with a cell cycle-dependent kinase and by association with its subtype." Mol Biol Cell **13**(6): 2016-2030.

Olson, M. O. and M. Dundr (2005). "The moving parts of the nucleolus." Histochem Cell Biol **123**(3): 203-216.

Olson, M. O., M. Dundr, et al. (2000). "The nucleolus: an old factory with unexpected capabilities." Trends Cell Biol **10**(5): 189-196.

Oskarsson, T. and A. Trumpp (2005). "The Myc trilogy: lord of RNA polymerases." Nat Cell Biol **7**(3): 215-217.

Palacios, I. M. and D. St Johnston (2001). "Getting the message across: the intracellular localization of mRNAs in higher eukaryotes." Annu Rev Cell Dev Biol **17**: 569-614.

Parrilla-Castellar, E. R., S. J. Arlander, et al. (2004). "Dial 9-1-1 for DNA damage: the Rad9-Hus1-Rad1 (9-1-1) clamp complex." DNA Repair (Amst) **3**(8-9): 1009-1014.

Pavlov, M. Y., D. V. Freistroffer, et al. (1997). "Fast recycling of Escherichia coli ribosomes requires both ribosome recycling factor (RRF) and release factor RF3." EMBO J **16**(13): 4134-4141.

Perkins, D. J. and G. N. Barber (2004). "Defects in translational regulation mediated by the alpha subunit of eukaryotic initiation factor 2 inhibit antiviral activity and facilitate the malignant transformation of human fibroblasts." Mol Cell Biol **24**(5): 2025-2040.

Perry, R. P. and O. Meyuhas (1990). "Translational control of ribosomal protein production in mammalian cells." Enzyme **44**(1-4): 83-92.

Petersen, C. P., M. E. Bordeleau, et al. (2006). "Short RNAs repress translation after initiation in mammalian cells." Mol Cell **21**(4): 533-542.

Pierrat, O. A., V. Mikitova, et al. (2007). "Control of protein translation by phosphorylation of the mRNA 5'-cap-binding complex." Biochem Soc Trans **35**(Pt 6): 1634-1637.

Pisarev, A. V., M. A. Skabkin, et al. (2010). "The role of ABCE1 in eukaryotic posttermination ribosomal recycling." Mol Cell **37**(2): 196-210.

Pokrywka, N. J. and E. C. Stephenson (1991). "Microtubules mediate the localization of bicoid RNA during Drosophila oogenesis." Development **113**(1): 55-66.

Proud, C. G. (2002). "Control of the translational machinery in mammalian cells." Eur J Biochem **269**(22): 5337.

Raska, I., K. Koberna, et al. (2004). "The nucleolus and transcription of ribosomal genes." Biol Cell **96**(8): 579-594.

Rice, A. P. (2009). "Dysregulation of positive transcription elongation factor B and myocardial hypertrophy." Circ Res **104**(12): 1327-1329.

Roegiers, F. (2003). "Insights into mRNA transport in neurons." Proc Natl Acad Sci U S A **100**(4): 1465-1466.

Roof, D. M., P. B. Meluh, et al. (1992). "Kinesin-related proteins required for assembly of the mitotic spindle." J Cell Biol **118**(1): 95-108.

Ross, J. (1996). "Control of messenger RNA stability in higher eukaryotes." Trends Genet **12**(5): 171-175.

Ross, J. L., K. Wallace, et al. (2006). "Processive bidirectional motion of dynein-dynactin complexes in vitro." Nat Cell Biol **8**(6): 562-570.

Roybal, C. N., L. A. Hunsaker, et al. (2005). "The oxidative stressor arsenite activates vascular endothelial growth factor mRNA transcription by an ATF4-dependent mechanism." J Biol Chem **280**(21): 20331-20339.

Rubbi, C. P. and J. Milner (2003). "Disruption of the nucleolus mediates stabilization of p53 in response to DNA damage and other stresses." EMBO J **22**(22): 6068-6077.

Saijo, T., G. Ishii, et al. (2006). "Eg5 expression is closely correlated with the response of advanced non-small cell lung cancer to antimitotic agents combined with platinum chemotherapy." Lung Cancer **54**(2): 217-225.

Saini, P., D. E. Eyler, et al. (2009). "Hypusine-containing protein eIF5A promotes translation elongation." Nature **459**(7243): 118-121.

Salmon, E. D. (1982). "Mitotic spindles isolated from sea urchin eggs with EGTA lysis buffers." Methods Cell Biol **25 Pt B**: 69-105.

Sanchez-Carbente Mdel, R. and L. Desgroseillers (2008). "Understanding the importance of mRNA transport in memory." Prog Brain Res **169**: 41-58.

Sarre, T. F. (1989). "The phosphorylation of eukaryotic initiation factor 2: a principle of translational control in mammalian cells." Biosystems **22**(4): 311-325.

Sawin, K. E., K. LeGuellec, et al. (1992). "Mitotic spindle organization by a plus-end-directed microtubule motor." Nature **359**(6395): 540-543.

Sawin, K. E. and T. J. Mitchison (1995). "Mutations in the kinesin-like protein Eg5 disrupting localization to the mitotic spindle." Proc Natl Acad Sci U S A **92**(10): 4289-4293.

Scheer, U. and R. Hock (1999). "Structure and function of the nucleolus." Curr Opin Cell Biol **11**(3): 385-390.

Schumm, D. E. and T. E. Webb (1982). "Site of action of colchicine on RNA release from liver nuclei." Biochem Biophys Res Commun **105**(1): 375-382.

Seal, R., R. Temperley, et al. (2005). "Serum-deprivation stimulates cap-binding by PARN at the expense of eIF4E, consistent with the observed decrease in mRNA stability." Nucleic Acids Res **33**(1): 376-387.

Sharp, D. J., G. C. Rogers, et al. (2000). "Microtubule motors in mitosis." Nature **407**(6800): 41-47.

Shcherbik, N., M. Wang, et al. (2010). "Polyadenylation and degradation of incomplete RNA polymerase I transcripts in mammalian cells." EMBO Rep **11**(2): 106-111.

Shestakova, E. A., R. H. Singer, et al. (2001). "The physiological significance of beta -actin mRNA localization in determining cell polarity and directional motility." Proc Natl Acad Sci U S A **98**(13): 7045-7050.

Shiloh, Y. (2001). "ATM (ataxia telangiectasia mutated): expanding roles in the DNA damage response and cellular homeostasis." Biochem Soc Trans **29**(Pt 6): 661-666.

Singer, R. H., G. L. Langevin, et al. (1989). "Ultrastructural visualization of cytoskeletal mRNAs and their associated proteins using double-label in situ hybridization." J Cell Biol **108**(6): 2343-2353.

Sivan, G., N. Kedersha, et al. (2007). "Ribosomal slowdown mediates translational arrest during cellular division." Mol Cell Biol **27**(19): 6639-6646.

Song, Z. and M. Wu (2005). "Identification of a novel nucleolar localization signal and a degradation signal in Survivin-deltaEx3: a potential link between nucleolus and protein degradation." Oncogene **24**(16): 2723-2734.

Stebbings, H. (1986). "Cytoplasmic transport and microtubnies in telotrophic ovarioles of hemiptaran insects." *Int. Rev. Cytol* **101**: 101-123.

Suprenant, K. A. (1993). "Microtubules, ribosomes, and RNA: evidence for cytoplasmic localization and translational regulation." Cell Motil Cytoskeleton **25**(1): 1-9.

Suprenant, K. A. and L. I. Rebhun (1983). "Assembly of unfertilized sea urchin egg tubulin at physiological temperatures." J Biol Chem **258**(7): 4518-4525.

Suprenant, K. A., L. B. Tempero, et al. (1989). "Association of ribosomes with in vitro assembled microtubules." Cell Motil Cytoskeleton **14**(3): 401-415.

Surjushe, A. and D. G. Saple (2008). "Mycophenolate mofetil." Indian J Dermatol Venereol Leprol **74**(2): 180-184.

Takahashi, A. and T. Ohnishi (2005). "Does gammaH2AX foci formation depend on the presence of DNA double strand breaks?" Cancer Lett **229**(2): 171-179.

Taneja, K. L., L. M. Lifshitz, et al. (1992). "Poly(A) RNA codistribution with microfilaments: evaluation by in situ hybridization and quantitative digital imaging microscopy." J Cell Biol **119**(5): 1245-1260.

Tang, S. J. and E. M. Schuman (2002). "Protein synthesis in the dendrite." Philos Trans R Soc Lond B Biol Sci **357**(1420): 521-529.

Tokai-Nishizumi, N., M. Ohsugi, et al. (2005). "The chromokinesin Kid is required for maintenance of proper metaphase spindle size." Mol Biol Cell **16**(11): 5455-5463.

Tokai, N., A. Fujimoto-Nishiyama, et al. (1996). "Kid, a novel kinesin-like DNA binding protein, is localized to chromosomes and the mitotic spindle." EMBO J **15**(3): 457-467.

Tomioka, S., M. Oyamada, et al. (1975). "[A case of pediculate neurofibroma of the visceral pleura (author's transl)]." Nihon Kyobu Shikkan Gakkai Zasshi **13**(5): 297-301.

Trere, D., C. Ceccarelli, et al. (2004). "Nucleolar size and activity are related to pRb and p53 status in human breast cancer." J Histochem Cytochem **52**(12): 1601-1607.

Tsai, R. Y. and R. D. McKay (2005). "A multistep, GTP-driven mechanism controlling the dynamic cycling of nucleostemin." J Cell Biol **168**(2): 179-184.

Turner, C. E., J. R. Glenney, Jr., et al. (1990). "Paxillin: a new vinculin-binding protein present in focal adhesions." J Cell Biol **111**(3): 1059-1068.

Turner, J. L. and J. R. McIntosh (1977). "Isolation of the mitotic apparatus." Methods Cell Biol **16**: 373-379.

van Venrooij, W. J., P. T. Sillekens, et al. (1981). "On the association of mRNA with the cytoskeleton in uninfected and adenovirus-infected human KB cells." Exp Cell Res **135**(1): 79-91.

Vessey, J. P., A. Vaccani, et al. (2006). "Dendritic localization of the translational repressor Pumilio 2 and its contribution to dendritic stress granules." J Neurosci **26**(24): 6496-6508.

von Hippel, P. H. and T. D. Yager (1991). "Transcript elongation and termination are competitive kinetic processes." Proc Natl Acad Sci U S A **88**(6): 2307-2311.

Vuppalanchi, D., J. Coleman, et al. "Conserved 3'-untranslated region sequences direct subcellular localization of chaperone protein mRNAs in neurons." J Biol Chem **285**(23): 18025-18038.

Walczak, C. E., T. J. Mitchison, et al. (1996). "XKCM1: a Xenopus kinesin-related protein that regulates microtubule dynamics during mitotic spindle assembly." Cell **84**(1): 37-47.

Walker, P. R. and J. F. Whitfield (1985). "Cytoplasmic microtubules are essential for the formation of membrane-bound polyribosomes." J Biol Chem **260**(2): 765-770.

Warner, J. R. (1999). "The economics of ribosome biosynthesis in yeast." Trends Biochem Sci **24**(11): 437-440.

Watkins, S. J. and C. J. Norbury (2002). "Translation initiation and its deregulation during tumorigenesis." Br J Cancer **86**(7): 1023-1027.

Wehrle-Haller, B. and B. A. Imhof (2003). "Actin, microtubules and focal adhesion dynamics during cell migration." Int J Biochem Cell Biol **35**(1): 39-50.

Wu, C. W., F. Zeng, et al. (2007). "mRNA transport to and translation in neuronal dendrites." Anal Bioanal Chem **387**(1): 59-62.

Yajima, J., M. Edamatsu, et al. (2003). "The human chromokinesin Kid is a plus end-directed microtubule-based motor." EMBO J **22**(5): 1067-1074.

Ye, K. (2005). "Nucleophosmin/B23, a multifunctional protein that can regulate apoptosis." Cancer Biol Ther **4**(9): 918-923.

Yisraeli, J. K., S. Sokol, et al. (1990). "A two-step model for the localization of maternal mRNA in Xenopus oocytes: involvement of microtubules and microfilaments in the translocation and anchoring of Vg1 mRNA." Development **108**(2): 289-298.

Yoon, Y. J. and K. L. Mowry (2004). "Xenopus Staufen is a component of a ribonucleoprotein complex containing Vg1 RNA and kinesin." Development **131**(13): 3035-3045.

Yu, Y., L. B. Maggi, Jr., et al. (2006). "Nucleophosmin is essential for ribosomal protein L5 nuclear export." Mol Cell Biol **26**(10): 3798-3809.

Zemp, I. and U. Kutay (2007). "Nuclear export and cytoplasmic maturation of ribosomal subunits." FEBS Lett **581**(15): 2783-2793.

Zha, S., F. W. Alt, et al. (2007). "Defective DNA repair and increased genomic instability in Cernunnos-XLF-deficient murine ES cells." Proc Natl Acad Sci U S A **104**(11): 4518-4523.

Zhu, C., J. Zhao, et al. (2005). "Functional analysis of human microtubule-based motor proteins, the kinesins and dyneins, in mitosis/cytokinesis using RNA interference." Mol Biol Cell **16**(7): 3187-3199.